NASA CONTRACTOR REPORT

NASA CR-

NASA CR-304

EXPERIMENTAL INVESTIGATION OF THERMAL ANNEALING OF NUCLEAR-REACTOR-INDUCED COLORATION IN FUSED SILICA

by F. C. Douglas and R. M. Gagosz

Prepared under Contract No. NASw-768 *by*
UNITED AIRCRAFT CORPORATION
East Hartford, Conn.
for

NATIONAL AERONAUTICS AND SPACE ADMINISTRATION • WASHINGTON, D. C. • SEPTEMBER 1965

NASA CR-304

EXPERIMENTAL INVESTIGATION OF THERMAL ANNEALING OF NUCLEAR-REACTOR-INDUCED COLORATION IN FUSED SILICA

By F. C. Douglas and R. M. Gagosz

Prepared under Contract No. NASw-768 by
UNITED AIRCRAFT CORPORATION
East Hartford, Conn.

for

NATIONAL AERONAUTICS AND SPACE ADMINISTRATION

For sale by the Clearinghouse for Federal Scientific and Technical Information
Springfield, Virginia 22151 – Price $4.00

Experimental Investigation of Thermal Annealing of Nuclear-Reactor-Induced Coloration in Fused Silica

TABLE OF CONTENTS

LIST OF TABLES

LIST OF FIGURES

LIST OF FIGURES (Contd.)

LIST OF FIGURES (Contd.)

LIST OF FIGURES (Contd.)

LIST OF FIGURES (Contd.)

LIST OF FIGURES (Contd.)

LIST OF FIGURES (Contd.)

LIST OF FIGURES (Contd.)

Experimental Investigation of Thermal Annealing of Nuclear-Reactor-Induced Coloration in Fused Silica

SUMMARY

An experimental investigation was conducted to determine the spectral transmission characteristics of fused silica over a range of temperatures prior to nuclear irradiation and during thermal annealing of reactor-induced coloration following exposure to a dose of 6×10^{17} nvt fast neutrons per cm^2. The investigation was conducted using commercially supplied specimens of Corning 7940, Amersil Infrasil, and Thermal American Spectrosil brands of fused silica which were selected because of their high purity but which were found to differ slightly in chemical composition. The pre-irradiation studies were carried out at a series of fixed temperatures. The annealing studies were carried out using both ramp variations of temperature with time and step-wise variations of temperature with time for temperatures between 22 and 1000 C. Most of the annealing data were obtained at a wavelength of 0.21 microns, although some annealing data were obtained following step-wise changes in temperature at wavelengths between 0.15 and 4.0 microns. Spectral transmission measurements also were made at wavelengths between 0.15 and 4.0 microns for all samples before nuclear irradiation and after thermal annealing.

The results of the tests indicate that nuclear-reactor-induced coloration is greater and more difficult to remove in the ultraviolet portion of the spectrum than in either the visible or the infrared portions of the spectrum. Induced coloration in the ultraviolet is annealed out at temperatures between 700 and 900 C, and the rate of annealing corresponds to activation energies of between 2.2 and 2.8 eV in a first-order kinetic annealing process with a frequency factor of 10^{10} sec^{-1}. The three brands of fused silica in order of their degree of induced coloration and the difficulty of annealing this induced coloration were: Amersil Infrasil, Corning 7940, and Thermal American Spectrosil.

This investigation was carried out under Contract NASw-768 with the National Aeronautics and Space Administration through the joint AEC-NASA Space Nuclear Propulsion Office.

RESULTS

1. Pre-irradiation studies of the optical transmission characteristics of fused silica indicated that:

   a. The ultraviolet wavelength below which the absorption coefficient is greater than 1.0 cm^{-1} was approximately equal to the following values at temperatures of 22 and 800 C, respectively: 0.154 and 0.170 microns for Thermal American Spectrosil, 0.159 and 0.176 microns for Corning 7940, and 0.162 and 0.180 microns for Amersil Infrasil.

   b. The absorption coefficient was too low to be measured (less than 0.002 cm^{-1}) in the portion of the spectrum between 0.3 and 1.0 microns for all specimens tested at temperatures between 22 and 1000 C.

   c. The Thermal American Spectrosil and Corning 7940 specimens exhibited absorption bands at wavelengths of 1.4, 2.23, and 2.8 microns (the 2.8-micron band is normally attributed to entrapped water) at both 22 and 800 C; these absorption bands were much less pronounced in the Amersil Infrasil specimens. The absorption coefficient of all samples tested was greater than 1.0 cm^{-1} at wavelengths greater than 3.6 microns at both 22 and 800 C.

2. Nuclear-reactor irradiation to a dose of 6×10^{17} nvt fast neutrons per cm^2 with the specimens at room temperature caused the following:

   a. Increases in absorption coefficient for all specimens of between 10 and 50 cm^{-1} at wavelengths less than 0.3 microns. A portion of this absorption was associated with a band centered at a wavelength of approximately 0.210 microns.

   b. Increases in absorption coefficient of between 1.0 and 6.0 cm^{-1} for Amersil Infrasil specimens, and increases in absorption coefficient of less than 0.2 cm^{-1} for Corning 7940 and Thermal American Spectrosil specimens at wavelengths between 0.35 and 0.8 microns.

   c. Increases in absorption coefficient of less than 0.05 cm^{-1} for all specimens at wavelengths greater than 1.4 microns.

3. The ease of removing the nuclear-reactor-induced color in the ultraviolet for the brands employed was in the order: Thermal American Spectrosil, Corning 7940, and Amersil Infrasil. For example, during annealing tests conducted using continuous variations of temperature with time, the reactor-induced absorption coefficient at a wavelength of 0.21 microns was reduced to 0.05 cm^{-1} at a temperature of approximately 720 C for Thermal American Spectrosil, 750 C for Corning 7940, and 900 C for Amersil Infrasil. Tests conducted with the specimens held at a series of fixed temperatures during the annealing process indicated that the rate of annealing was independent of wavelength for wavelengths between approximately 0.17 and 0.25 microns.

4. Reactor-induced coloration in the visible and infrared portions of the spectrum was annealed out at temperatures below 600 C for all specimens studied.

5. Activation energies calculated for a first-order annealing process (assuming a frequency factor of 10^{10} sec^{-1}) from the variation of reactor-induced absorption coefficient with time during the annealing process were between 2.2 and 2.6 eV for Thermal American Spectrosil and Corning 7940, and between 2.2 and 2.8 eV for Amersil Infrasil. Calculated activation energies were approximately 0.8 eV higher for a frequency factor of 10^{14} sec^{-1} than for a frequency factor of 10^{10} sec^{-1}.

6. Spectral transmission data measured following complete annealing were in agreement with spectral transmission data measured before irradiation within the accuracy of the procedures employed.

7. The indicated optical transmission of the fused silica specimens employed was influenced by their heating history and surface condition.

INTRODUCTION

It is desirable in many applications to employ a material which is transparent to optical radiation over a wide range of wavelengths in a nuclear radiation environment. Two competing processes will affect such applications: first, coloration induced by nuclear radiation; and second, annealing of coloration by exposure to elevated temperatures. Therefore, it would appear possible to reduce the coloration present in a transparent material while it is in a nuclear environment by maintaining it at an elevated temperature.

The only available data concerning annealing of reactor-induced coloration has been obtained from room-temperature measurements following exposure of the irradiated specimen to high temperatures (see, for example, Refs. 1 and 2). The results of these experimental studies indicate that reactor-induced color in fused silica can be annealed by exposure of the specimens to temperatures between 700 and 1000 C. However, these experiments have not yielded information concerning the rate of annealing of the reactor-induced coloration. Such rate information is required, as well as information on the rate of creation of coloration, to permit determination of the temperature dependence of the equilibrium coloration during the combined processes of reactor-induced coloration and of thermal annealing.

Therefore, a program was initiated at the United Aircraft Research Laboratories to obtain annealing-rate information. The first portion of this program was the development, under Corporate sponsorship, of a spectrophotometer which could be employed to obtain transient transmission characteristics of high-temperature transparent specimens. The second portion of this program, the actual measurement of rates of annealing for fused silica, was carried out under sponsorship of the National Aeronautics and Space Administration, and is described in the following sections.

DESCRIPTION OF EQUIPMENT

UAC High-Temperature Spectrophotometer

Spectrophotometer Description

The UAC high-temperature spectrophotometer is a dual-beam instrument which measures the spectral transmission characteristics of optical materials when the specimen under study is at any temperature between 22 and 1100 C. This spectrophotometer is comprised of three chambers as shown in Fig. 1. The portions of the instrument corresponding to the numbers in Fig. 1 are listed in Fig. 2. The largest chamber contains the monochromator section, ultraviolet, visible and near-infrared sources, infrared thermocouple detector, and collimating and beam-splitting mirrors. Radiant energy from either of the two sources located in this chamber is selected and focused by the spherical condensing mirror into the entrance slit of the monochromator. The monochromator section is of basic Littrow design utilizing an off-axis parabolic mirror to collimate light from the entrance slit onto the plane diffraction grating and to focus the diffracted light from the grating to the exit slit. Four diffraction gratings are utilized to cover the spectral range of operation and are mounted on a turntable. The monochromatized energy emerging from the exit slit is collimated by another

off-axis parabola and then directed by two circular plane mirrors through the chopper system into the furnace chamber. Two furnace tubes are used to mount and to heat the specimens. Each furnace is comprised of a 12-in.-long, 1 1/4-in.-dia, 0.020-in.-wall tantalum tube supported at each end by water-cooled copper electrodes. These electrodes are carbon lined to allow the tantalum tubes to slide as they elongate at elevated temperatures. After passing through the sample chamber the transmitted energy enters the third chamber and is directed by two circular plane mirrors onto the photomultiplier or the lead sulfide detector. The lead sulfide detector is mounted on a turntable and may be positioned directly in front of the photomultiplier. The infrared source system located in this chamber consists of a Nernst glower to provide radiant energy and an arsenic trisulfide lens to collimate this energy. Mounted on the same turntable with the lead sulfide detector are a pair of rectangular plane mirrors which direct the radiant energy from the infrared source system to circular plane mirrors and thence into the sample chamber and on to the monochromator section. These three chambers are connected with high-vacuum ball valves so that the furnace chamber may be opened independent of the rest of the system for the insertion or removal of sample specimens. The whole system is capable of being evacuated to 20 mm of Hg or can be run when filled with an inert gas. It has been the practice to operate the instrument with the chambers filled with argon.

The radiant energy in the ultraviolet, visible, and near-infrared regions are monochromatized before entering the sample chamber whereas the infrared spectrum is monochromatized after sampling. There are two reasons for this configuration; monochromatizing of the shorter wavelengths is done initially to eliminate or minimize any optical bleaching of a colored sample which may occur by allowing the full ultraviolet spectrum to be incident upon the sample, while monochromatizing of the longer wavelengths is done terminally to minimize the amount of direct furnace and sample radiation incident upon the thermocouple detector when running the system at elevated temperatures. In addition to the reversed optical beam paths, the optical chopping for each beam direction is accomplished prior to entering the furnace chamber so that any furnace radiation which may be directed onto the operating photodetector will produce a constant signal and thus not be passed by the chopper rectification circuitry to affect the recorded signal. Output is presented onto a recording strip chart which displays the ratio of energy transmitted in the sample beam to that transmitted in the reference beam with respect to wavelength.

Spectrophotometer Optical Specifications

The spectral wavelength range of operation for the high-temperature spectrophotometer is 0.15 to 4.5 microns. In covering the full spectrum, several light sources, detectors and dispersing elements are required, and are summarized in Table I. The four different gratings were chosen so that the blaze angle (angle

at which the grating grooves are cut) would concentrate first-order diffraction in the appropriate ranges. Theoretical resolving powers for the instrument are 0.00005 microns at 0.2 microns, and 0.0004 microns at 2 microns. However, because of energy requirements, the normal band pass at which specimens have been studied are 20 Å in the visible and ultraviolet (wavelengths between 1500 and 7000 Å) and 0.02 microns in the infrared (wavelengths between 1.0 and 4.5 microns). These are sufficiently narrow band passes, since the materials to be examined do not have sharp absorption bands.

The particular type of optical beam chopping and signal rectification circuitry employed in the high-temperature spectrophotometer requires that a positive and therefore recordable "zero" signal be present even when the sample beam is blocked. This is accomplished by introducing a small percentage (referred to as the percent of phasing) of the reference signal into the sample signal. The accuracy with which transmittance data may be obtained on the high-temperature spectrophotometer is dependent upon this percent of phasing. Table II compares the transmittance values obtained by measuring ten neutral-density filters and screens varying in transmittance from 97.7 percent to 12.2 percent on a Cary-14R spectrophotometer and subsequently on the high-temperature spectrophotometer at three different percents of phasing. In general, the tests discussed in the following sections were conducted using one-percent phasing. The average difference in the transmission measurements for one-percent phasing is $\pm$ 0.3 percent as shown in Table II. In some cases the deviation is larger than one-percent arising from the fact that the filters are not uniform over the area through which the optical beam passes. An accuracy in transmittance of $\pm$ 0.3 percent corresponds to a measurement of the absorption coefficient of a 30-mm sample to within $\pm$ 0.001 cm^{-1} when τ= 95 percent. Table III shows the accuracy of the measurements of α for two-specimen thicknesses at a range of transmissivities. The standard deviation of the reproducibility of the transmittance data at 0.475 microns is 0.5 percent as shown in Fig. 3. Measurements were made at wavelengths in the different spectral regions and show, in Fig. 3, the transmittance data reproducibility of the spectrophotometer over a 10-day period.

Wavelength calibration of the spectrophotometer was performed using interference filters. As a typical example of the reproducibility of these measurements, Fig. 4 is presented showing the scatter obtained at a wavelength of 0.39016 microns. This measurement can be made to within $\pm$ 0.00007 microns. Since this indicates the reproducibility with which the grating normal may be located with respect to the incident beam, similar values may be obtained for the other spectral regions. In the ultraviolet the measurements can be obtained to $\pm$ 0.00014 microns and in the infrared to $\pm$ 0.00056 microns.

Measurements of Transmission Properties

The dual-beam design of the high-temperature instrument, in which the ratio of the transmitted energies of the two beams is measured, allows specimens to be studied in either a two-specimen or one-specimen mode of operation, as illustrated in Fig. 5. In the two-specimen mode, a thick specimen is placed in the sample beam and a thin specimen in the reference beam. In this mode, the transmissivity of the net specimen thickness (difference between sample and reference thicknesses) is measured directly since the identical reflection losses of each sample do not appear in the recorded ratio as shown in Fig. 5. The spectral absorption coefficient, $\alpha_{\lambda,T}$, is then obtained employing the measured transmissivity and a form of the Lambert-Beer Law:

$$\tau = e^{-\alpha_{\lambda,T}(X_s - X_r)} \tag{1}$$

where X_s = sample specimen thickness

X_r = reference specimen thickness

τ = transmissivity

Measurements of transmissivity and absorption coefficient are made by using the two-specimen mode of operation in the following way. Three spectral runs are made over the spectral range of interest: (1) a 100-percent transmissivity run (no specimens in either beam); (2) a zero transmissivity run (sample beam completely blocked and no specimen in the reference beam); and (3) a sample run (sample and reference specimens in their respective beams). The transmissivity is obtained from these three runs from the following equation.

$$\tau_{X_s - X_r} = \frac{\text{Sample value (3) - zero value (2)}}{\text{100\% value (1) - zero value (2)}} \tag{2}$$

Transmittance data are obtained by operating the spectrophotometer in the one-specimen mode with the specimen placed in the sample beam and performing the same operations as above (Eq. (2)). To obtain detailed information concerning the spectral absorption edges in the ultraviolet and infrared regions where α is greater than 1.5 cm^{-1}, it is necessary to study thin specimens using the one-specimen mode of operation. Thin specimens are required because the transmissivity of a 30-mm specimen is 1.1 percent when α = 1.5 cm^{-1}, but a 1-mm specimen has a transmissivity of 86 percent at α = 1.5 cm^{-1}, and 13.6 percent at α = 20 cm^{-1}. Furthermore, the one-specimen mode of operation is required since the insertion of a specimen into the reference beam raises the spectrophotometer cut-off wavelength to a value dependent

upon the specimen's thickness, material, and temperature. For example, a 1-mm Thermal American Spectrosil specimen in the reference beam increases this cut-off wavelength from 0.150 to 0.158 microns. Therefore, measurements cannot be made below this wavelength using the two-specimen mode of operation.

The transmittance as measured includes reflection losses since, in this case, the compensating reflection losses are not present in the reference beam. The transmittance is related to the absorption coefficient as shown in Fig. 5 by the relation

$$I_s/I_o = (1 - \rho_{\lambda,T})^2 e^{-\alpha_{\lambda,T} X_s} \tag{3}$$

where I_s/I_o = transmittance of specimen

$\rho_{\lambda,T}$ = surface reflectivity

$\alpha_{\lambda,T}$ = absorption coefficient

X_s = specimen thickness

The absorption coefficient can be obtained from Eq. (3) if the reflectivity is known, or by measuring the transmittances of two samples of different thicknesses. The ratio of the transmittances of two specimens of different thicknesses yields the absorption coefficient from the relation

$$\frac{I_s/I_o}{I_r/I_o} = e^{-\alpha_{\lambda,T}(X_s - X_r)} \tag{4}$$

where I_s/I_o = transmittance of thick specimen

I_r/I_o = transmittance of thin specimen

The technique employed to obtain the data shown in each figure is noted in the relevant portion of the text.

Temperature Calibration

When taking transmission data with the specimen above room temperature, it is necessary to have a correlation between monitored furnace temperature and actual specimen temperature. Both furnace tubes are instrumented with thermocouples to provide a means for measuring high temperatures. To provide a time correlation between specimen temperature and furnace temperature a 30-mm specimen was instrumented by drilling three holes, 15-mm deep, and inserting thermocouples at the center, at one-half the radius and at nine-tenths the radius. Various time-versus-temperature

programs were obtained using this instrumented specimen in the sample furnace tube. Figure 6 is a plot showing the temperature of the specimen center line and furnace during an 88-min linear ramp from 200 to 1000 C and Fig. 7 shows the specimen response for a 6-min change of furnace temperature from 200 to 1000 C. Additional programs were obtained for 44- and 150-min linear ramps. The 44- and 88-min ramps and some step programs were used in the annealing of the reactor-induced coloration. When the specimen is held at constant temperature, the difference between the monitored furnace temperature and the actual specimen temperature is less than one deg C and this condition is reached in approximately 1.5 min at the desired constant temperature.

Cary Model 14R

Some measurements were obtained using the Cary Model 14R spectrophotometer. The Model 14R is a dual-beam instrument with a wavelength range of 0.2 to 2.5 microns with a wavelength accuracy of 4 A and reproducibility to 0.5 Å. It records absorbance in a range of from 0 to 2.0 optical density units to within $\pm$ 0.002 O.D. The optical density is related to the transmittance in the following way:

$$O.D. = \log_{10} \frac{1}{I_s/I_o} \tag{5}$$

Measurements performed on the Cary 14R must be made with the specimen at room temperature, hence, the variation of transmissivity with temperature cannot be measured on this instrument. This instrument was used for calibrating the transmittance scale of the high-temperature spectrophotometer.

SPECIMEN DESCRIPTION AND HANDLING HISTORY

The specimens used for the optical transmissivity studies were fused silica of the following brands and types: Amersil "Infrasil", Corning "7940", and Thermal American "Spectrosil". They have been designated SA, SC, and ST, respectively, "S" referring to "silica" and the second letter to the manufacturer. Numbers following these letters represent the length of the specimen, and the specimen number. For example, SC 2-11 denotes silica, Corning 7940, 2 mm, specimen No. 11.

The specimens used were of thicknesses 1, 2, 8, and 30 mm. Maximum accuracy in the determination of absorption coefficient was obtained by using thick specimens in wavelength regions of low absorption and thin specimens in wavelength regions of high absorption. Each specimen was polished by the manufacturer to a flatness of one-half wavelength, sodium "D" line, and a parallelism of 0.025 mm or better. Each specimen was 25 mm in diameter.

Two of the three types of fused silica tested, Corning 7940 and Thermal American Spectrosil, were reported by the manufacturer to have good transmission characteristics in the ultraviolet, while Amersil Infrasil was reported to have good transmission characteristics in the infrared. It will be shown in following sections that the two types of fused silica which transmit further into the ultraviolet have poor transmission in the infrared, while the fused silica which has good transmission in the infrared does not transmit as far into the ultraviolet. Preliminary tests also were conducted using a fourth type of fused silica, Amersil Ultrasil, which was reported to have good transmission characteristics in the ultraviolet. However, no further tests of this material were conducted because the transmission in the ultraviolet was poorer than either Corning 7940 or Thermal American Spectrosil, and because there was a large difference in ultraviolet transmission from sample to sample.

The results of a spectrochemical analysis of each type of fused silica are summarized in Table IV. The accuracy of the analysis is approximately $\pm$ 50 percent. The major differences between the impurities in the samples analyzed are 40 ppm Al in the Amersil as compared to 2 ppm Al for Corning and 1 ppm for Thermal American, and 20 ppm Na in the Thermal American as compared to less than 5 ppm Na for the Corning and Amersil brands.

The handling procedure for the specimens included a number of cleaning processes. Initially the specimens were cleaned with an organic solvent such as acetone or alcohol, cleaned in a soap solution in an ultrasonic cleaner, then rinsed in distilled water. After the pre-irradiation studies had been completed, the same cleaning process was repeated prior to encapsulation for irradiation. Some specimens also were cleaned chemically using chromic acid (sodium dichromate or potassium dichromate). Table V summarizes the handling and cleaning history for all specimens.

Prior to irradiation at the Union Carbide Nuclear Research Reactor Facility, all specimens were packaged in clean aluminum foil and packed in an aluminum tube. To insert the samples into the reactor this aluminum tube was closed by welding and inserted in an aluminum filler container of sufficient size to fill the stringer tube which allowed the sample to be placed in the core of the nuclear reactor. The aluminum filler container was used to exclude the reactor cooling water from the stringer tube, so that the generation of thermal neutrons due to moderation of fast neutrons by the water would be minimized. In general, it was found that contamination of the samples due to their exposure to the nuclear-reactor irradiation consisted of by-products from the aluminum-to-sodium transition which occurred in the aluminum container. A sufficient decay time for safe handling was allowed at the Union Carbide Nuclear Research Reactor Facility. Samples were then shipped to the Research Laboratories where they were cleaned again in an ultrasonic

cleaner using soap and water solution plus special cleaning agents. In some cases, the chromic acid glass cleaning solution was used. The cleaning procedure was continued until the contamination of the samples was shown to be negligible.

The monitors for flux determination to obtain the radiation dose given the specimens consisted of nickel wires and cadmium shielded and unshielded gold wires placed next to the specimens during the irradiation. The results of the monitoring procedure show a negligible variation in dose given specimens in the various positions during any single exposure, and only small differences in total dose given each of the three groups of specimens irradiated. Table VI gives the specific results for each specimen, and Table VII gives the variation of flux with position.

FACTORS AFFECTING DATA REPRODUCIBILITY

A series of factors have been encountered in the test program which can lead to inconsistencies in the data. For instance, the initial experiments with the Amersil Infrasil fused silica showed that the transmission properties of the specimens changed after they were heated either in argon or in air. The transmissivity measured on a specimen at 800 C as received from the manufacturer was greater than the transmissivity obtained with the same specimen at 22 C prior to heating at wavelengths in the ultraviolet portion of the spectrum. After this specimen had been heated, its transmissivity properties became stable as a function of temperature. A second specimen was pre-heated to 850 C prior to transmissivity measurements. The transmissivity of this pre-heated specimen is reproducible at temperatures of measurement below 850 C, and drops with increased specimen temperature. Figure 8 compares the transmissivity of the pre-heated Amersil 30-mm specimen SA 30-5 with the transmissivity of the non-pre-heated Amersil 30-mm specimen SA 30-2, at 22 C and at 800 C, illustrating this effect. Since the effect of heating proved irreversible, all specimens employed in subsequent tests were conditioned by heating for one hour at 850 C prior to transmissivity measurements. The changes observed with the heat treatment may be due to the relieving of strains induced by the polishing procedure.

A decrease in specimen transmissivity in the ultraviolet portion of the spectrum at all specimen temperatures was found in conjunction with tests in which the specimen was held at 1075 C for a period of approximately 10 min. Figure 9 summarizes the measurements of transmittance taken at 22 C, 800 C, and 1075 C before and after the 10-min exposure to 1075 C for the pre-heated specimen SC 2-10. The data taken after the heat treatment at 1075 C (solid lines) indicates lower transmittance than the data taken prior to the heat treatment (dashed lines). However,

data taken after subsequent exposure to 1000 C for units of time totaling 30 min indicated no further change in transmittance due to heating the specimen. This same effect--a decrease in transmittance after exposure to 1075 C--for preheated specimens occurred for Corning 2-mm specimens SC 2-11 and SC 1-1, as shown in Fig. 10. The test results shown in Fig. 10 were obtained before the irradiation studies of these specimens.

In one early test it was found that a film was present on the faces of the specimen. An X-ray diffraction investigation identified this film as α -quartz, showing that the surface of this specimen had devitrified after only a few minutes at temperatures of 950 C or less. A series of tests indicated that the observed film was the result of surface impurity catalyzation of the phase transformation: glassy phase fused silica → crystalline quartz. Precautions were taken in all following tests to avoid any surface contamination of the specimens which would result in such films.

The surface-impurity-catalyzed devitrification prompted an investigation into the specimen cleaning procedures used. A comparison was made of the transmittance of Corning 2-mm specimen SC 2-10 (which had been chemically cleaned with hot chromic acid) with that of Corning 2-mm specimen SC 2-11 (cleaned with solvents and detergents). Although the data, given in Fig. 11, shows that the chemically cleaned specimen has consistently higher transmittance at 22 C in the ultraviolet than the specimen not chemically cleaned, the difference in transmittance is of the same order of magnitude as that which has been observed between other specimens from the same manufacturer which had not been chemically cleaned. Therefore, it cannot be concluded definitely that the improvement in the 22 C transmittance is due to chemical cleaning. It is to be noted, however, that the transmittance of the chemically cleaned specimen always decreased with increasing specimen temperature. This was not always the case with specimens not chemically cleaned, both thick and thin. Such results are illustrated in Figs. 12 and 13. For Thermal American 30-mm specimen ST 30-1 in Fig. 13, the indicated transmissivity at wavelengths between approximately 0.190 and 0.300 microns is greater than 100 percent at a temperature of 800 C, although it is approximately equal to 100 percent for wavelengths greater than 0.300 microns. Data obtained at room temperature subsequent to heating to 800 C was in agreement with that obtained prior to heating to 800 C. Transmissivities greater than unity can be explained only by the assumption of high spectral absorption or scattering of light by the 1-mm specimen in the reference beam of the spectrophotometer. The cause of such a characteristic in the 1-mm specimen is not known.

The effects discussed in preceding paragraphs were encountered primarily in the ultraviolet portions of the spectrum, and little or no effect was noted in the visible and infrared regions. It is obvious that many more tests are required to investigate all of the factors which affect the ultraviolet transmission of fused silica.

PRE-NUCLEAR-REACTOR-IRRADIATION STUDIES OF OPTICAL TRANSMISSION

The purposes of the pre-irradiation studies were two-fold: to study the reversible effects of temperature on the transmission properties of fused silica, and to establish a basis for comparison of transmission properties to be measured after the anneal of radiation-induced color. As discussed in preceding sections, several effects were noted in conjunction with the transmission properties of the specimens at temperatures between 22 and 1000 C which limit the accuracy of the absorption coefficient data. Representative data showing the effects of temperature on the transmission properties for 30-mm specimens of each brand are presented in Figs. 14 through 22. Measurement conditions concerning wavelength and temperature for all specimens are summarized in Table VIII. The Thermal American Spectrosil specimens have the deepest and broadest infrared absorption bands, with the Corning 7940 nearly the same. The Amersil Infrasil, as the name implies is an infrared transmitting type of fused silica, and shows only a weak water band at 2.8 microns, its magnitude being only 0.6 cm^{-1}, as compared to complete absorption from 2.68 to 2.82 microns for the Corning 7940 and Thermal American Spectrosil. Figure 23 is a summary of the infrared transmissivity spectra at 22 C for these three brands. The following figure, (Fig. 24), shows that raising the temperature of the specimens to 800 C depresses the transmissivity of the Corning and Thermal American 30-mm specimens from 66 to 19 percent at 3.35 microns, a wavelength between the water band and the long wavelength cut-off. This is apparently due to a broadening of the water band and to the long wavelength cut-off shift to shorter wavelengths. The effect at the same wavelength on the Amersil 30-mm specimen is from 67 to 30 percent.

The transmission properties in the ultraviolet region may be correlated to the amount of water in the specimens, the Thermal American having the lowest ultraviolet cut-off wavelength and the most water (compare Fig. 23 and 25). Since the actual cut-off wavelength is difficult to measure exactly using 30-mm specimens, the wavelengths at which the specimens have 1 cm^{-1} of absorption are compared. These wavelengths are approximately 0.154 microns for Thermal American Spectrosil (ST 30-4), 0.159 microns for Corning 7940 (SC 30-8), and 0.162 microns for Amersil Infrasil (SA 30-5), as shown in Fig. 25. Heating the specimens to 800 C shifts this point to longer wavelengths, as shown in Fig. 26. In general, the shift is some 0.015 microns.

A comparison of transmissivity data for 1-mm samples of each of the three types of fused silica (SC 1-3, SA 1-5, and ST 1-6) is given in Figs. 27 through 29. Because both the specimen in the sample beam and the specimen in the reference beam have thicknesses of 1 mm, departures from 100-percent transmissivity are an indication of differences in either internal absorption coefficient or surface conditions for the two samples employed during the tests.

Absorption coefficient data obtained on all specimens at 22 and at 800 C is summarized in Figs. 30 through 33. The first two figures compare the absorption coefficient in the ultraviolet region for the three brands tested, while the second pair of figures compare the absorption in the infrared region.

Transmittance or transmissivity data were obtained at specific wavelengths as a function of temperature for several specimens. These data are presented in Figs. 34 through 39. The transparency of the specimens drops most rapidly for the shorter wavelengths in the ultraviolet. In the infrared region, the transparency of the specimen at a particular wavelength and temperature depends on the location of that wavelength with respect to the long wavelength cut-off or the 2.80 micron water band.

POST-NUCLEAR-REACTOR-IRRADIATION STUDIES OF OPTICAL TRANSMISSION

A comparison of absorption coefficients determined for specimens following nuclear-reactor irradiation but before annealing for wavelengths between 0.15 and 1.3 microns is given in Fig. 40 along with similar data obtained before irradiation. It can be seen that the coloration of all specimens tested is greatest at wavelengths below 0.3 microns. It can also be seen from Fig. 40 that a major portion of the absorption in the ultraviolet portion of the spectrum appears to be due to a band which is centered at a wavelength between 0.20 and 0.23 microns. The coloration induced in the Corning 7940 and Thermal American Spectrosil specimens is small at wavelengths above 0.3 microns, but is substantial for the Amersil Infrasil specimen for wavelengths up to approximately 1.2 microns.

A comparison of infrared transmittance at wavelengths between 2.4 and 4.0 microns of Thermal American specimen ST 1-6 obtained after irradiation but before annealing with similar data obtained from Thermal American specimen ST 1-4 before irradiation is given in Fig. 41. It can be seen from this figure that any effect of nuclear-reactor irradiation in the infrared portion of the spectrum is small, particularly relative to the coloration caused by nuclear-reactor irradiation in the ultraviolet portion of the spectrum.

After exposure to the nuclear-reactor irradiation, the Corning and Thermal American specimens were transparent and slightly blue, indicating some absorption of visible wavelengths in the yellow region around 0.62 microns. The Amersil specimens were quite opaque, appearing purple to black. This difference in absorption in the visible region correlates to the relatively large amount of aluminum impurity in the Amersil and to the small amount of aluminum impurity in the Corning and Thermal American fused silicas.

OPTICAL TRANSMISSION PROPERTIES DURING ANNEALING PROCESS

The purpose of studying the removal of reactor-induced color while a specimen is being heated is to evaluate the rate of decrease of the optical absorption of the specimen during the annealing process. As summarized in Tables IX and X, the annealing studies were conducted using 15 different specimens and several types of heating schedules. The character of the annealing data is discussed in this section, and the rate information is discussed in the following section.

For the annealing studies, the high-temperature spectrophotometer was operated in the one-specimen mode, yielding the transmittance of the specimen being annealed as a function of time or wavelength, for a known heating schedule. Figures 42 through 50 present the transmittance-versus-time data during the specimen anneals. Figures 51, 52, and 53 present transmittance data obtained at 22 C after the specimen being studied had been annealed by exposure to various high temperatures, as obtained using the Cary 14R spectrophotometer. The details of the variations in the transmittance-versus-time curves depend on the heating schedule used, although in all cases the transmittance increased with time during the anneal. It is to be noted in particular that the coloration at wavelengths greater than 0.30 microns is rapidly removed at moderate temperatures (Fig. 53). Further, the data in Figs. 41 and 54 indicate there is little induced color in the infrared region, and that it, too, vanishes rapidly at moderate temperatures.

The absorption coefficient due to reactor-induced coloration at a given wavelength has been determined from data on transmittance during and after anneal at the same temperature. This calculation has been made using the following two equations:

$$\tau_n = \frac{(I_s/I_o) \text{ during anneal}}{(I_s/I_o) \text{ after anneal}} = \frac{1}{e^{\alpha_n X_s}} , \qquad (6)$$

which yields

$$\alpha_n = - \frac{1}{X_s} \ln (\tau_n). \qquad (7)$$

The variation of reactor-induced absorption coefficient with time during anneal is given for 11 specimens in Figs. 55 through 65. The α_n values were obtained from the transmittance data using Eq. 7. Figures 66 and 67 show the decrease of the reactor-induced absorption in the ultraviolet region at successively higher specimen annealing temperatures for Corning 1-mm specimen SC 1-3 and for Amersil 1-mm specimen SA 1-2. Figures 68 and 69 are comparison plots of the absorption of these two specimens after anneals to temperatures of approximately 400 and 600 C. Figure 70 shows that the coloration at 0.210 microns, which is approximately the center of an absorption band, is removed from Corning, Amersil, and Thermal American specimens by a linear temperature-versus-time heating schedule in the order (1) Thermal American, (2) Corning, and (3) Amersil. It is to be noted that the depth of the infrared absorption bands for the specimens may be correlated with the temperature required for anneal of coloration at 0.21 microns. It appears that the material with the deepest infrared absorption bands, and containing the most water, has the greatest resistance to radiation damage, and that the coloration which occurs anneals out at the lowest temperature. Figure 71 shows the same annealing behavior as indicated in Fig. 70 for 30-mm Corning and Thermal American specimens using two different linear temperature-versus-time heating schedules, viz., the reactor-induced color is removed from the Thermal American specimen first.

Examination of the curves of α_n versus time for the 1-mm specimens shows that the absorption coefficient characterizing the induced coloration at 0.21 microns is of order 50 cm^{-1} prior to the anneal. Thus, the anneal of coloration observed using the 30-mm specimens is characteristic only of the tail of the full α_n versus time annealing curve and is representative of the highest activation energy present. This will be discussed in the following section. Two such tails are compared in Fig. 72. In this case, each specimen was subjected to an isochronal anneal of 10 min. at constant temperature, the temperature steps increasing incrementally by 50 C. Again, the color in the Thermal American fused silica is removed more readily than from the Corning 7940. For both Corning and Thermal American brands, Fig. 72 shows that the induced absorption coefficient is reduced to zero by the 10-min. anneal at 750 C. This is to be compared to the required temperature of 800 C when a linear temperature-versus-time

heating schedule is used (see curves, Fig. 71). Similarly, the Amersil Infrasil fused silica requires a temperature of 850 C to remove the color at 0.210 microns under an isochronal anneal, and 900 C when a linear heating schedule is used (Figs. 61 and 67).

DETERMINATION OF ACTIVATION ENERGIES FROM ANNEALING DATA

An analysis of the annealing data, α_n versus time, has been made assuming that the removal of coloration at a given wavelength is described by a first-order kinetics equation of the form

$$\frac{d\alpha_n}{dt} = -\nu\alpha_n \exp(-\epsilon_a/kT) \text{ cm}^{-1} \text{ sec}^{-1} \qquad (8)$$

This equation states that the rate of decrease of induced absorption at any time is proportional to the remaining value of the induced absorption at that time and also proportional to a Boltzmann probability factor which contains the ratio of an activation energy ϵ_a to the thermal energy of the specimen, kT. k is the Boltzmann constant, T is the absolute temperature of the specimen, and kT has units of energy. The frequency factor, ν, is the proportionality constant, with units of inverse time, and is interpreted as a frequency characteristic of the type of color center being annealed.

Two theoretical curves are shown in Figs. 73 and 74 which are provided as an aid in the interpretation of the annealing data which has been shown in preceding figures. It is seen from Fig. 73 that the variation of induced absorption coefficient with time during a constant-temperature step is linear on a semi-log plot if a single activation energy is associated with the coloration during that period of anneal. However, it is seen from Fig. 74 that the presence of two different activation energies in the same specimen will cause the variation of induced absorption coefficient with time on a semi-log plot to be non-linear in nature. The experimental data on Fig. 75 and some of the experimental data on Fig. 76 are curved in a manner similar to the theoretical data in Fig. 74, thereby indicating that the annealing process is sometimes characterized by more than one activation energy. However, some of the data in Fig. 76 is relatively linear, indicating that at least some of the annealing process is characterized by a single activation energy.

Values of the frequency factor ν have been obtained in some tests reported in the literature from measurements of the change in slope on a semi-logarithmic plot of some measure of radiation damage due to a sudden change in specimen temperature (see data for annealing of copper in Ref. 3). Determination of the frequency factor in this manner requires that the annealing of damage during the adjacent annealing steps be

characterized by a single activation energy for both steps. Determination of frequency factors by this technique from data in the present report obtained during tests with step-wise increases in temperature yielded inconsistent results. This inconsistency may be due to the simultaneous anneal of several color centers (characterized by different activation energies) according to the temperature programs used or to the time lag present in changing the temperature of the sample in successive steps (Figs. 6 and 7).

It has been estimated by Dr. W. Dale Compton, a consultant to the Research Laboratories, that the frequency factor ν should be between 10^{10} and 10^{14} sec^{-1}. This estimate is based on experience with determination of activation energies for anneal of radiation-induced coloration in a number of materials. Therefore, all of the data discussed in following paragraphs has been reduced on the basis of activation energies both of 10^{10} and 10^{14} sec^{-1}.

Attempts have been made using several different techniques to derive activation energies from the induced absorption coefficient curves shown in Figs. 55 through 65. The technique which has been selected for use in the present report is the simplest of these and involves calculation of an activation energy from Eq. (8) using values of α_n and $d\alpha_n/dt$ determined at a series of different times during the annealing process. This data reduction procedure yields exact values of activation energy only when a single activation energy characterizes all of the change of absorption coefficient with time for a given specimen. If two activation energies influence the rate of change of absorption coefficient with time, the calculation procedure employed yields a value of activation energy somewhere between the two true activation energies. Therefore, activation energies determined in this manner are denoted apparent activation energy, ϵ_a.

Apparent activation energies determined in the manner described in the preceding paragraph from the data shown in Figs. 55 through 65 are presented in Figs. 77 through 87 for frequency factors of 10^{10} and 10^{14} sec^{-1} as a function of the ratio α_n/α_{no}. It can be seen that the activation energies calculated for a frequency factor of 10^{14} sec^{-1} are approximately 0.8 eV higher than those calculated for an activation energy of 10^{10} sec^{-1}.

A summary of values of apparent activation energy for the 11 samples for which data are presented in Figs. 77 through 87 is shown in Fig. 88 as a function of the absolute value of α_n existing at the time for which the apparent activation energy was determined. Approximate faired lines have been drawn through the data for each brand of fused silica. The differences between the apparent activation energies for each of the types of fused silica correspond to the different temperatures at which annealing takes place for the different brands of fused silica as indicated on Figs. 70 through 72. It can be seen that the apparent activation energies for Corning

7940 and Thermal American Spectrosil fall between 2.2 and 2.6 eV, whi
activation energies for Amersil Infrasil fall between 2.2 and 2.8 eV
$\nu = 10^{10}$ sec^{-1}.

COMPARISON OF OPTICAL CHARACTERISTICS MEASURED BEFORE IRRADIATION AND AFTER ANNEALING

After the annealing tests described in the preceding section wer
portion of the transmissivity-versus-wavelength spectrum was obtained
comparison with similar data obtained at 22 C prior to the nuclear-re
process. The purpose of this comparison was to find any effects on t
properties of the specimens which could be attributed to non-removabl
damage. The comparison plots for these specimens are presented in Fi
98. Two specimens, SA 30-1 and SA 1-1, have no comparison data, sinc
irradiation studies were conducted at wavelengths between 1.2 and 4.0
while the anneal and post-anneal studies were conducted at 0.210 micr
of some of this data for each of the three types of fused silica are
Figs. 99 through 101. The figures show that in some cases the post-a
missivities are higher than the pre-irradiation transmissivities, and
the reverse is true. The conclusion is that the scatter in the data,
to the variations in handling procedure required as the experimental
is greater than any observable effect which could be correlated with
radiation damage. These results, which were obtained following expos
of 6×10^{17} nvt fast neutrons per cm^2, do not permit conclusions to b
the effect of higher dosage.

REFERENCES

1. Levy, P. W.: Annealing of Radiation Induced Defects in Fused Silica. BNL 6053, Presented at the Second International Conference on "Radiation Effects in Glass and Related Materials," Rochester, New York, April 12-13, 1962.

2. Burkig, V. C.: A Progress Report on Radiation Damage Studies for the Glow Plug Reactor. Douglas Report SM-44885, November 15, 1963.

3. Overhauser, A. W.: Isothermal Annealing Effects in Irradiated Copper. Physical Review, 90, 393-400 (May 1953).

LIST OF SYMBOLS

$e^{(\ )}$	Exponential function
I_o	Incident intensity of optical radiation
I_r	Intensity transmitted through reference specimen
I_s	Intensity transmitted through sample specimen
I_s / I_o	Transmittance
k	Boltzmann constant, 8.612×10^{-5} eV/deg K
$\bar{R}$	Average reading
t	Time, min or sec
T	Temperature, deg C or deg K
X_r	Reference specimen thickness, cm or mm
X_s	Sample specimen thickness, cm or mm
α	Absorption coefficient, cm^{-1}
α_n	Nuclear-reactor-irradiation-induced absorption coefficient, cm^{-1}
α_{no}	First measurable value of α_n during anneal process, cm^{-1}
$\alpha_{\lambda,T}$	Absorption coefficient, cm^{-1}, function of λ and T
ϵ_a	Apparent activation energy, for anneal of reactor-induced coloration, eV
λ	Wavelength, microns
ν	Frequency factor, sec^{-1}
$\rho_{\lambda,T}$	Surface reflectivity, function of λ and T
σ	Standard deviation
τ	Transmissivity
τ_n	$e^{(\alpha_n X_s)}$

Subscripts

$( )_{theor.}$	Calculation from first-order kinetics
$( )'$	Denotes value at specific time during anneal
$( )^*$	Denotes value at beginning of constant temperature during anneal

APPENDIX I

The method used to obtain the values of activation energy, ϵ_a eV, from the experimental annealing data is to associate one value of ϵ_a with each value of α_n observed during the annealing process. The experimental data required are α_n and temperature as function of time. The first-order kinetics equation used gives the relation

$$(d\alpha_n/dt) = -\alpha_n \nu \exp(-\epsilon_a/kT) \tag{9}$$

To evaluate ϵ_a, eV, at a time, t', the slope from the α_n versus time curve at $t = t'$ is needed as well as the temperature from the T-versus-time curve. These values are denoted $(d\alpha_n/dt)_{t'}$ and T'.

Thus
$$\left(\frac{-1}{\nu \alpha_n}\right)\left(\frac{d\alpha_n}{dt}\right)_{t'} = \exp(-\epsilon_a'/kT) \tag{10}$$

and
$$\epsilon' = kT' \ln\left[\left(\frac{-1}{\nu \alpha_n'}\right)\left(\frac{d\alpha_n'}{dt}\right)_{t'}\right] \tag{11}$$

With reference to Fig. 61, take $t' = 40$ min; $T' = 879$ K; $\alpha' = 8.78$ cm^{-1}; $(d\alpha_n/dt)_{t'} = -0.016$ cm^{-1}sec^{-1}. Assuming $\nu = (10)^{10}$ sec^{-1}, then $\epsilon_a' = 2.2$ eV.

TABLE I

UAC. HIGH-TEMPERATURE SPECTROPHOTOMETER COMPONENTS

Spectral Range	Source	Grating	Detector
0.15 to 0.4 microns	Hanovia 906 A-32 Hydrogen Discharge	Bausch & Lomb 33-53-06-05	Ascop #543-1014 Photomultiplier
0.35 to 0.65 microns	GE 9 AT-8¼ Tungsten Ribbon Filament	Bausch & Lomb 33-53-06-34	Ascop #543-1014
0.6 to 1.5 microns	GE 9 AT-8¼	Bausch & Lomb 33-43-06-76	Infrared Industries SA-11 Lead Sulfide Cell
1.3 to 4.5 microns	Perkin Elmer 013-0059 Nernst Glower	Bausch & Lomb 33-53-06-76	Reeder RP-5W Thermocouple

TABLE II

COMPARISON OF HIGH-TEMPERATURE SPECTROPHOTOMETER DATA UNDER VARIOUS PHASING CONDITIONS TO CARY MODEL 14R TRANSMITTANCE DATA OBTAINED USING NEUTRAL DENSITY SCREENS

See Text for Definition of Phasing

Neutral Density Screen No.	Cary % Transmittance	H.T.S. $\%I_s/I_o$ 1% Phasing	Difference 1% Phasing	H.T.S. $\%I_s/I_o$ 3% Phasing	Difference 3% Phasing	H.T.S. $\%I_s/I_o$ 5% Phasing	Difference 5% Phasing
IX	97.70	97.80	0.10	97.80	0.10	97.60	0.10
VIII	92.40	92.70	0.30	92.80	0.40	92.50	0.10
0.1	78.40	77.10	1.30	77.50	0.90	77.70	0.70
0.2	62.0	62.40	0.40	63.00	1.00	63.20	1.20
0.3	47.85	47.90	0.15	48.50	0.65	48.90	1.05
0.4	37.35	37.10	0.25	37.90	0.45	38.30	0.95
0.6	24.30	23.90	0.40	24.65	0.35	24.80	0.50
0.7	18.10	18.15	0.05	18.72	0.62	18.90	0.70
0.8	12.95	12.90	0.05	13.50	0.55	13.65	0.70
0.9	12.25	12.20	0.05	12.62	0.37	12.90	0.65
	average difference		0.31		0.54		0.77

TABLE III

ESTIMATED INSTRUMENT ACCURACY OF ABSORPTION COEFFICIENT MEASUREMENTS USING U.A.C. HIGH-TEMPERATURE SPECTROPHOTOMETER

Transmissivity		Absorption Coefficient			
		30-mm Specimen		1-mm Specimen	
τ, %	Uncertainty, %	α, cm^{-1}	Uncertainty, cm^{-1}	α, cm^{-1}	Uncertainty, cm^{-1}
95	$\pm$0.3	0.0172	$\pm$0.0012	0.5164	$\pm$0.033
50	$\pm$0.3	0.2310	$\pm$0.0021	6.931	$\pm$0.060
5	$\pm$0.3	0.9985	$\pm$0.0216	29.95	$\pm$0.590

TABLE IV

SPECTROCHEMICAL ANALYSIS OF TYPICAL AMERSIL INFRASIL, CORNING 7940 AND THERMAL AMERICAN SPECTROSIL FUSED SILICA SPECIMENS

Impurity	Amersil Infrasil	Corning 7940	Thermal American Spectrosil
Aluminum	40	2	1
Beryllium	0.4	0.1	< 0.5
Boron	< 0.5	< 0.5	2
Iron	3	2	3
Magnesium	1	1	13
Manganese	1	0.5	1
Titanium	2	0.2	0.5
Calcium	3	1	1.5
Sodium	< 5	< 5	20

Concentration in parts per million (ppm)
All other elements undetectable
< = less than

NOTE: These materials differed in water content, which does not show up under spectrochemical analysis--such differences do appear in infrared absorption spectra. For a comparison of the amount of water contained in the structure of these specimens, compare the absorption bands at 1.4 and 2.8 microns (Fig. 23)

TABLE V

SUMMARY OF SPECIMEN HANDLING HISTORY

Brand	Type	Specimen	Pre-Heat to 850 C		Nuclear Reactor Irradiated**	Cleaning History*
			Prior to Irrad Studies	Prior to Reactor Irradiation		
Corning	7940	SC 1-1	yes	yes	yes	A, D^1
		SC 1-2	yes	yes	no	A
		SC 1-3	yes	yes	yes	A, C^1
		SC 2-10	yes	yes	no	B^2
		SC 2-11	yes	yes	yes	A, D^1
		SC 30-4	yes	yes	yes	A, D^1
		SC 30-8	yes	yes	yes	A, C^1
Amersil	Infrasil	SA 1-1	yes	yes	yes	A
		SA 1-2	yes	yes	yes	A
		SA 1-5	yes	yes	yes	A, C^1
		SA 1-6	yes	yes	no	A
		SA 2-3	yes	yes	no	B^2
		SA 8-2	yes	yes	no	B^2
		SA 30-1	no	yes	yes	A
		SA 30-2	no	yes	yes	A
		SA 30-5	yes	yes	yes	A, C^1
Thermal American	Spectrosil	ST 1-3	yes	yes	no	A
		ST 1-6	yes	yes	yes	A, C^1
		ST 30-1	yes	yes	yes	A, C^1
		ST 30-4	yes	yes	yes	A, C^1
		ST 30-5	no	yes	yes	A, D^1

*A - Not Chemically Cleaned for Pre-Irradiation Studies
B - Chemically Cleaned for Pre-Irradiation Studies
C - Chemically Cleaned Prior to Anneal Only
D - Chemically Cleaned Prior to Irradiation and Prior to Anneal
Superscripts: 1 - Sodium Dichromate used in Chromic Acid; 2 - Potassium Dichromate used in Chromic Acid
**See Table VI

TABLE VI

SUMMARY OF NUCLEAR-REACTOR-IRRADIATION DOSES FOR SPECIMENS TESTED

Group	Brand	Type	Specimen	Integrated Fast Flux Neutrons/cm^2	Fast* Neutron Flux Neutrons/cm^2-sec	Thermal** Neutron Flux Neutrons/cm^2-sec
1	Amersil	Infrasil	SA 1-1	$6.36(10)^{17}$	$4.11(10)^{12}$	Not monitored
			SA 1-2	$6.36(10)^{17}$	$4.11(10)^{12}$	-
			SA 30-1	$6.36(10)^{17}$	$4.11(10)^{12}$	-
			SA 30-2	$6.36(10)^{17}$	$4.11(10)^{12}$	-
2	Amersil	Infrasil	SA 1-5	$7.38(10)^{17}$	$5.0(10)^{12}$	$1.4(10)^{13}$
			SA 30-5	$7.38(10)^{17}$	$5.0(10)^{12}$	$1.4(10)^{13}$
	Corning	7940	SC 1-3	$7.38(10)^{17}$	$5.0(10)^{12}$	$1.4(10)^{13}$
			SC 30-8	$7.38(10)^{17}$	$5.0(10)^{12}$	$1.4(10)^{13}$
	Thermal American	Spectrosil	ST 1-6	$7.38(10)^{17}$	$5.0(10)^{12}$	$1.4(10)^{13}$
			ST 30-1	$7.38(10)^{17}$	$5.0(10)^{12}$	$1.4(10)^{13}$
			ST 30-4	$7.38(10)^{17}$	$5.0(10)^{12}$	$1.4(10)^{13}$
3	Corning	7940	SC 1-1	$8.3(10)^{17}$	$5.5(10)^{12}$	$1.9(10)^{13}$
			SC 2-11	$8.3(10)^{17}$	$5.5(10)^{12}$	$1.9(10)^{13}$
			SC 30-4	$8.3(10)^{17}$	$5.5(10)^{12}$	$1.9(10)^{13}$
	Thermal American	Spectrosil	ST 30-5	$8.3(10)^{17}$	$5.5(10)^{12}$	$1.9(10)^{13}$

*Fast neutron (energy >0.4 mev) flux monitor - nickel wire

**Thermal neutron flux monitor - gold wire and gold wire with cadmium shield

See Table VII for comparison of fast neutron flux over length of sample container during nuclear reactor irradiation

TABLE VII

VARIATION OF FAST NEUTRON FLUX WITH POSITION
OF SPECIMEN IN NUCLEAR REACTOR

Group	Position	Fast Neutron Flux* Neutrons/cm^2-sec
2	Top	$4.3\ (10)^{12}$
	Center	$4.2\ (10)^{12}$
	Bottom	$4.8\ (10)^{12}$
3	Top	$5.5\ (10)^{12}$
	Center	$5.6\ (10)^{12}$
	Bottom	$5.5\ (10)^{12}$

*UACRL nickel wire monitor; specimen holder length: 8-12 inches

TABLE VIII

SUMMARY OF PRE-IRRADIATION MEASUREMENT CONDITIONS

All Measurements Made on UAC Dual-Beam High-Temperature Spectrophotometer

Manufacturer	Type	Sample Beam		Reference Beam		Temperature deg C	Wavelength Range Microns
		Specimen	Thickness mm	Specimen	Thickness mm		
Corning	7940	SC 1-1	1	---	-	22,256,524,800,1070	0.15 → 1.5
		SC 1-3	1	SC 1-2	1	22,800	0.15 → 4.0
		SC 2-11	2	---	-	22,256,524,800,1070	0.15 → 1.5
		SC 30-4	30	SC 1-3	1	22,800	0.15 → 0.65, 1.2 → 4.0
		SC 30-8	30	SC 1-2	1	22,800	0.15 → 4.0
Amersil	Infrasil	SA 1-5	1	SA 1-6	1	22,800	0.15 → 4.0
		SA 8-2	8	SA 2-3	2	22,230,420,620,860	0.15 → 4.0
		SA 30-1	30	SA 1-1	1	22,310,568,854	1.2 → 4.0
		SA 30-2	30	SA 1-2	1	22,310,568,854	0.15 → 0.65, 1.2 → 4.0
		SA 30-5	30	SA 1-6	1	22,800	0.15 → 4.0
Thermal American	Spectrosil	ST 1-6	1	ST 1-3	1	22,800	0.15 → 4.0
		ST 30-1	30	ST 1-3	1	22,204,416,628,800	0.15 → 4.0
		ST 30-1	30	ST 1-6	1	22,800	0.15 → 0.65, 1.2 → 4.0
		ST 30-4	30	ST 1-3	1	22,800	0.15 → 4.0
		ST 30-5	30	ST 1-3	1	22,738	0.15 → 0.65, 1.2 → 4.0

TABLE IX

SUMMARY OF ANNEALING MEASUREMENT CONDITIONS

Brand	Type	Specimen	Annealing Temp. History		Wavelength Span of Observation Microns	Single Wavelength of Observation Microns
			Class*	Detail		
Corning	7940	SC 1-1	F	---	---	0.215
		SC 1-3	B	t_B = 10 min	0.15 - 0.25	0.215
		SC 2-11	G	---	---	0.215
		SC 30-4	C	t_C = 44 min	---	0.210
		SC 30-8	C	t_C = 88 min	---	0.210
Amersil	Infrasil	SA 1-1	D	---	0.2 - 2.0	---
		SA 1-2	B	t_B = 10 min	0.15 - 1.4	0.21
		SA 1-5	C	t_C = 88 min	---	0.21
		SA 30-1	E	---	---	0.21
		SA 30-2	E	---	---	0.23
		SA 30-5	B	t_B = 10 min	2.2 - 4.0	3.15
Thermal American	Spectrosil	ST 1-6	C	t_C = 88 min	---	0.164
		ST 30-1	C	t_C = 88 min	---	0.215
		ST 30-4	C	t_C = 44 min	---	0.215
		ST 30-5	A	t_A = 10 min	---	0.215

*See Table X for class code

TABLE X

CLASS CODE FOR TABLE IX

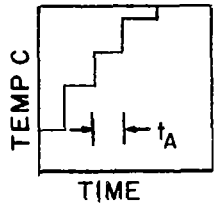

A. 50 C step in 10 min. intervals

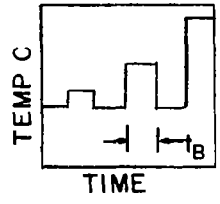

B. 50 C incremental rise after drop to temperature at which data was taken

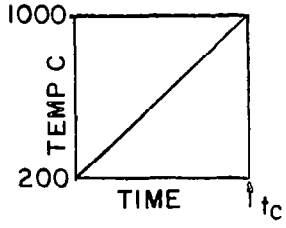

C. Linear

D. Specimen heated in 25 C incremental steps. Held at each temperature until equilibrium coloration attained. Observed on Cary - 14 Spectrophotometer at 22 C.

E. Approximately lin.: 22-1000 C in 90 min.

F. Step: 22 C to 646 C; held until no further change observed, then specimen completely annealed.

G. Step: 22 C to 708 C; held until no further change observed, then specimen completely annealed.

SPECIMEN DATA TO FIGURE NUMBER CROSS-REFERENCE INDEX

Specimen	Pre-Irradiation - 22 C			Pre-Irradiation - 800 C			Post-Irradiation Pre-Anneal		Annealing			Activation Energy	Pre-Irradiation vs Post-Anneal	Comments
	Ultraviolet	Visible	Infrared	Ultraviolet	Visible	Infrared	UV-Vis.	IR	I_t/I_o vs t	α_n vs t	α_n/α_{no} vs t			
SC 1-1	10,34			34			40		42	55		77	89	
SC 1-3	27	27	27	27	27	27			43	56,66,68 69,72	73	78	98	
SC 2-10	9,11			9										
SC 2-11	10,11,12,35	12		12,35	12				44	57		79	90,99	
SC 30-4									45	58,71		80	91,99	
SC 30-8	14,17,25	14	14,20,23	14,17,26	14	14,20,24	40		46	59,70,71		81	92,99	
SA 1-1									51,52,53					
SA 1-2										60,67,68,69	74	82	93	
SA 1-5	28	28	28	28	28	28	40		47	61,70		83	98	
SA 8-2	36		37	36		37								
SA 30-1														Test specimen; film on surfaces - no data
SA 30-2	8			8						62		84	93,100	
SA 30-5	8,15,18,25	15	15,21,23	8,15,18,26	15	15,21,24				54			94	
ST 1-6	29	29	29	29	29	29	40	41					98	Measured for anneal at 0.164 microns; temperature effect overrides anneal.
ST 30-1	13,38	13	39	13,38	13	39	40		48	63,70,71		85	95,101	
ST 30-4	16,19,25	16	16,22,23	16,19,26	16	16,22,24			49	64,71		86	96,101	
ST 30-5									50	65,72		87	97,101	
Summary	30		32	31		33	40					88	99,100,101	

UAC HIGH-TEMPERATURE SPECTROPHOTOMETER

SEE FIG. 2 FOR EXPLANATION OF NUMBER CODE

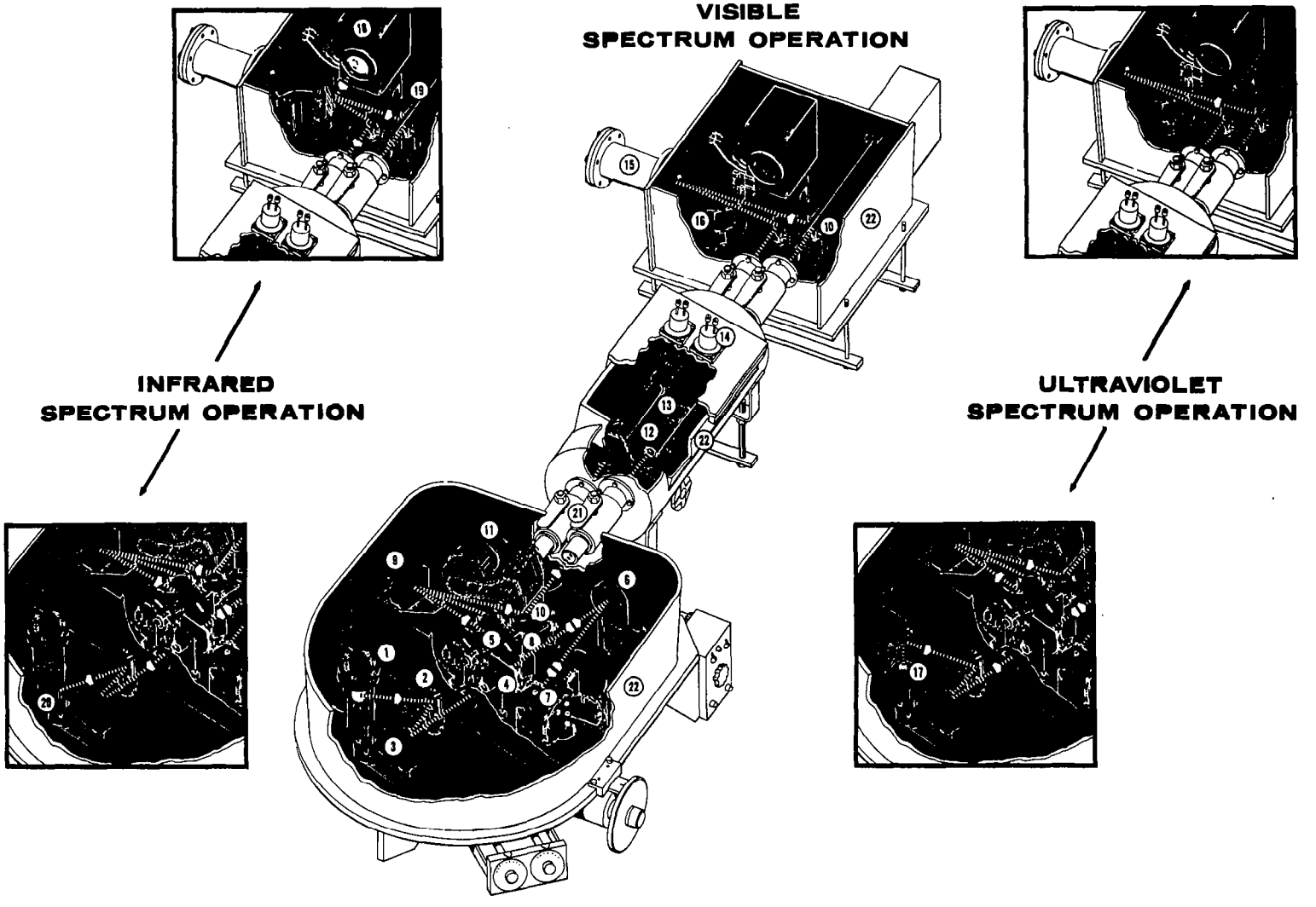

FIG. 1

NUMBER CODE USED IN FIG. 1

1 TUNGSTEN LAMP
2 SOURCE SELECTING MIRROR
3 SPHERICAL MIRROR
4 ENTRANCE SLIT
5 BAND PASS FILTERS
6 PARABOLIC MIRROR
7 DIFFRACTION GRATING
8 EXIT SLIT
9 PARABOLIC MIRROR
10 FOLDING MIRRORS
11 VISIBLE & ULTRAVIOLET CHOPPER
12 FURNACE TUBE
13 SPECIMEN
14 FURNACE ELECTRODES
15 PHOTOMULTIPLIER TUBE
16 LEAD SULFIDE DETECTOR
17 HYDROGEN DISCHARGE LAMP
18 NERST GLOWER ASSEMBLY
19 INFRARED CHOPPER
20 THERMOCOUPLE DETECTOR
21 VACUUM VALVES
22 VACUUM CHAMBERS

FIG. 2

FIG. 3

REPRODUCIBILITY OF UAC HIGH-TEMPERATURE SPECTROPHOTOMETER READINGS AT ROOM TEMPERATURE

NO SAMPLE IN EITHER BEAM
DATA POINTS TAKEN ON CONSECUTIVE DAYS

WAVELENGTH λ - microns	AVERAGE READING, $\bar{R}$	STANDARD DEVIATION σ_R	$\sigma_R / \bar{R}$
0.149	0.666	0.007	0.011
0.235	0.758	0.004	0.005
0.475	0.963	0.005	0.005
2.47	0.799	0.004	0.005

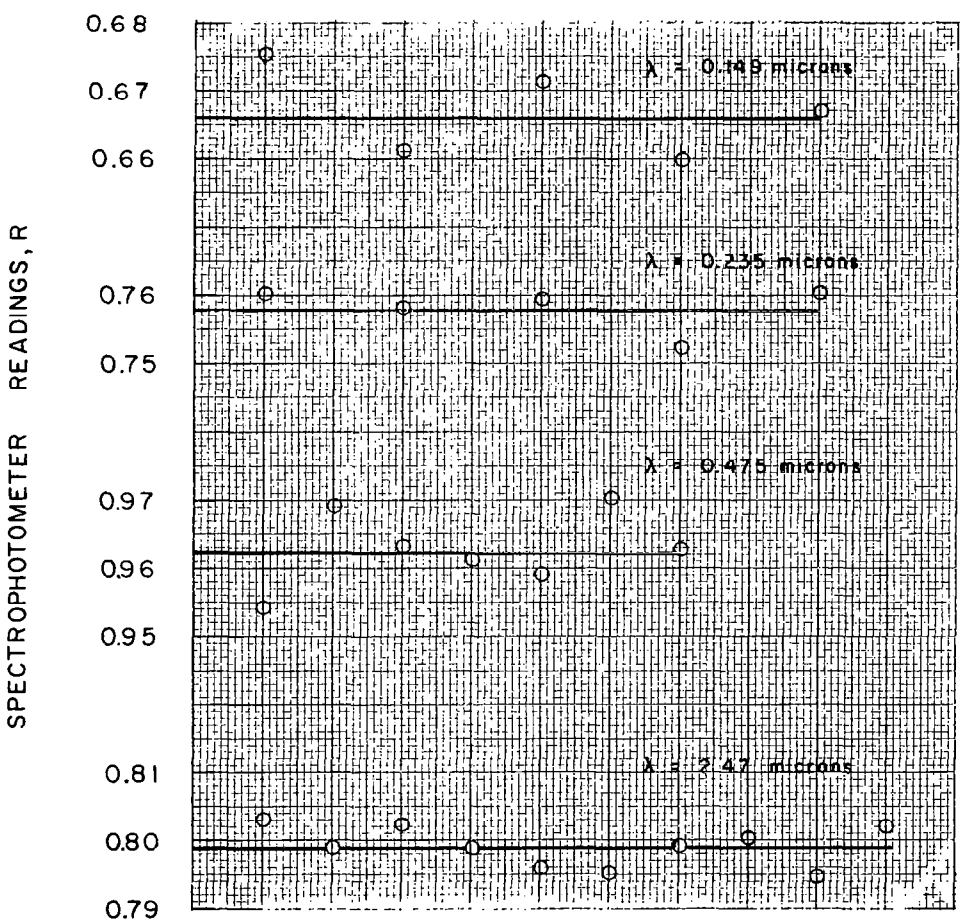

FIG. 4

REPRODUCIBILITY OF UAC HIGH-TEMPERATURE SPECTROPHOTOMETER WAVELENGTH MEASUREMENTS AT ROOM TEMPERATURE USING A 0.3901 micron INTERFERENCE FILTER

.ALL DATA POINTS TAKEN ON SAME DAY
AVERAGE VALUE = 0.39016 microns
STANDARD DEVIATION = ± 0.00007microns

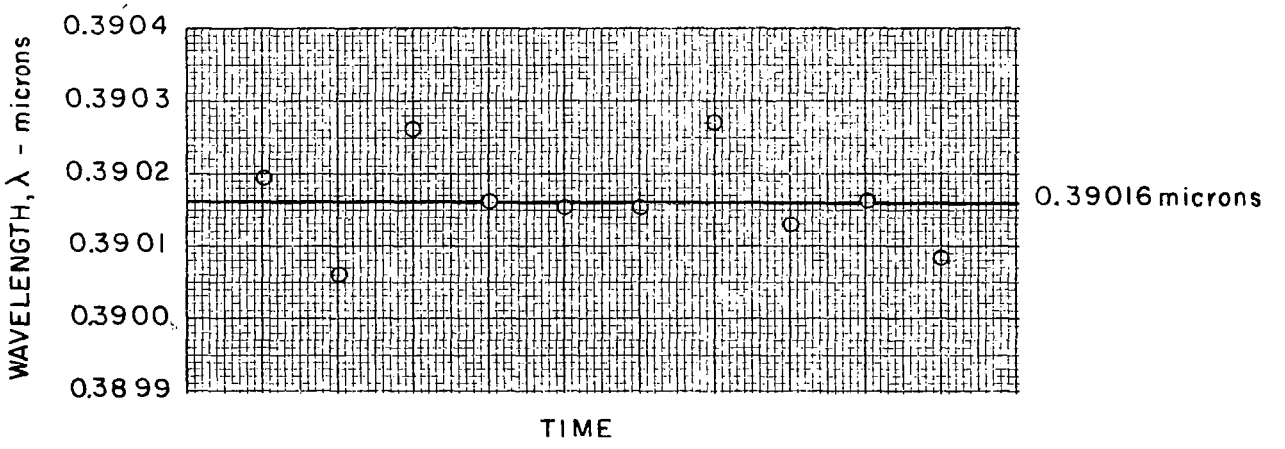

FIG. 5

MODES OF OPERATION OF UAC HIGH-TEMPERATURE SPECTROPHOTOMETER

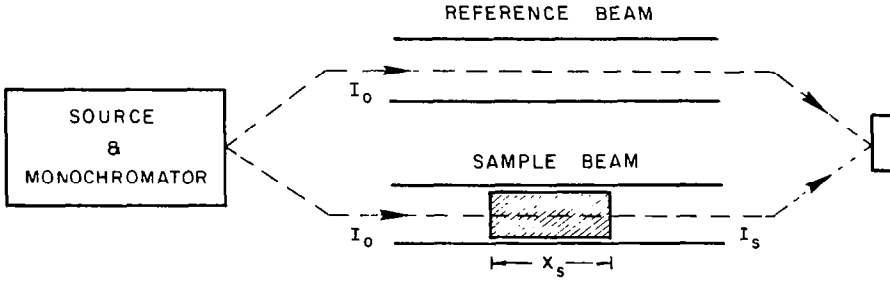

1 - SPECIMEN MODE

$$I_s / I_o = (1 - \rho_{\lambda,T})^2 e^{-\alpha_{\lambda,T} X_s}$$

$\rho_{\lambda,T}$ = SURFACE REFLECTIVITY

$\alpha_{\lambda,T}$ = ABSORPTION COEFFICIENT

X_s = SAMPLE SPECIMEN THICKNESS

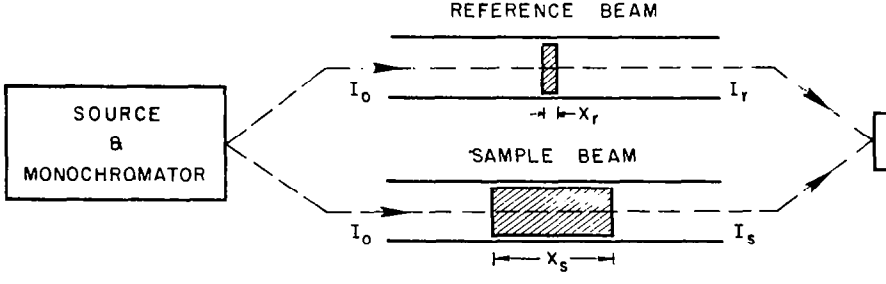

2 - SPECIMEN MODE

$$\tau = \frac{I_s / I_o}{I_r / I_o} = e^{-\alpha_{\lambda,T} (X_s - X_r)}$$

I_s / I_o = TRANSMITTANCE OF SAMPLE SPECIMEN

I_r / I_o = TRANSMITTANCE OF REFERENCE SPECIMEN

FIG. 6

30mm SPECIMEN TEMPERATURE CALIBRATION WITH SLOW TEMPERATURE CHANGE

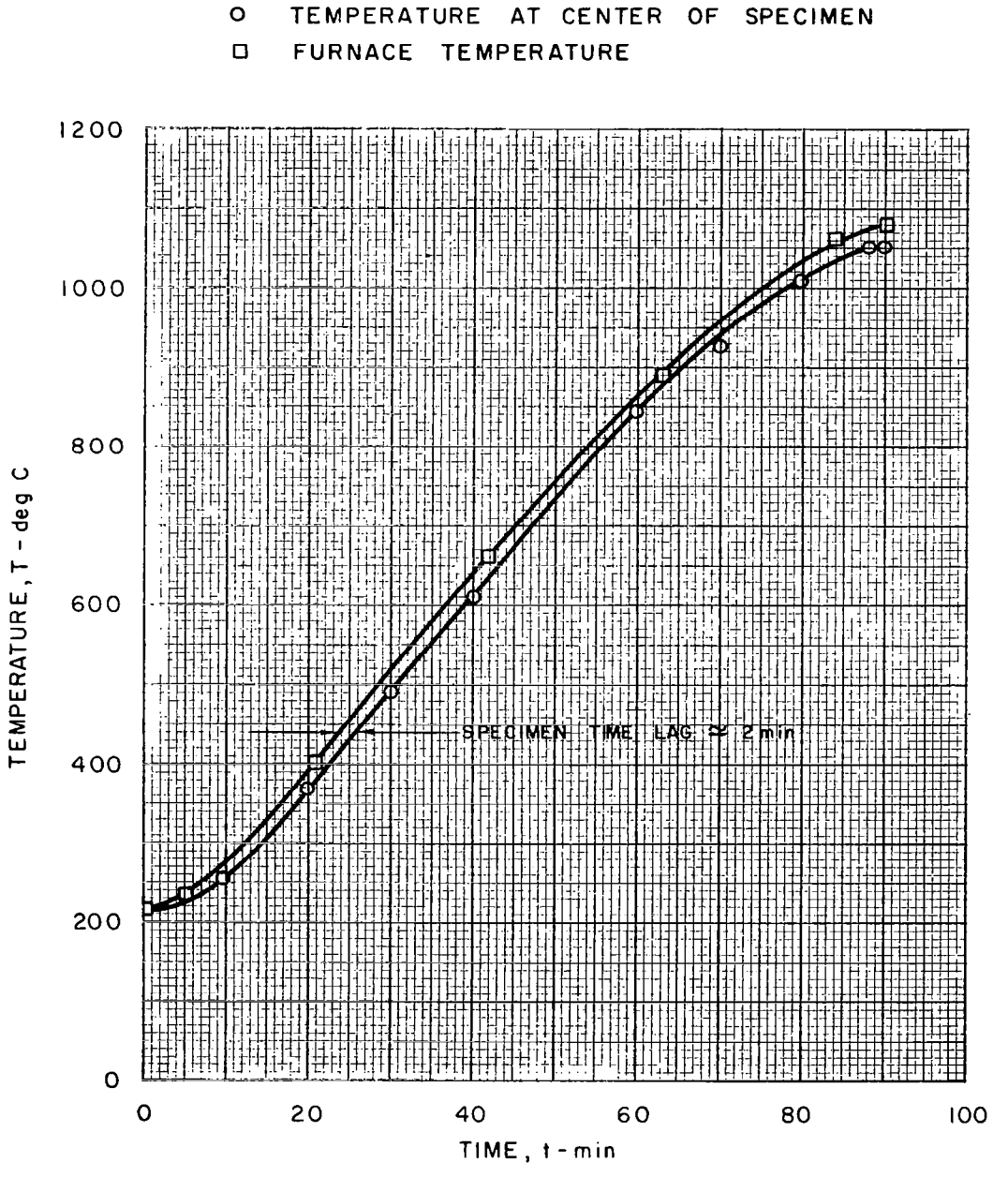

FIG. 7

30mm SPECIMEN TEMPERATURE CALIBRATION WITH FAST TEMPERATURE CHANGE

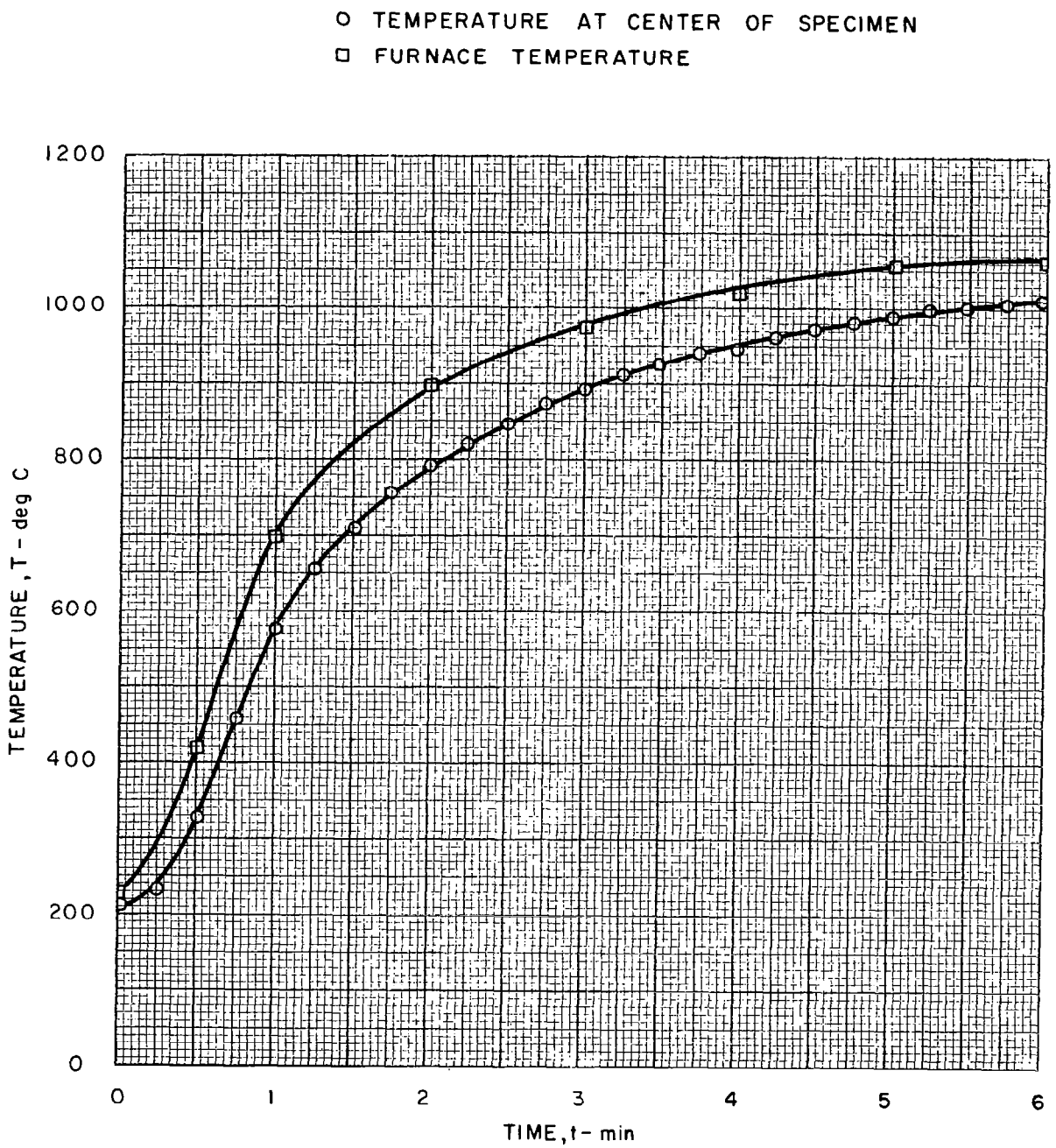

COMPARISON OF THE EFFECT OF TEMPERATURE ON THE TRANSMISSIVITY OF NON-PRE-HEATED AND PRE-HEATED AMERSIL 30 mm SPECIMENS

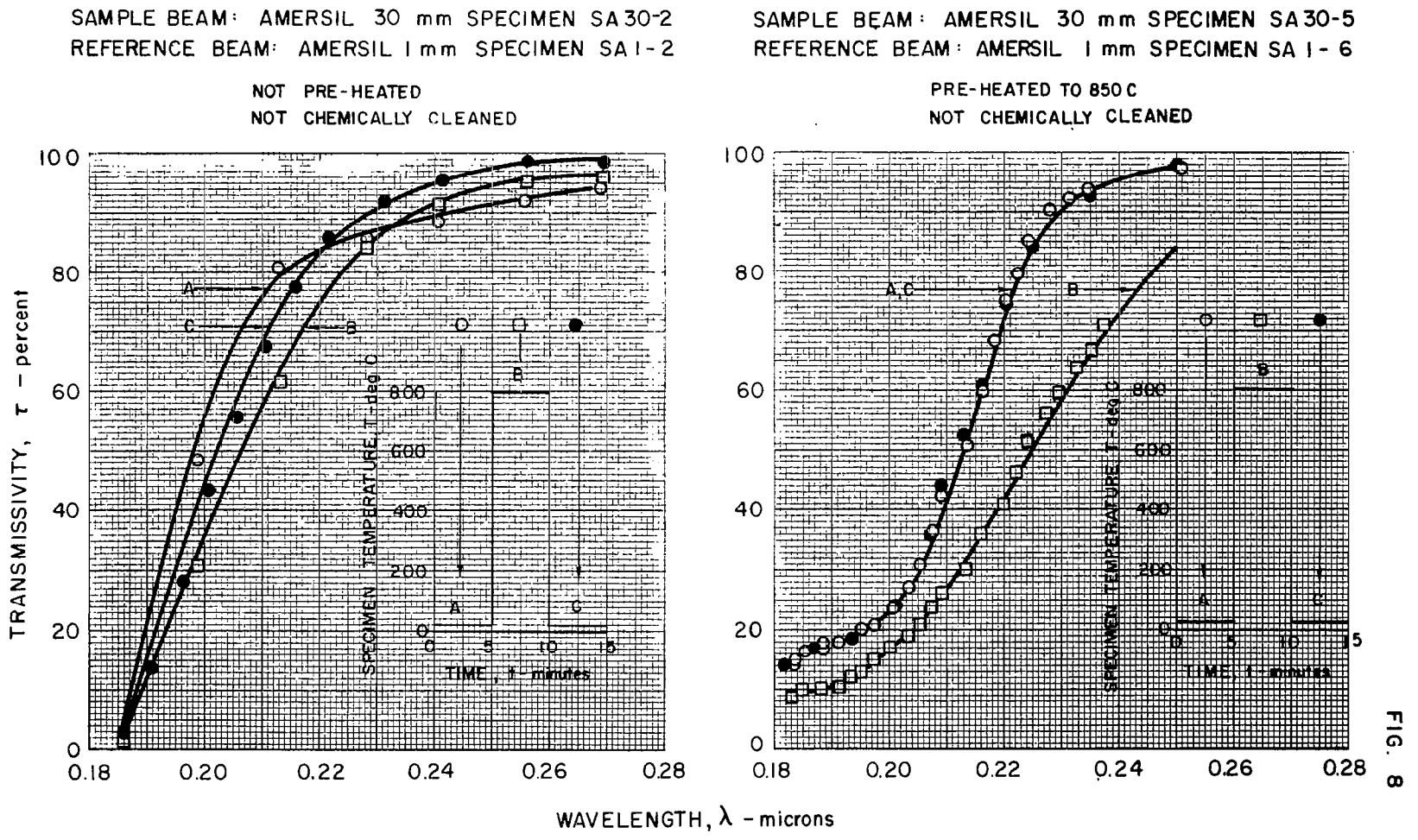

FIG. 8

FIG. 9

EFFECT OF HEATING ON THE TRANSMITTANCE OF THE CHEMICALLY CLEAN CORNING 2mm SPECIMEN SC 2-10

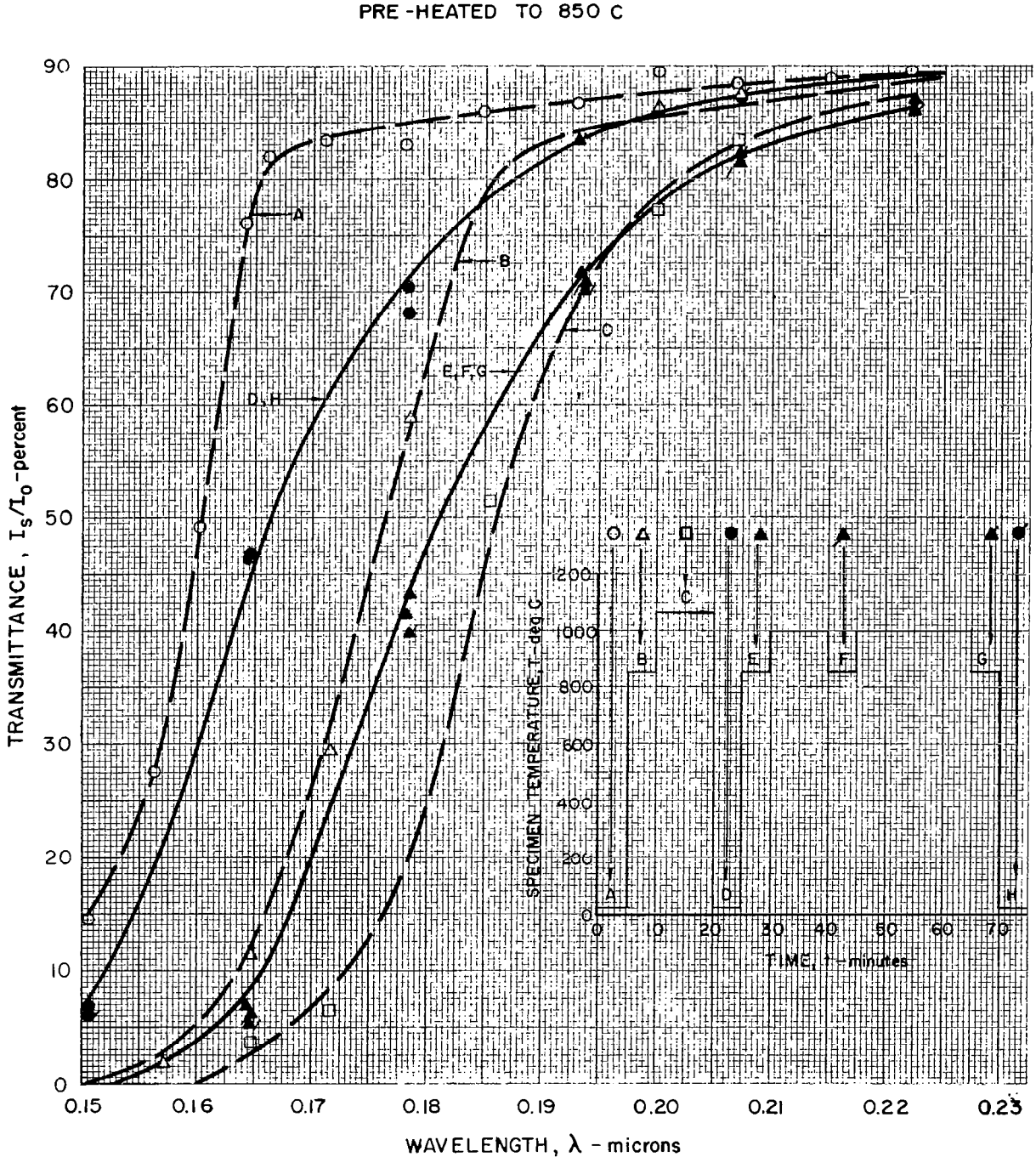

EFFECT ON 22 C TRANSMITTANCE OF A 10-minute EXPOSURE TO 1075 C ON CORNING 2mm AND 1mm SPECIMENS

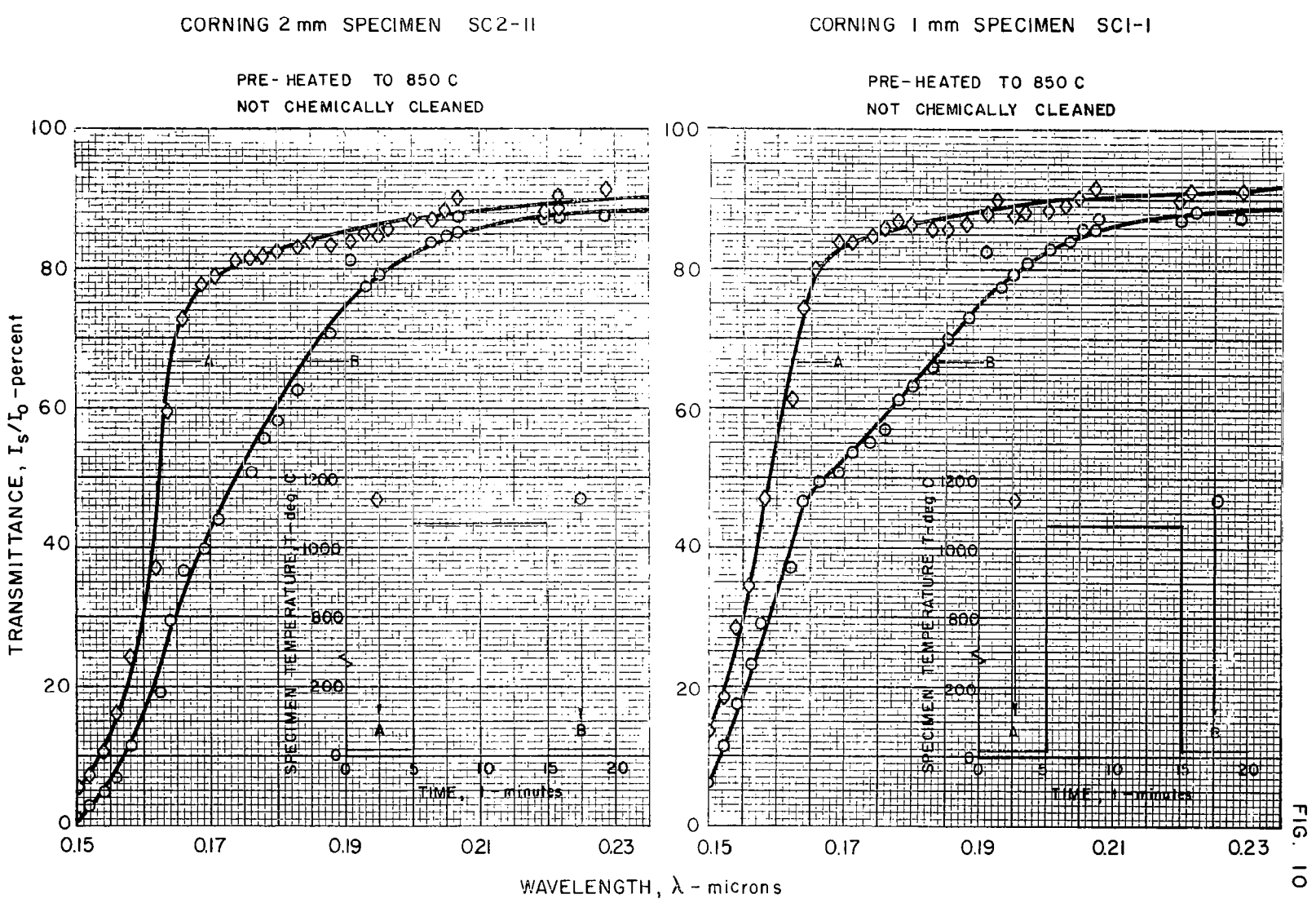

FIG. 10

FIG. 11

COMPARISON OF 22C TRANSMITTANCES OF TWO CORNING 2mm SPECIMENS SUBJECTED TO DIFFERENT CLEANING PROCEDURES

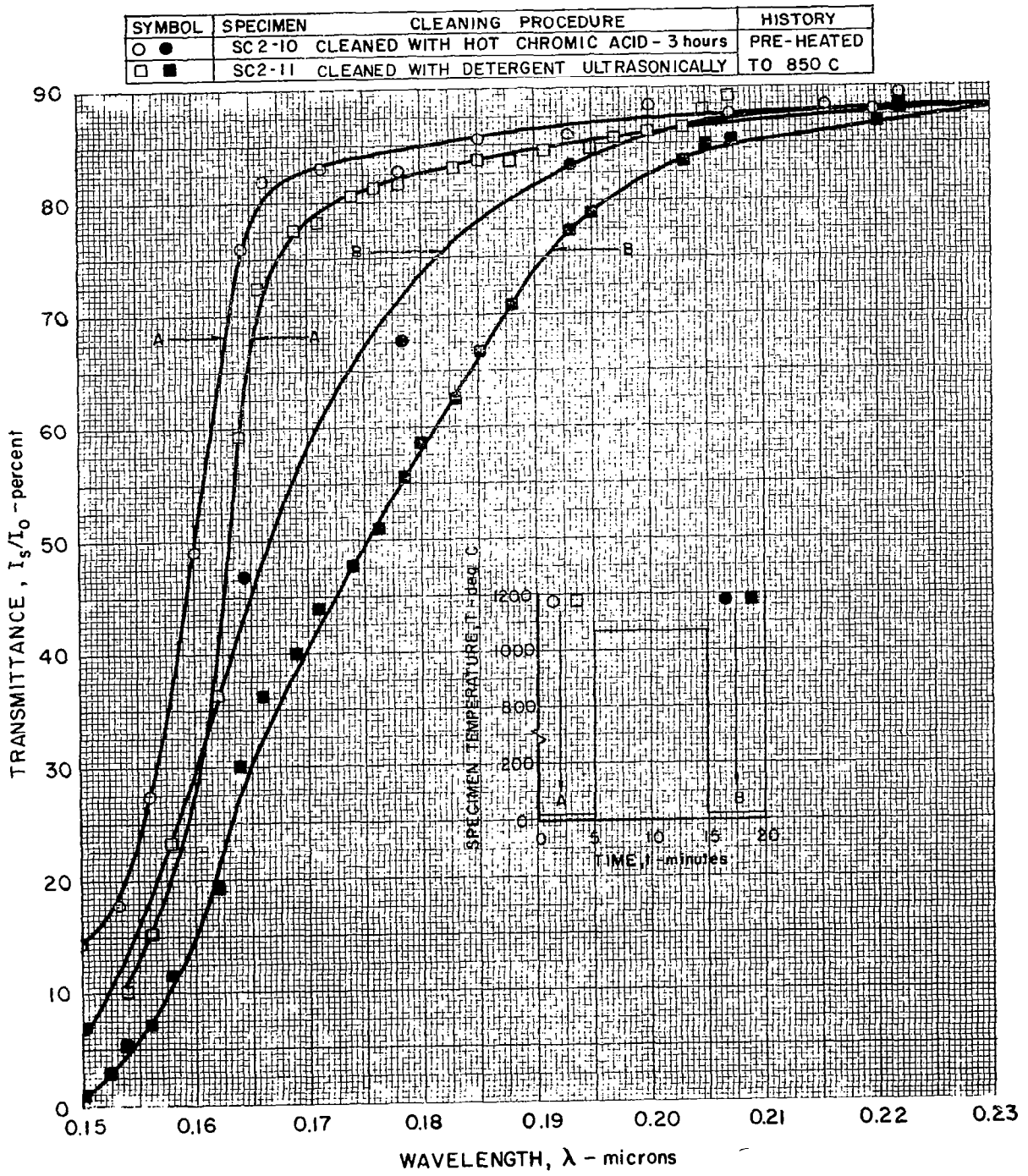

EFFECT OF TEMPERATURE ON THE TRANSMITTANCE OF CORNING 2 mm SPECIMEN SC2-II

SYMBOL	TEMP C	SAMPLE BEAM		REFERENCE BEAM		HISTORY
		THICKNESS, m m	SPECIMEN	THICKNESS, m m	SPECIMEN	
○	22	2.0	SC 2-II	NONE	NONE	PRE-HEATED TO 850 C
□	800	2.0	SC 2-II	NONE	NONE	NOT CHEMICALLY CLEANED

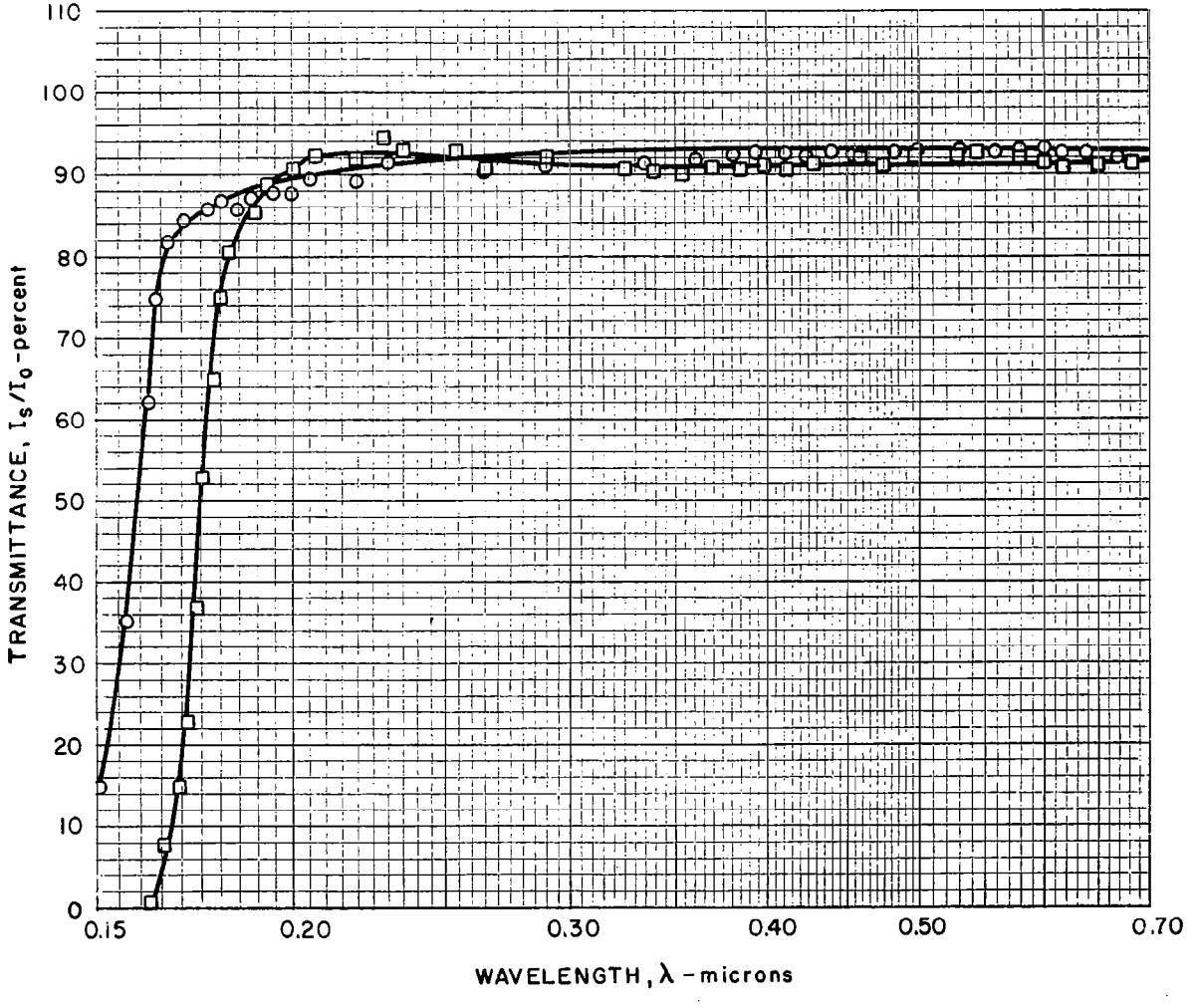

FIG. 12

FIG. 13

EFFECT OF TEMPERATURE ON THE TRANSMISSIVITY OF THERMAL AMERICAN 30 mm SPECIMEN ST30-1

SYMBOL	TEMP C	SAMPLE BEAM		REFERENCE BEAM		HISTORY
		THICKNESS, mm	SPECIMEN	THICKNESS, mm	SPECIMEN	
○	22	30.0	ST 30-1	1.0	ST 1-3	PRE-HEATED TO 850 C NOT CHEMICALLY CLEANED
□	800	30.0	ST 30-1	1.0	ST 1-3	

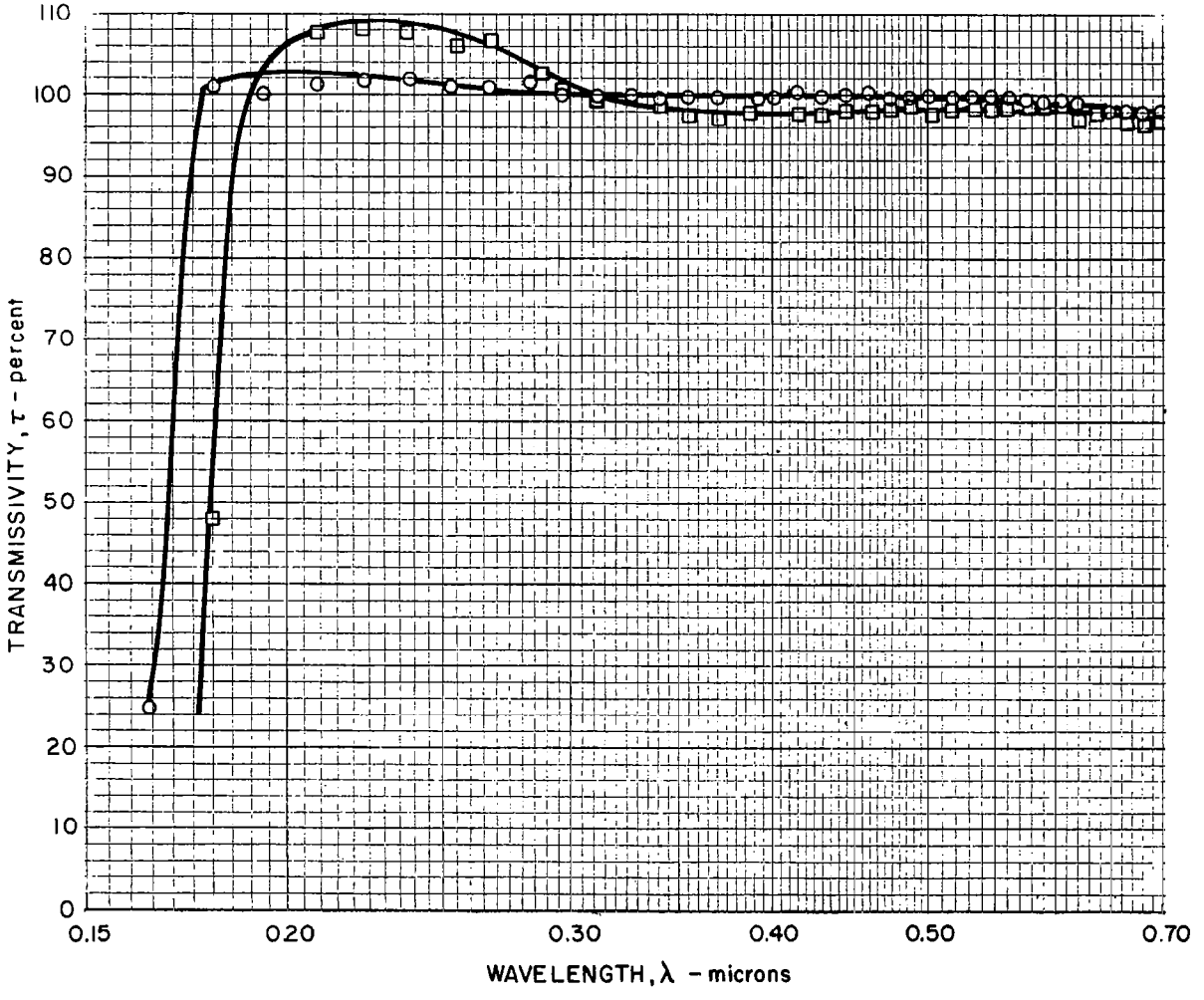

VARIATION OF TRANSMISSIVITY WITH WAVELENGTH OF CORNING 30 mm SPECIMEN SC 30-8

SYMBOL	TEMP C	SAMPLE BEAM		REFERENCE BEAM		HISTORY
		THICKNESS, mm	SPECIMEN	THICKNESS, mm	SPECIMEN	
○	22	30 0	SC 30-8	1.0	SC 1-2	PRE-HEATED TO 850 C
□	800	30.0	SC 30-8	1.0	SC 1-2	NOT CHEMICALLY CLEANED

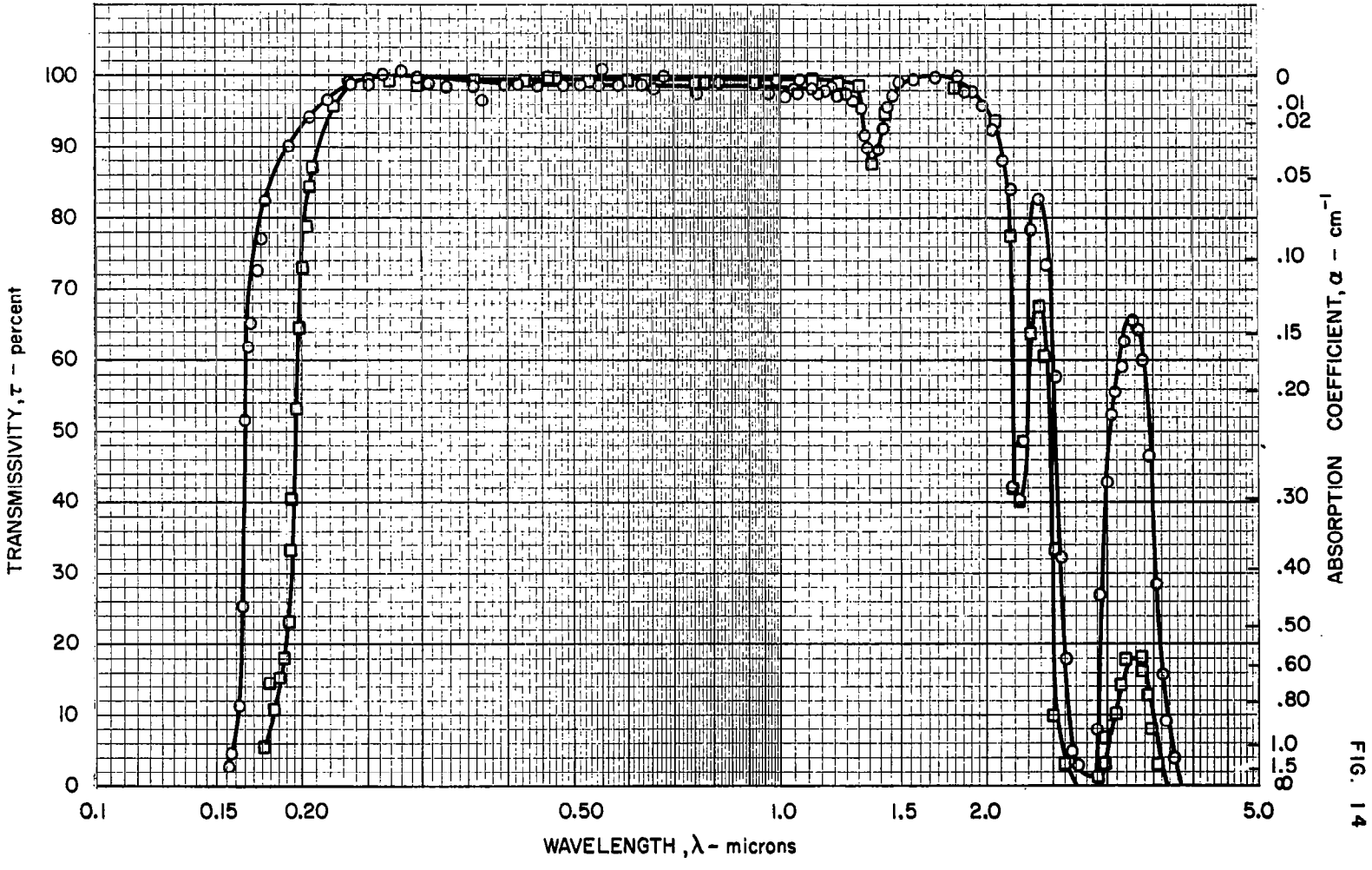

FIG. 14

FIG. 15

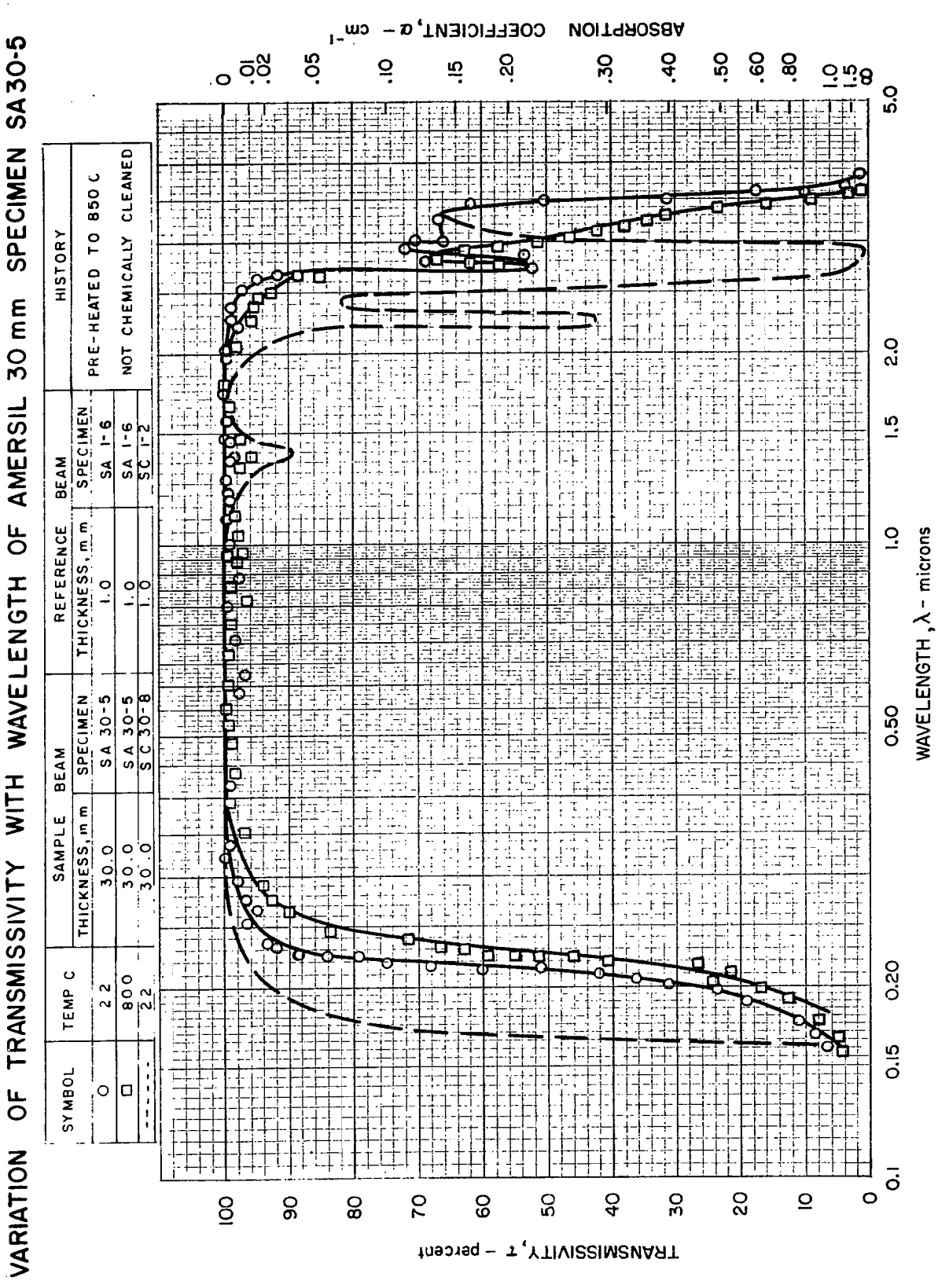
VARIATION OF TRANSMISSIVITY WITH WAVELENGTH OF AMERSIL 30 mm SPECIMEN SA30-5
SYMBOL
TEMP C
SAMPLE BEAM
THICKNESS, mm
SPECIMEN
REFERENCE BEAM
THICKNESS, mm
SPECIMEN
HISTORY
○ 22 30.0 SA 30-5 1.0 SA 1-6 PRE-HEATED TO 850 C
□ 800 30.0 SA 30-5 1.0 SA 1-6 NOT CHEMICALLY CLEANED
------ 22 30.0 SC 30-8 1.0 SC 1-2
TRANSMISSIVITY, τ – percent
ABSORPTION COEFFICIENT, α – cm⁻¹
WAVELENGTH, λ - microns

VARIATION OF TRANSMISSIVITY WITH WAVELENGTH OF THERMAL AMERICAN 30 mm SPECIMEN ST 30-4

SYMBOL	TEMP C	SAMPLE BEAM		REFERENCE BEAM		HISTORY
		THICKNESS, mm	SPECIMEN	THICKNESS, mm	SPECIMEN	
○	22	30.0	ST 30-4	1.0	ST 1-3	PRE-HEATED TO 850 C
□	800	30.0	ST 30-4	1.0	ST 1-3	NOT CHEMICALLY CLEANED
-----	22	30.0	SC 30-8	1.0	SC 1-2	

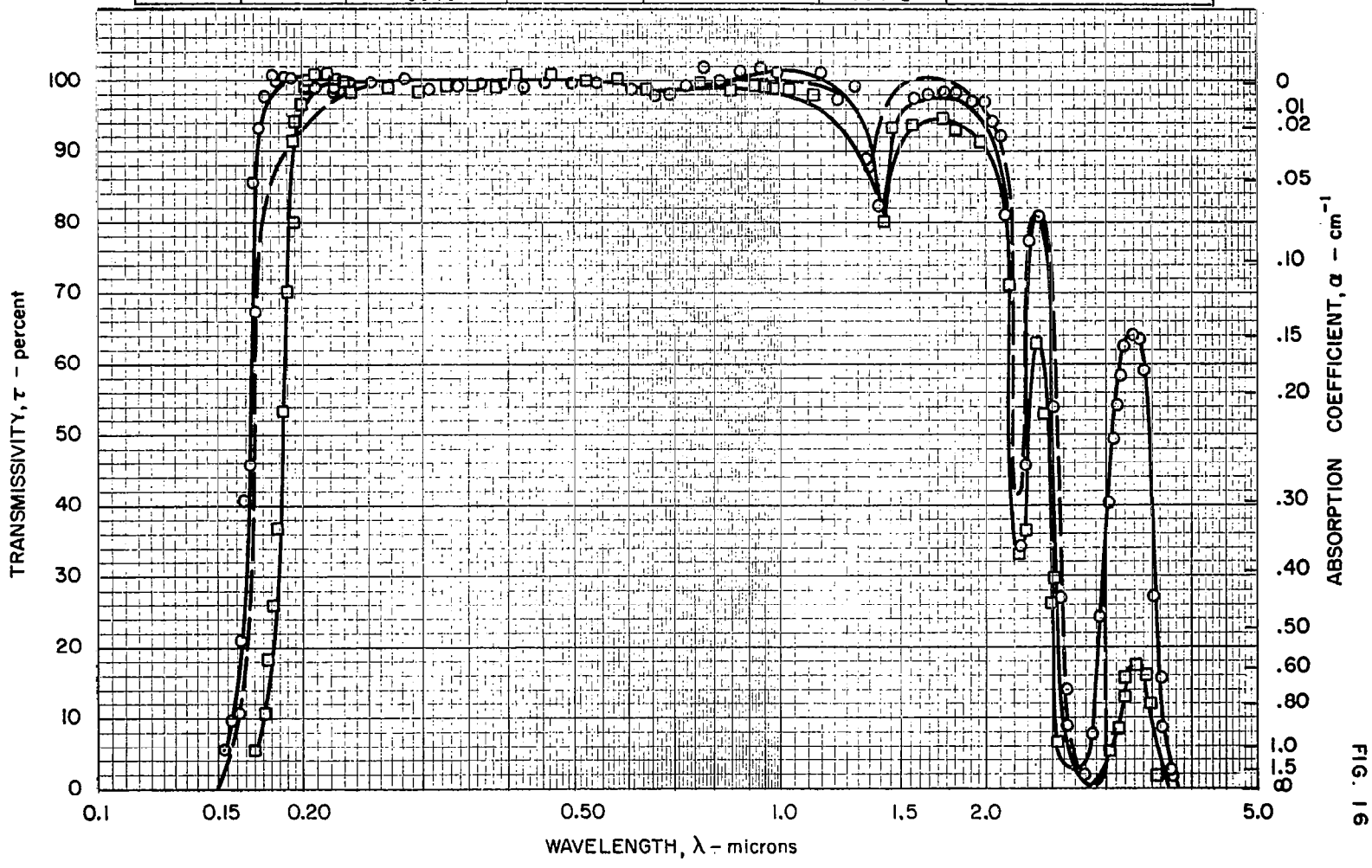

FIG. 16

FIG. 17

ULTRAVIOLET TRANSMISSIVITY OF CORNING 30 mm SPECIMEN SC 30-8

SYMBOL	TEMP C	SAMPLE BEAM		REFERENCE BEAM	
		THICKNESS, mm	SPECIMEN	THICKNESS, mm	SPECIMEN
○ □	22 800	30.0	SC 30-8	1.0	SC 1-2

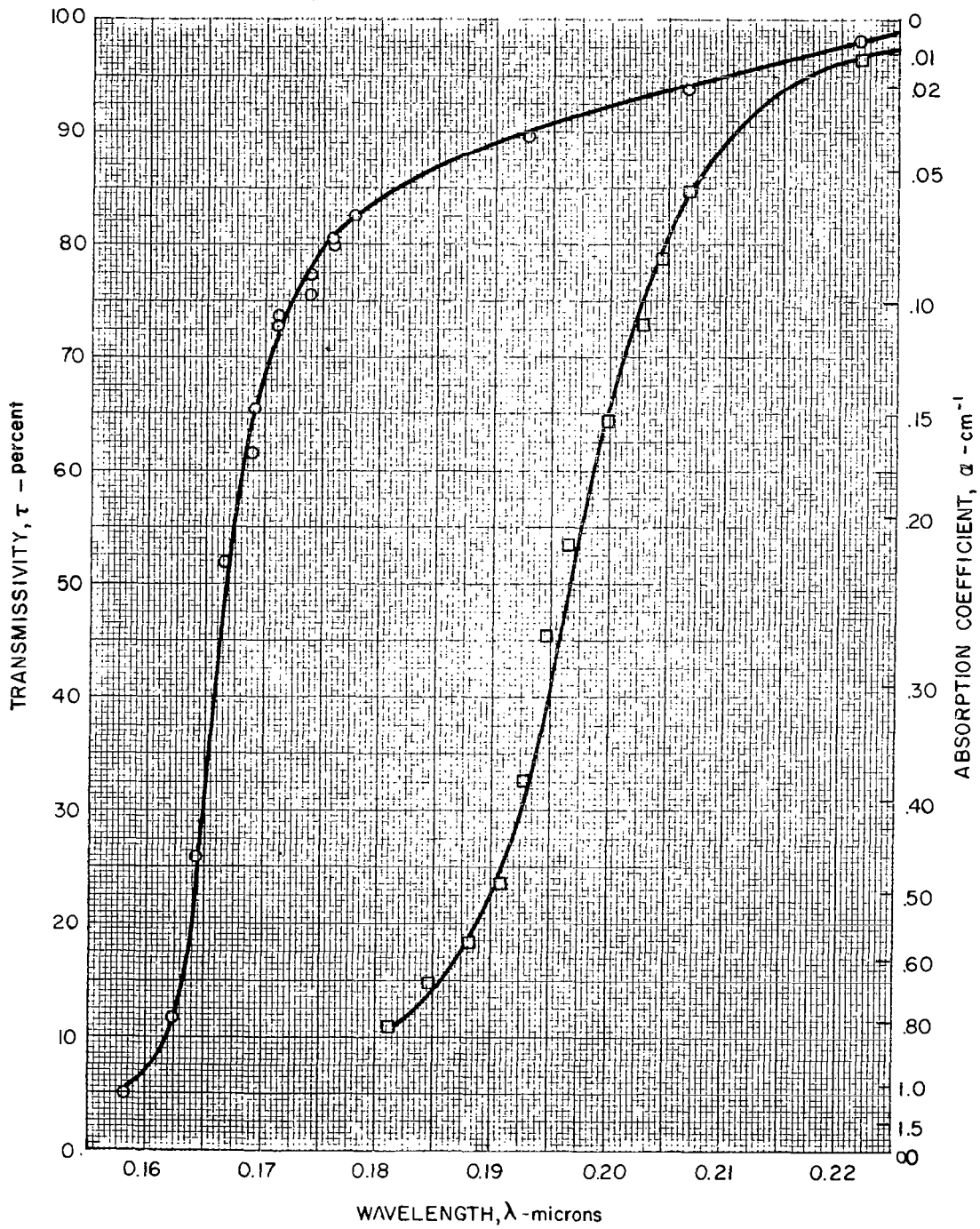

FIG. 18

ULTRAVIOLET TRANSMISSIVITY OF AMERSIL 30 mm SPECIMEN SA 30-5

SYMBOL	TEMP C	SAMPLE BEAM		REFERENCE BEAM	
		THICKNESS, m m	SPECIMEN	THICKNESS, m m	SPECIMEN
○ □	22 800	30.0	SA 30-5	1.0	SA 1-6
------	22	30.0	SC 30-8	1.0	SC 1-2

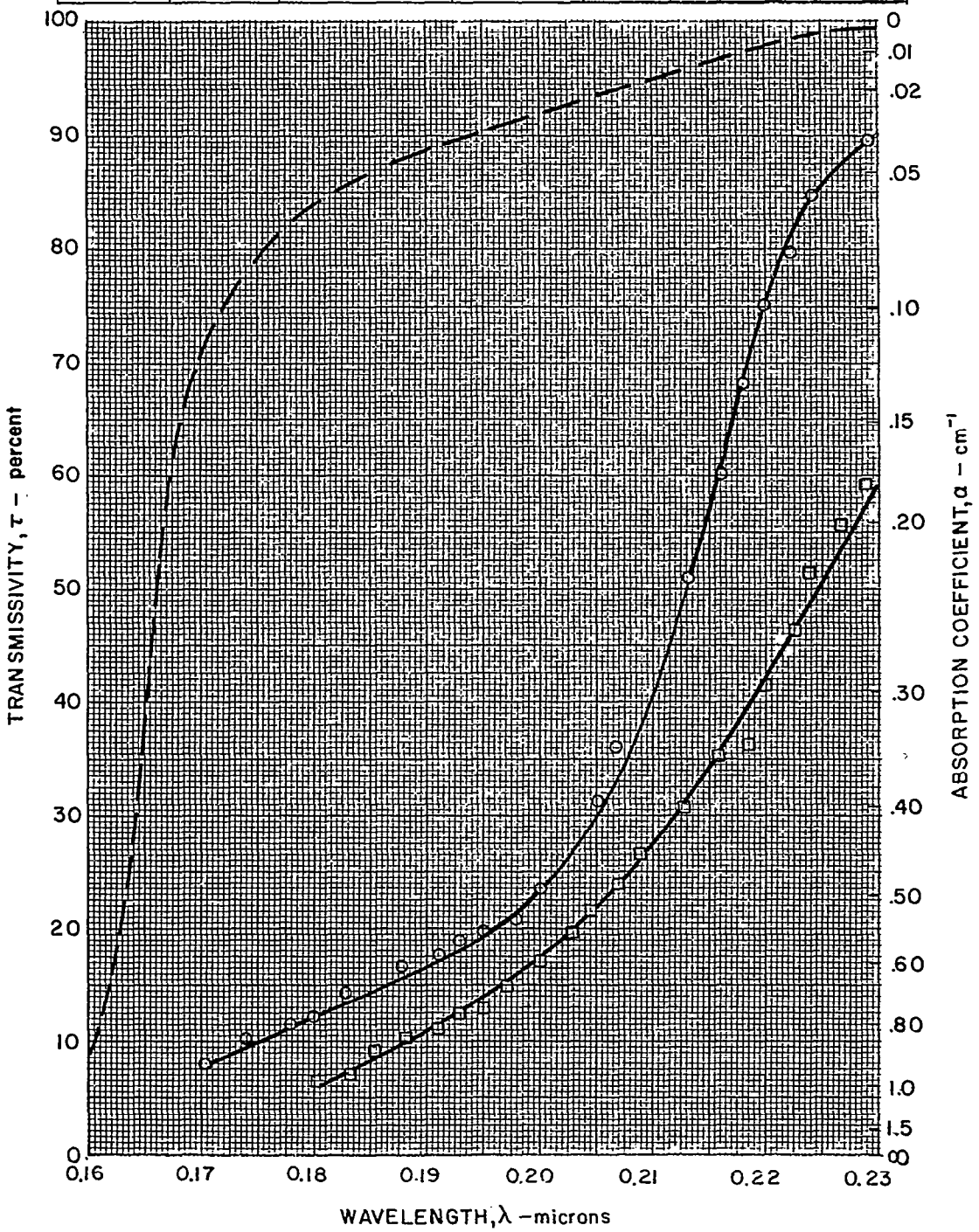

FIG. 19

ULTRAVIOLET TRANSMISSIVITY OF THERMAL AMERICAN 30 mm SPECIMEN ST 30-4

SYMBOL	TEMP C	SAMPLE BEAM		REFERENCE BEAM	
		THICKNESS, mm	SPECIMEN	THICKNESS, mm	SPECIMEN
○ □	22 800	30.0	ST 30-4	1.0	ST 1-3
----	22	30.0	SC 30-8	1.0	SC 1-2

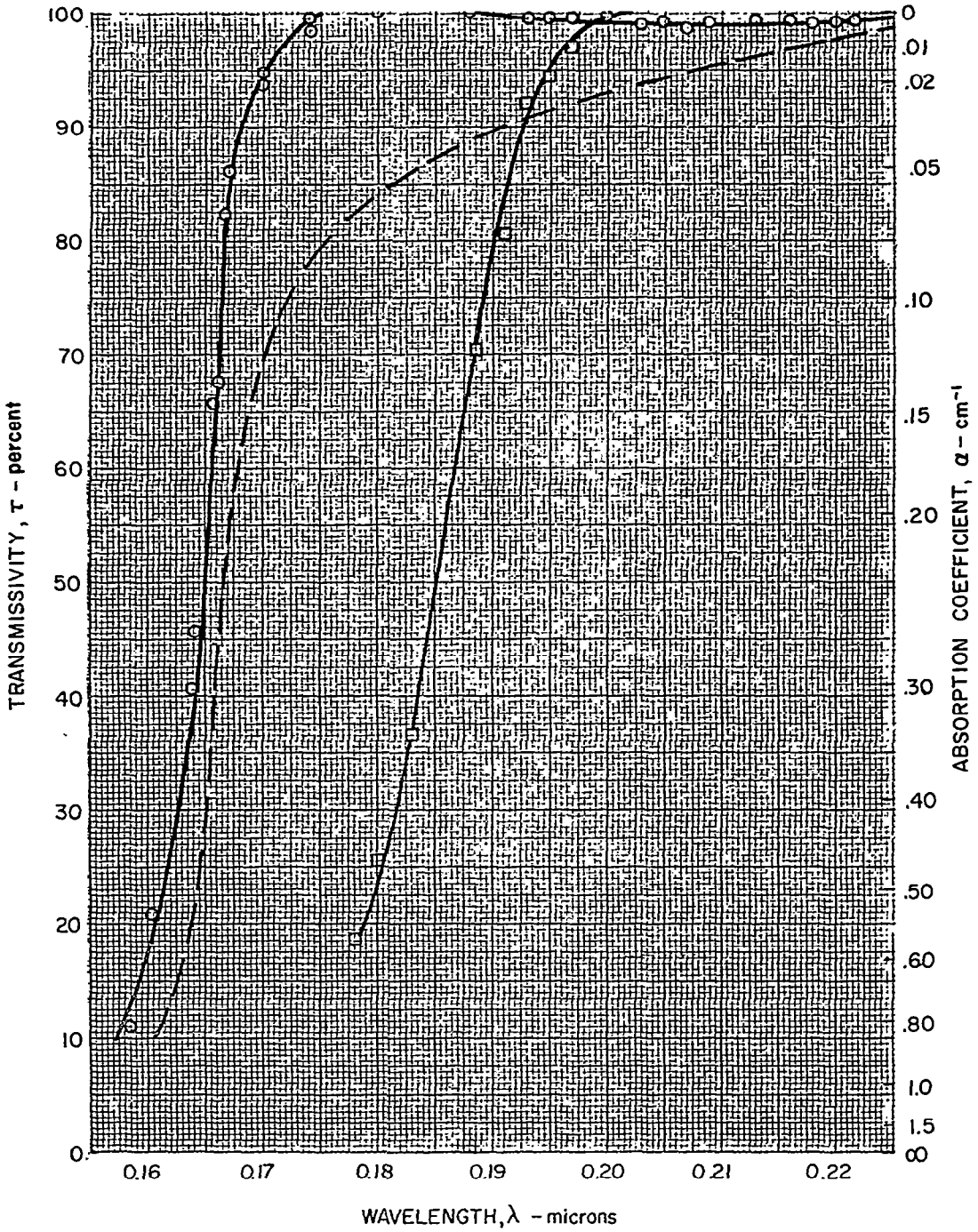

FIG. 20

INFRARED TRANSMISSIVITY OF CORNING 30mm SPECIMEN SC 30 - 8

SYMBOL	TEMP C	SAMPLE BEAM		REFERENCE BEAM	
		THICKNESS, mm	SPECIMEN	THICKNESS, mm	SPECIMEN
○	22	30.0	SC 30 - 8	1.0	SC 1 - 2
□	800	30.0	SC 30 - 8	1.0	SC 1 - 2

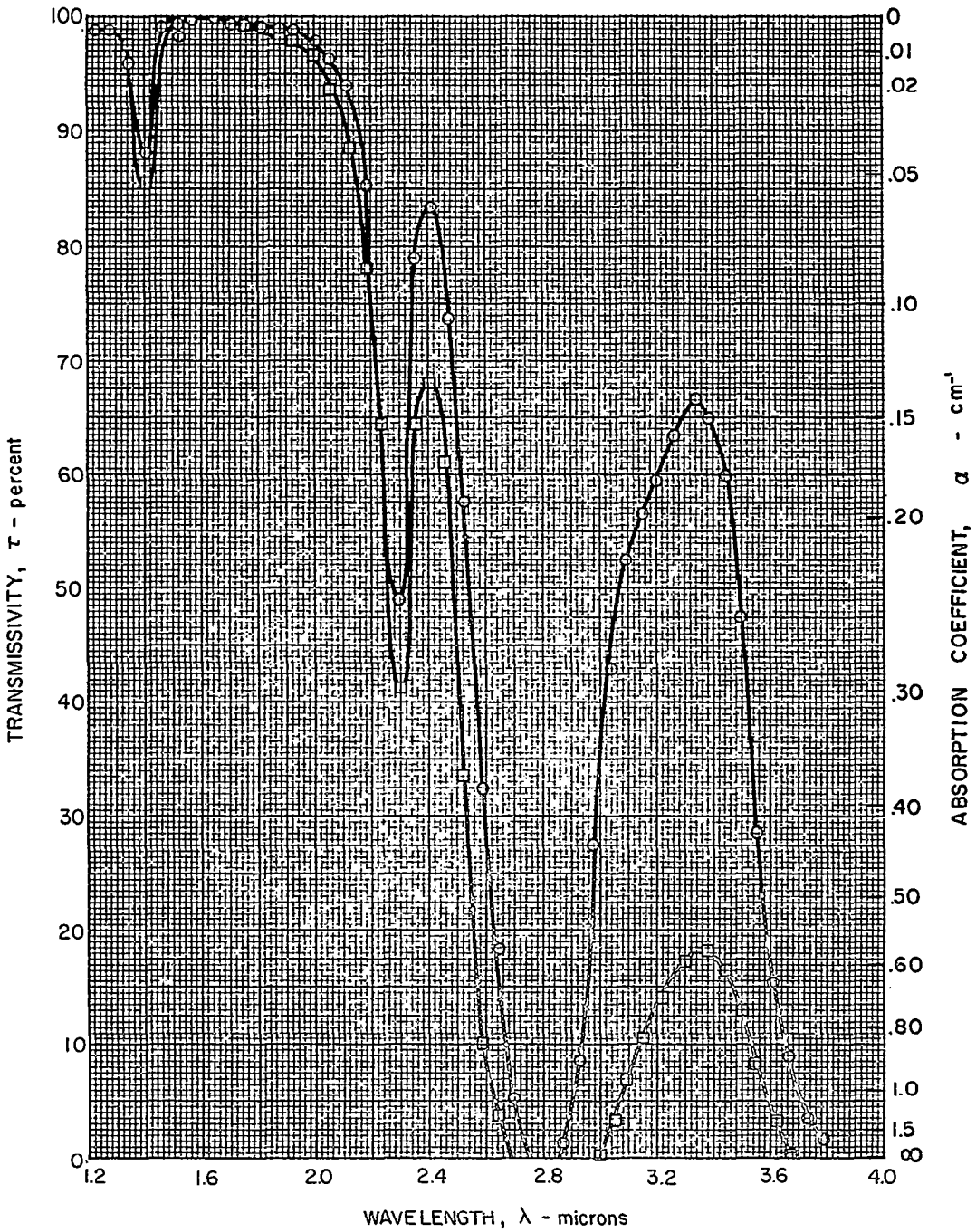

FIG. 21

INFRARED TRANSMISSIVITY OF AMERSIL 30 mm SPECIMEN SA 30-5

SYMBOL	TEMP C	SAMPLE BEAM		REFERENCE BEAM	
		THICKNESS, mm	SPECIMEN	THICKNESS, mm	SPECIMEN
O	22	30.0	SA 30-5	1.0	SA 1-6
□	800	30.0	SA 30-5	1.0	SA 1-6

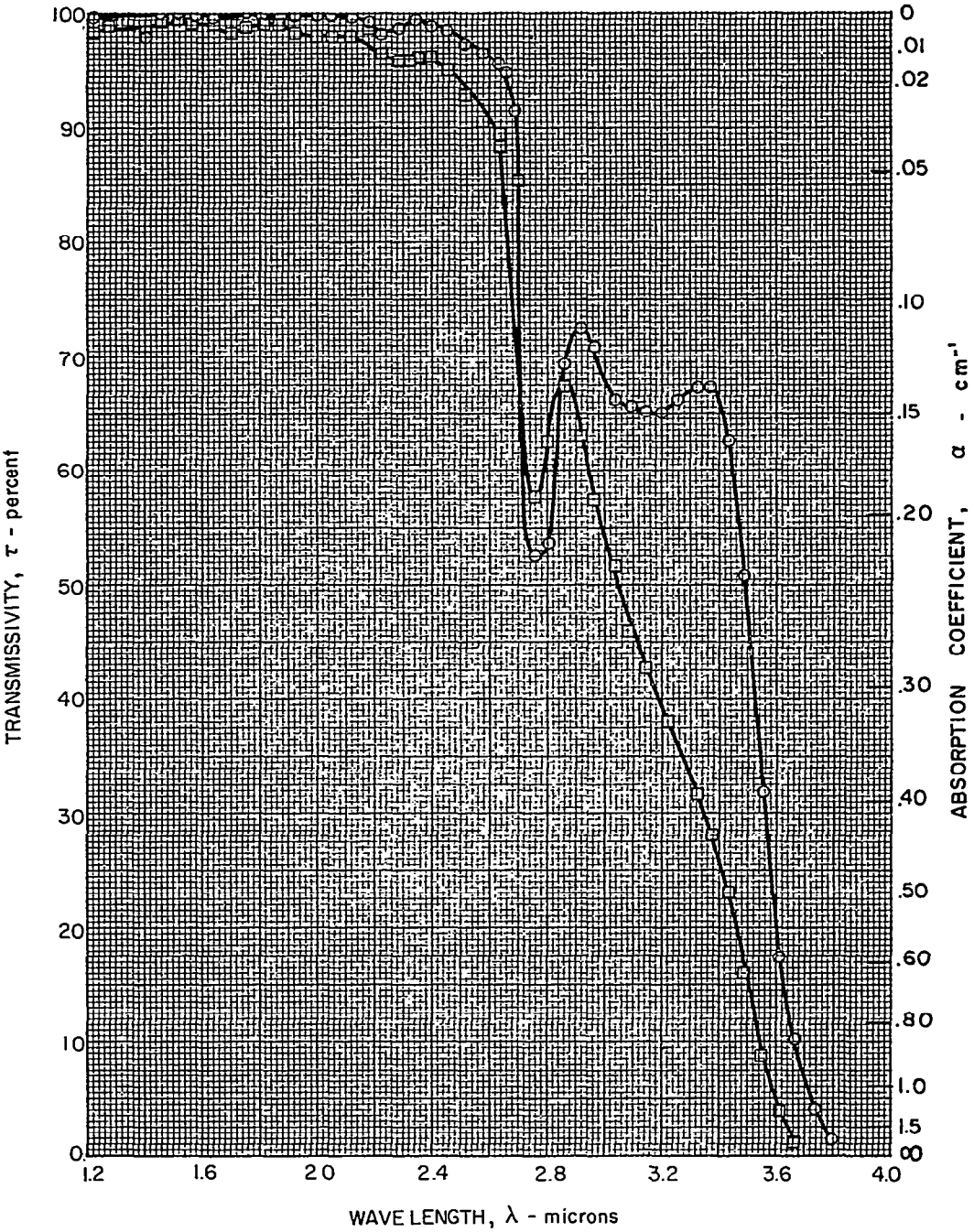

FIG. 22

INFRARED TRANSMISSIVITY OF THERMAL AMERICAN 30 mm SPECIMEN ST 30-4

SYMBOL	TEMP C	SAMPLE BEAM		REFERENCE BEAM	
		THICKNESS, mm	SPECIMEN	THICKNESS, mm	SPECIMEN
○	22	30.0	ST 30 - 4	1.0	ST 1 - 3
□	800	30.0	ST 30 - 4	1.0	ST 1 - 3

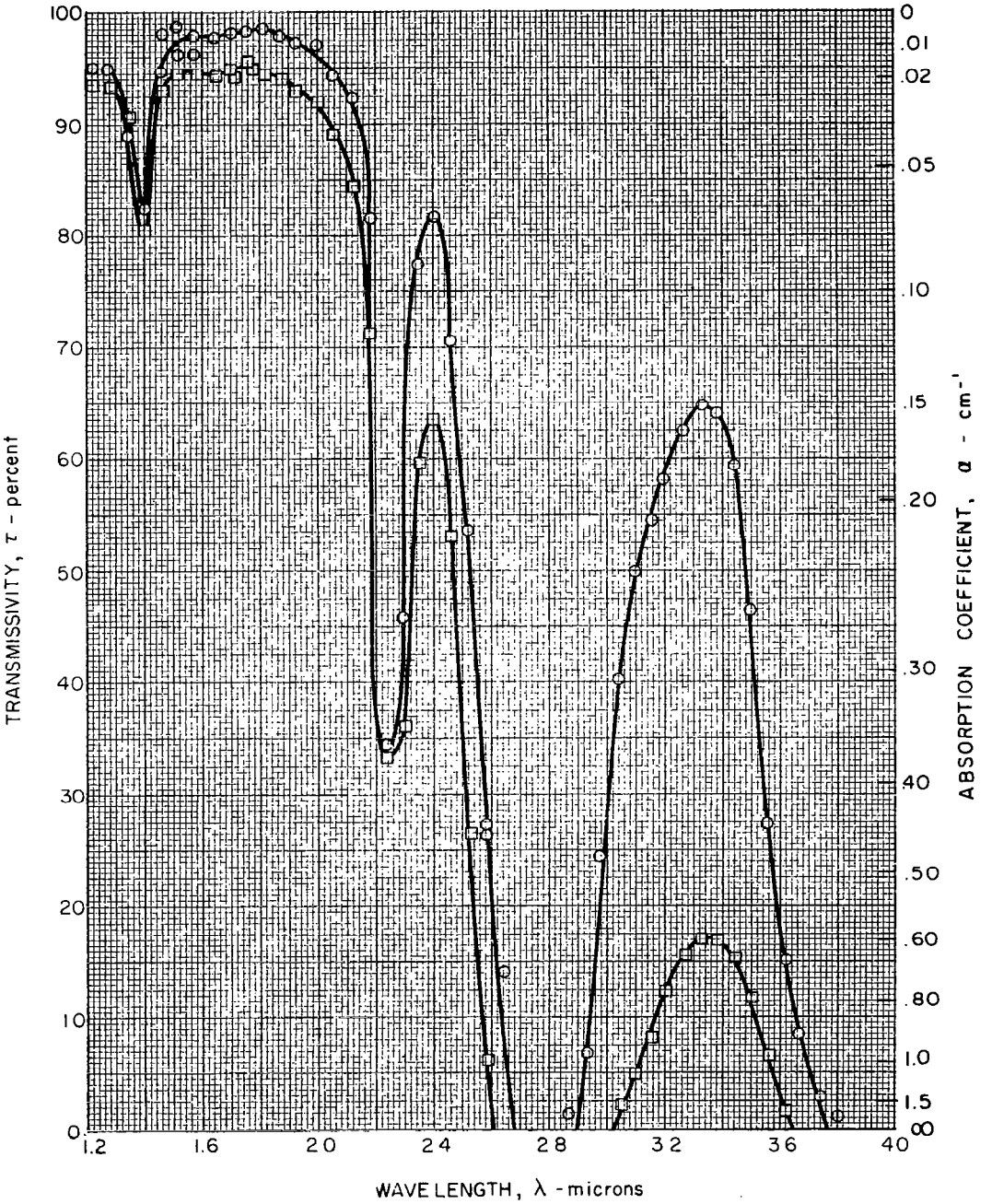

FIG. 23

COMPARISON OF 22 C INFRARED TRANSMISSIVITY OF CORNING, AMERSIL, AND THERMAL AMERICAN 30 mm SPECIMENS

SYMBOL	TEMP C	SAMPLE BEAM		REFERENCE BEAM	
		THICKNESS, mm	SPECIMEN	THICKNESS, mm	SPECIMEN
□	22	30.0	SA 30 - 5	1.0	SA 1 - 6
△	22	30.0	SC 30 - 8	1.0	SC 1 - 2
○	22	30 0	ST 30 - 4	1.0	ST 1 - 3

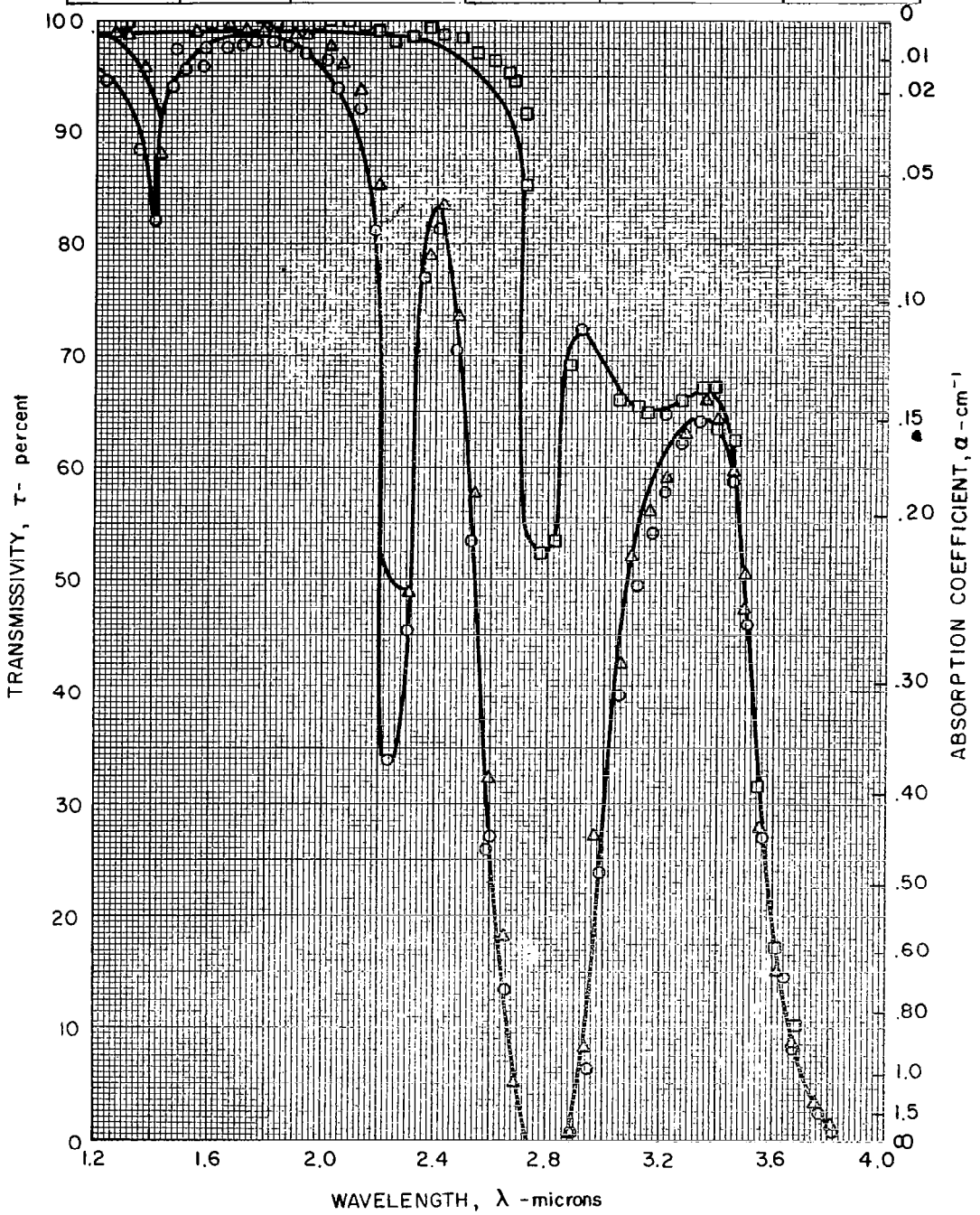

FIG. 24

COMPARISON OF 800 C INFRARED TRANSMISSIVITY OF CORNING, AMERSIL, AND THERMAL AMERICAN 30 mm SPECIMENS

SYMBOL	TEMP C	SAMPLE BEAM		REFERENCE BEAM	
		THICKNESS, mm	SPECIMEN	THICKNESS, mm	SPECIMEN
□	800	30	SA 30-5	1.0	SA 1-6
△	800	30	SC 30-8	1.0	SC 1-2
○	800	30	ST 30	1.0	ST 1-3

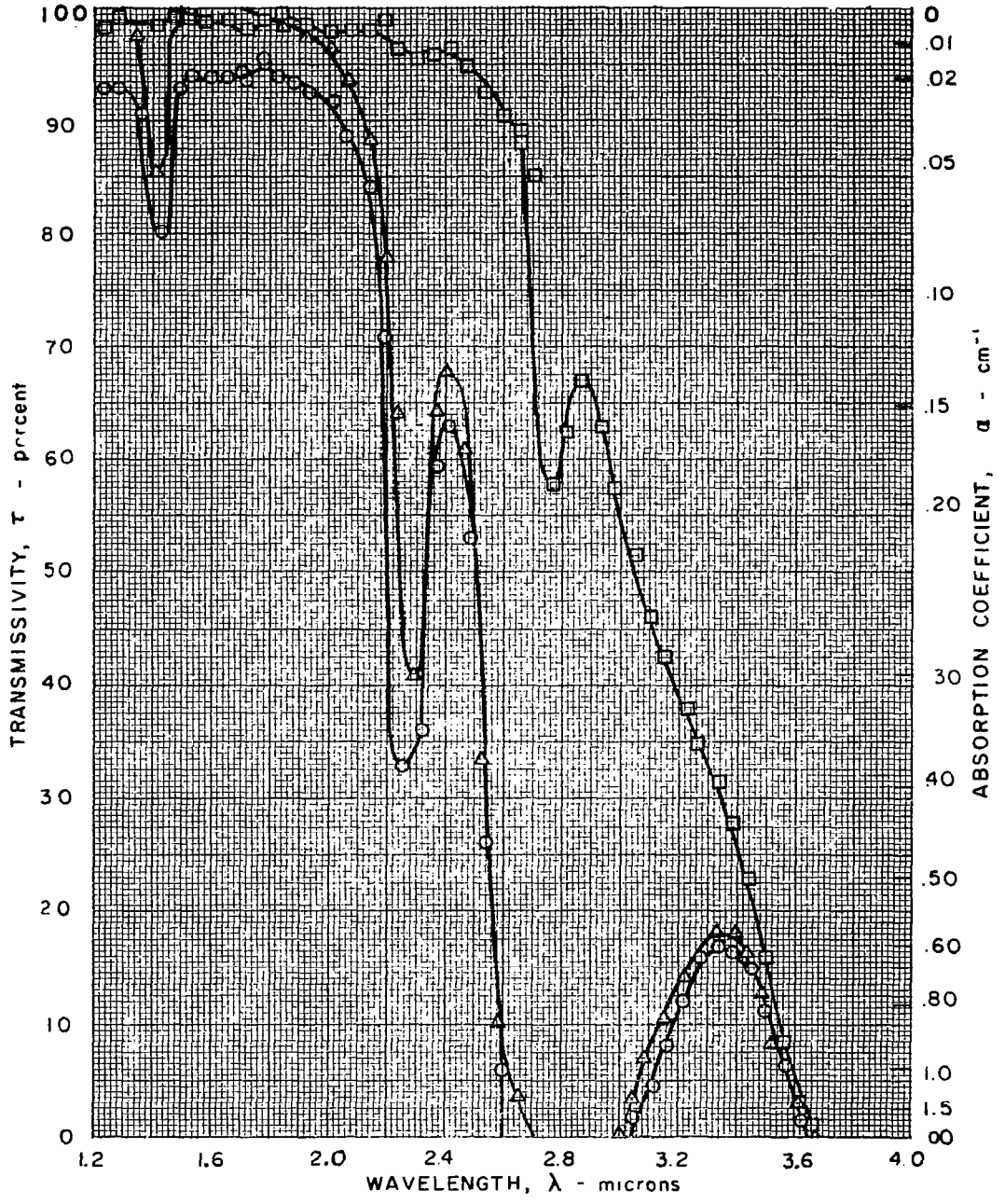

FIG. 25

COMPARISON OF 22 C ULTRAVIOLET TRANSMISSIVITY OF CORNING, AMERSIL, AND THERMAL AMERICAN 30 mm SPECIMENS

SYMBOL	TEMP C	SAMPLE BEAM		REFERENCE BEAM	
		THICKNESS, mm	SPECIMEN	THICKNESS, mm	SPECIMEN
○	22	30.0	ST 30-4	1.0	ST 1-3
△	22	30.0	SC 30-8	1.0	SC 1-2
□	22	30.0	SA 30-5	1.0	SA 1-6

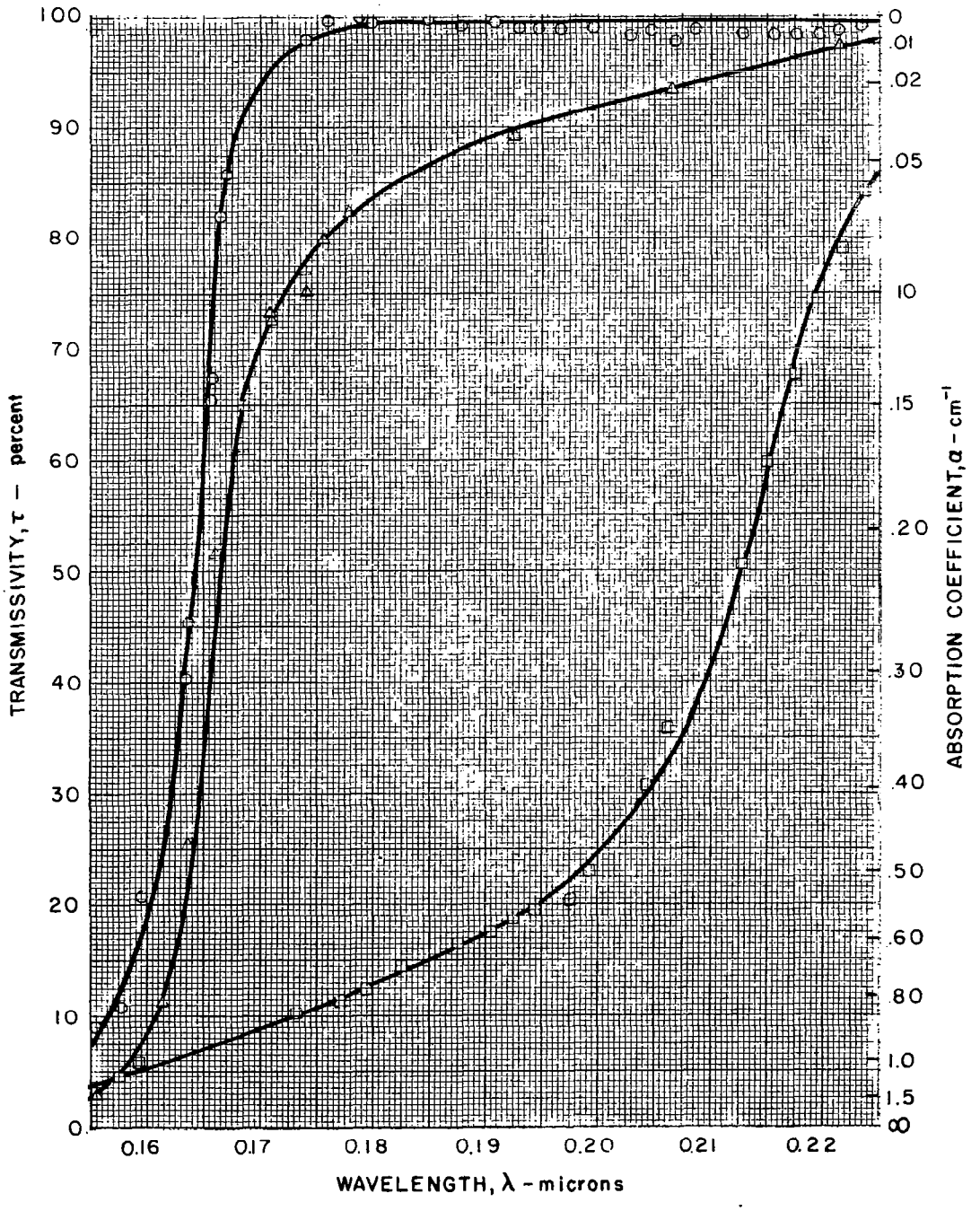

FIG. 26

COMPARISON OF 800C ULTRAVIOLET TRANSMISSIVITY OF CORNING, AMERSIL, AND THERMAL AMERICAN 30 mm SPECIMENS

SYMBOL	TEMP C	SAMPLE BEAM		REFERENCE BEAM	
		THICKNESS, mm	SPECIMEN	THICKNESS, mm	SPECIMEN
○	800	30.0	ST 30-4	1.0	ST 1-3
△	800	30.0	SC 30-8	1.0	SC 1-2
□	800	30.0	SA 30-5	1.0	SA 1-6

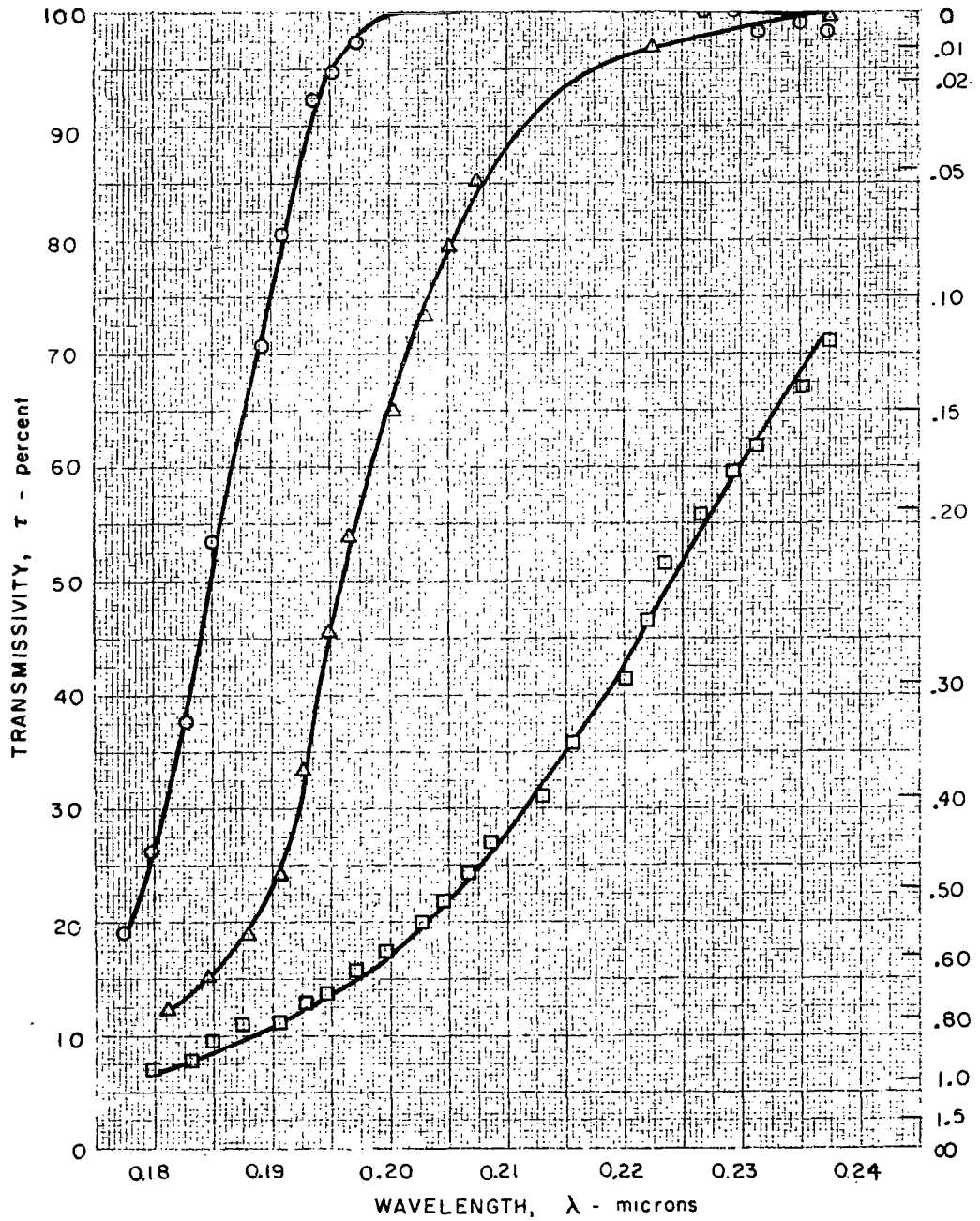

VARIATION OF TRANSMISSIVITY WITH WAVELENGTH OF CORNING 1 mm SPECIMEN SC 1-3

SYMBOL	TEMP C	SAMPLE BEAM		REFERENCE BEAM		HISTORY
		THICKNESS, mm	SPECIMEN	THICKNESS, mm	SPECIMEN	
O	22	1.0	SC 1 - 3	1.0	SC 1-2	PRE - HEATED TO 850 C
□	750	1.0	SC 1 - 3	1.0	SC 1-2	NOT CHEMICALLY CLEANED

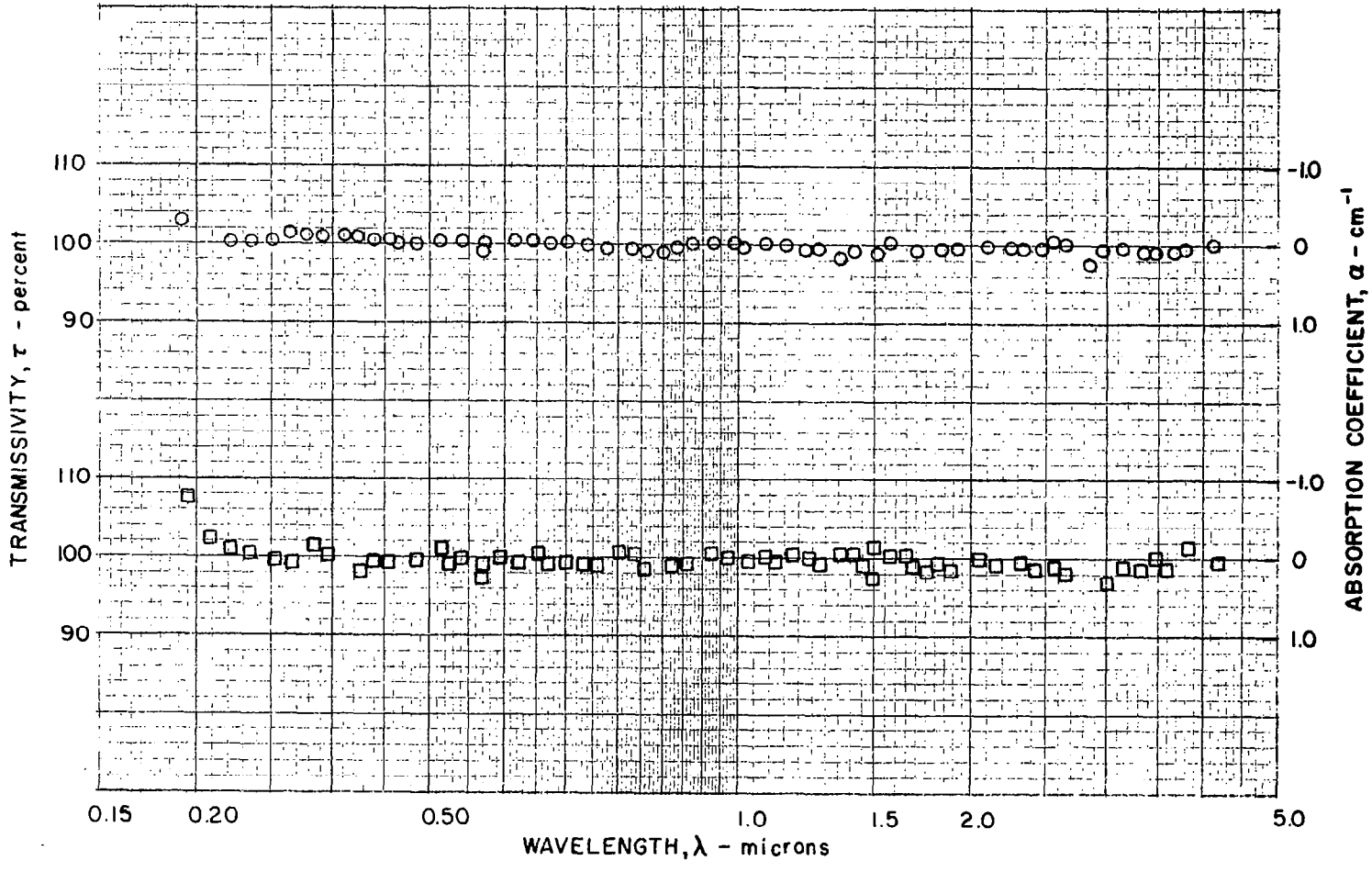

FIG. 27

VARIATION OF TRANSMISSIVITY WITH WAVELENGTH OF AMERSIL 1mm SPECIMEN SA 1-5

SYMBOL	TEMP C	SAMPLE BEAM		REFERENCE BEAM		HISTORY
		THICKNESS, m m	SPECIMEN	THICKNESS, m m	SPECIMEN	
O	22	1.0	SA 1-5	1.0	SA 1-6	PRE-HEATED TO 850 C
□	800	1.0	SA 1-5	1.0	SA 1-6	NOT CHEMICALLY CLEANED

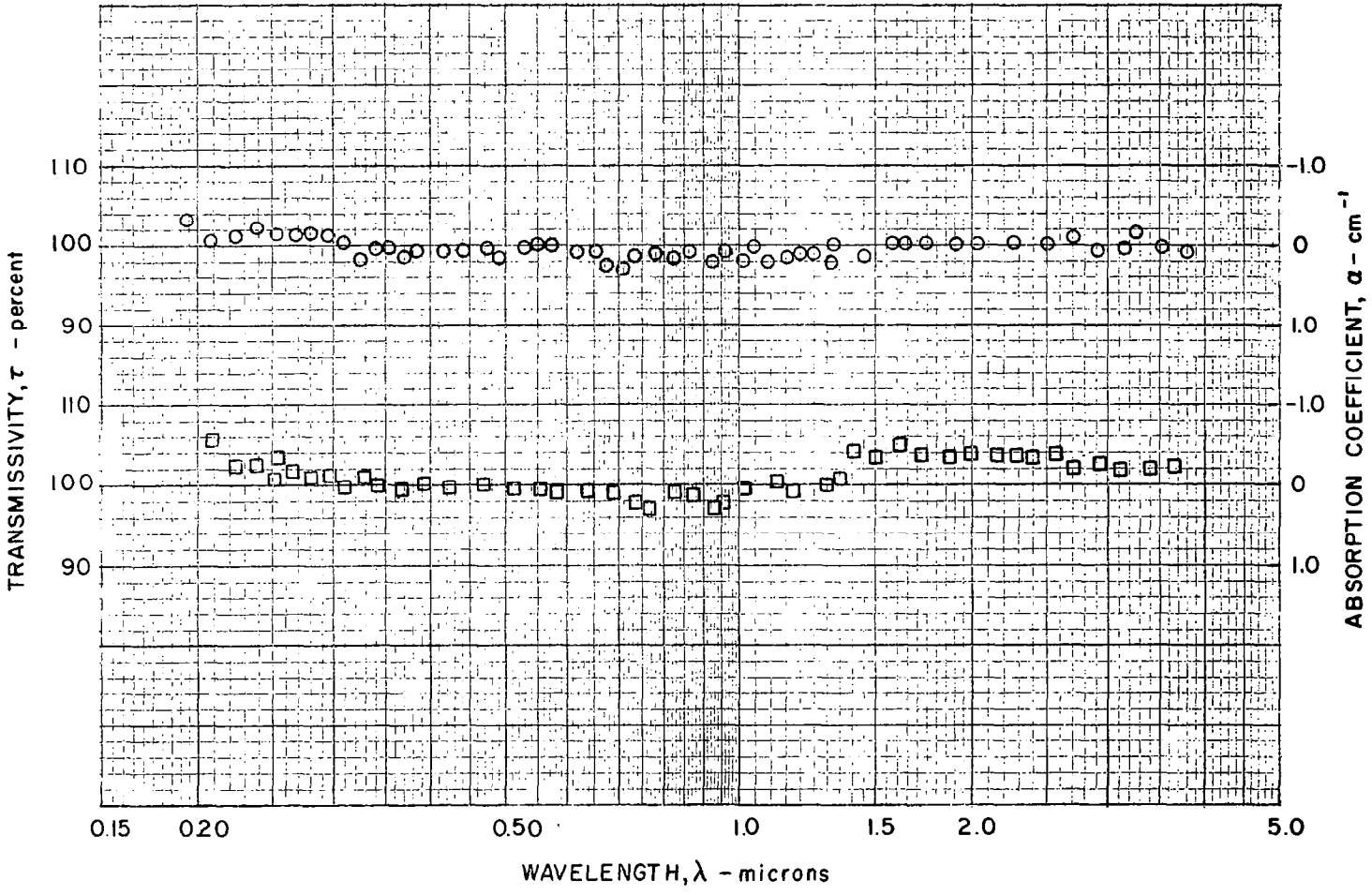

FIG. 28

VARIATION OF TRANSMISSIVITY WITH WAVELENGTH OF THERMAL AMERICAN 1mm SPECIMEN ST 1-6

SYMBOL	TEMP C	SAMPLE BEAM		REFERENCE BEAM		HISTORY
		THICKNESS, mm	SPECIMEN	THICKNESS, mm	SPECIMEN	
○	22	1.0	ST 1-6	1.0	ST 1-3	PRE-HEATED TO 850 C
□	800	1.0	ST 1-6	1.0	ST 1-3	NOT CHEMICALLY CLEANED

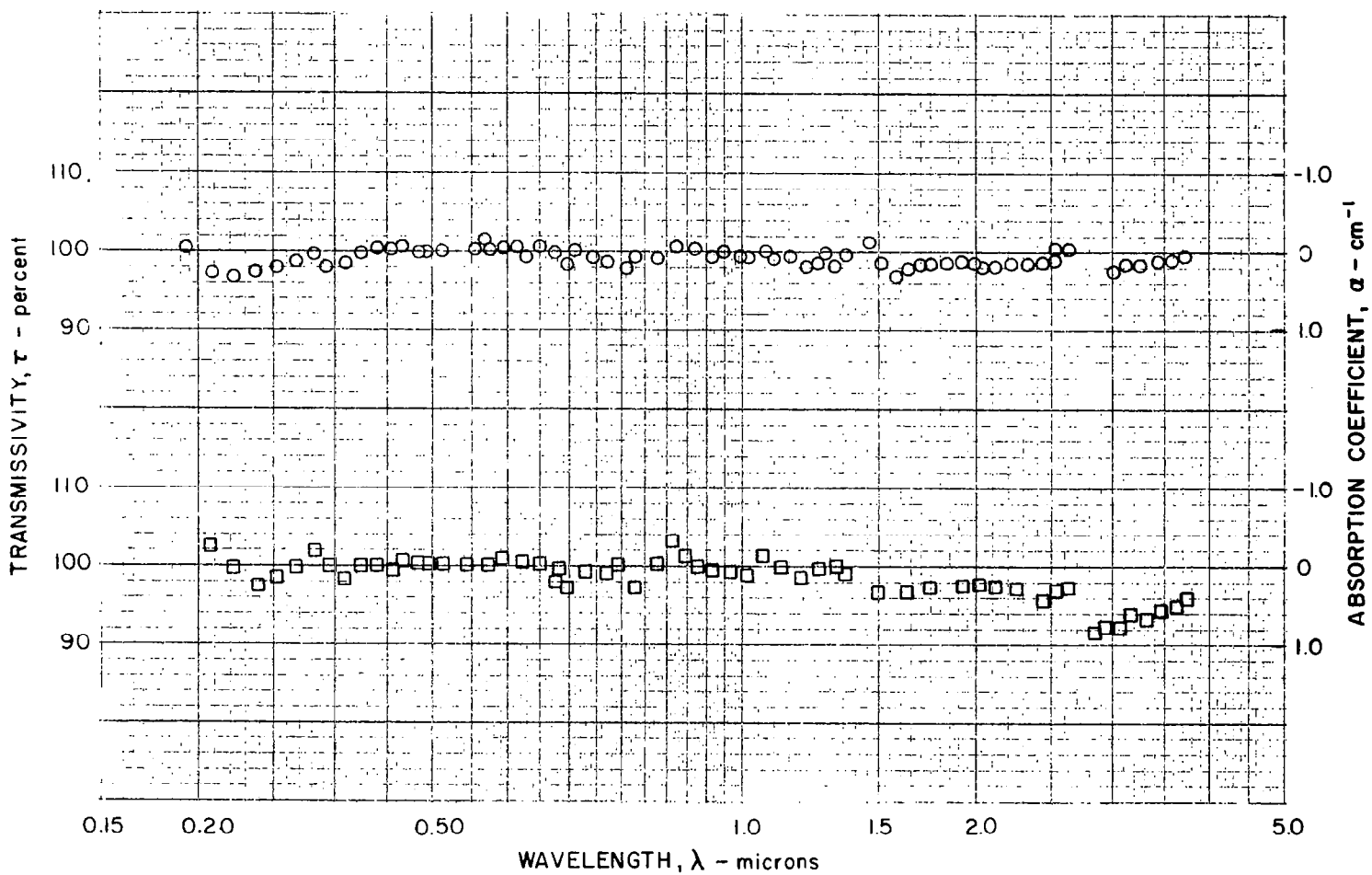

FIG. 29

FIG. 30

SUMMARY OF THE 22 C ULTRAVIOLET ABSORPTION COEFFICIENT DATA FOR CORNING, AMERSIL, AND THERMAL AMERICAN BRANDS OF FUSED SILICA

SYMBOL	BRAND	HISTORY
△	CORNING	PRE-HEATED TO 850 C NOT CHEMICALLY CLEANED
□	AMERSIL	
○	THERMAL AMERICAN	

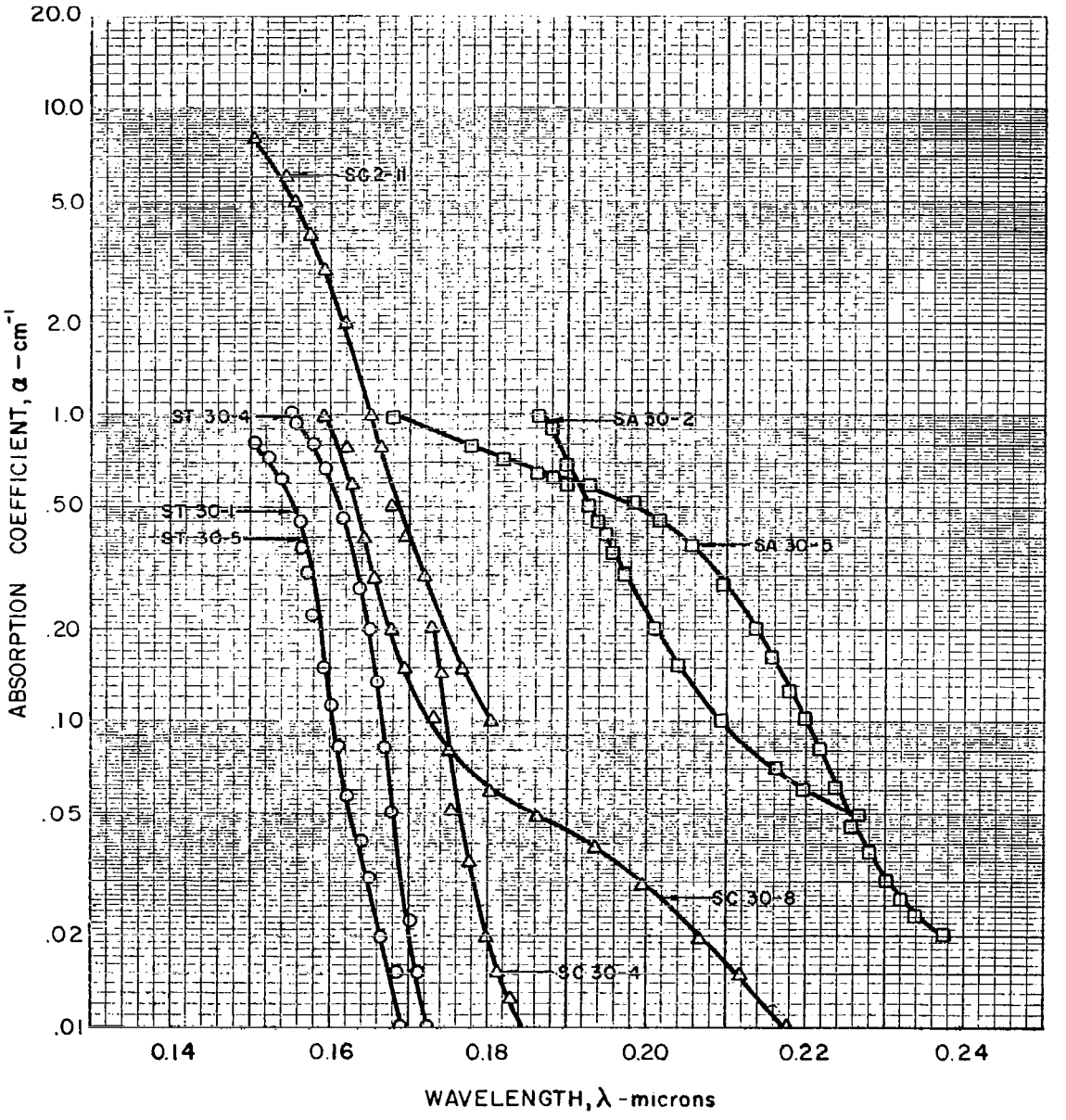

FIG. 31

SUMMARY OF THE 800 C ULTRAVIOLET ABSORPTION COEFFICIENT DATA FOR CORNING, AMERSIL, AND THERMAL AMERICAN BRANDS OF FUSED SILICA

SYMBOL	BRAND	HISTORY
△	CORNING	PRE-HEATED TO 850 C NOT CHEMICALLY CLEANED
□	AMERSIL	
○	THERMAL AMERICAN	

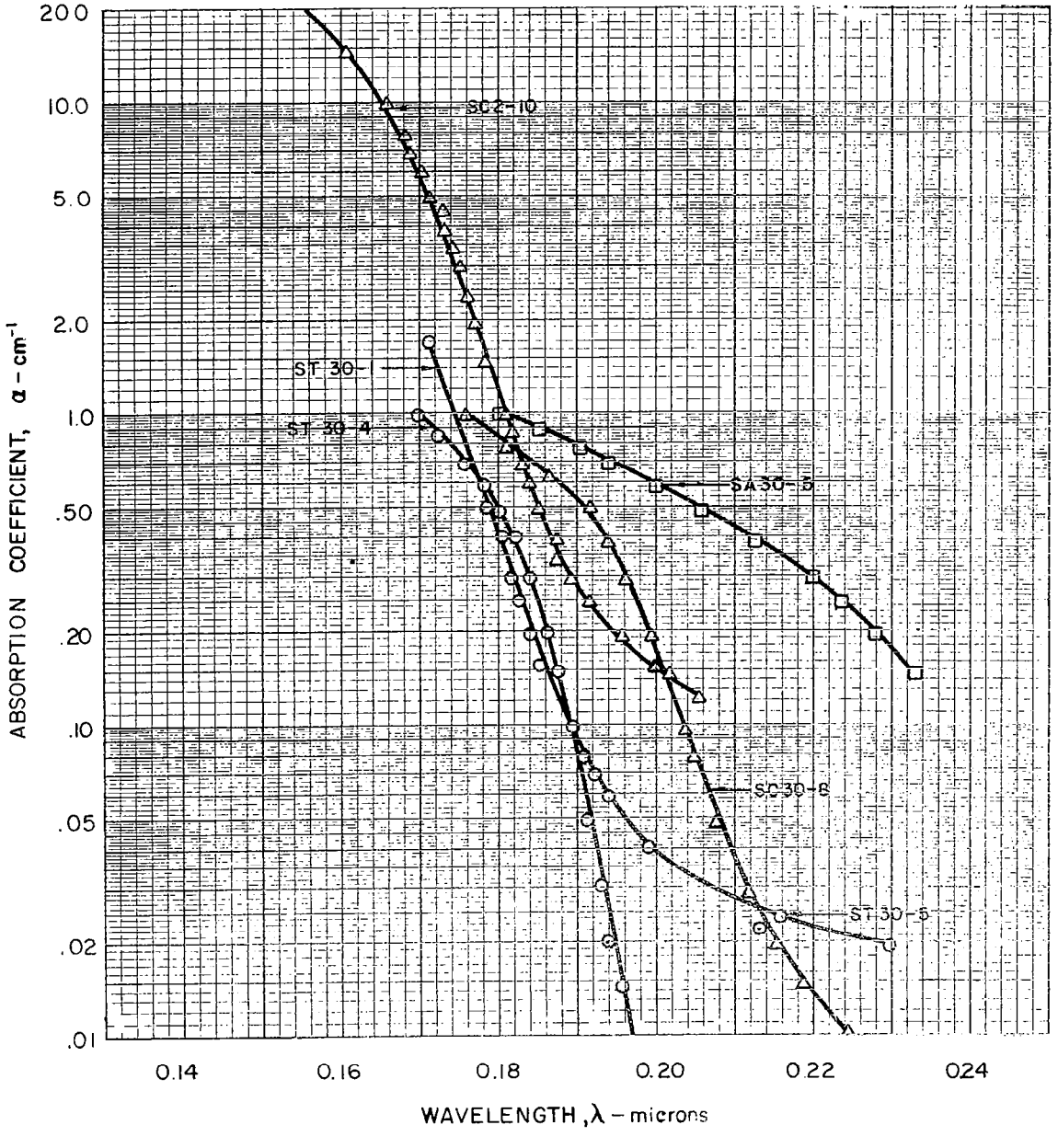

SUMMARY OF THE 22C INFRARED ABSORPTION COEFFICIENT DATA FOR CORNING, AMERSIL, AND THERMAL AMERICAN BRANDS OF FUSED SILICA

SYMBOL	BRAND	HISTORY
△	CORNING	PRE-HEATED TO 850 C
□	AMERSIL	NOT CHEMICALLY CLEANED
○	THERMAL AMERICAN	

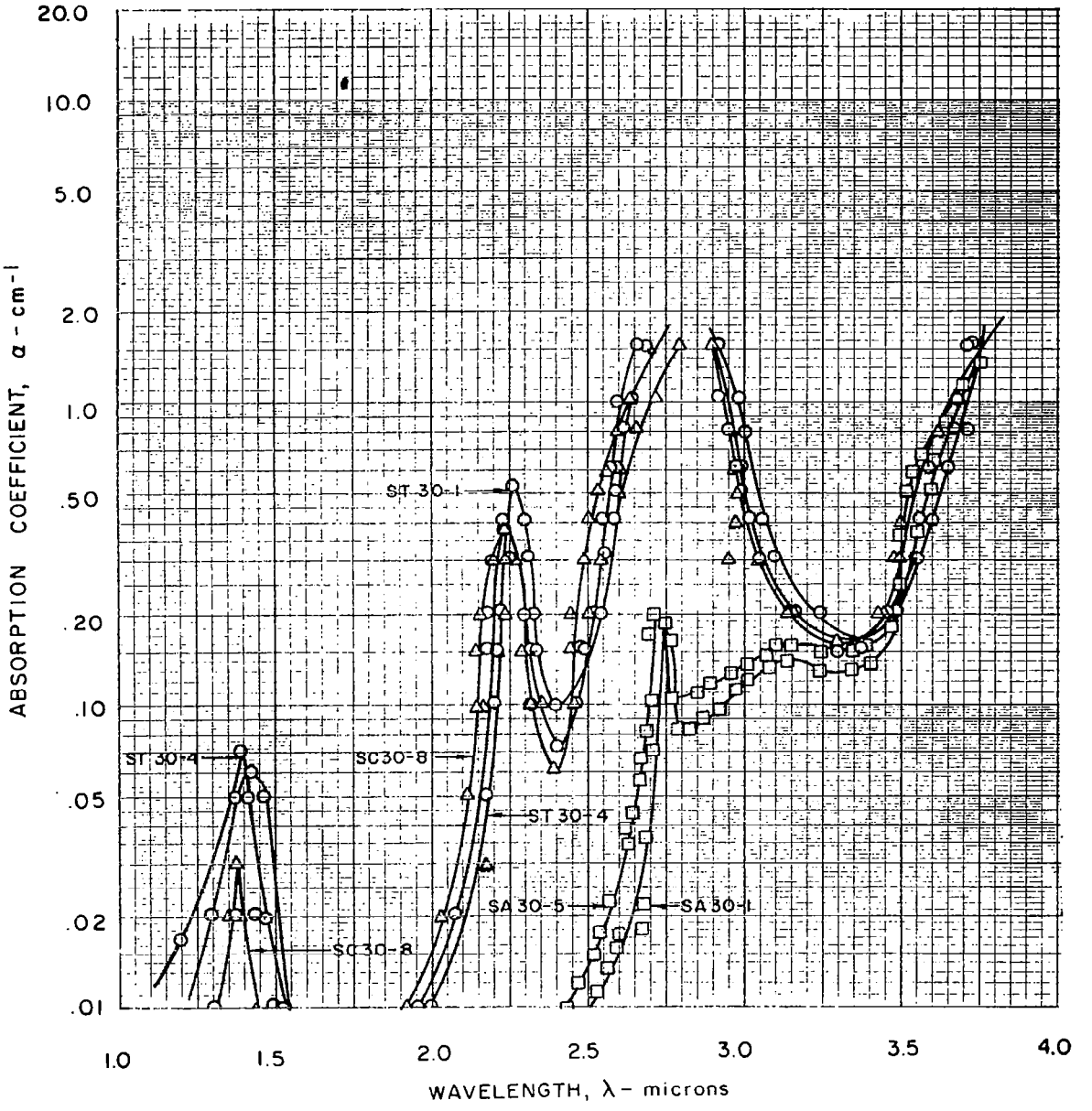

FIG. 33

SUMMARY OF THE 800 C INFRARED ABSORPTION COEFFICIENT DATA FOR CORNING, AMERSIL, AND THERMAL AMERICAN BRANDS OF FUSED SILICA

SYMBOL	BRAND	HISTORY
△	CORNING	PRE-HEATED TO 850C NOT CHEMICALLY CLEANED
□	AMERSIL	
○	THERMAL AMERICAN	

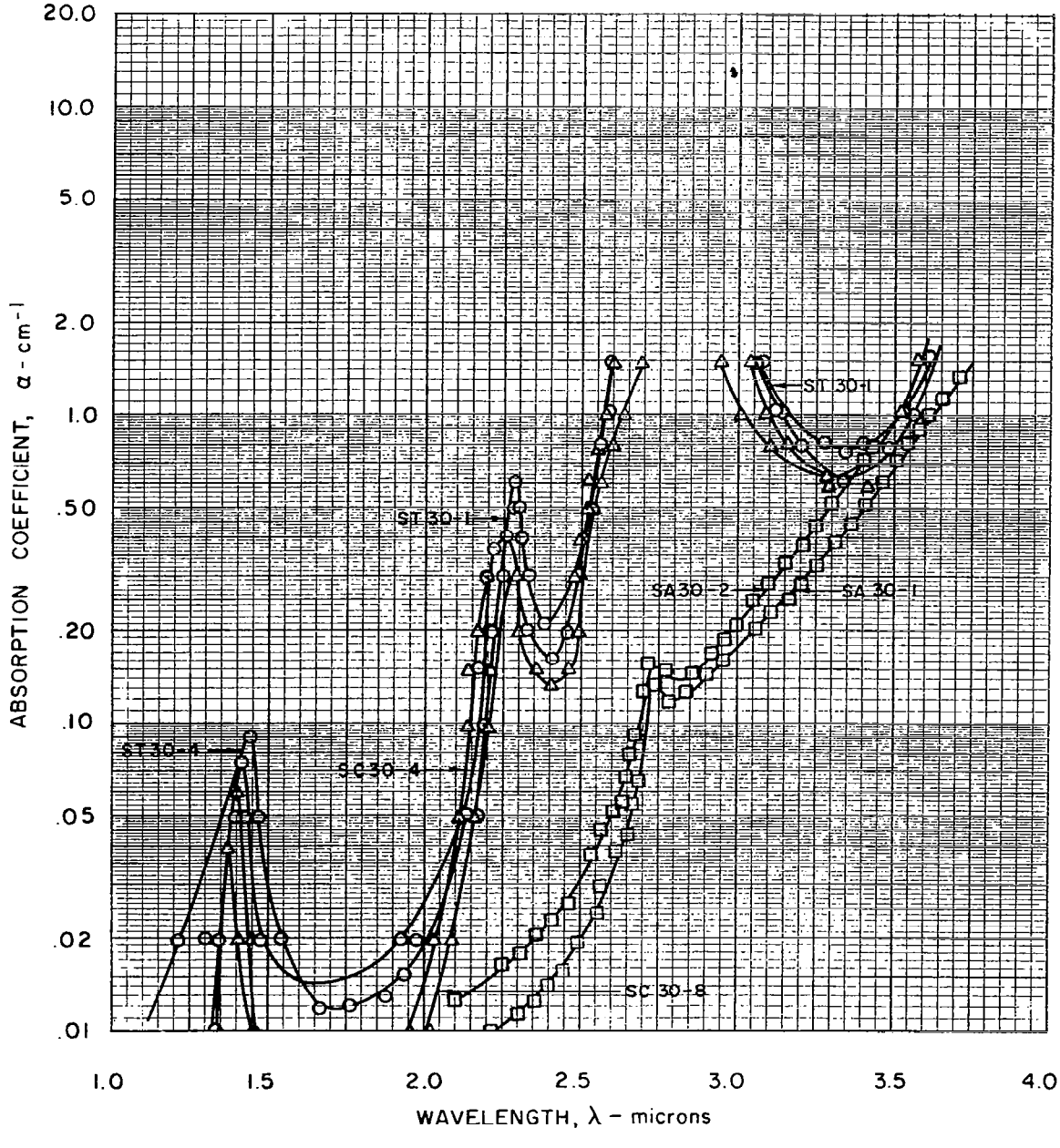

FIG. 34

VARIATION OF ULTRAVIOLET TRANSMITTANCE OF CORNING 1 mm SPECIMEN SC 1-1 WITH TEMPERATURE

HISTORY- PRE-HEATED TO 850 C- NOT CHEMICALLY CLEANED

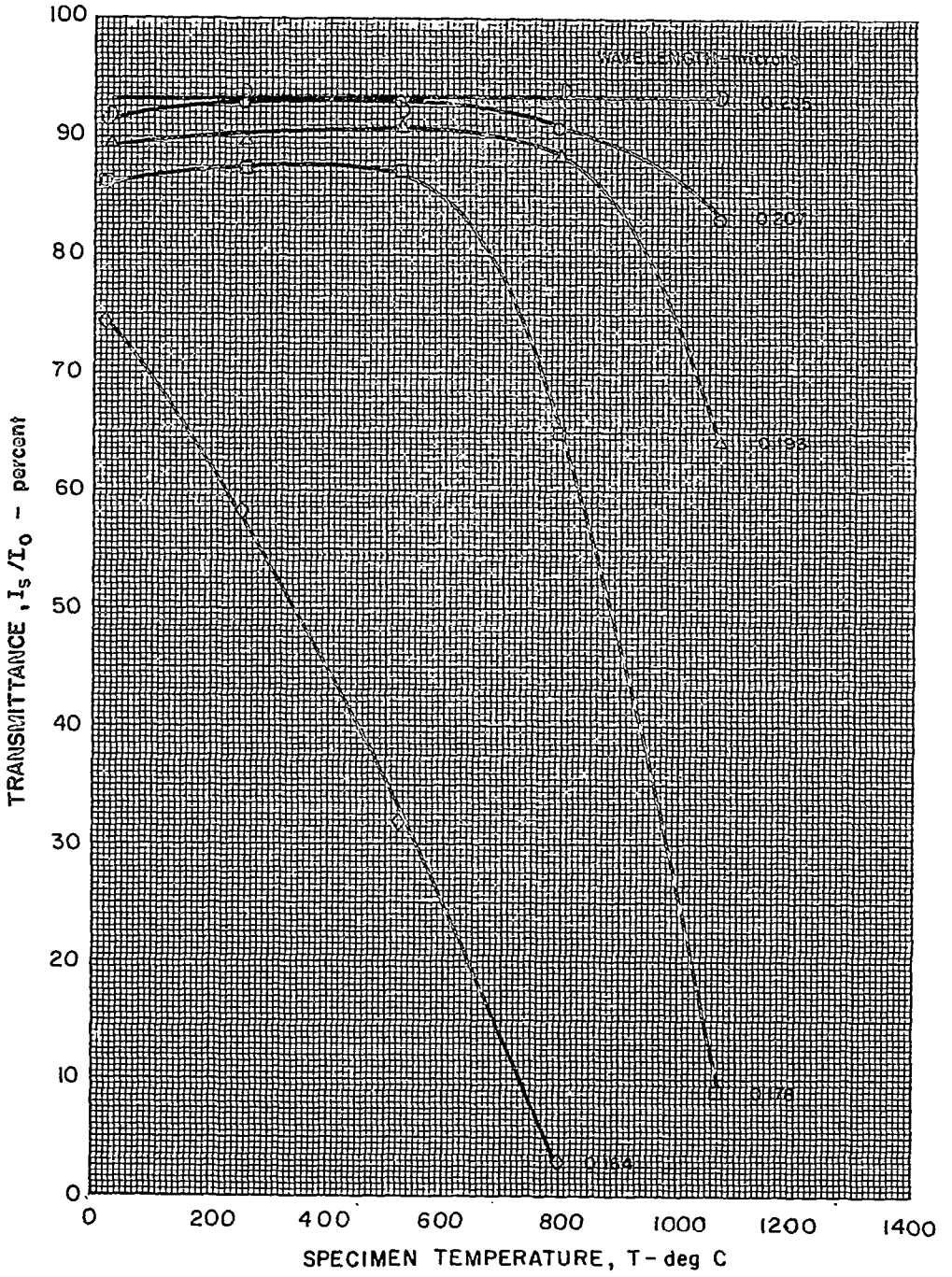

FIG. 35

VARIATION OF ULTRAVIOLET TRANSMITTANCE OF CORNING 2 mm SPECIMEN SC 2-11 WITH TEMPERATURE

HISTORY - PRE-HEATED TO 850 C - NOT CHEMICALLY CLEANED

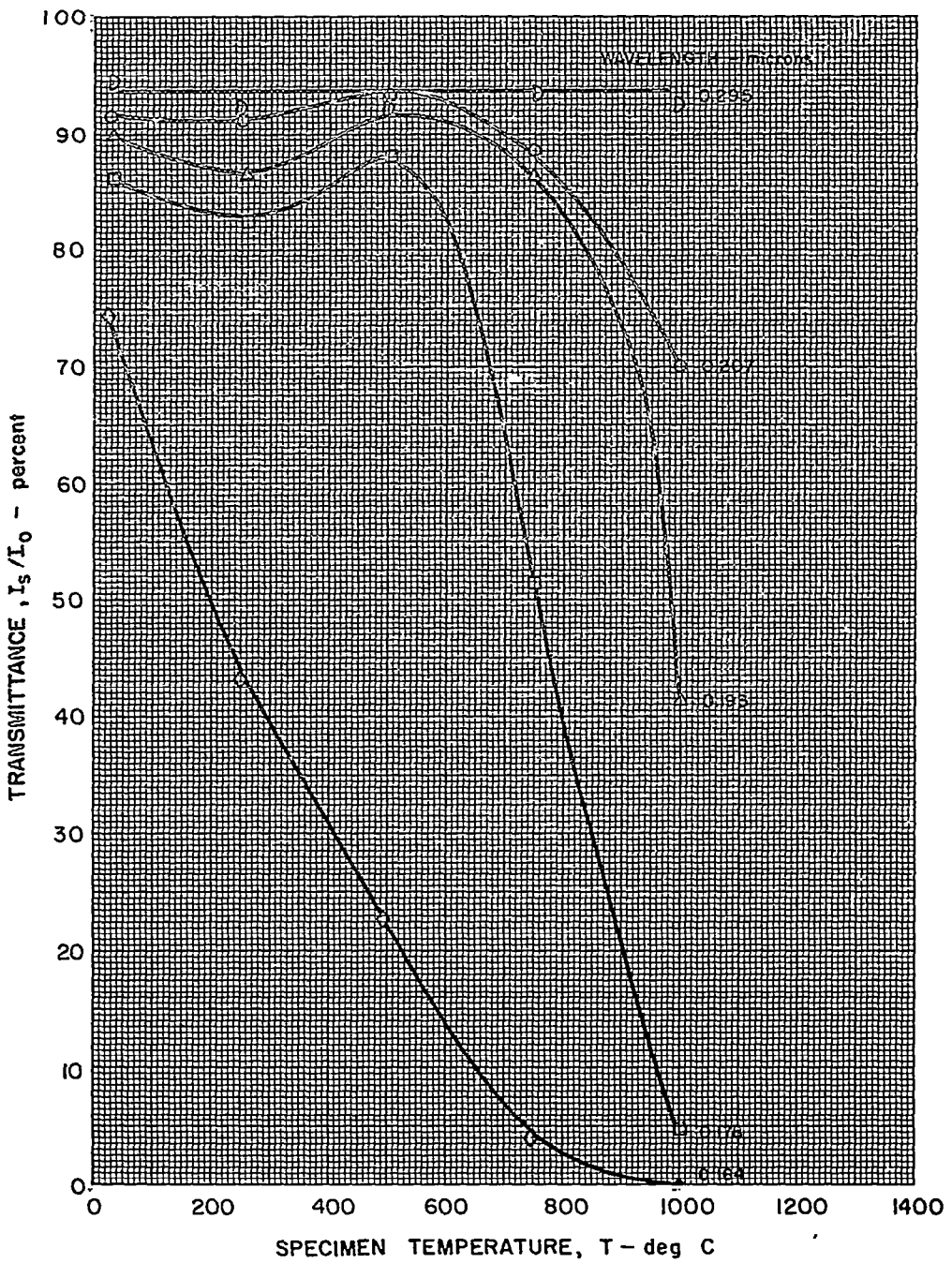

FIG. 36

VARIATION OF ULTRAVIOLET TRANSMISSIVITY OF AMERSIL 8 mm SPECIMEN SA 8-2 WITH TEMPERATURE

HISTORY - PRE-HEATED TO 850 C - NOT CHEMICALLY CLEANED
REFERENCE BEAM - SPECIMEN SA 2-3

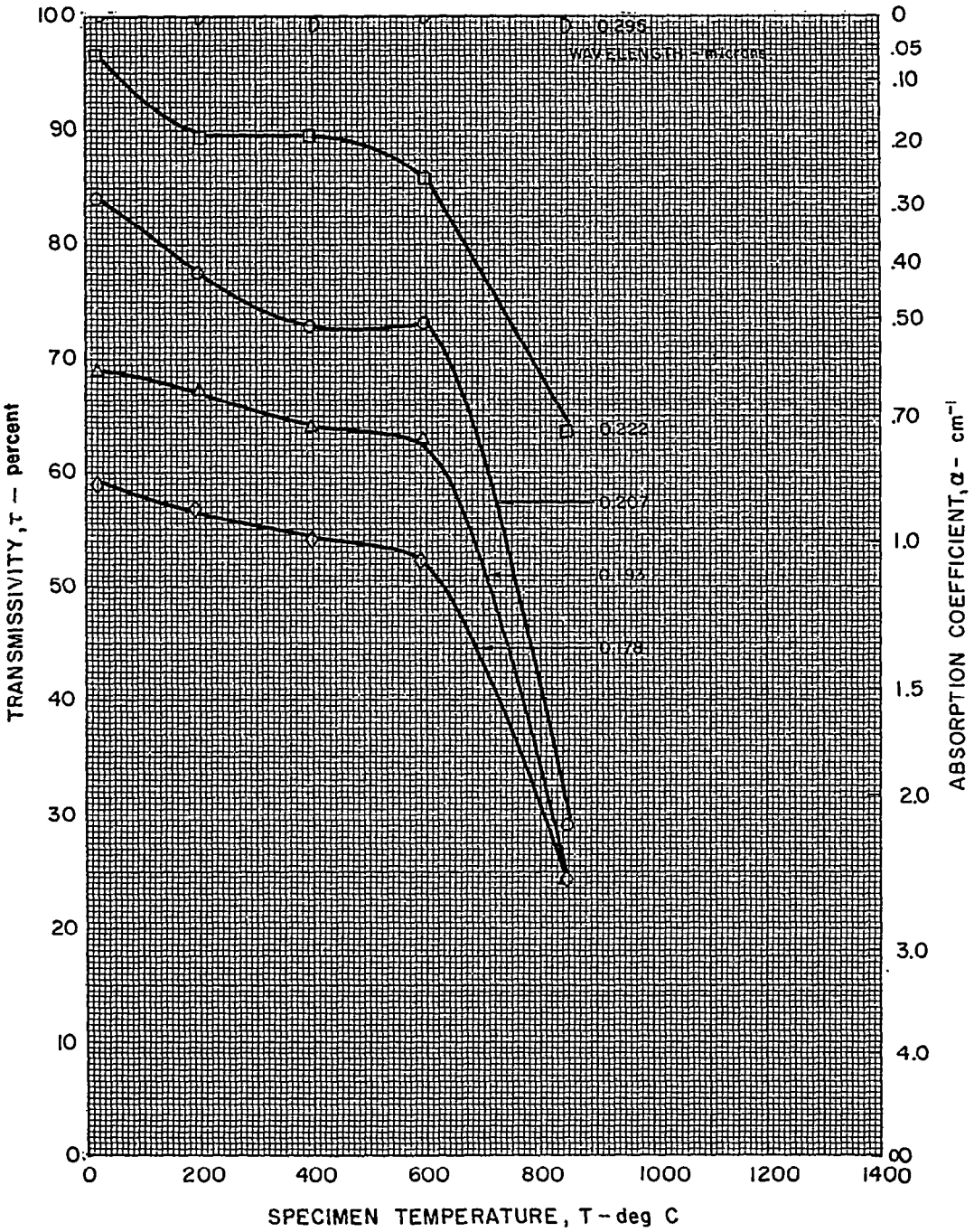

FIG. 37

VARIATION OF INFRARED TRANSMISSIVITY OF AMERSIL 8 mm SPECIMEN SA 8-2 WITH TEMPERATURE

HISTORY - PRE-HEATED TO 850 C - NOT CHEMICALLY CLEANED
REFERENCE BEAM - SPECIMEN SA 2-3

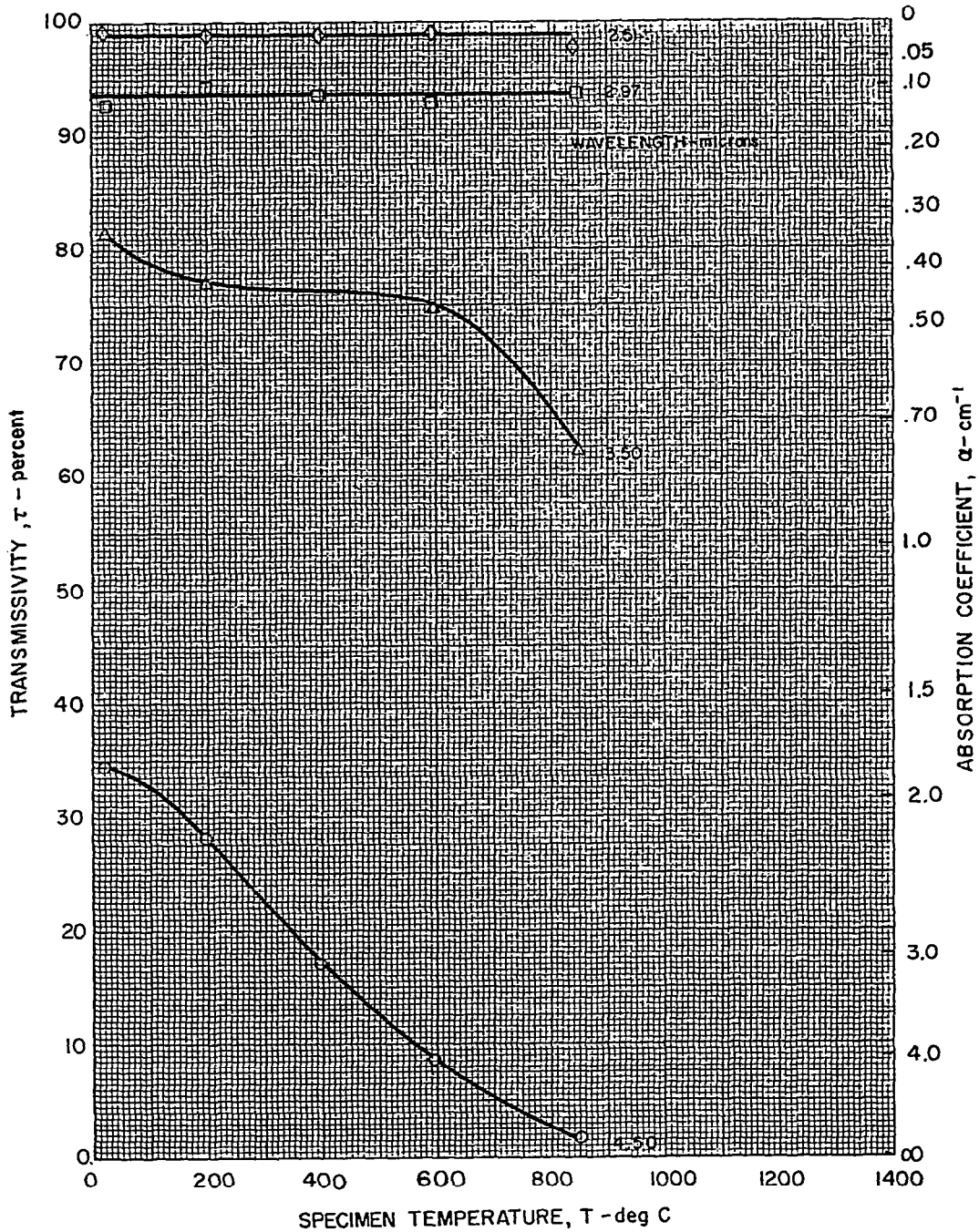

VARIATION OF ULTRAVIOLET TRANSMISSIVITY OF THERMAL AMERICAN 30 mm SPECIMEN ST 30-1 WITH TEMPERATURE

HISTORY - PRE-HEATED TO 850 C - NOT CHEMICALLY CLEANED
REFERENCE BEAM ST 1-3

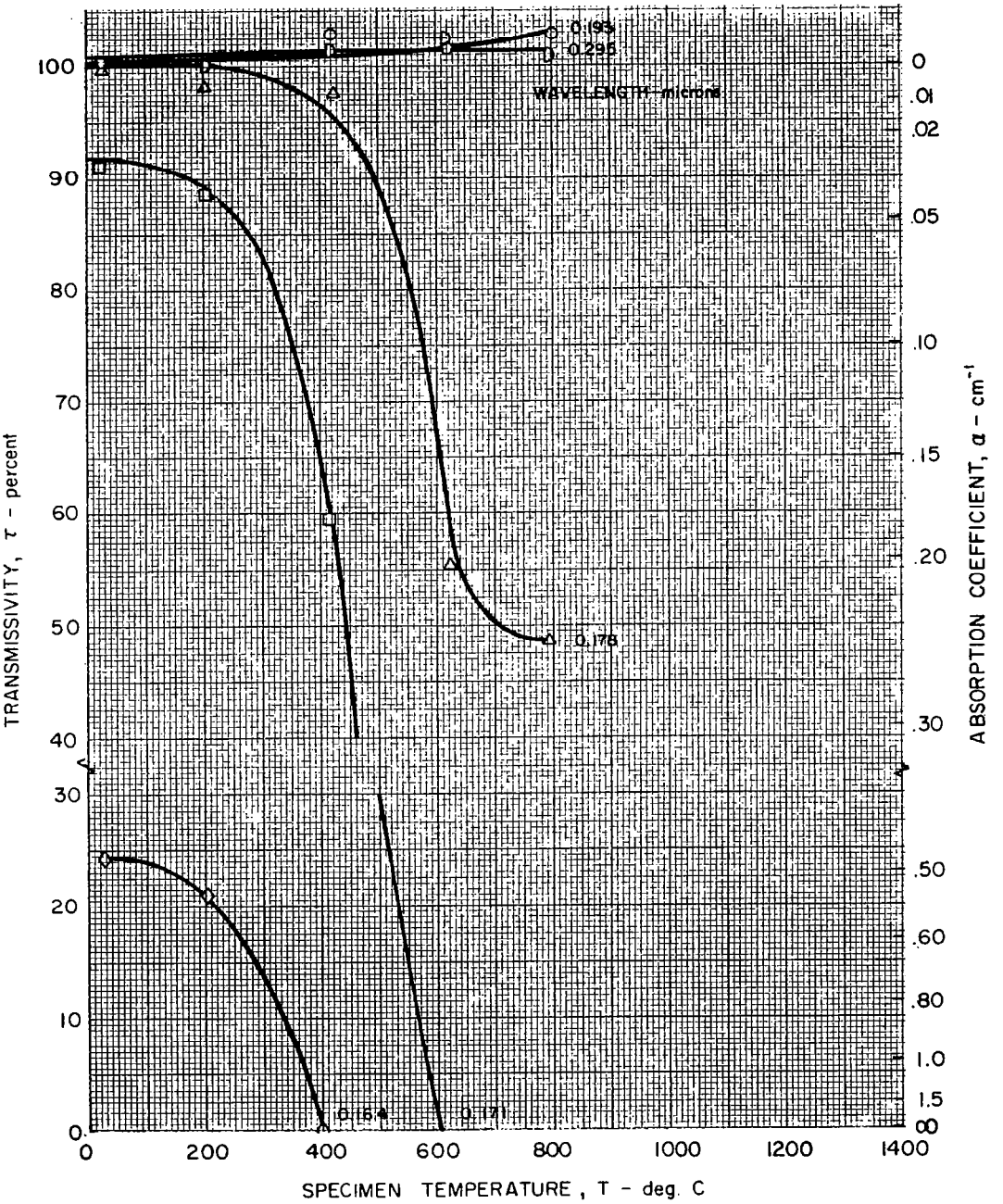

FIG. 39

VARIATION OF INFRARED TRANSMISSIVITY OF THERMAL AMERICAN 30 mm SPECIMEN ST 30-1 WITH TEMPERATURE

HISTORY - PRE-HEATED TO 850 C - NOT CHEMICALLY CLEANED
REFERENCE BEAM - SPECIMEN ST 1-3

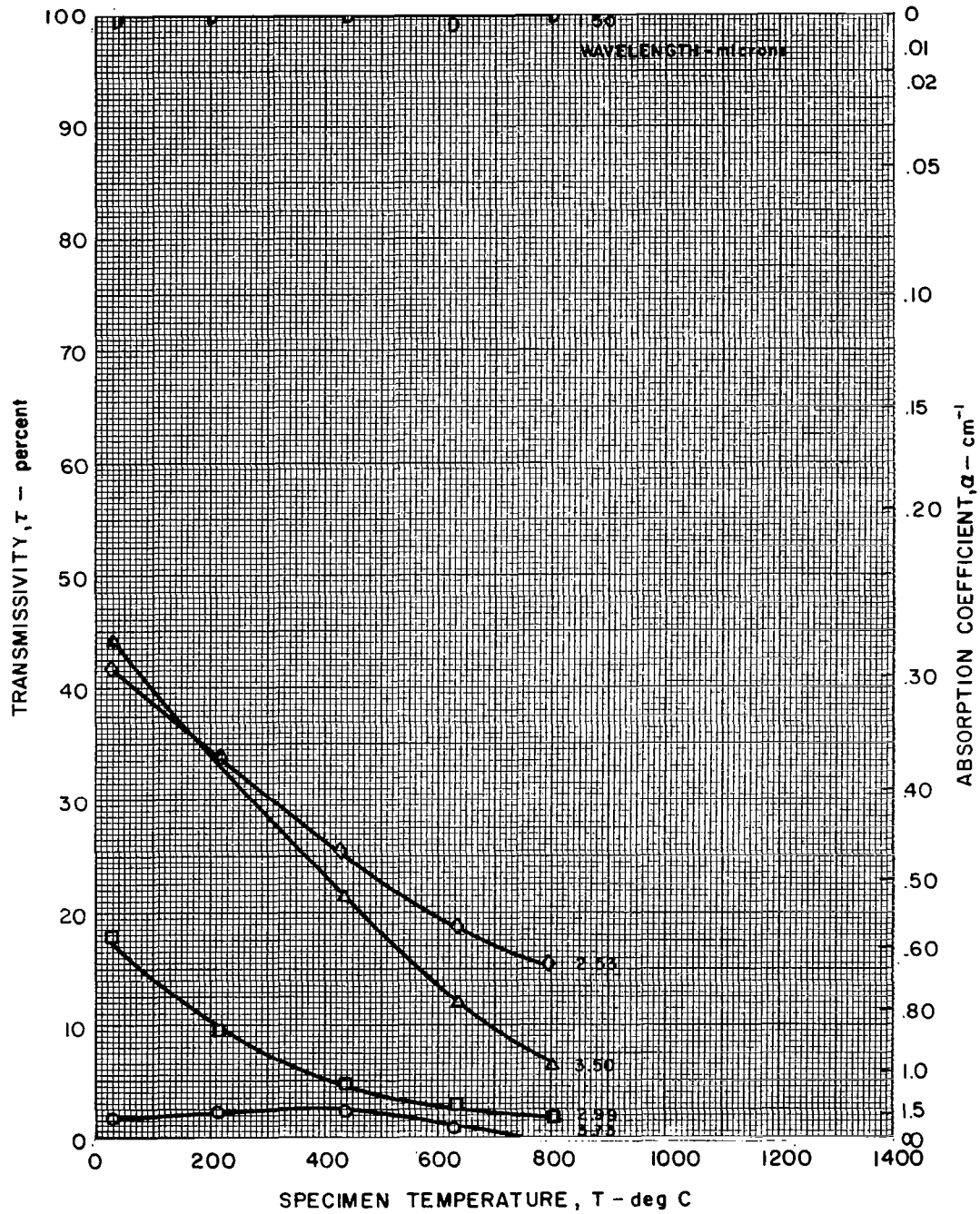

COMPARISON OF PRE-IRRADIATION TO POST-IRRADIATION, PRE-ANNEAL 22 C ABSORPTION COEFFICIENT DATA FOR CORNING, AMERSIL, AND THERMAL AMERICAN SPECIMENS

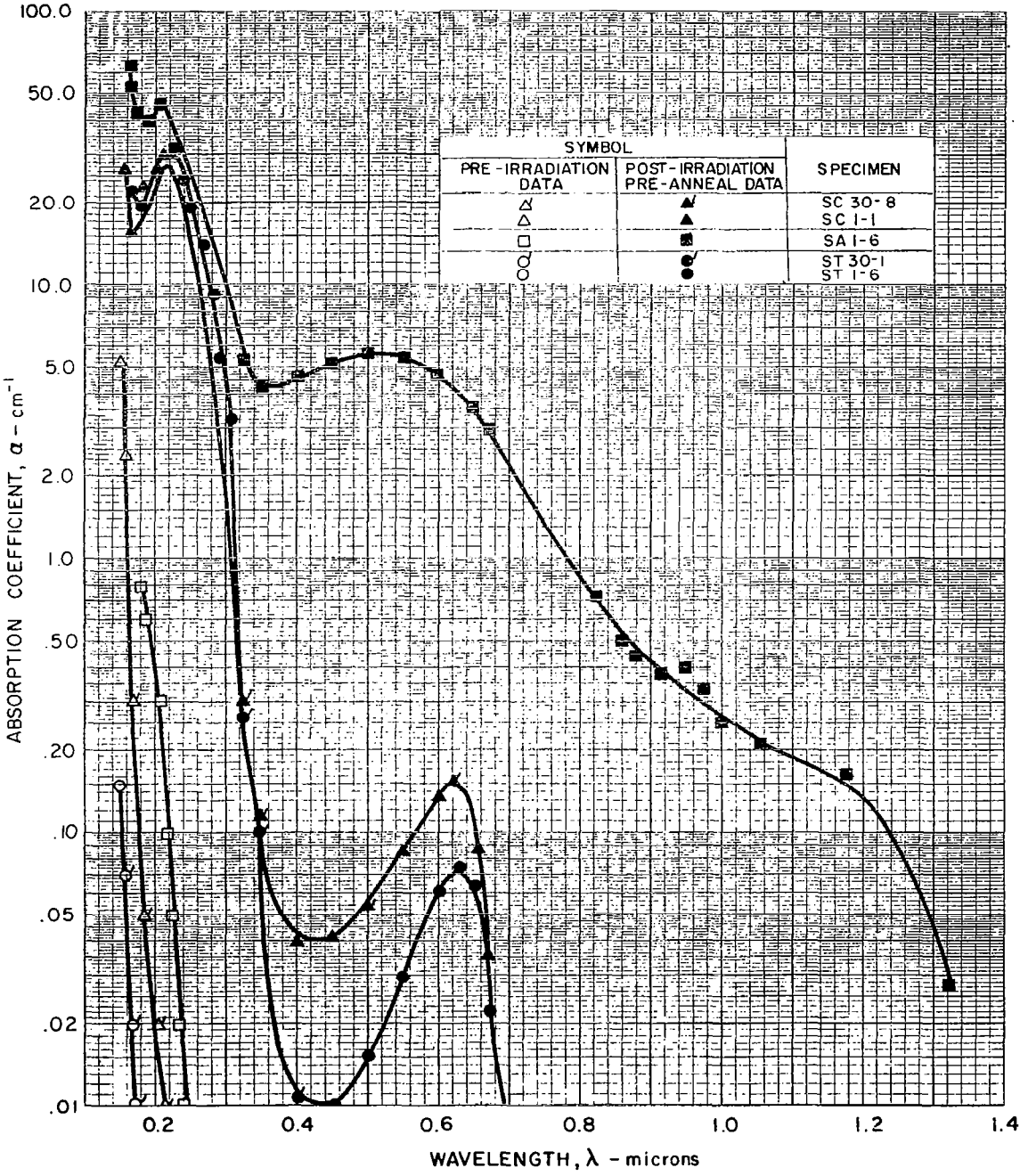

FIG. 41

COMPARISON OF 22 C INFRARED TRANSMITTANCE OF THERMAL AMERICAN 1 mm SPECIMEN ST 1-6 AFTER IRRADIATION BUT BEFORE ANNEALING WITH THERMAL AMERICAN 1 mm SPECIMEN ST 1-4 BEFORE IRRADIATION

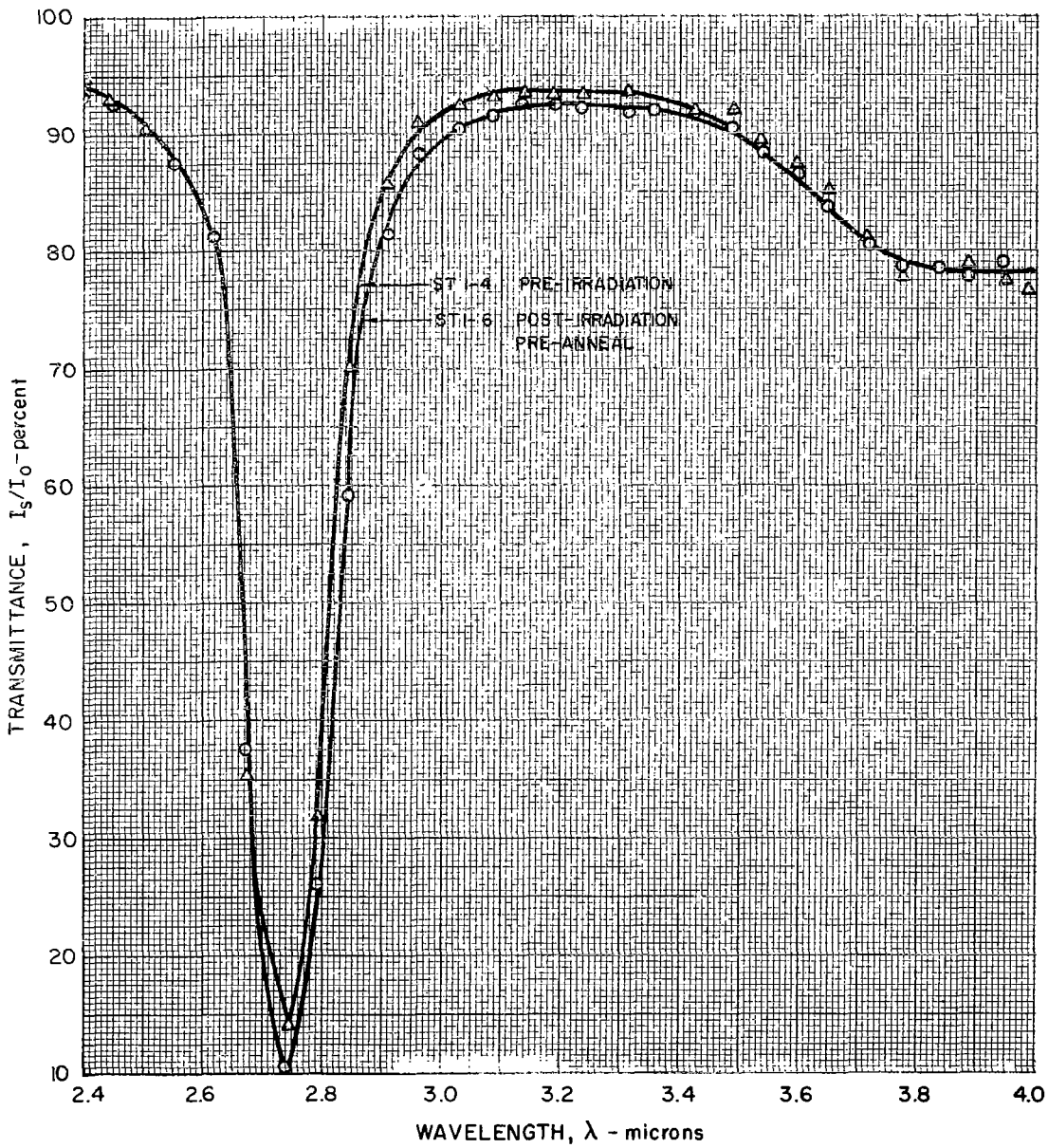

FIG. 42

VARIATION OF TRANSMITTANCE OF CORNING 1 mm SPECIMEN SC 1-1 MEASURED AT 0.215 microns DURING ANNEAL OF REACTOR-INDUCED COLOR

NO SPECIMEN IN REFERENCE BEAM

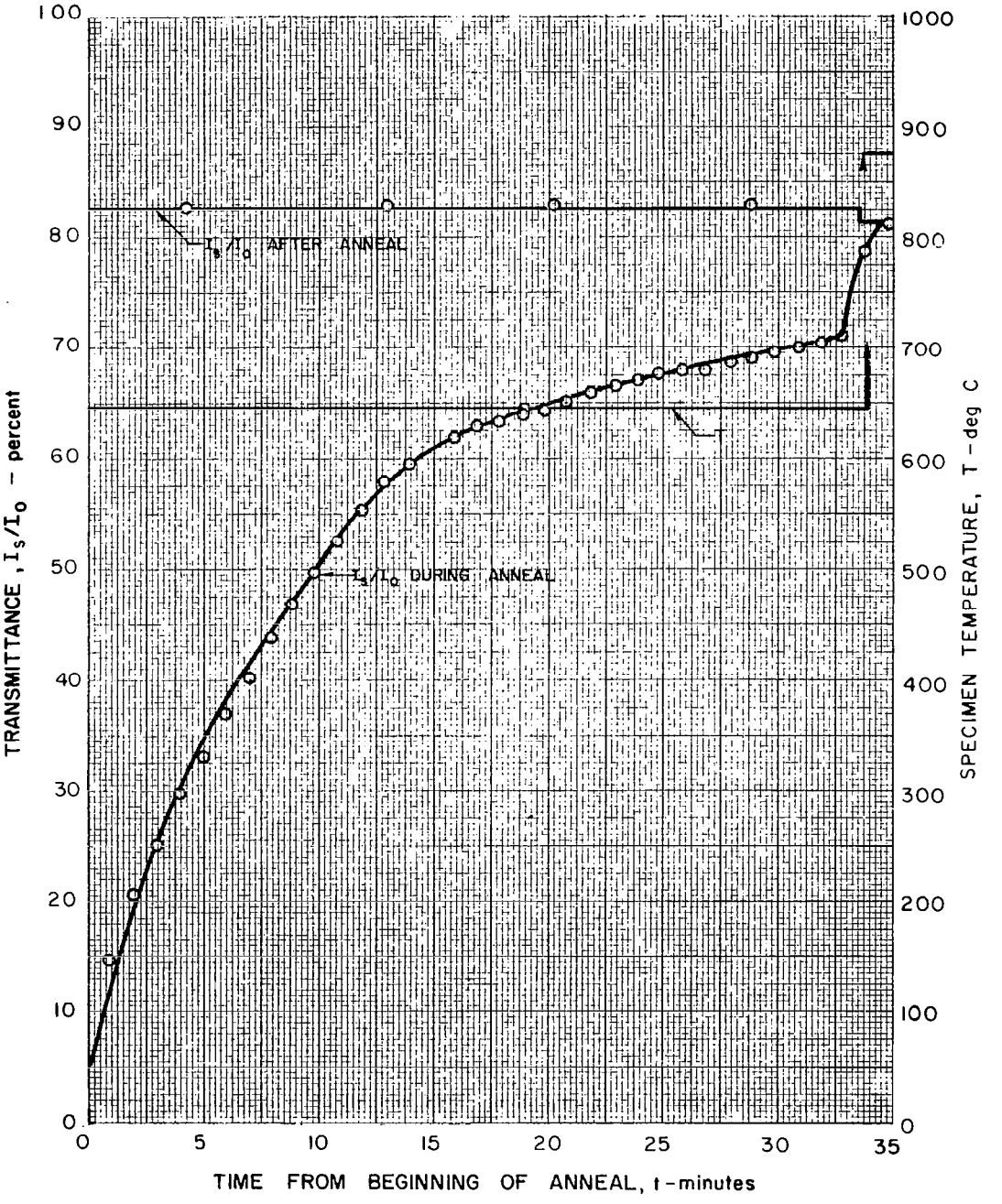

FIG. 43

VARIATION OF TRANSMITTANCE OF CORNING 1 mm SPECIMEN SC 1-3 MEASURED AT 0.215 microns DURING ANNEAL OF REACTOR-INDUCED COLOR

NO SPECIMEN IN REFERENCE BEAM

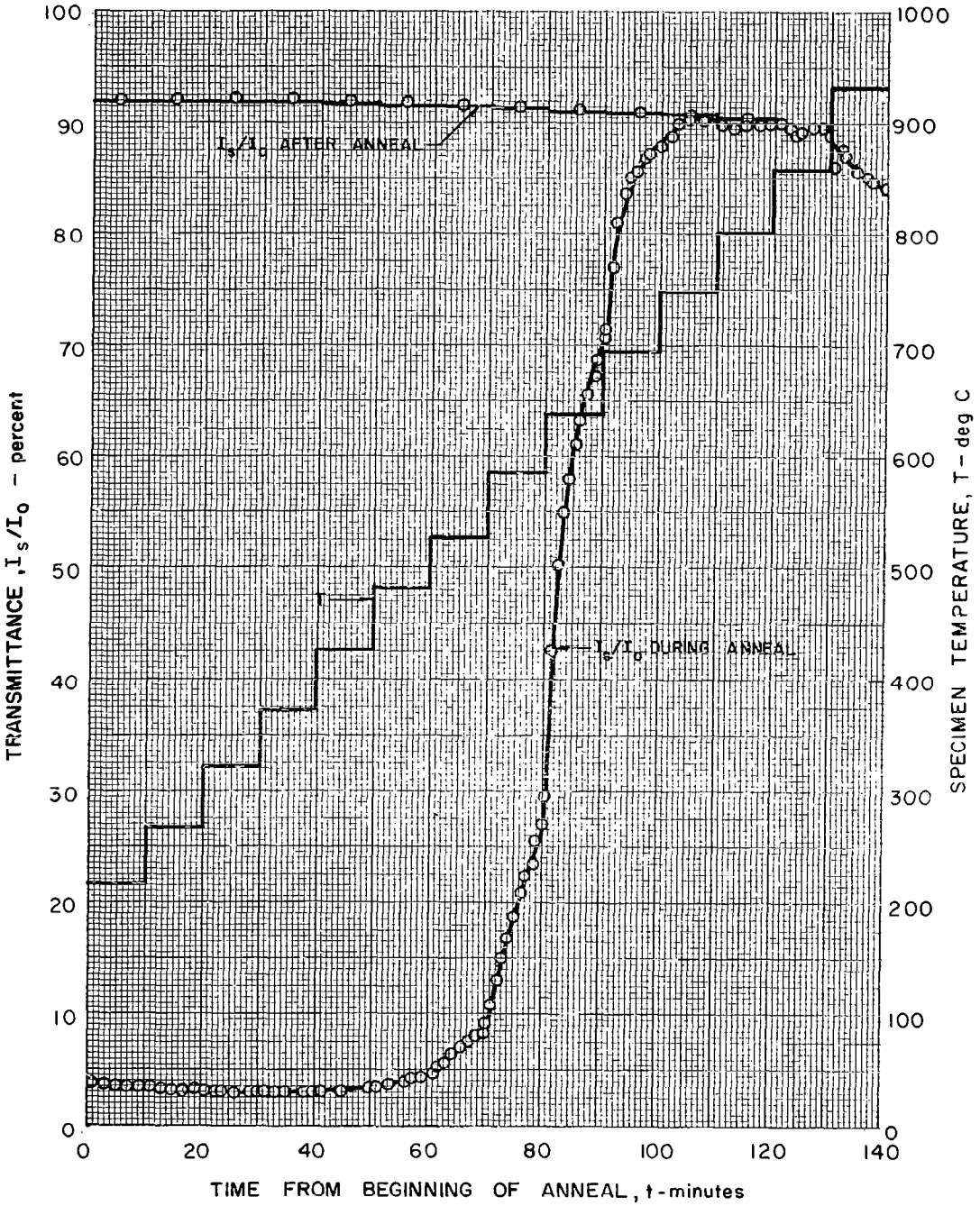

FIG. 44

VARIATION OF TRANSMITTANCE OF CORNING 2 mm SPECIMEN SC 2-II MEASURED AT 0.215 microns DURING ANNEAL OF REACTOR-INDUCED COLOR

NO SPECIMEN IN REFERENCE BEAM

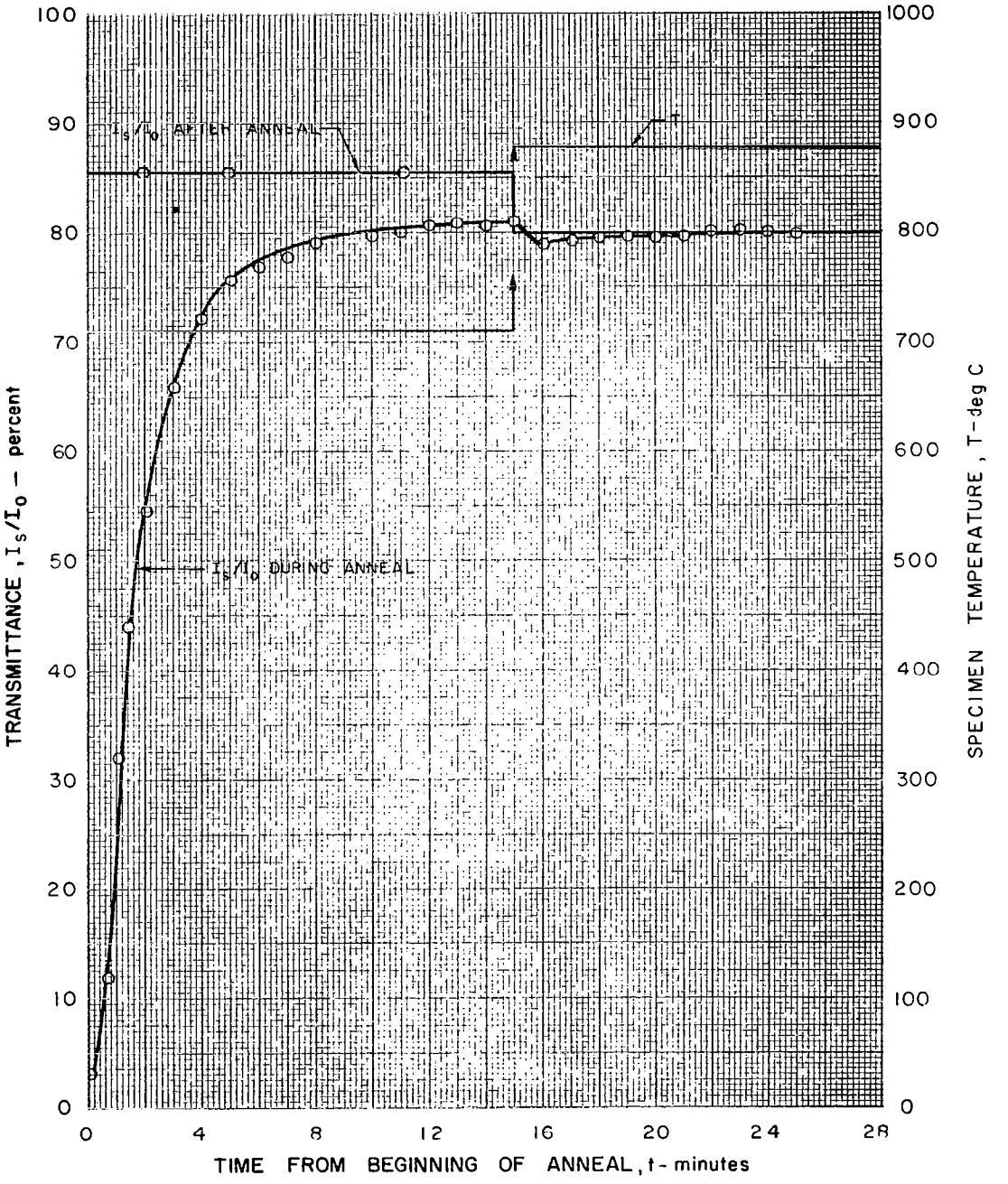

FIG. 45

VARIATION OF TRANSMITTANCE OF CORNING 30mm SPECIMEN SC30-4 MEASURED AT 0.215 microns DURING ANNEAL OF REACTOR-INDUCED COLOR

NO SPECIMEN IN REFERENCE BEAM

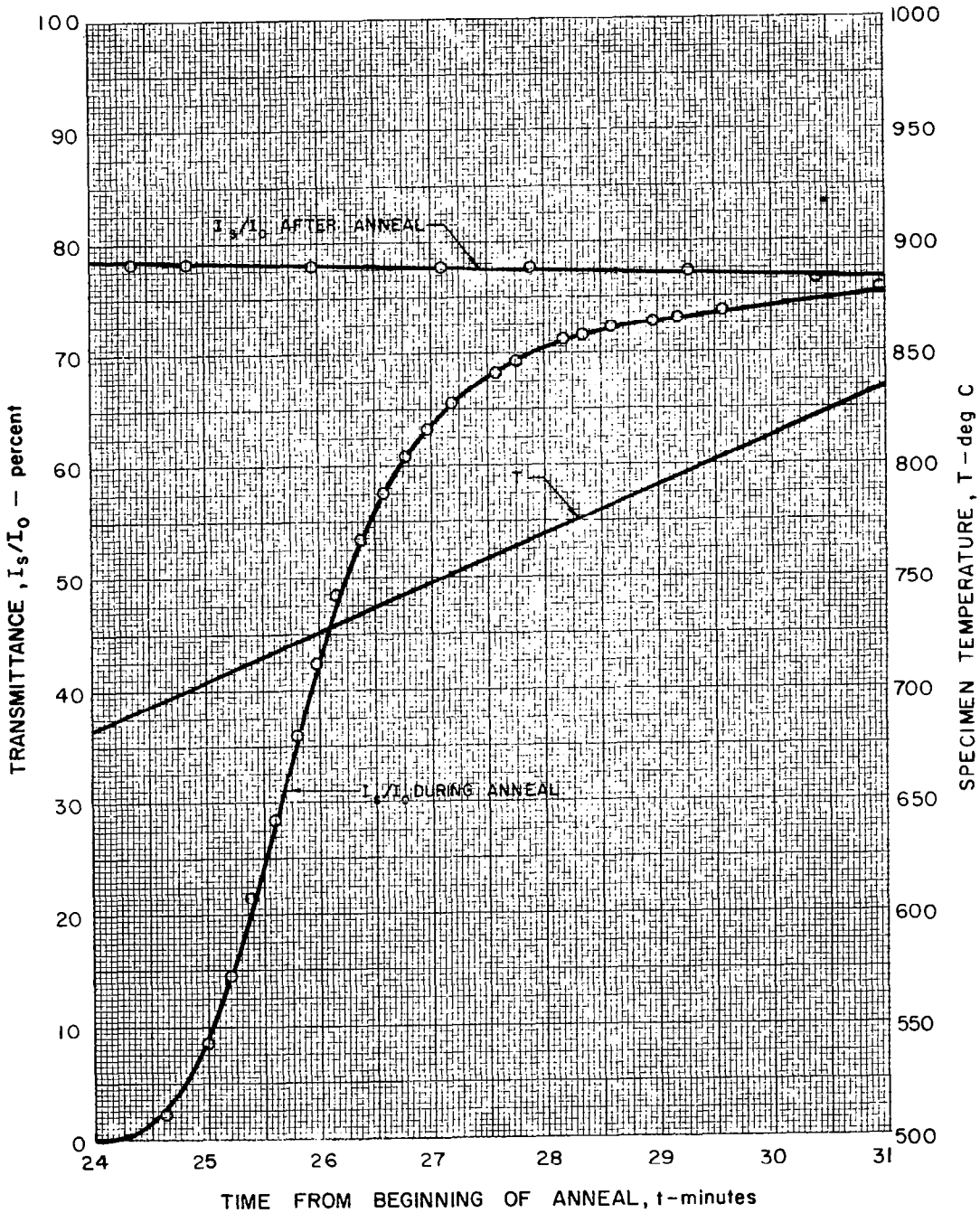

FIG. 46

VARIATION OF TRANSMITTANCE OF CORNING 30mm SPECIMEN SC30-8 MEASURED AT 0.210 microns DURING ANNEAL OF REACTOR-INDUCED COLOR

NO SPECIMEN IN REFERENCE BEAM

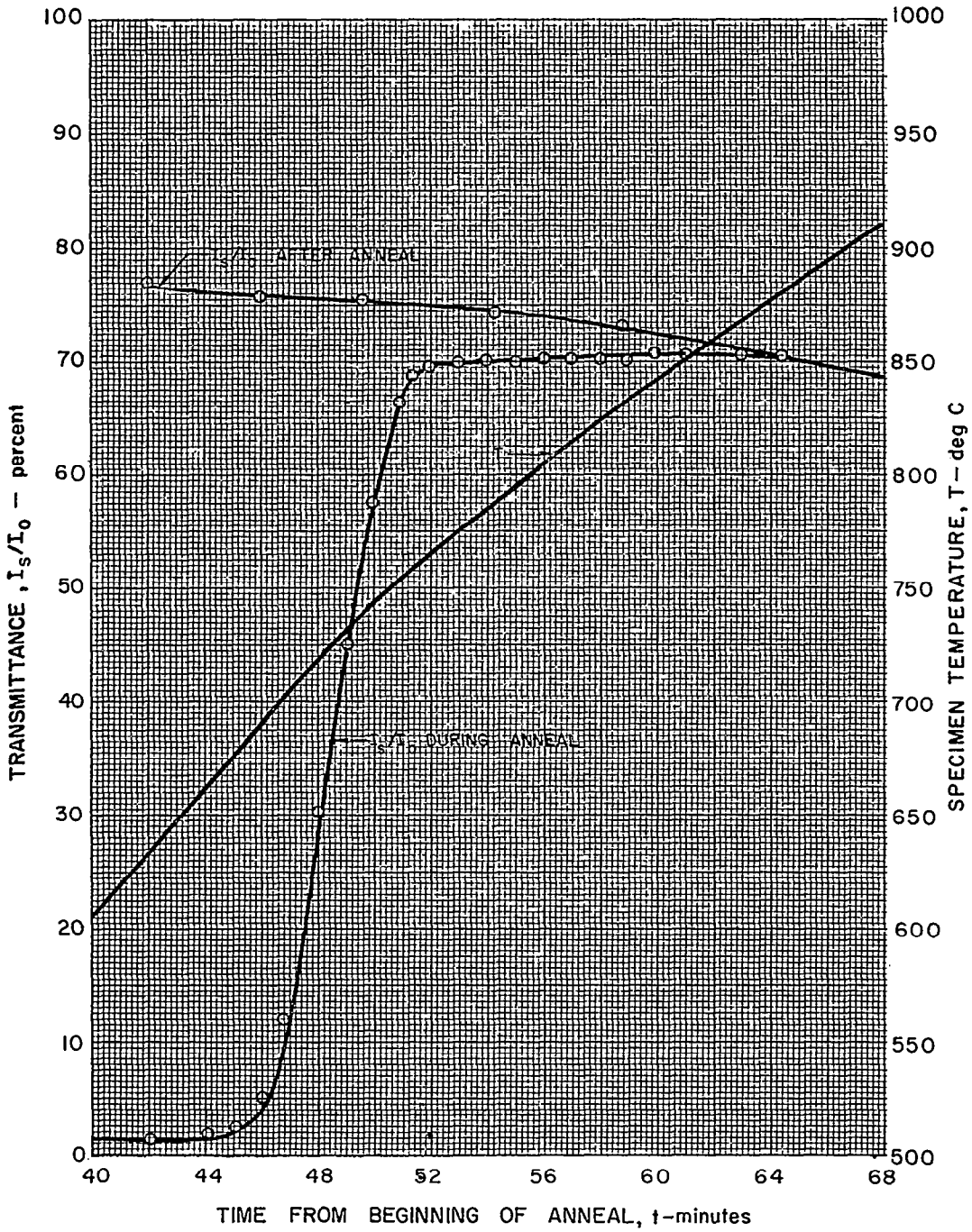

FIG. 47

VARIATION OF TRANSMITTANCE OF AMERSIL 1 mm SPECIMEN SA 1-5 MEASURED AT 0.210 microns DURING ANNEAL OF REACTOR-INDUCED COLOR

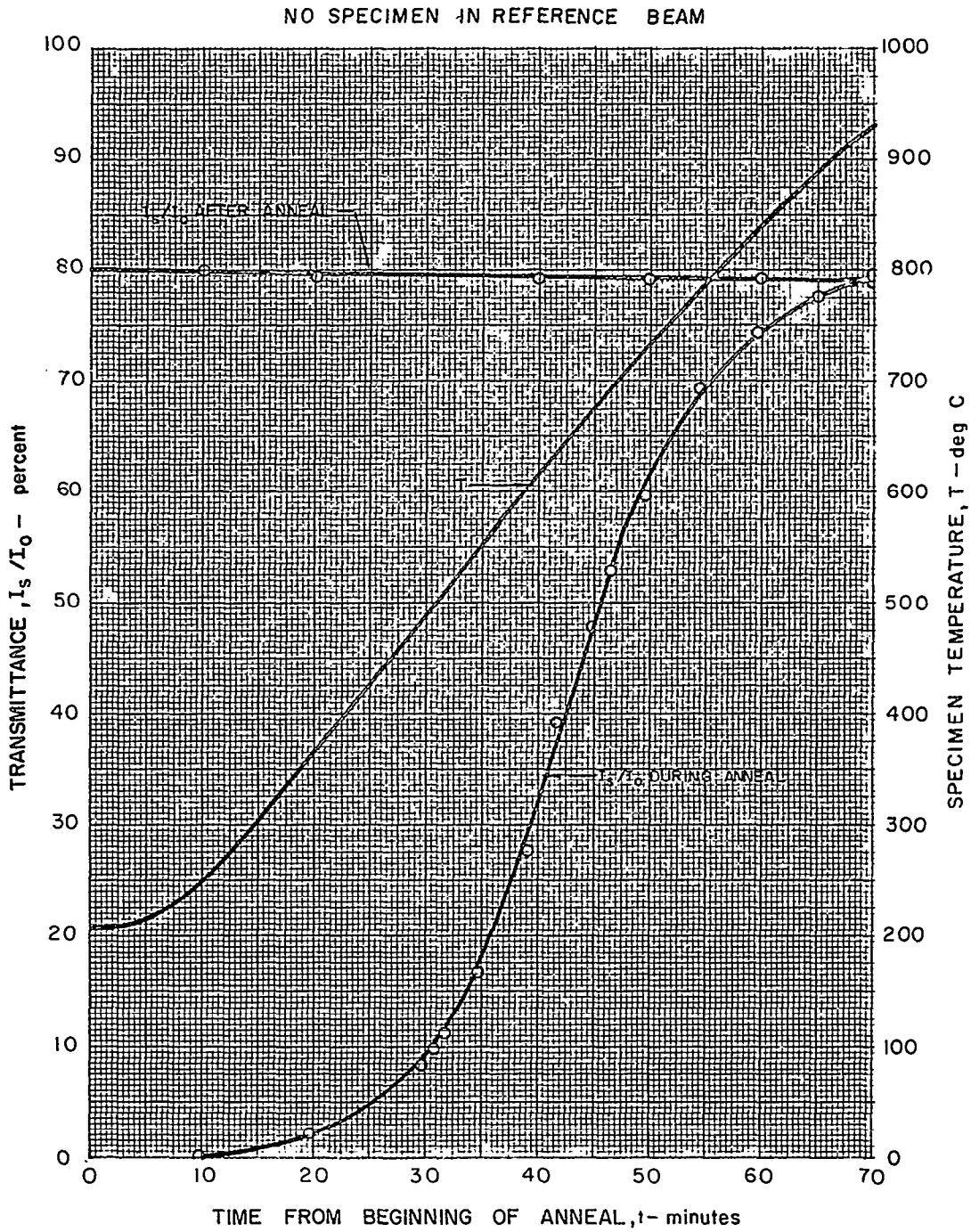

FIG. 48

VARIATION OF TRANSMITTANCE OF THERMAL AMERICAN 30 mm SPECIMEN ST 30-1 MEASURED AT 0.210 microns DURING ANNEAL OF REACTOR-INDUCED COLOR

NO SPECIMEN IN REFERENCE BEAM

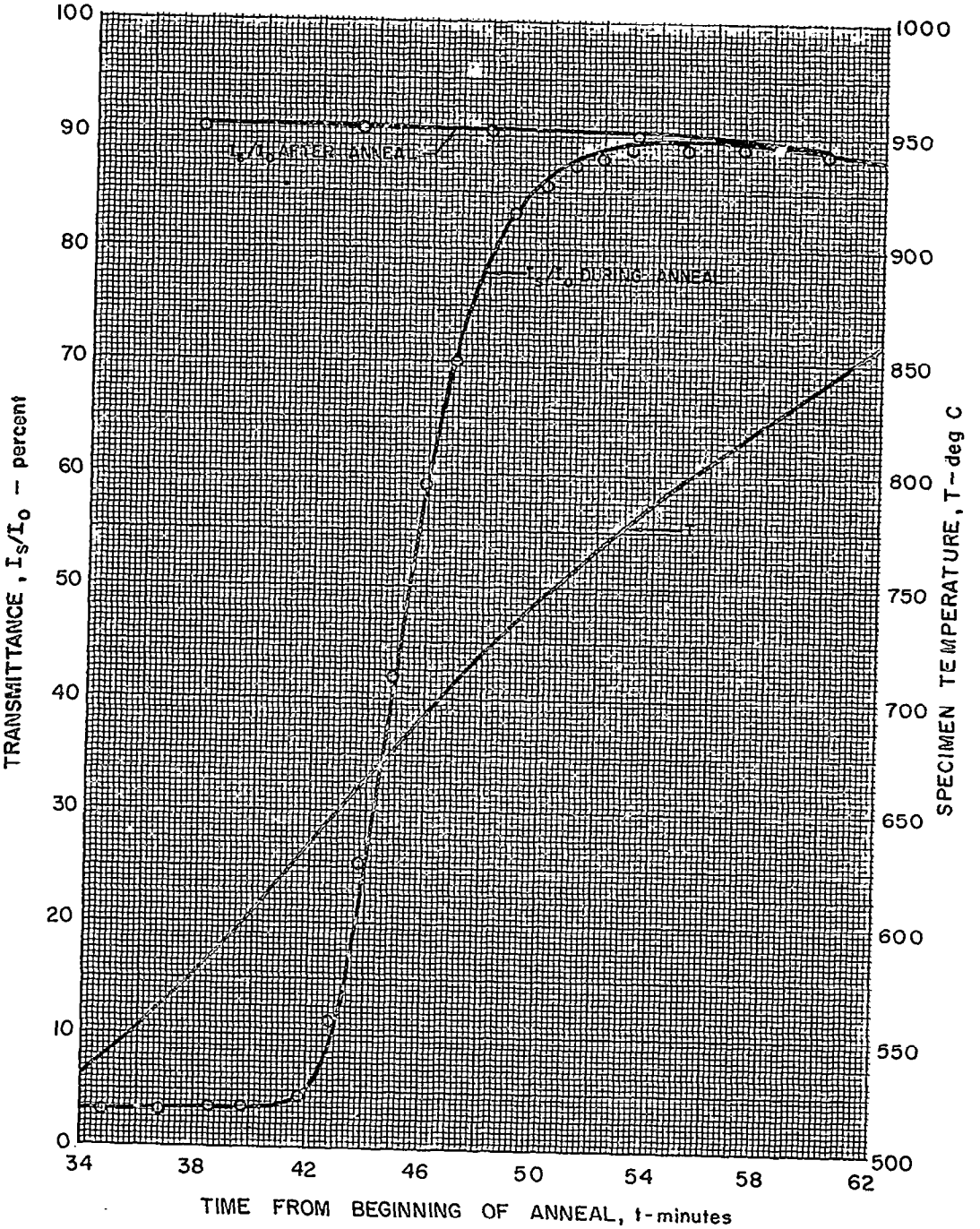

FIG. 49

VARIATION OF TRANSMITTANCE OF THERMAL AMERICAN 30 mm SPECIMEN ST 30-4 MEASURED AT 0.215 microns DURING ANNEAL OF REACTOR-INDUCED COLOR

NO SPECIMEN IN REFERENCE BEAM

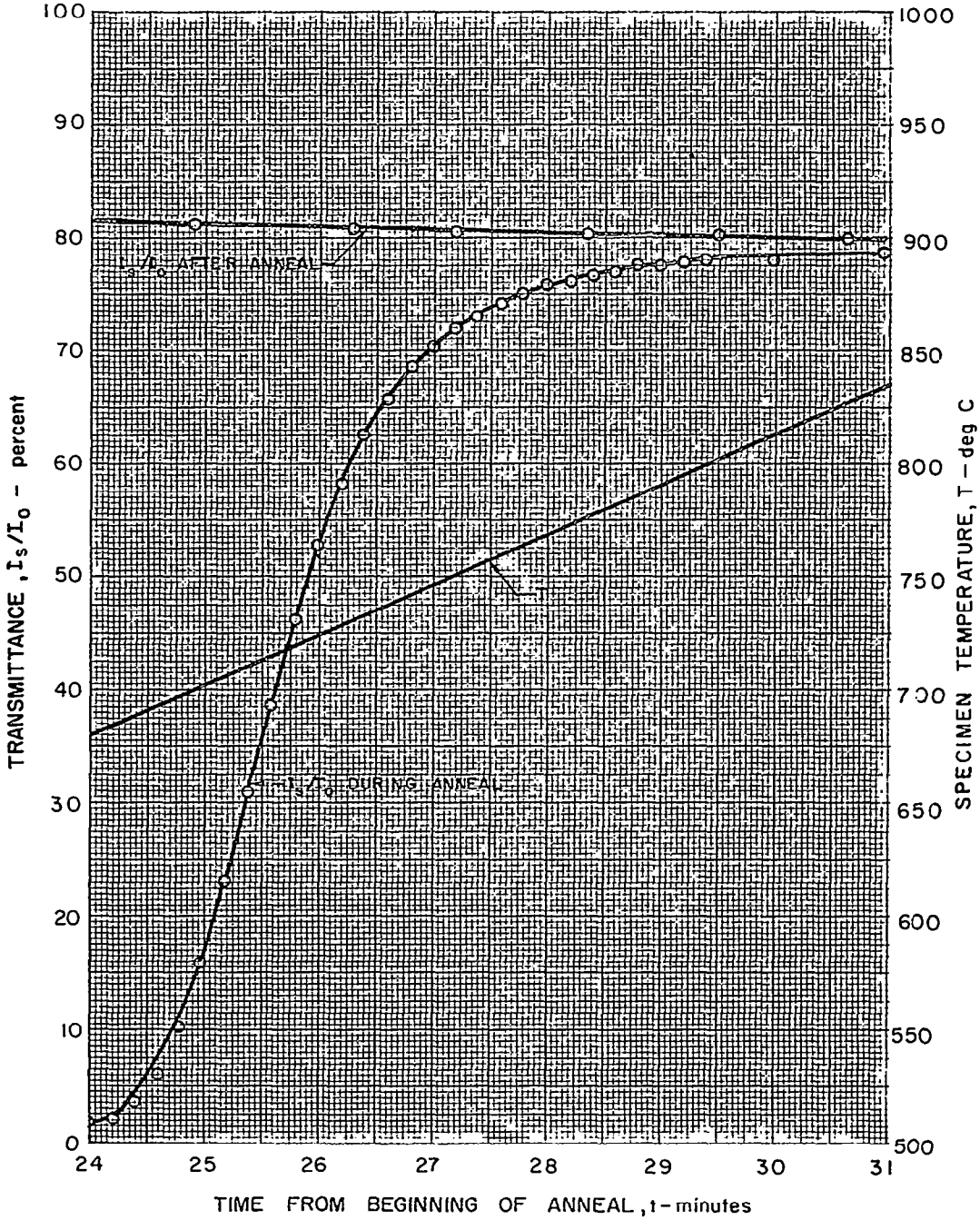

FIG. 50

VARIATION OF TRANSMITTANCE OF THERMAL AMERICAN 30mm SPECIMEN ST 30-5 MEASURED AT 0.215 microns DURING ANNEAL OF REACTOR-INDUCED COLOR

NO SPECIMEN IN REFERENCE BEAM

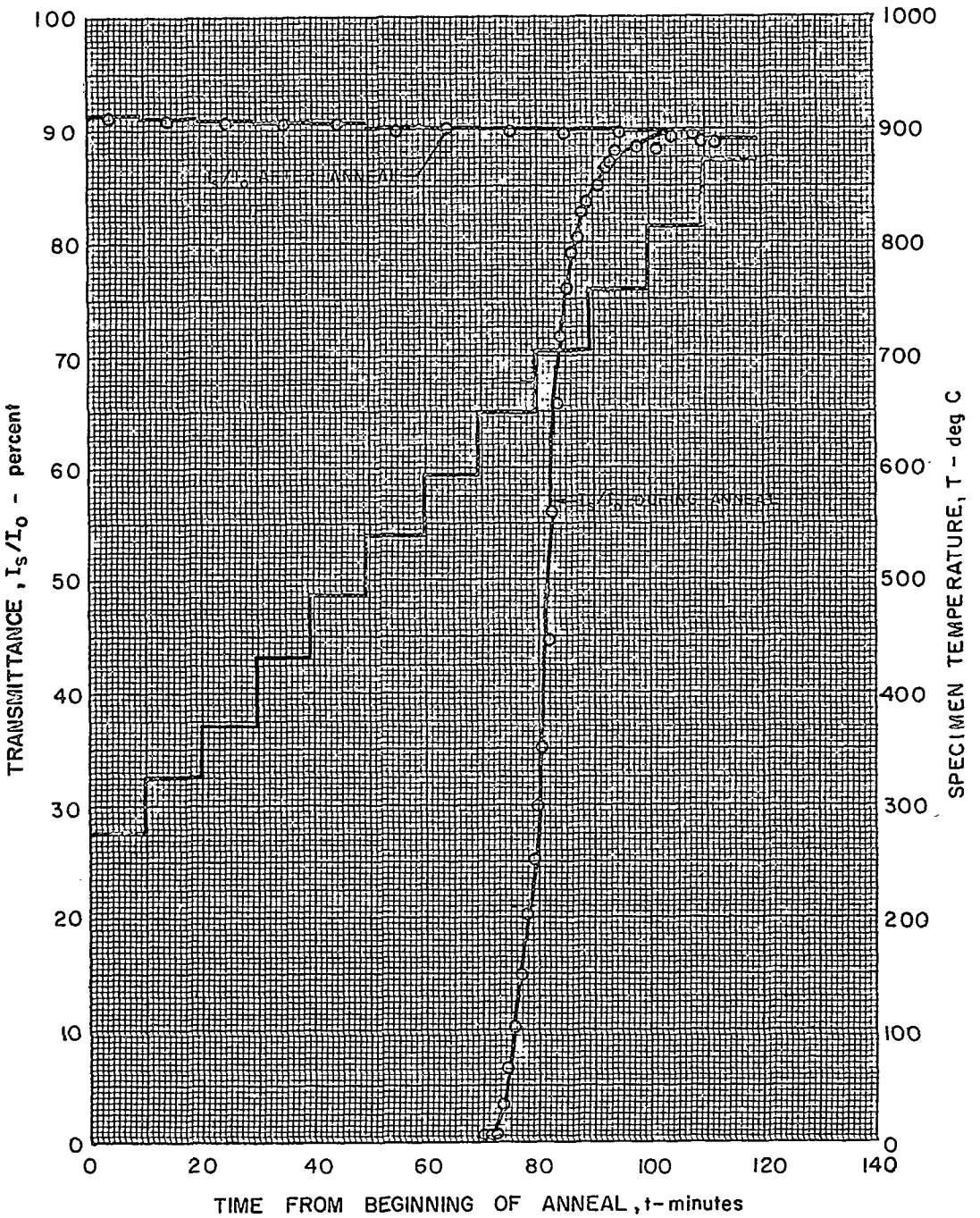

FIG. 51

VARIATION OF 22 C TRANSMITTANCE OF AMERSIL 1mm SPECIMEN SA1-1 MEASURED AT 0.210 microns DURING ANNEAL OF REACTOR-INDUCED COLOR

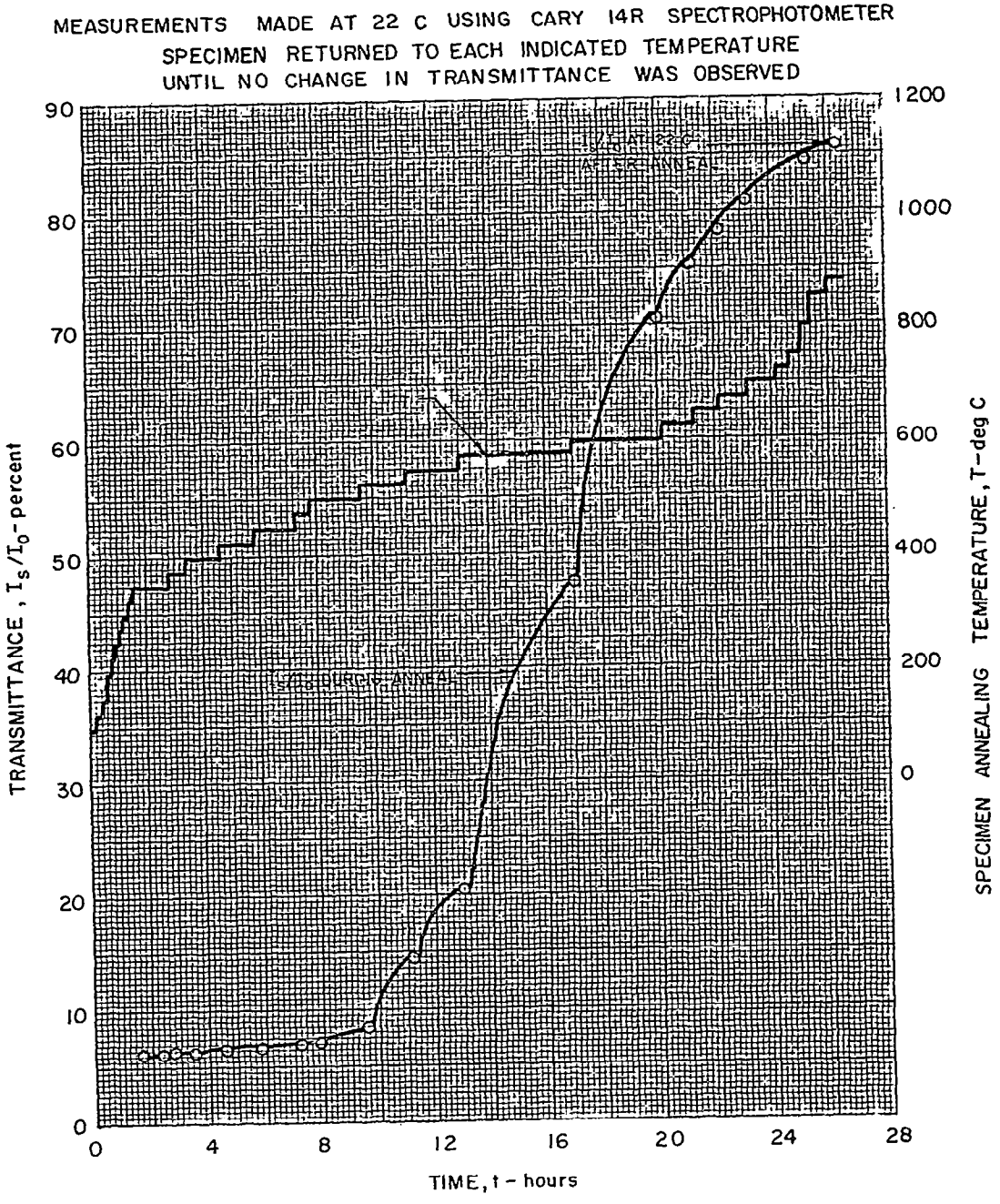

FIG. 52

VARIATION OF 22 C TRANSMITTANCE OF AMERSIL 1mm SPECIMEN SA1-1 MEASURED AT 0.50 microns DURING ANNEAL OF REACTOR-INDUCED COLOR

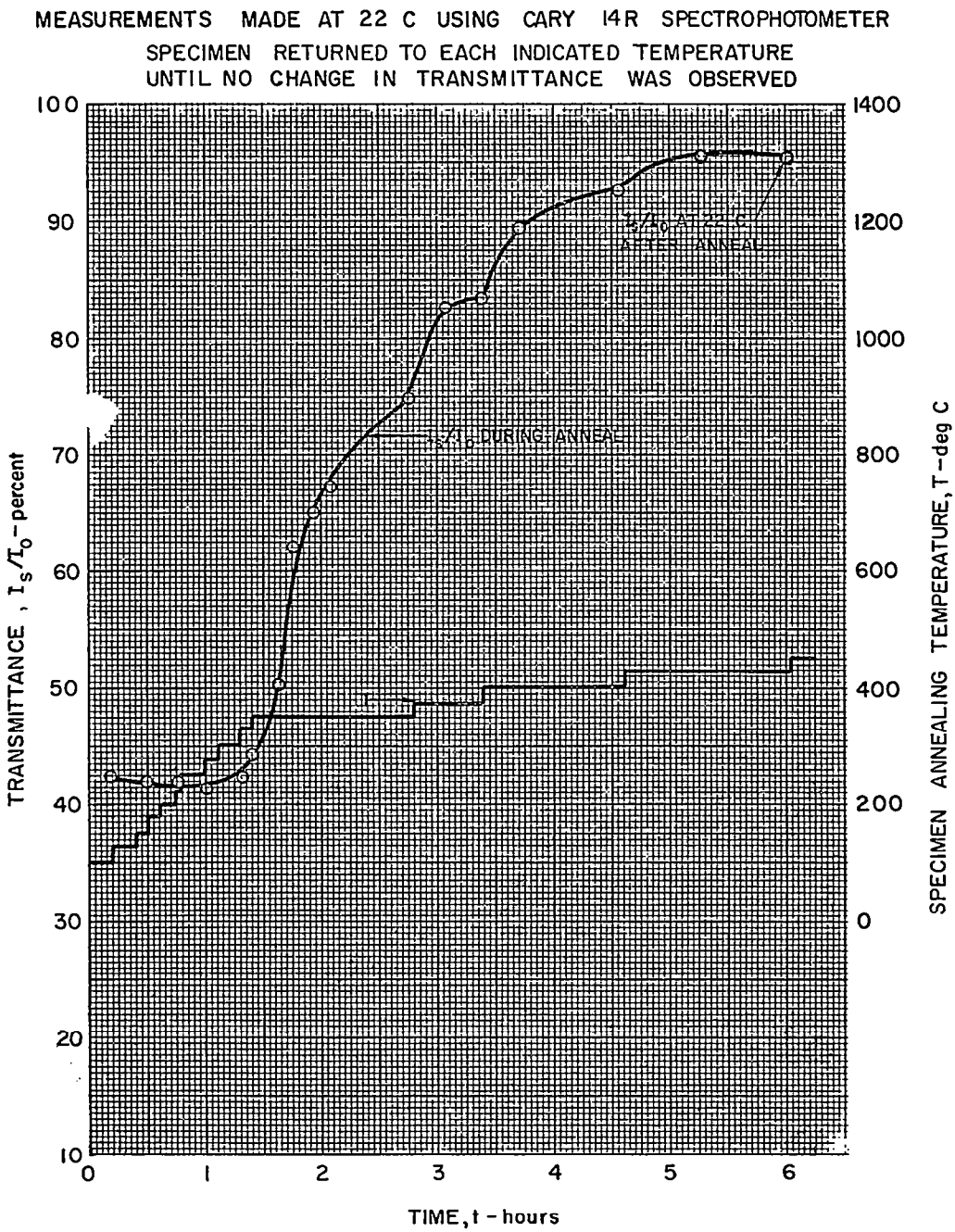

22 C TRANSMITTANCE OF AMERSIL 1 mm SPECIMEN SA1-1 AFTER ANNEAL AT CONSTANT TEMPERATURE UNTIL NO CHANGE OF ABSORPTION WAS OBSERVED

FIG. 53

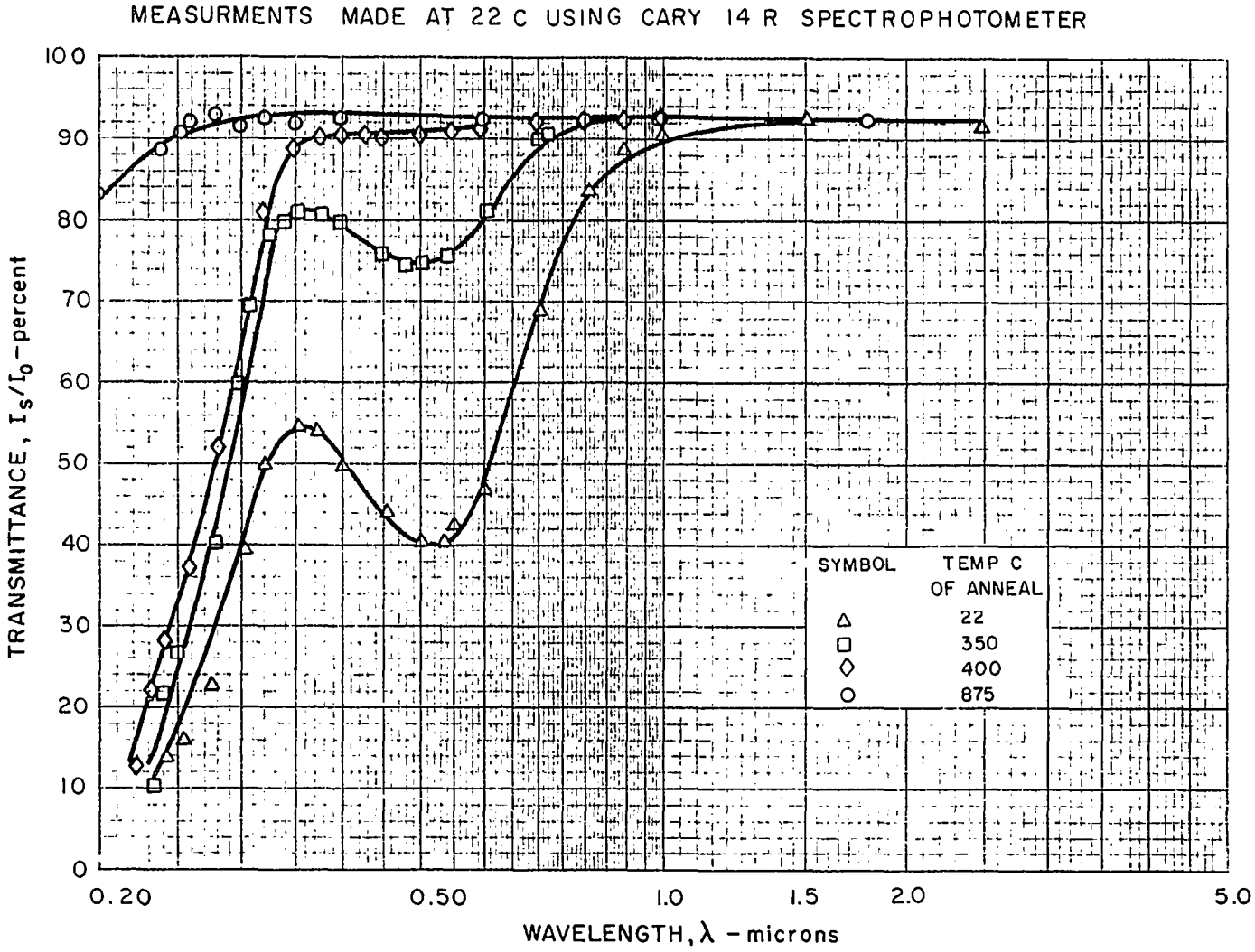

FIG. 54

REMAINING REACTOR-INDUCED COLOR IN INFRARED AFTER CUMULATIVE 100 C INCREMENT, 10-minute-CONSTANT-TEMPERATURE ANNEALS FOR AMERSIL 30 mm SPECIMEN SA 30-5

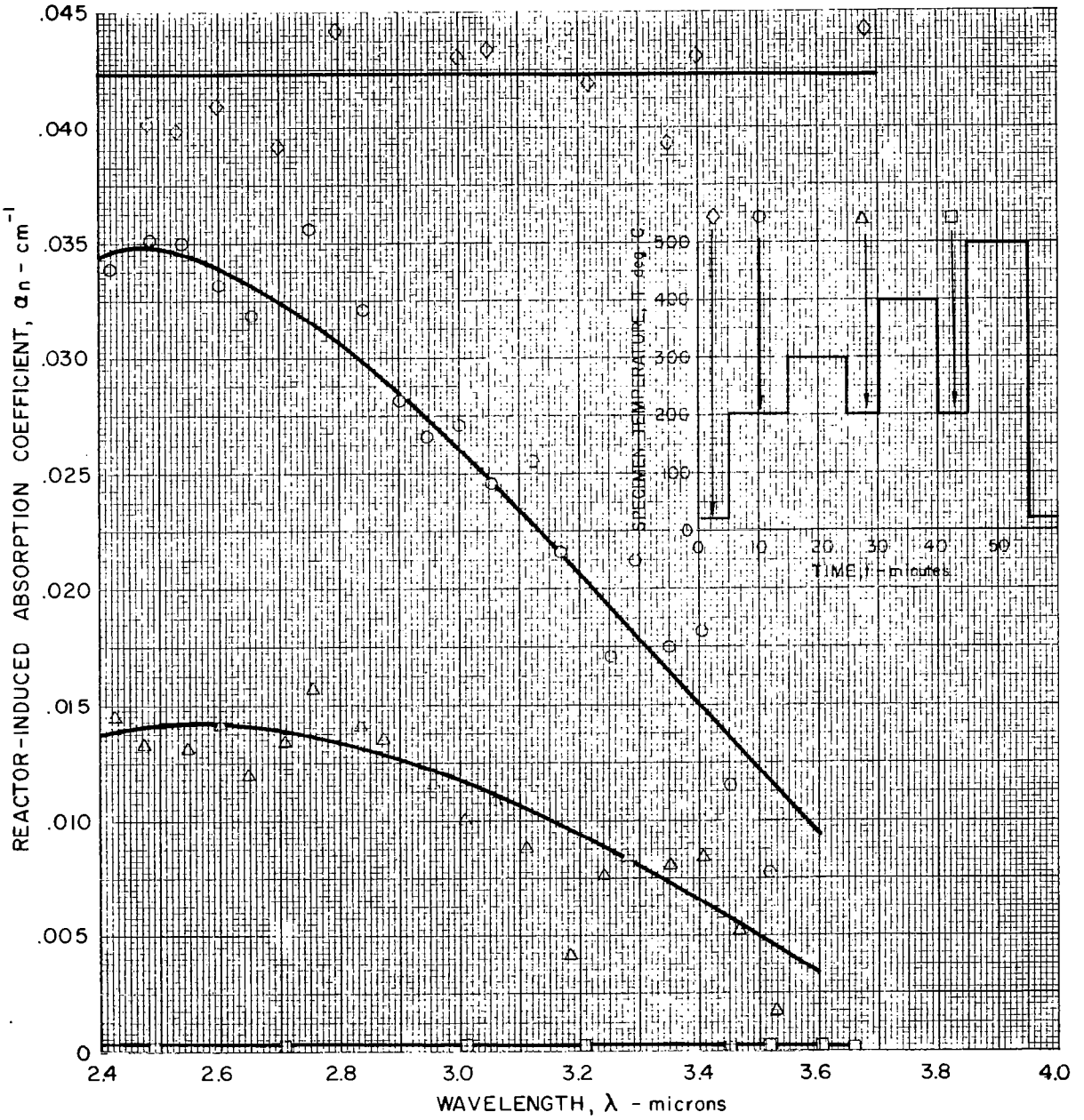

FIG. 55

VARIATION OF INDUCED ABSORPTION COEFFICIENT FOR CORNING 1 mm SPECIMEN SC 1-1 MEASURED AT 0.215 microns DURING ANNEAL OF REACTOR-INDUCED COLOR

α_n VALUES BASED ON DATA FROM FIG. 42

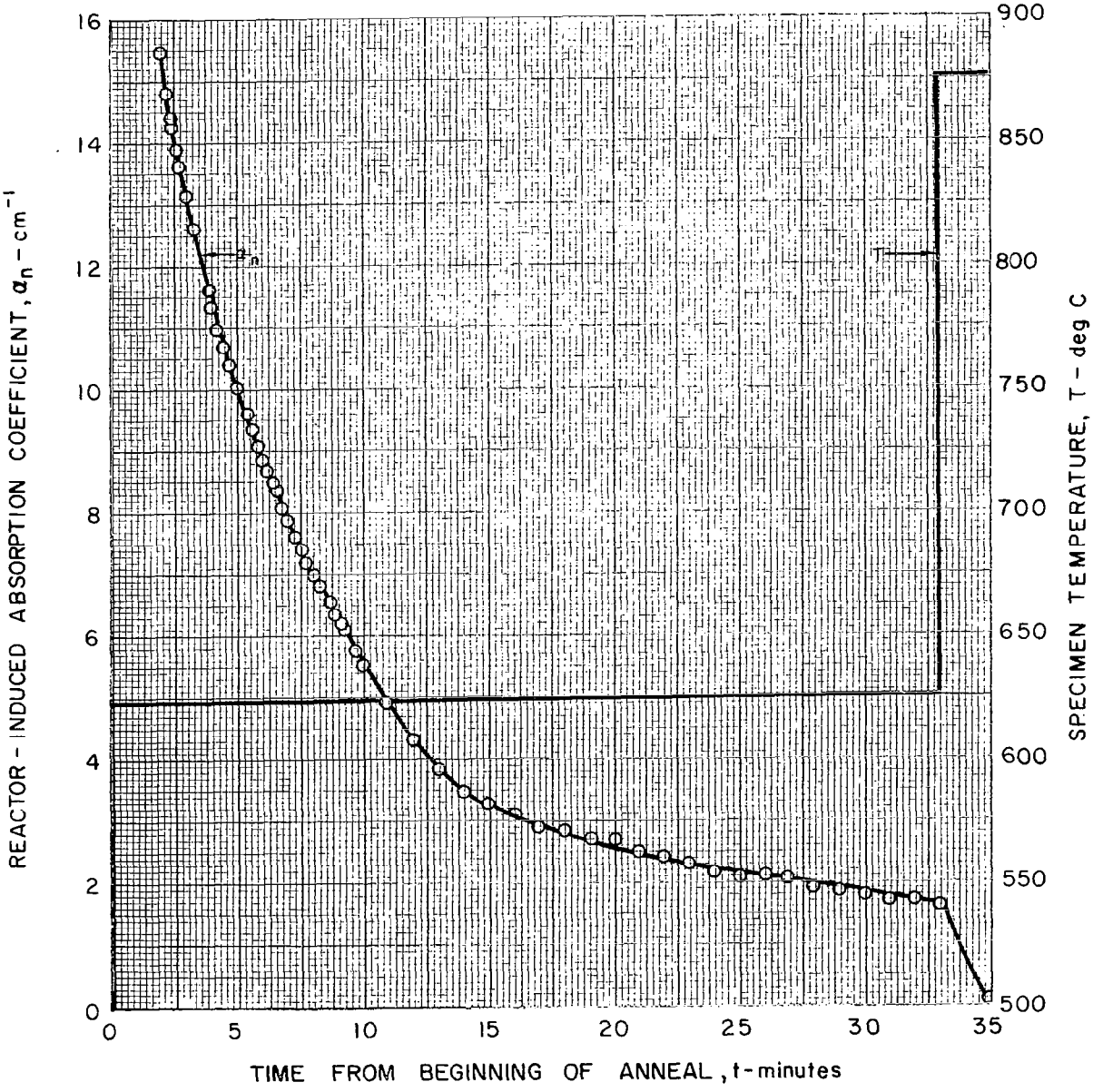

FIG. 56

VARIATION OF INDUCED ABSORPTION COEFFICIENT FOR CORNING 1 mm SPECIMEN SC 1 - 3 MEASURED AT 0.215 microns DURING ANNEAL OF REACTOR-INDUCED COLOR

α_n VALUES BASED ON DATA FROM FIG. 43

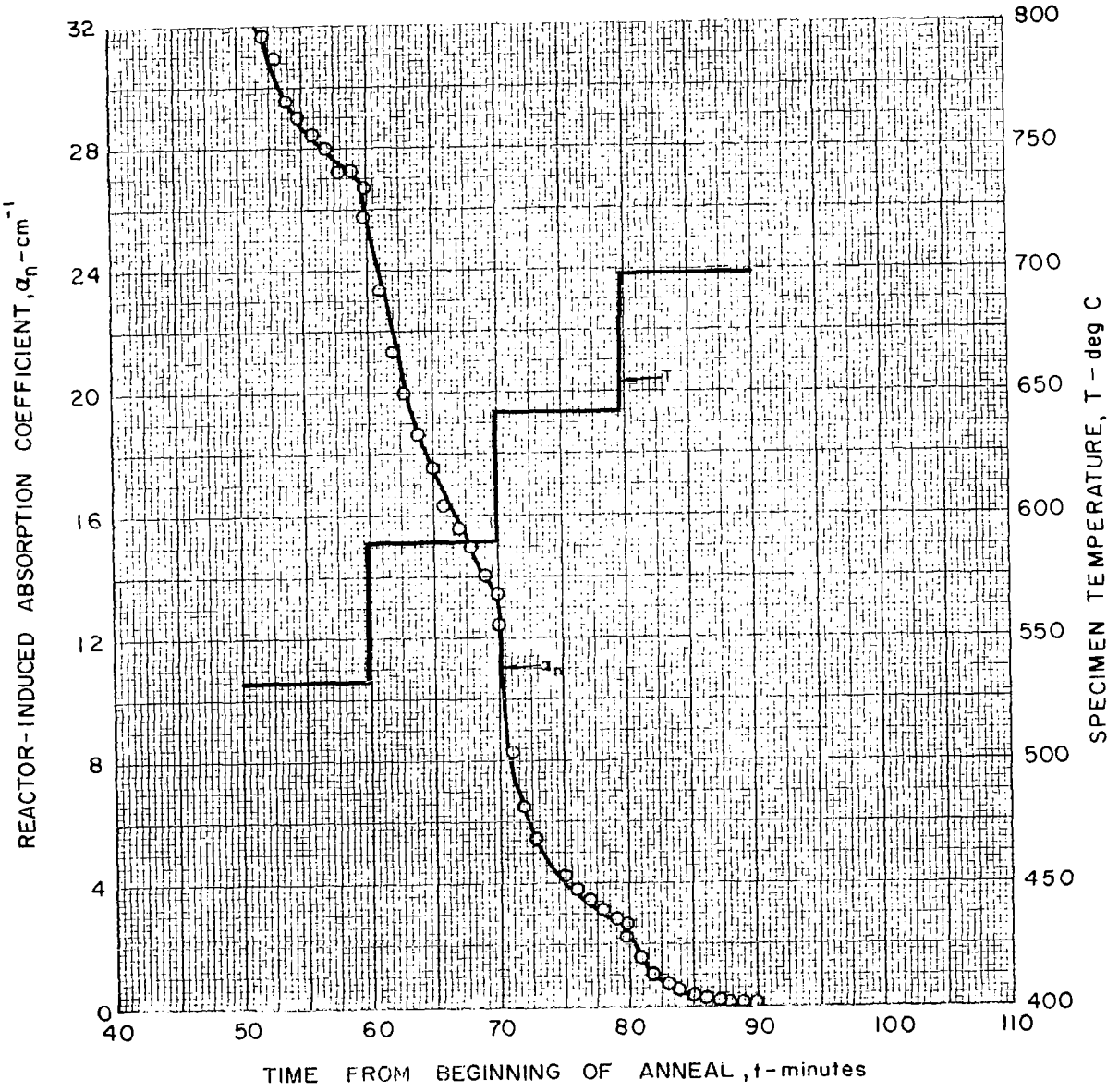

FIG. 57

VARIATION OF INDUCED ABSORPTION COEFFICIENT FOR CORNING 2 mm SPECIMEN SC 2-11 MEASURED AT 0.215 microns DURING ANNEAL OF REACTOR-INDUCED COLOR

α_n VALUES BASED ON DATA FROM FIG. 44

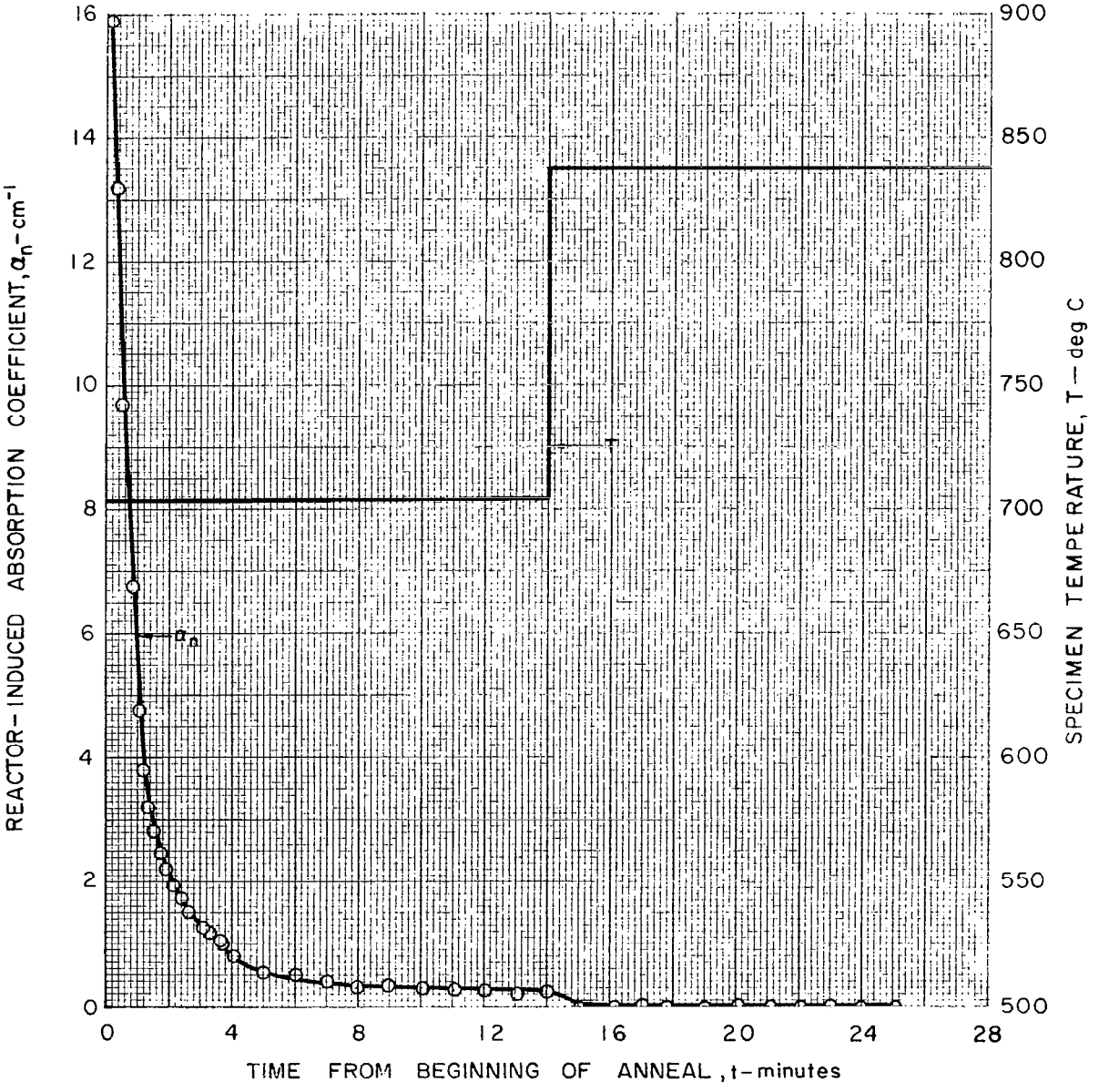

FIG. 58

VARIATION OF INDUCED ABSORPTION COEFFICIENT FOR CORNING 30mm SPECIMEN SC30-4 MEASURED AT 0.215 microns DURING ANNEAL OF REACTOR-INDUCED COLOR

α_n VALUES BASED ON DATA FROM FIG. 45

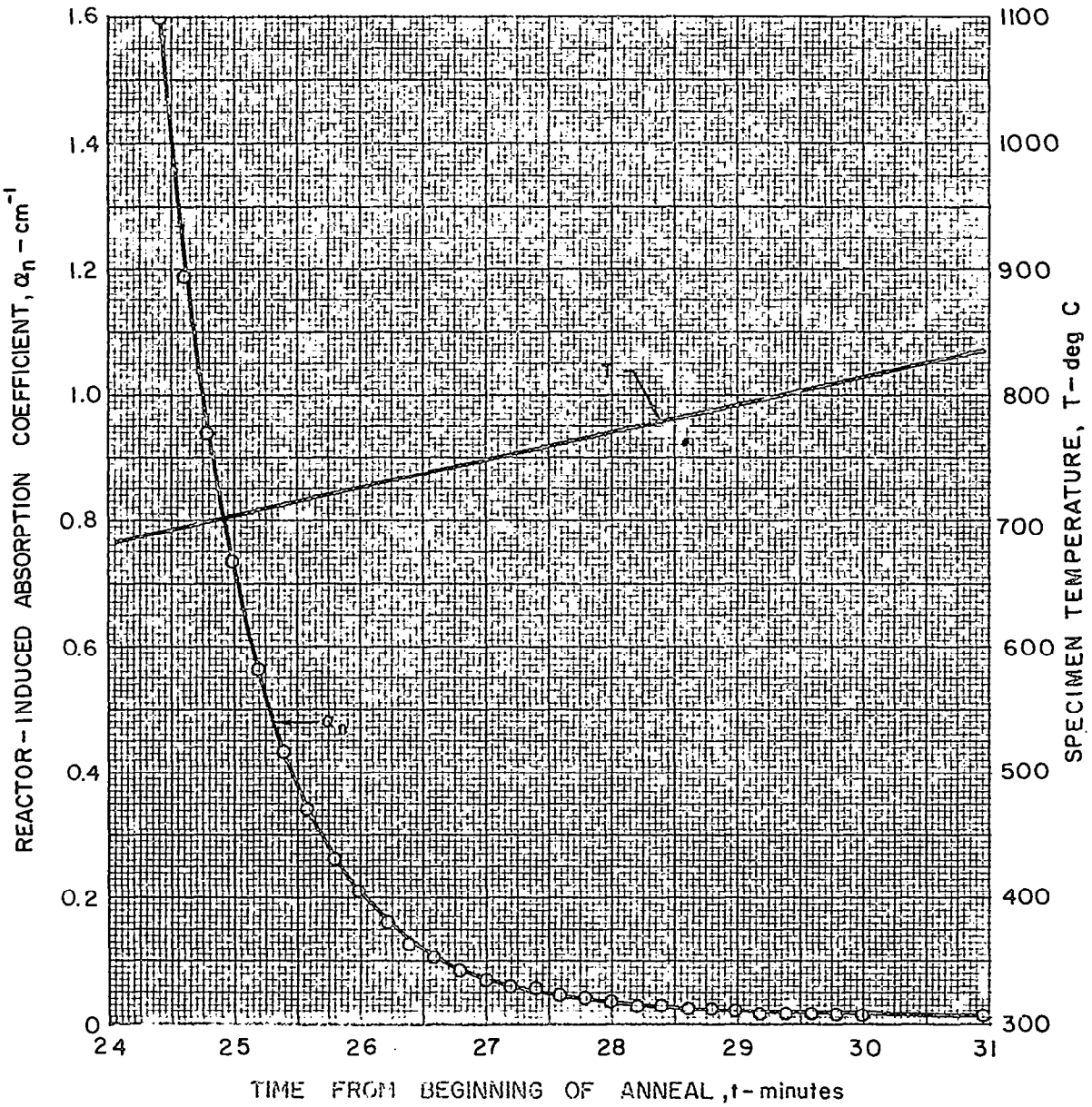

FIG. 59

VARIATION OF INDUCED ABSORPTION COEFFICIENT FOR CORNING 30 mm SPECIMEN SC30-8 MEASURED AT 0.210 microns DURING ANNEAL OF REACTOR-INDUCED COLOR

α_n VALUES BASED ON DATA FROM FIG. 46

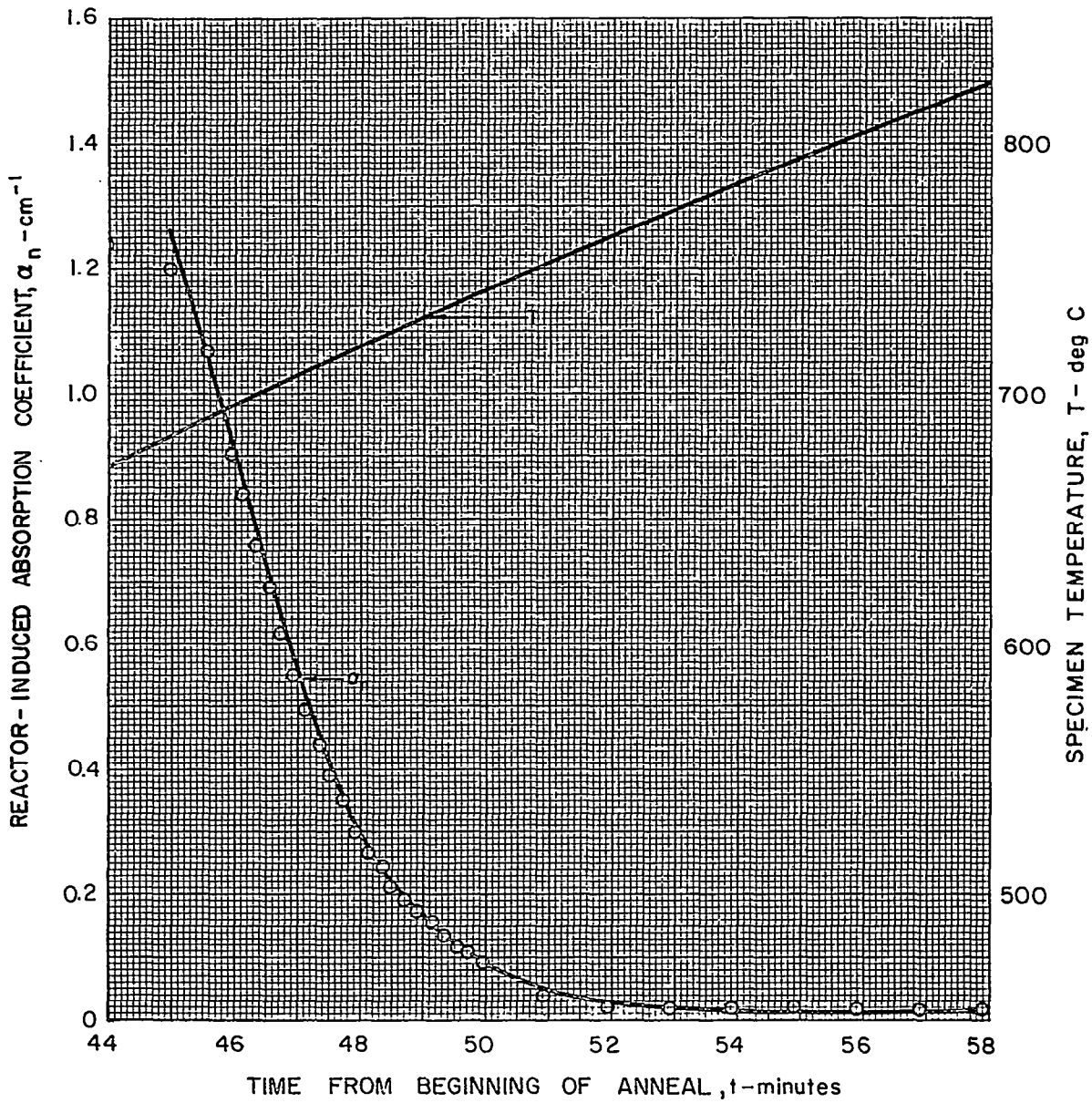

FIG. 60

VARIATION OF INDUCED ABSORPTION COEFFICIENT FOR AMERSIL 1 mm SPECIMEN SA 1-2 MEASURED AT 0.210 microns DURING ANNEAL OF REACTOR-INDUCED COLOR

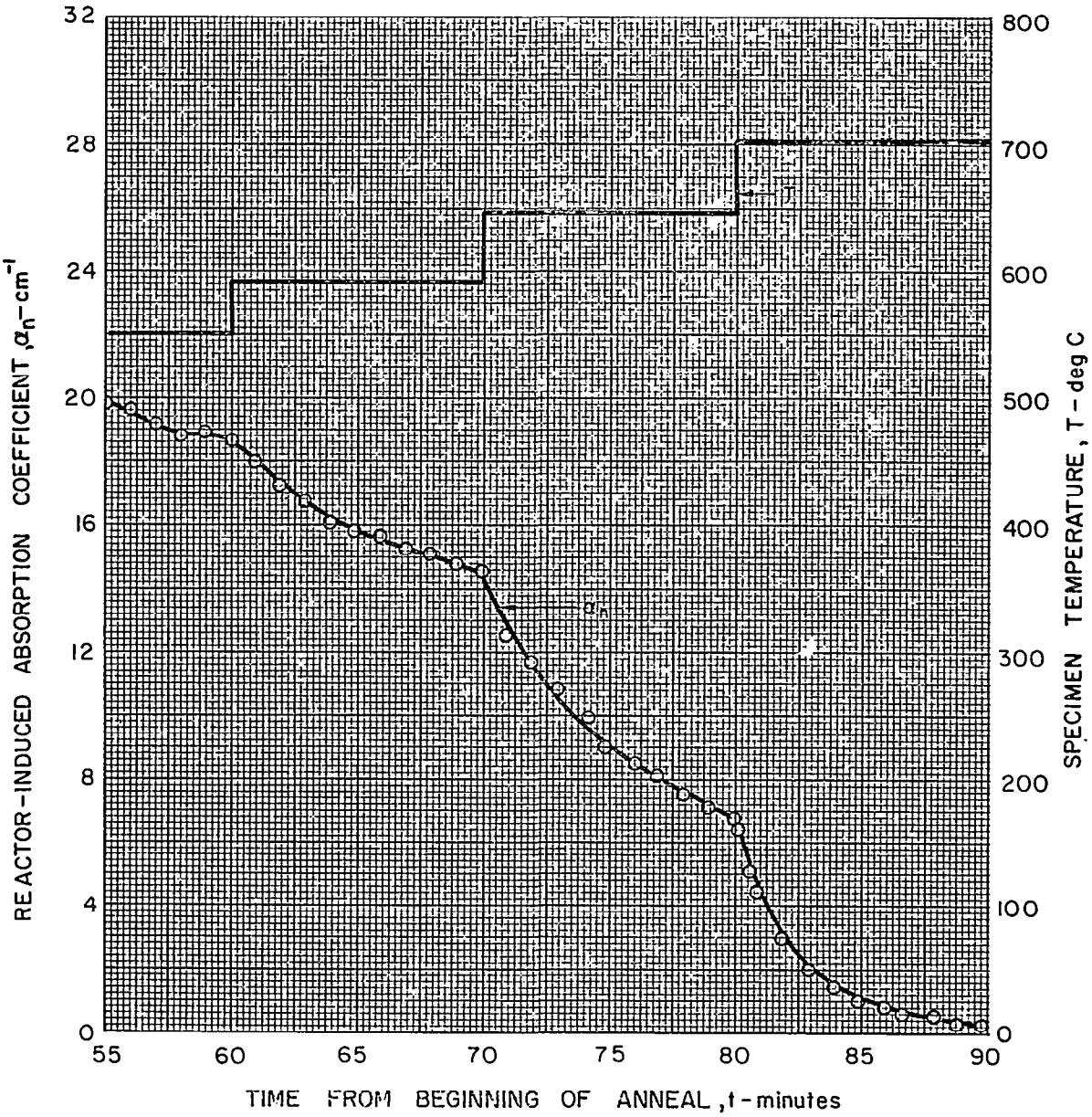

FIG. 61

VARIATION OF INDUCED ABSORPTION COEFFICIENT FOR AMERSIL 1 mm SPECIMEN SA 1-5 MEASURED AT 0.210 microns DURING ANNEAL OF REACTOR-INDUCED COLOR

α_n VALUES BASED ON DATA FROM FIG. 47

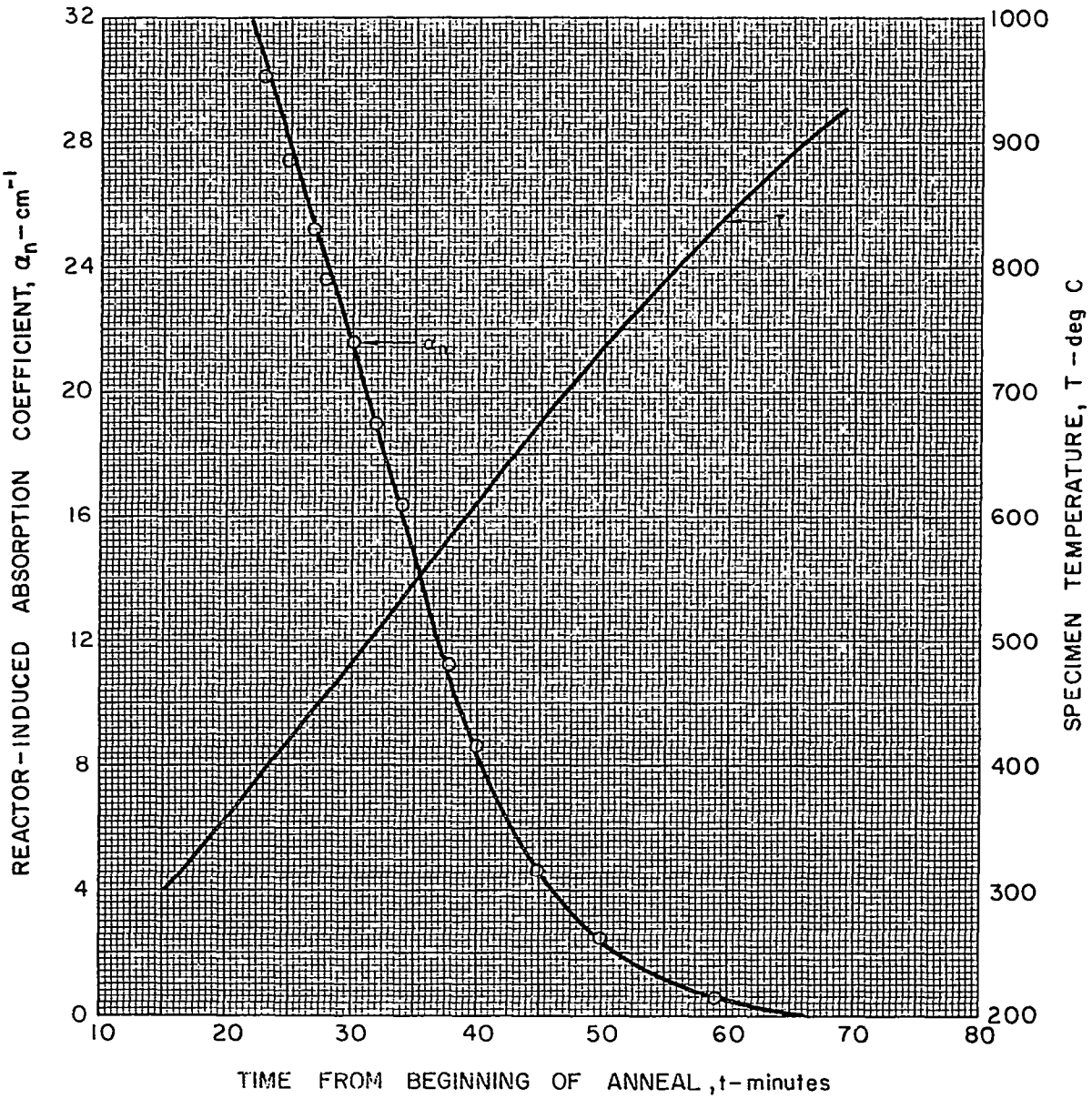

FIG. 61

VARIATION OF INDUCED ABSORPTION COEFFICIENT FOR AMERSIL 1 mm SPECIMEN SA 1-5 MEASURED AT 0.210 microns DURING ANNEAL OF REACTOR-INDUCED COLOR

α_n VALUES BASED ON DATA FROM FIG. 47

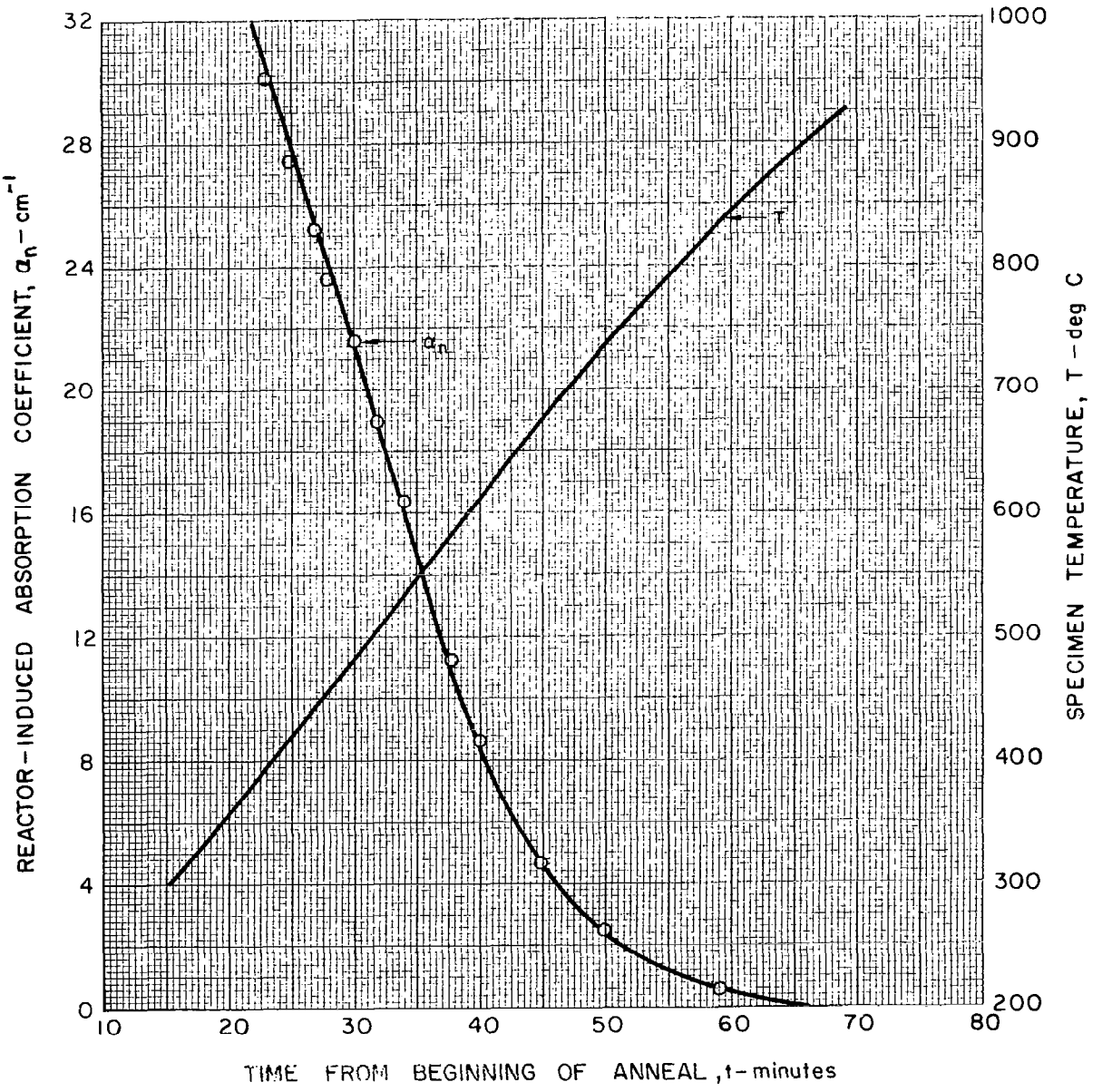

FIG. 62

VARIATION OF INDUCED ABSORPTION COEFFICIENT FOR AMERSIL 30 mm SPECIMEN SA30-2 MEASURED AT 0.23 microns DURING ANNEAL OF REACTOR-INDUCED COLOR

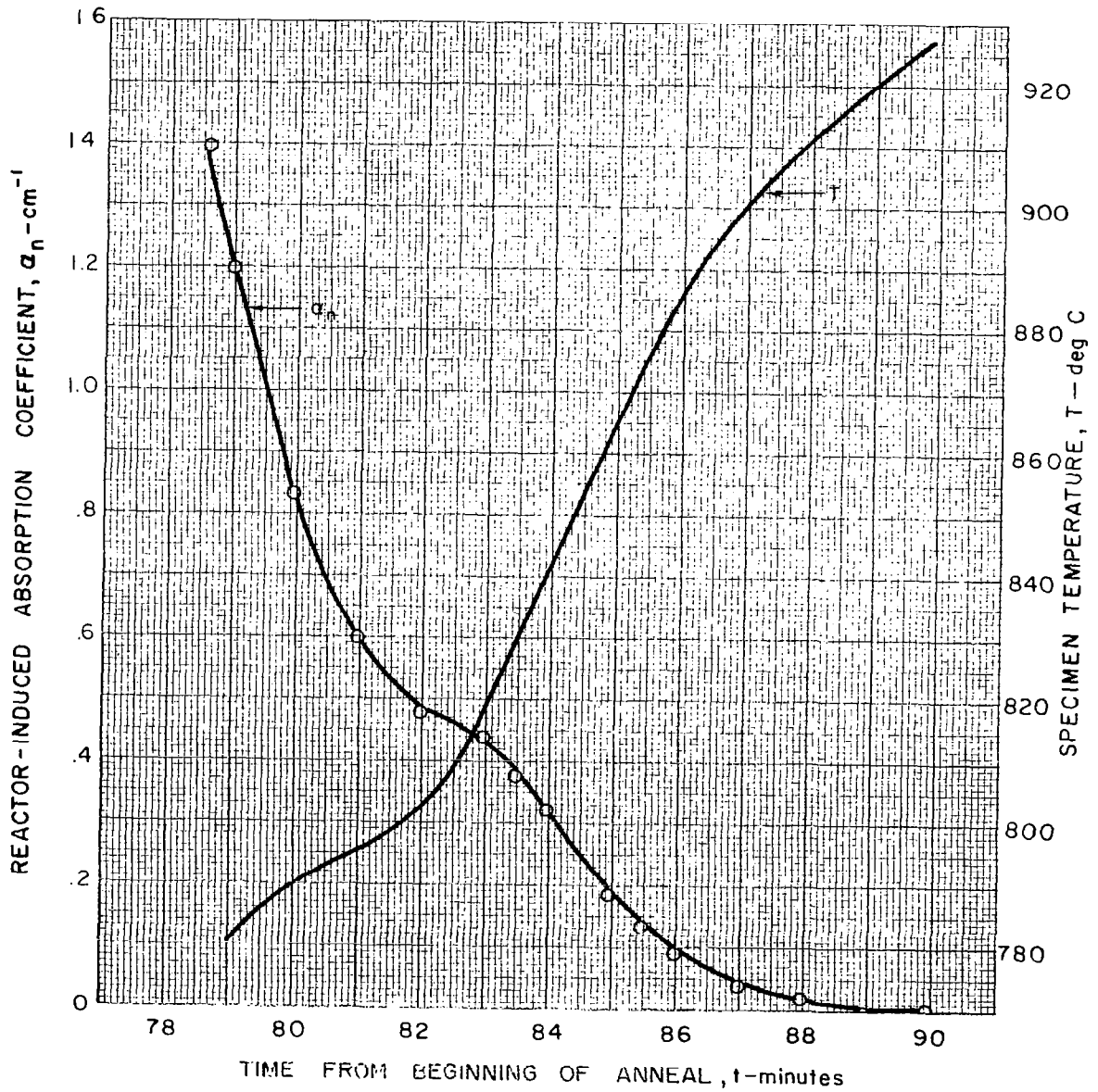

FIG. 63

VARIATION OF INDUCED ABSORPTION COEFFICIENT FOR THERMAL AMERICAN 30 mm SPECIMEN ST 30-1 MEASURED AT 0.210 microns DURING ANNEAL OF REACTOR-INDUCED COLOR

α_n VALUES BASED ON DATA FROM FIG. 48

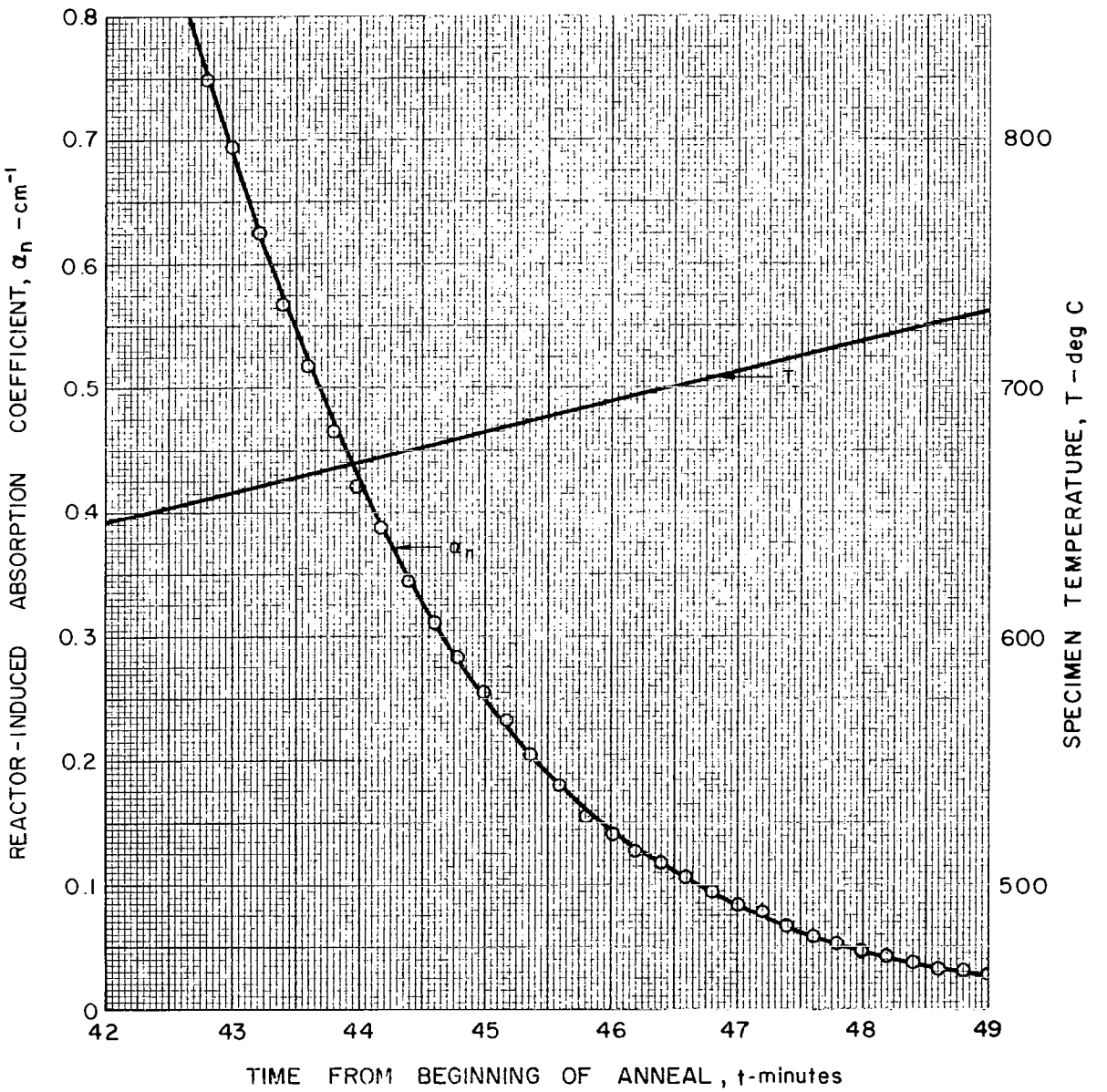

FIG. 64

VARIATION OF INDUCED ABSORPTION COEFFICIENT FOR THERMAL AMERICAN 30 mm SPECIMEN ST 30-4 MEASURED AT 0.215 microns DURING ANNEAL OF REACTOR-INDUCED COLOR

α_n VALUES BASED ON DATA FROM FIG. 49

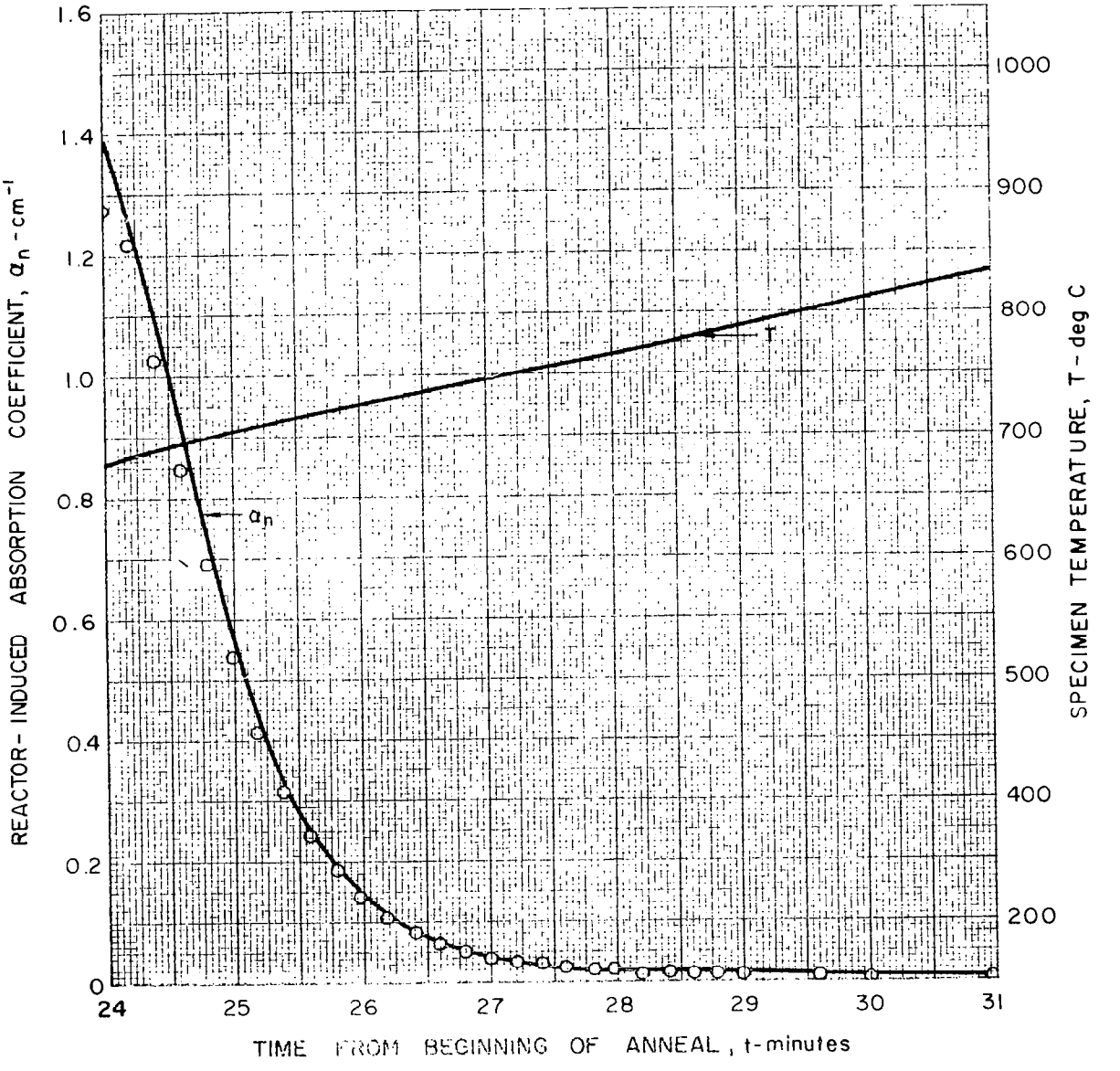

FIG. 65

VARIATION OF INDUCED ABSORPTION COEFFICIENT FOR THERMAL AMERICAN 30 mm SPECIMEN ST 30-5 MEASURED AT 0.215 microns DURING ANNEAL OF REACTOR-INDUCED COLOR

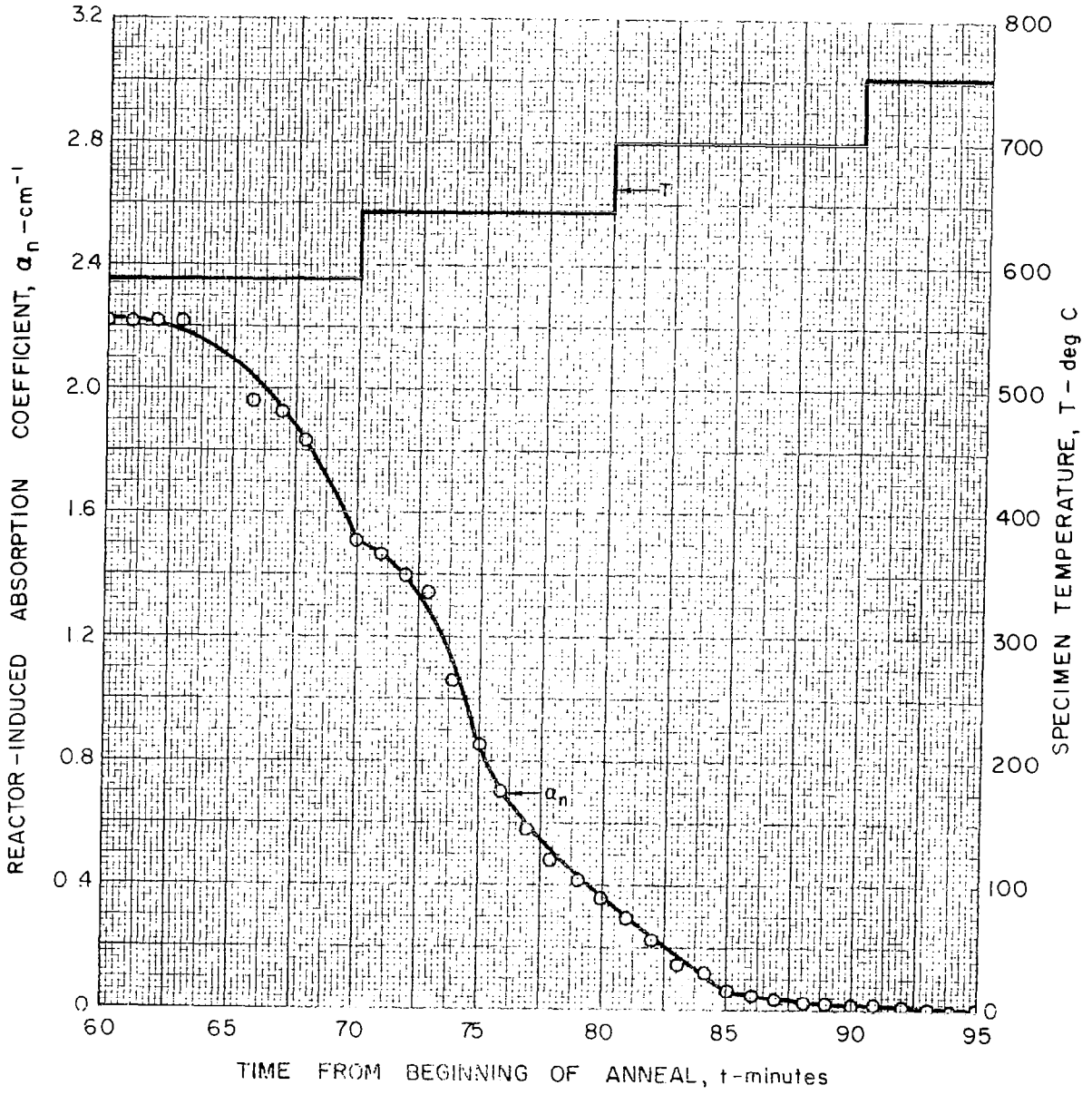

FIG. 66

REMAINING REACTOR-INDUCED COLOR AFTER CUMULATIVE 50 C INCREMENT, 10-minute-CONSTANT-TEMPERATURE ANNEALS FOR CORNING 1 mm SPECIMEN SC 1-3

MEASUREMENTS MADE AT 200 C AFTER ANNEAL AT TEMPERATURE NOTED ON CURVE

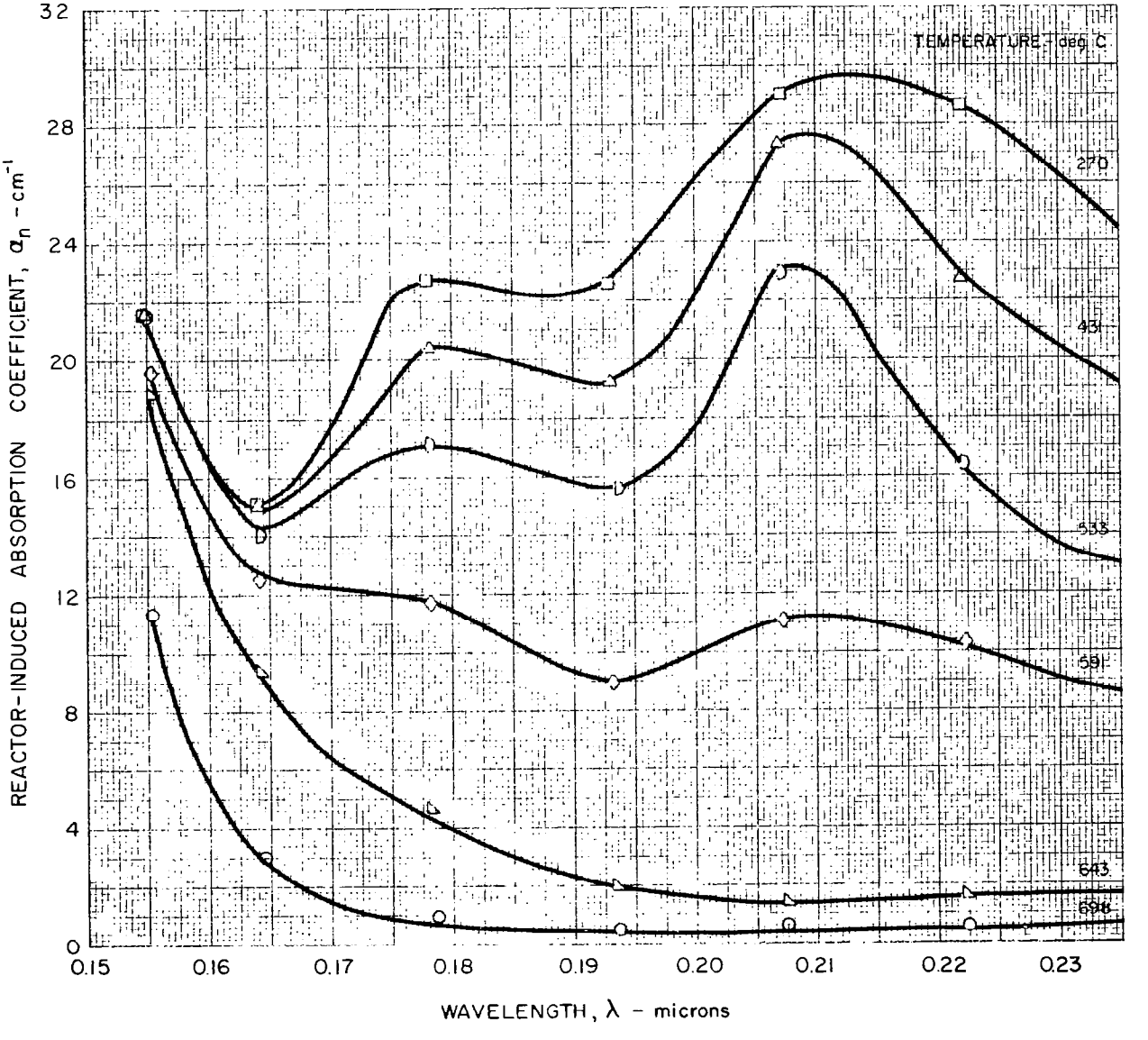

FIG. 67

REMAINING REACTOR-INDUCED COLOR AFTER CUMULATIVE 50 C INCREMENT, 10-minute-CONSTANT-TEMPERATURE ANNEALS FOR AMERSIL 1mm SPECIMEN SA1-2

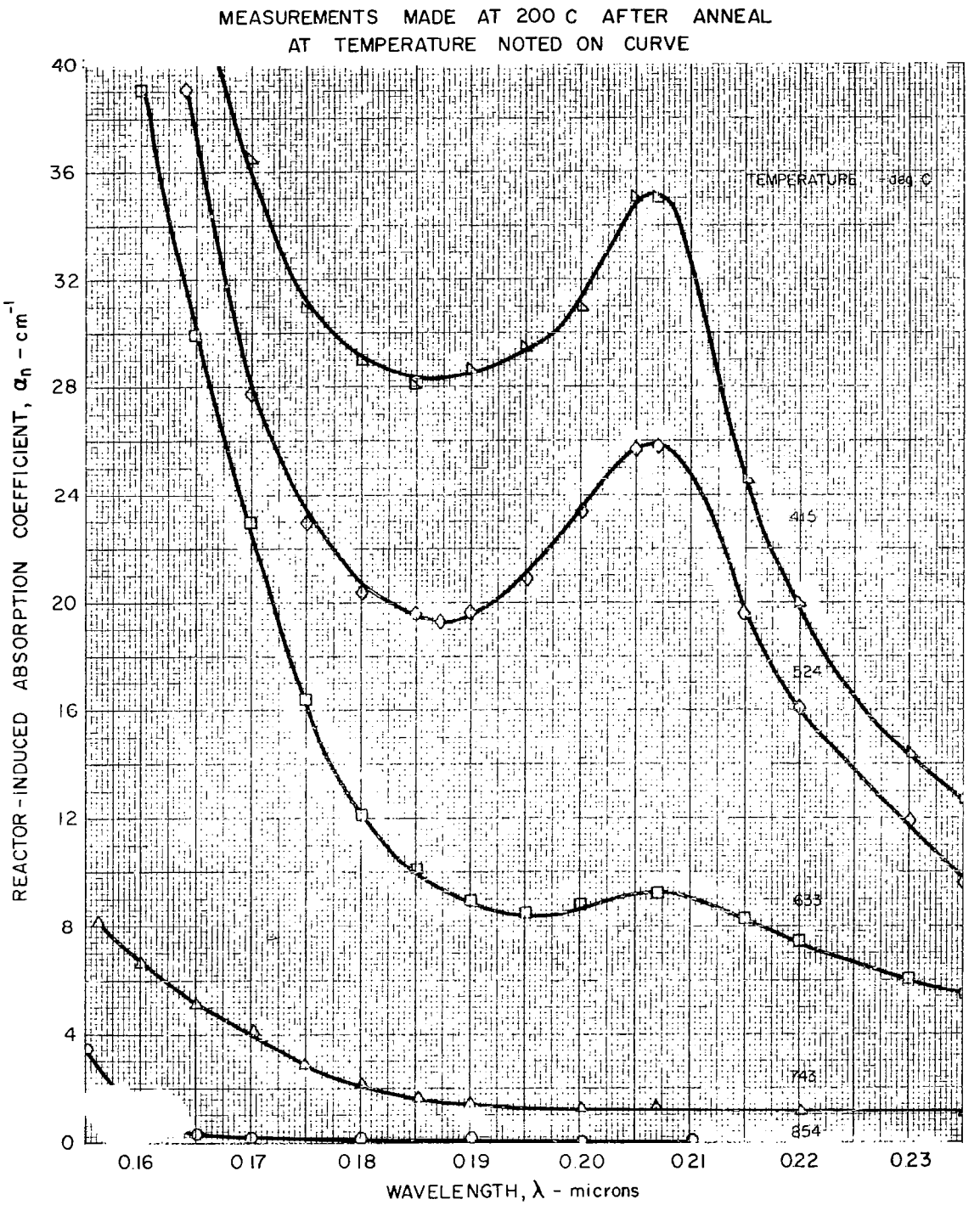

FIG. 68

COMPARISON OF REMAINING REACTOR-INDUCED COLOR AFTER CUMULATIVE 50 C INCREMENT, 10-minute-CONSTANT-TEMPERATURE ANNEALS FOR AMERSIL AND CORNING FUSED SILICAS

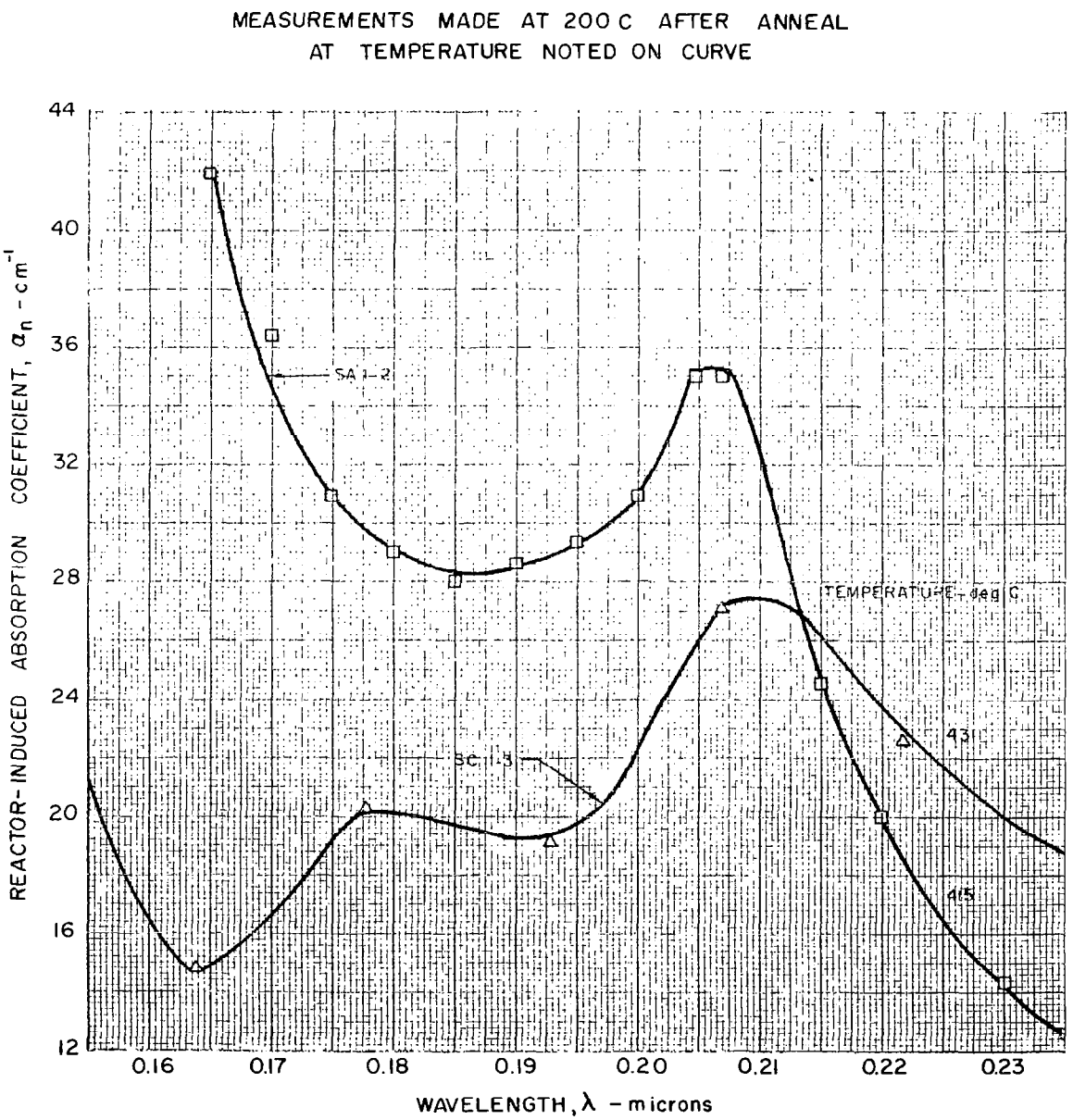

FIG. 69

COMPARISON OF REMAINING REACTOR-INDUCED COLOR AFTER CUMULATIVE 50 C INCREMENT, 10-minute-CONSTANT-TEMPERATURE ANNEALS FOR AMERSIL AND CORNING FUSED SILICAS

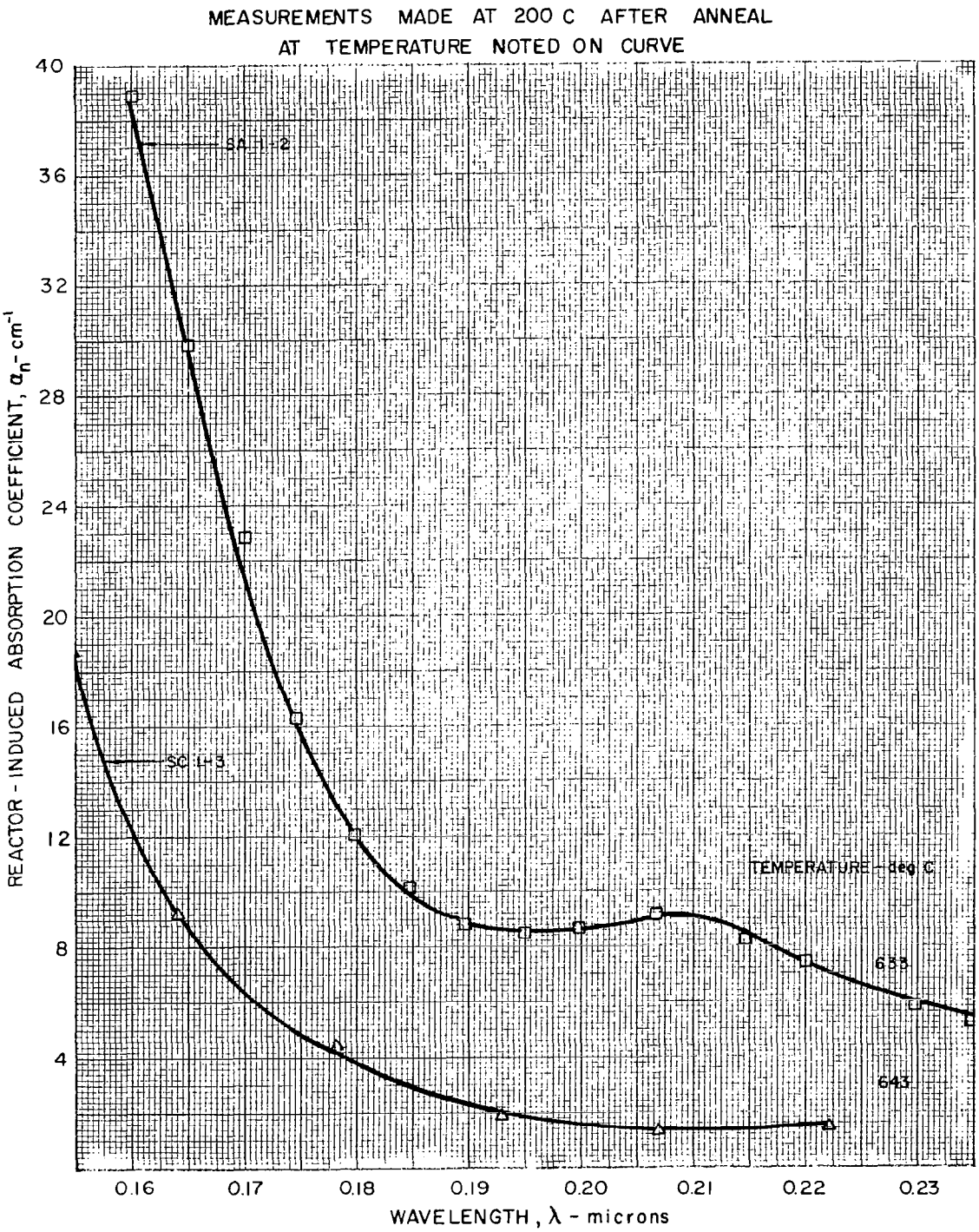

COMPARISON OF ANNEALING RESULTS FOR CORNING, AMERSIL, AND THERMAL AMERICAN SPECIMENS AT 0.210 microns

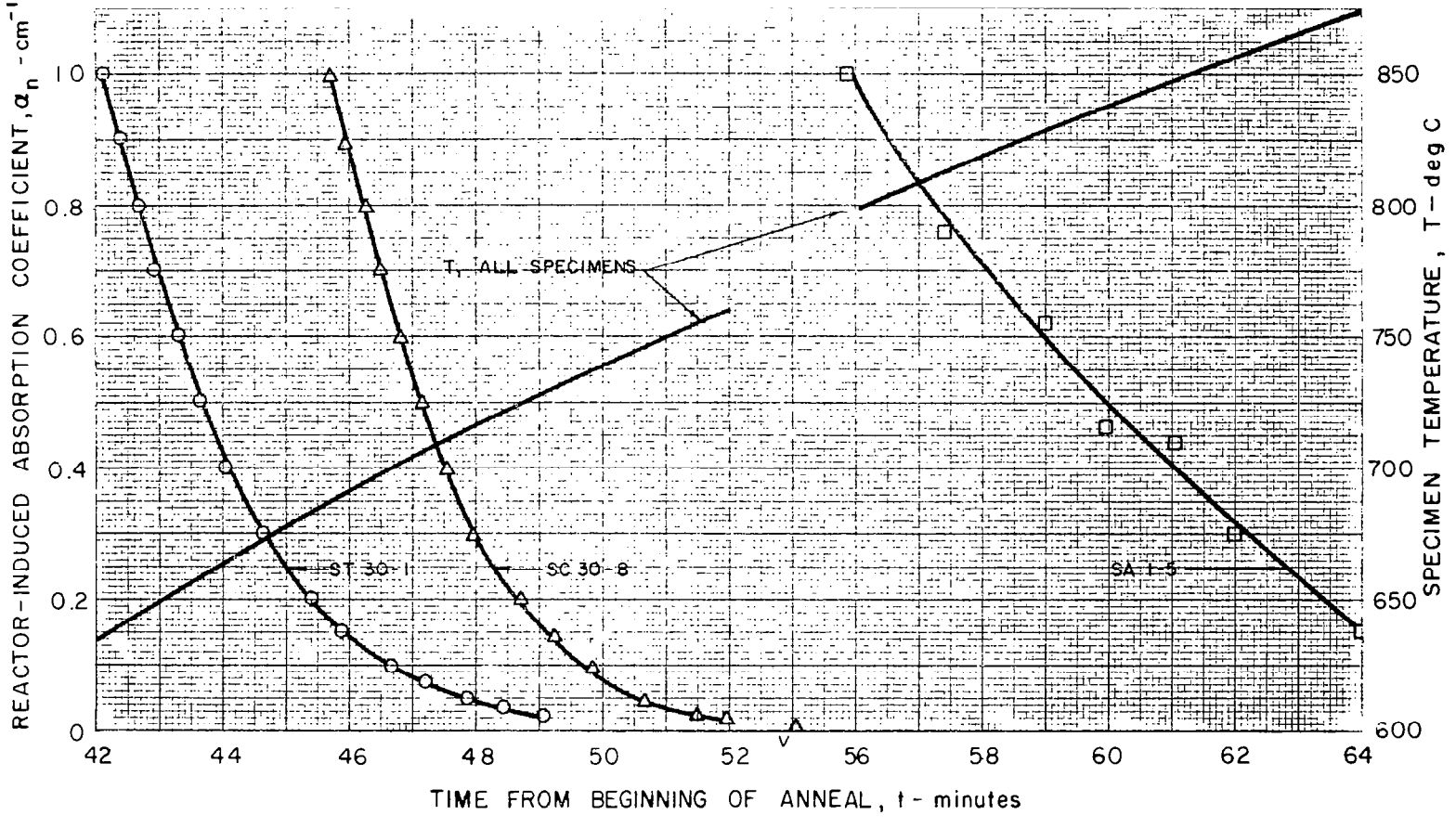

FIG. 70

COMPARISON OF ANNEALING RESULTS FOR CORNING AND THERMAL AMERICAN 30 mm SPECIMENS

SYMBOL	SPECIMEN	WAVELENGTH – microns
○	ST 30-4	0.215
△	SC 30-4	0.215
●	ST 30-1	0.210
▲	SC 30-8	0.210

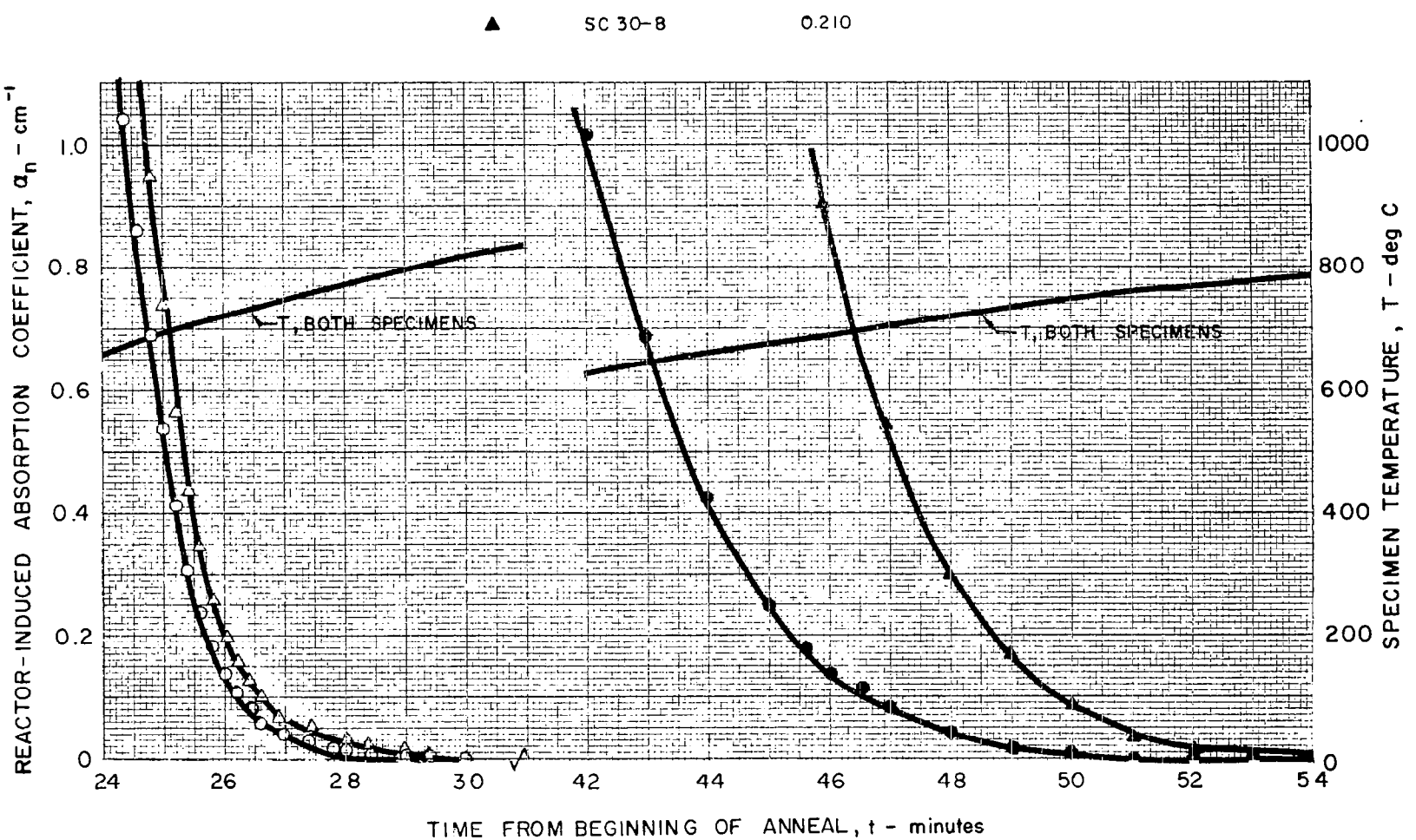

FIG. 71

FIG. 72

COMPARISON OF ANNEALING RESULTS FOR CORNING AND THERMAL AMERICAN SPECIMENS MEASURED AT 0.215 microns DURING ANNEAL OF REACTOR - INDUCED COLOR

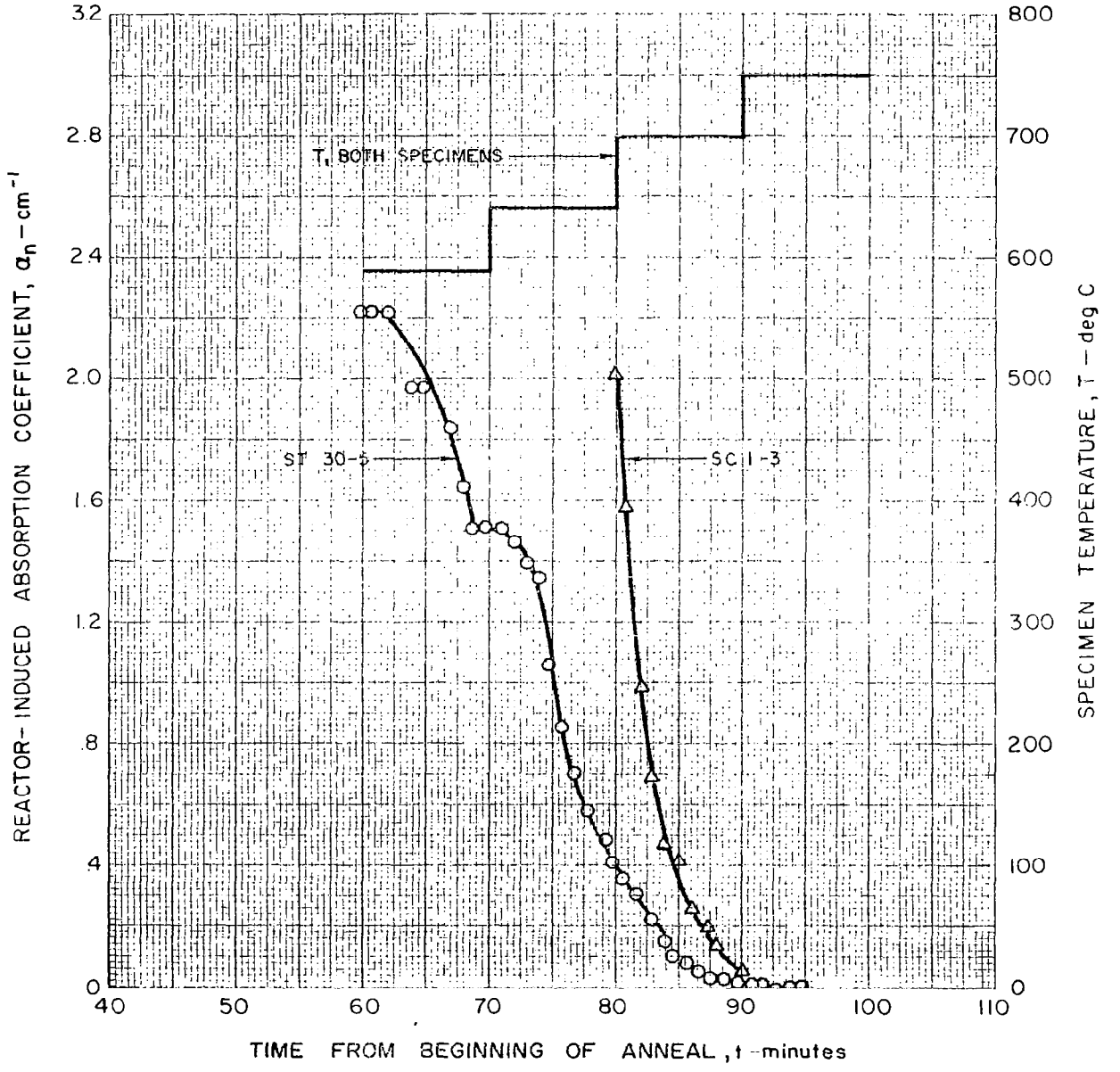

FIG. 73

THEORETICAL NORMALIZED INDUCED ABSORPTION COEFFICIENT WITH FIRST ORDER KINETICS AND SINGLE ACTIVATION ENERGY

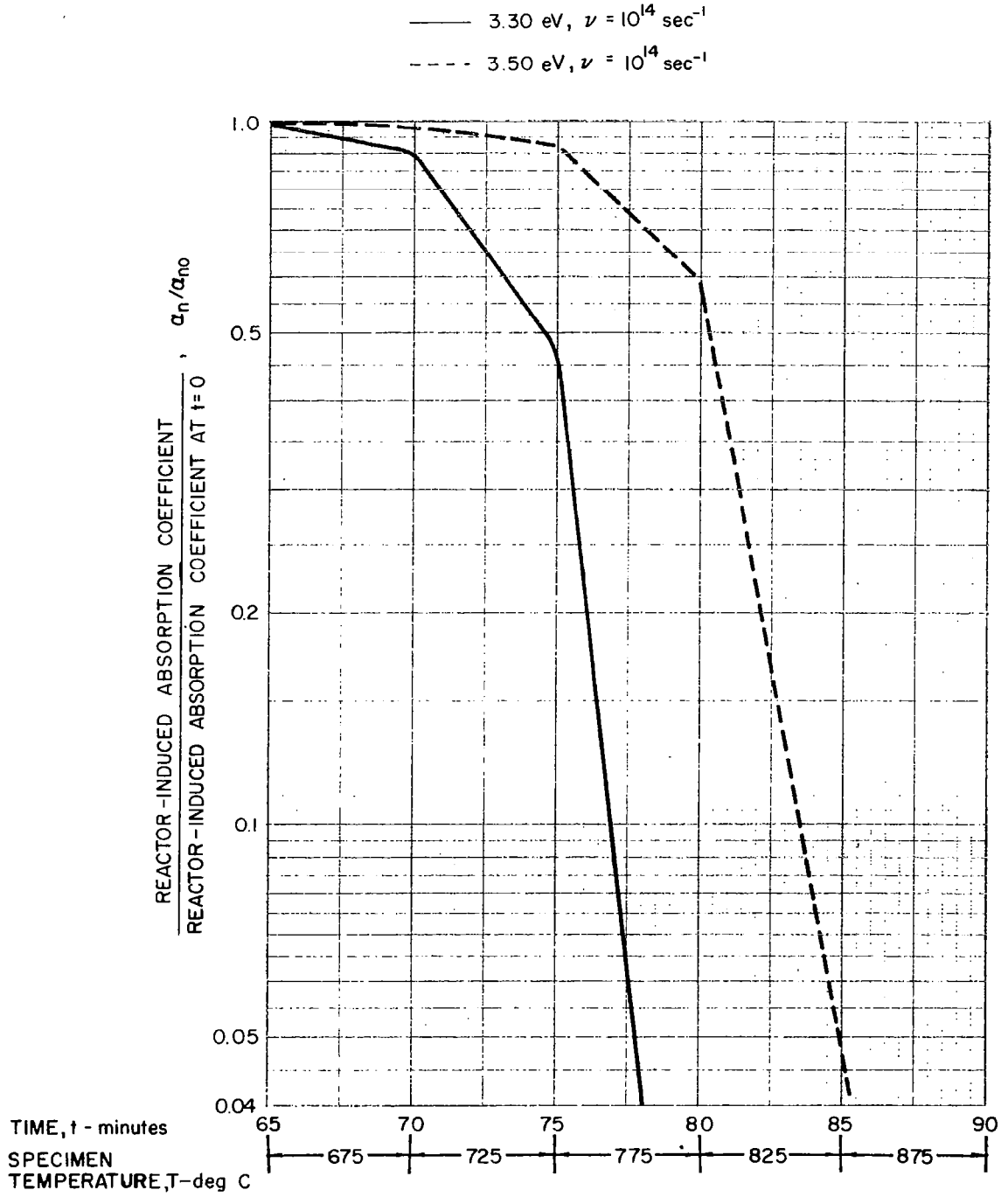

FIG. 74

THEORETICAL NORMALIZED INDUCED ABSORPTION COEFFICIENT WITH FIRST ORDER KINETICS AND TWO SIMULTANEOUSLY EFFECTIVE ACTIVATION ENERGIES

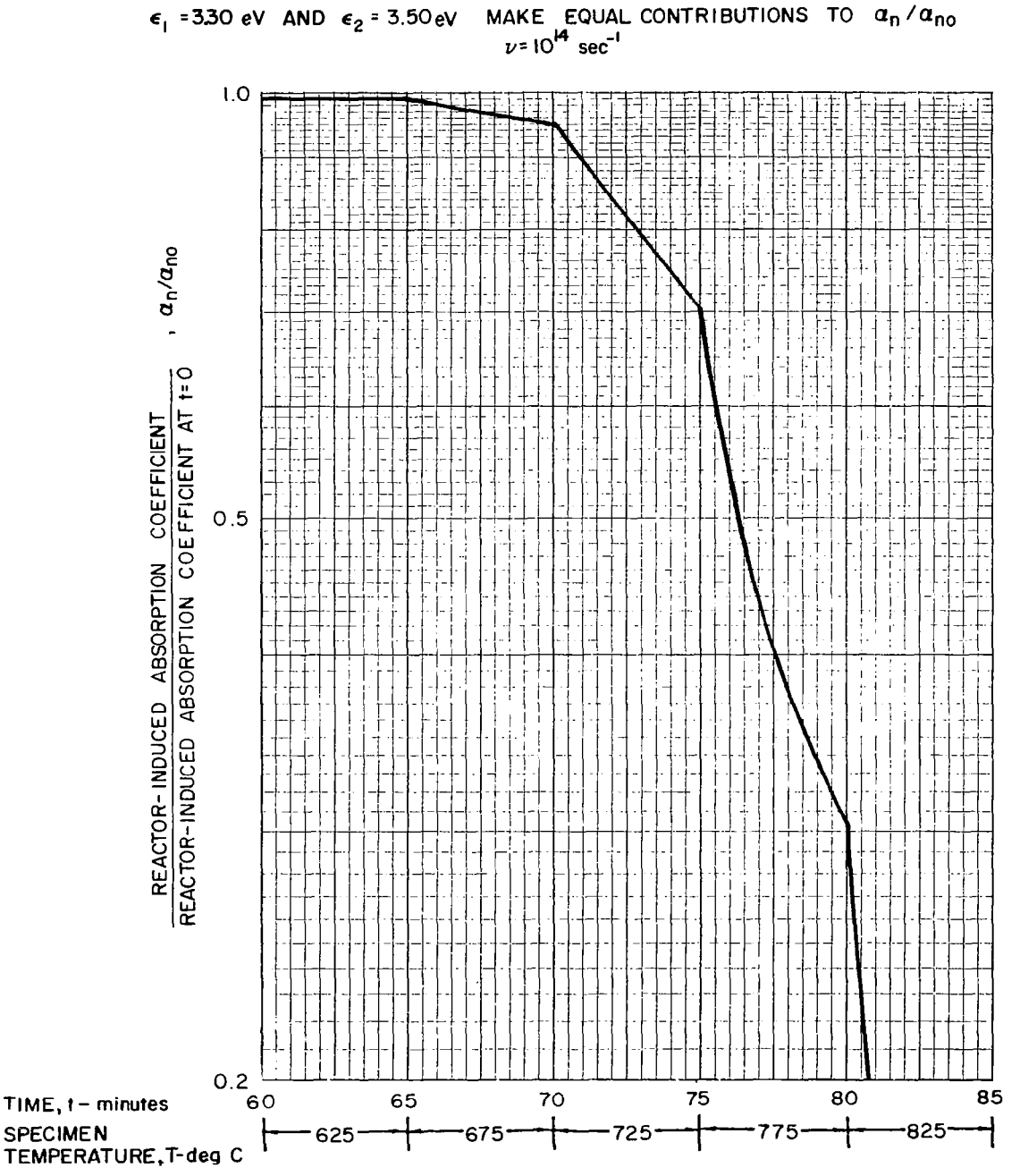

FIG. 75

VARIATION OF NORMALIZED INDUCED ABSORPTION COEFFICIENT WITH TIME FROM BEGINNING OF ANNEAL FOR CORNING 1mm SPECIMEN SC 1-3 AT 0.215 microns

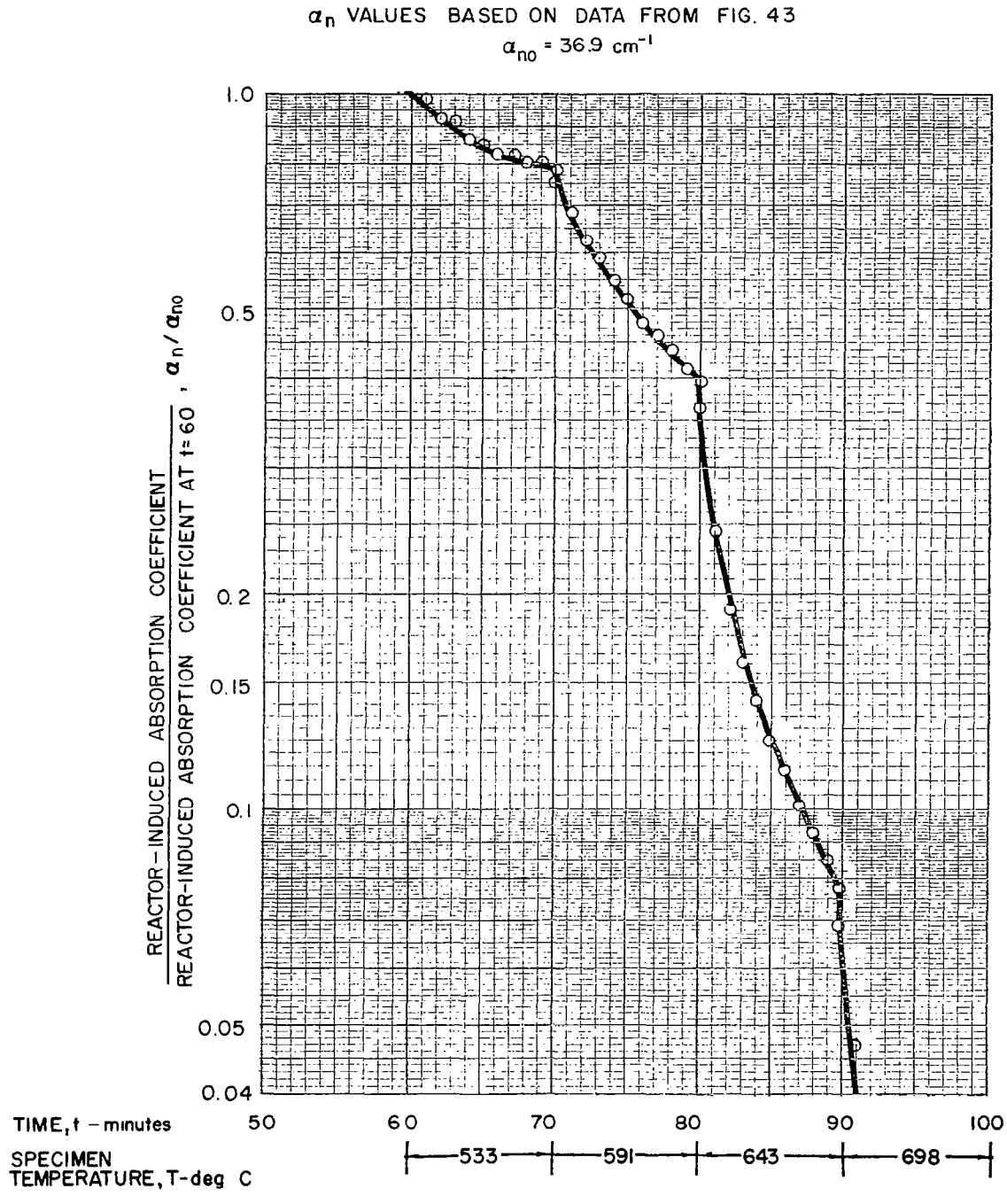

VARIATION OF NORMALIZED INDUCED ABSORPTION COEFFICIENT WITH TIME FROM BEGINNING OF ANNEAL FOR AMERSIL 1mm SPECIMEN SA 1-2 AT 0.210 microns

α_n VALUES BASED ON DATA FROM FIG. 60

$\alpha_{no} = 18.8\ cm^{-1}$

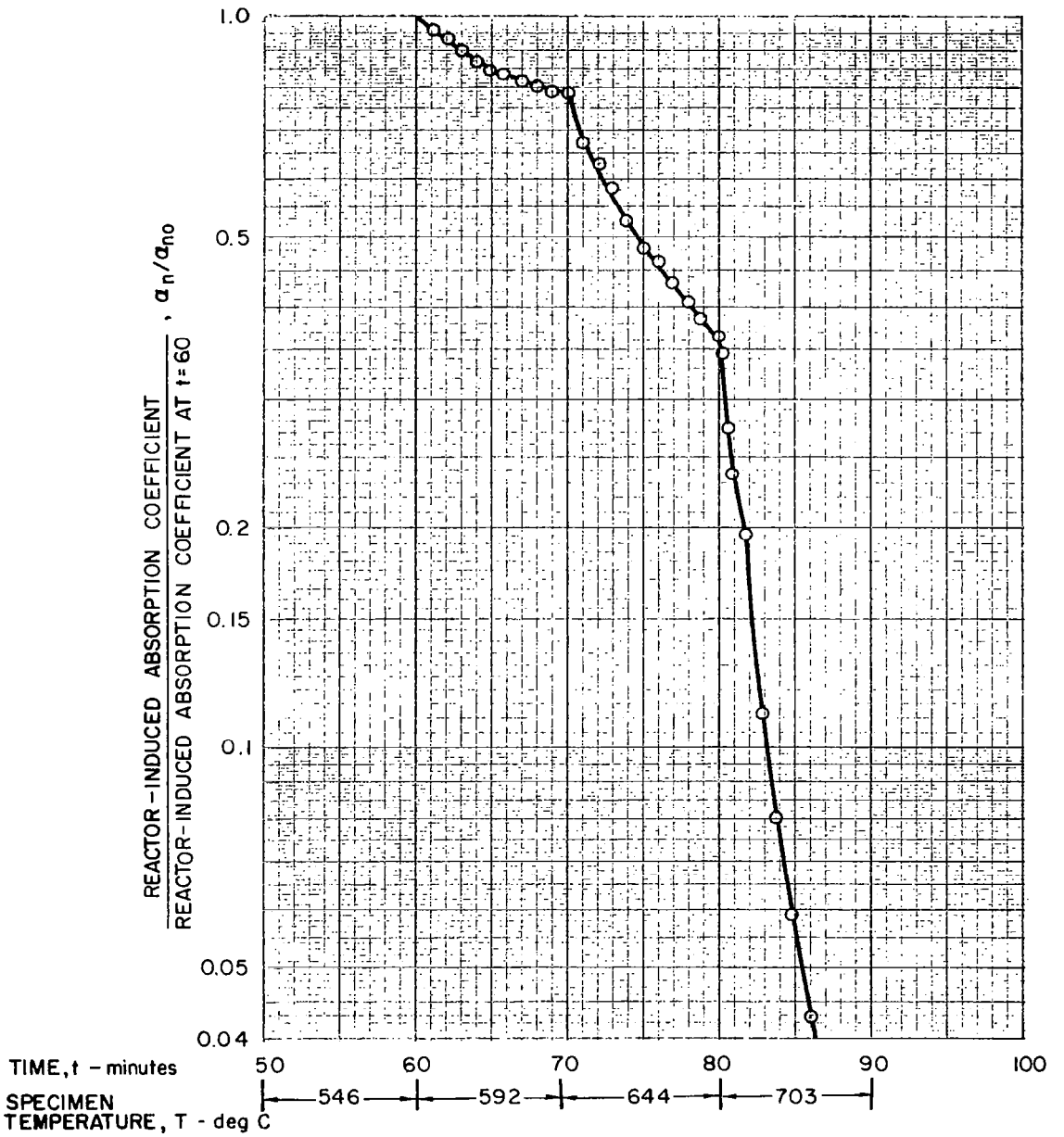

FIG. 77

APPARENT ACTIVATION ENERGY VS REACTOR-INDUCED ABSORPTION COEFFICIENT FOR CORNING 1mm SPECIMEN SC 1-1 AT 0.215 microns

$\alpha_{no} = 19.2\ cm^{-1}$
○ $\nu = 10^{10}\ sec^{-1}$
□ $\nu = 10^{14}\ sec^{-1}$

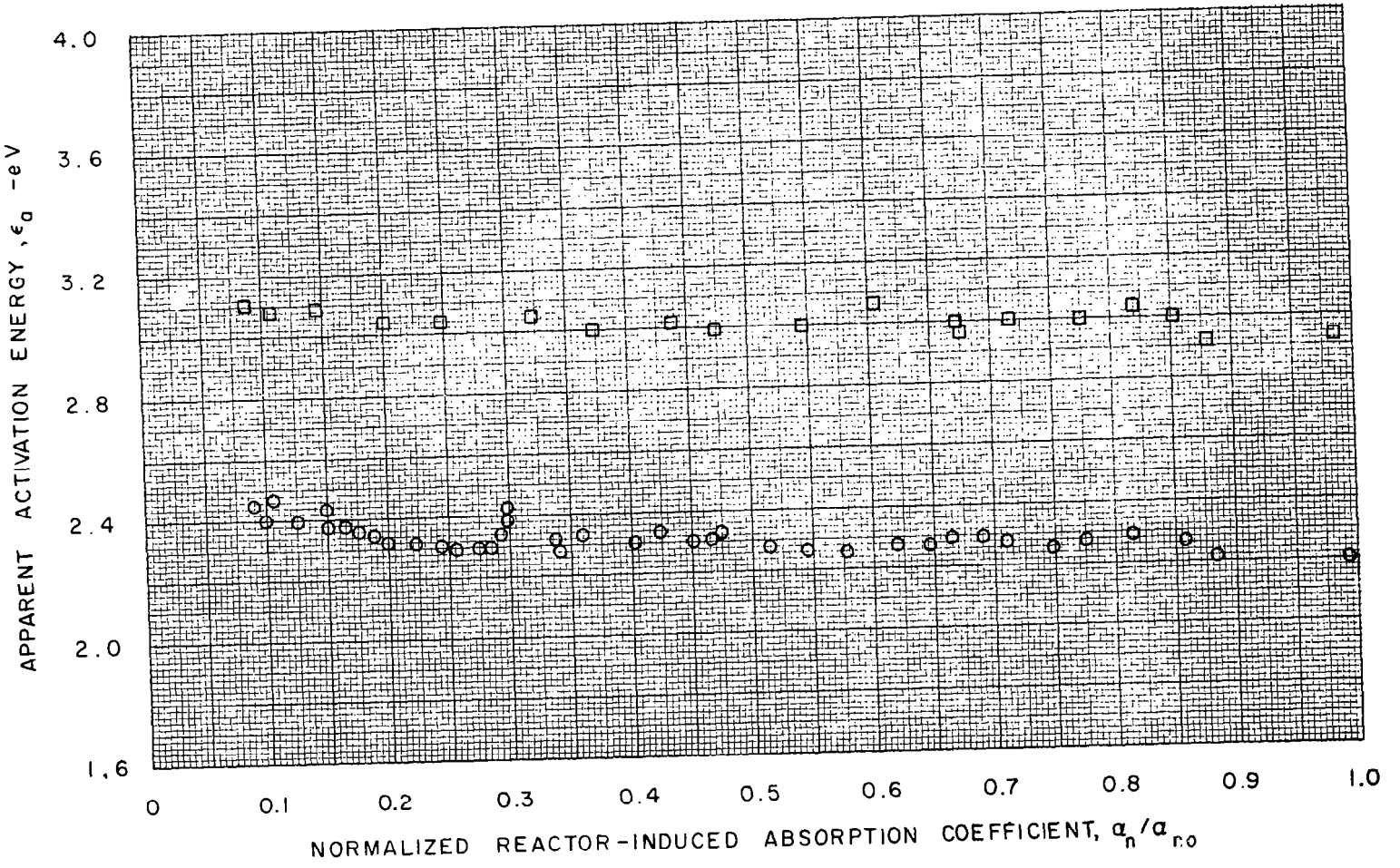

APPARENT ACTIVATION ENERGY VS REACTOR-INDUCED ABSORPTION COEFFICIENT FOR CORNING 1mm SPECIMEN SC 1-3 AT 0.215 microns

α_{no} = 36.9 cm^{-1}
○ ν = 10^{10} sec^{-1}
□ ν = 10^{14} sec^{-1}

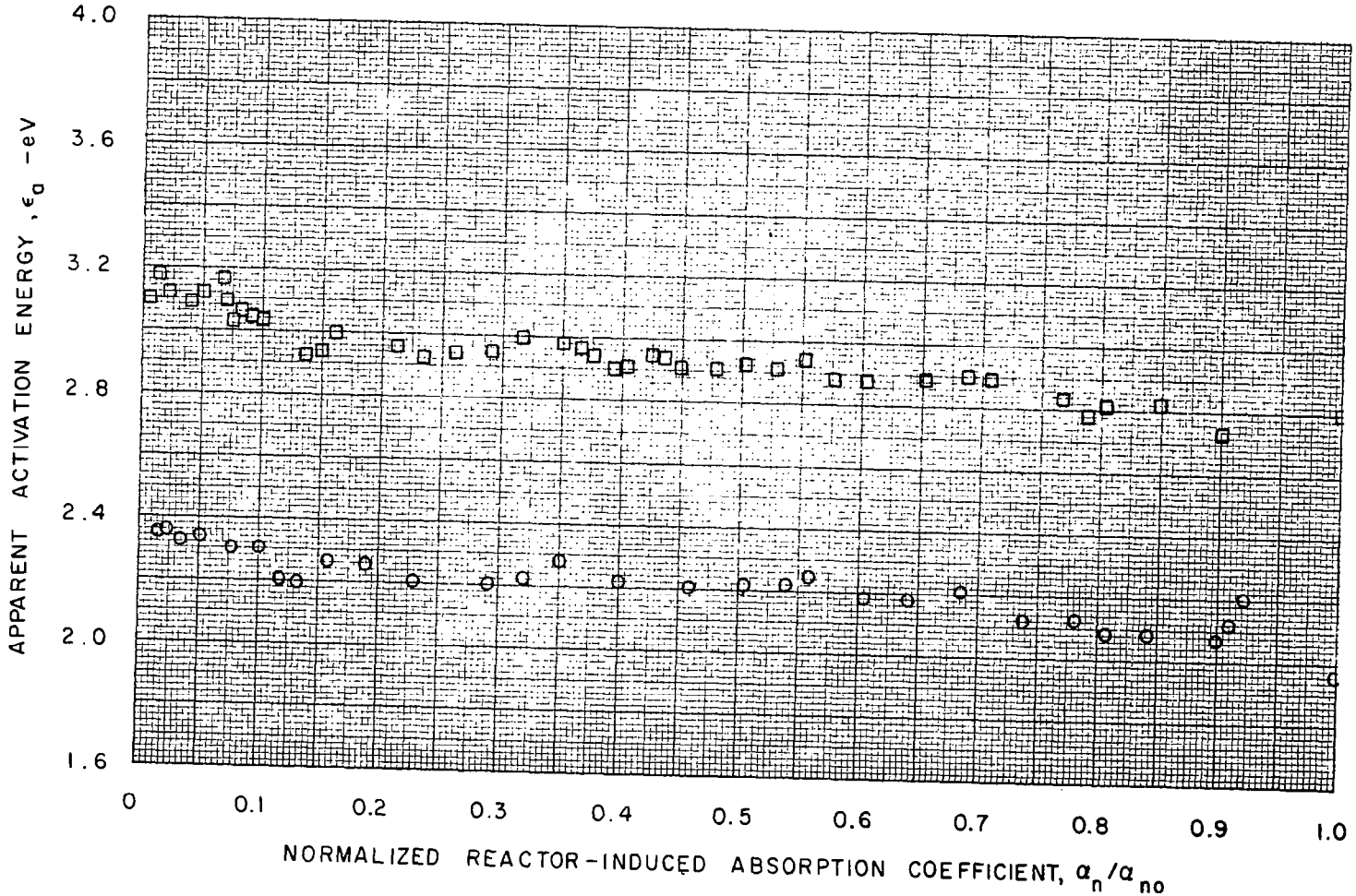

FIG. 78

APPARENT ACTIVATION ENERGY VS REACTOR-INDUCED ABSORPTION COEFFICIENT FOR CORNING 2mm SPECIMEN SC2-11 AT 0.215 microns

FIG. 79

$\alpha_{no} = 15.9\ cm^{-1}$
○ $\nu = 10^{10}\ sec^{-1}$
□ $\nu = 10^{14}\ sec^{-1}$

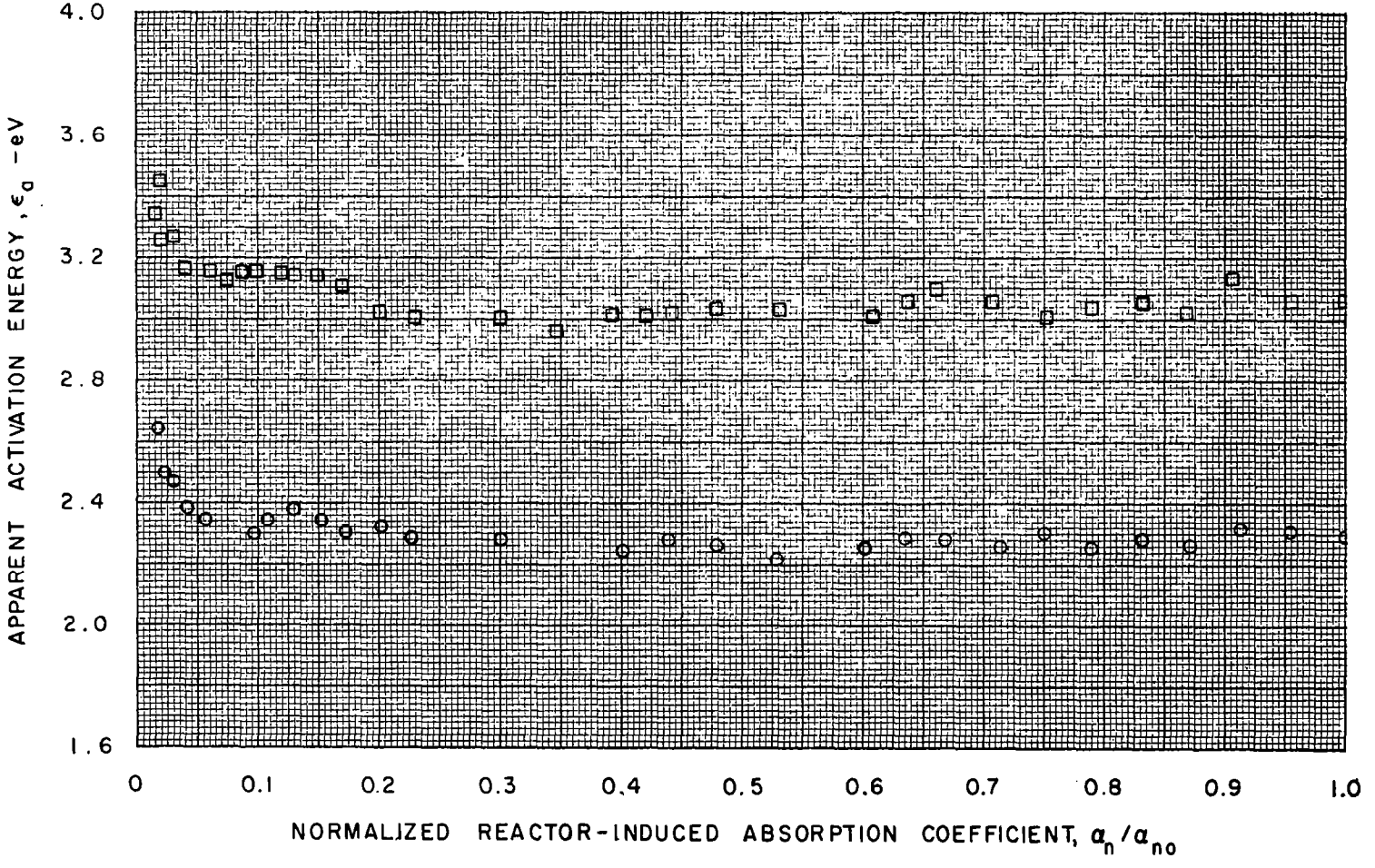

APPARENT ACTIVATION ENERGY VS REACTOR-INDUCED ABSORPTION COEFFICIENT FOR CORNING 30mm SPECIMEN SC30-4 AT 0.215 microns

$\alpha_{no} = 2.2\ cm^{-1}$

○ $\nu = 10^{10}\ sec^{-1}$

□ $\nu = 10^{14}\ sec^{-1}$

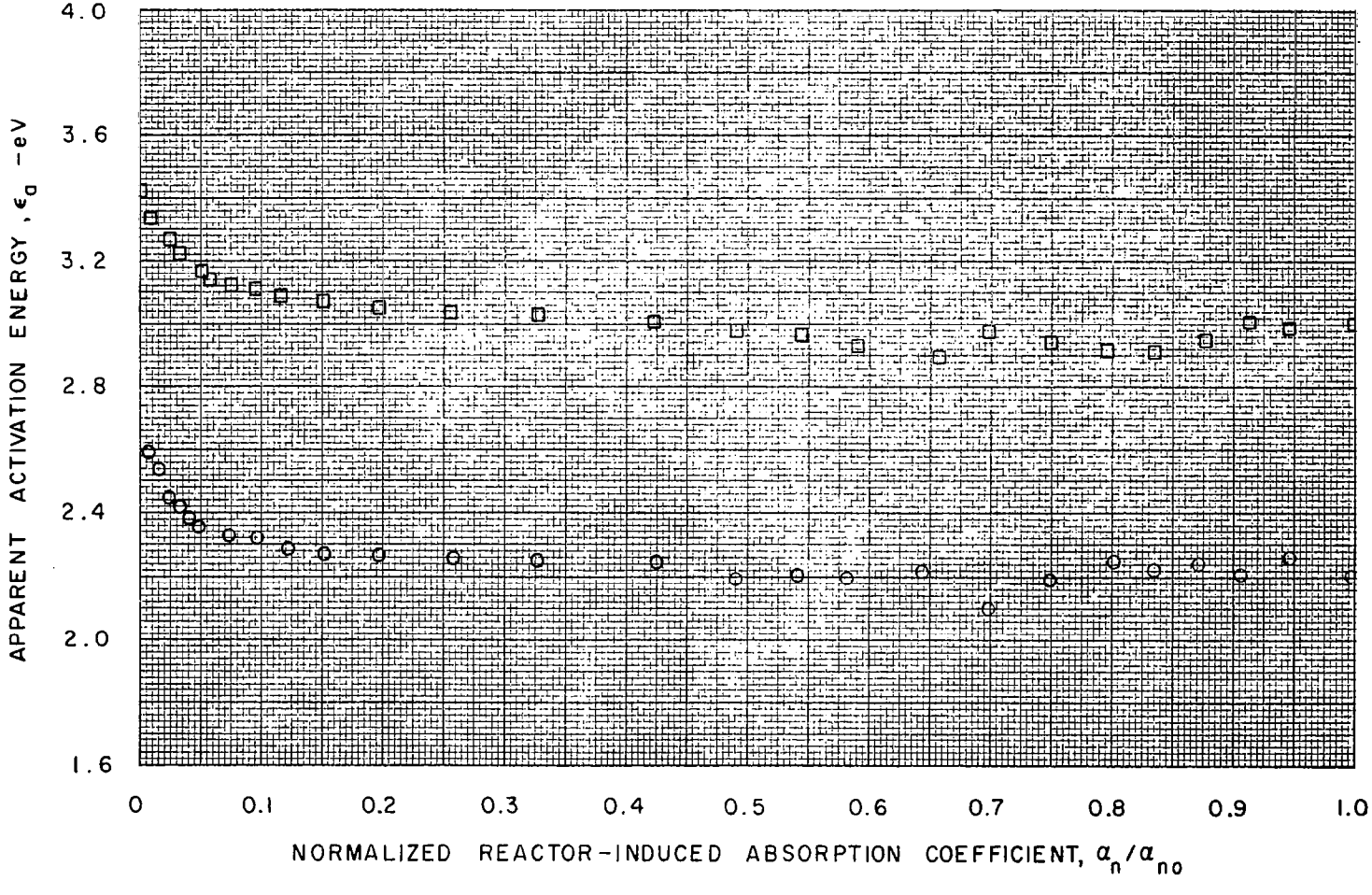

FIG. 80

FIG. 81

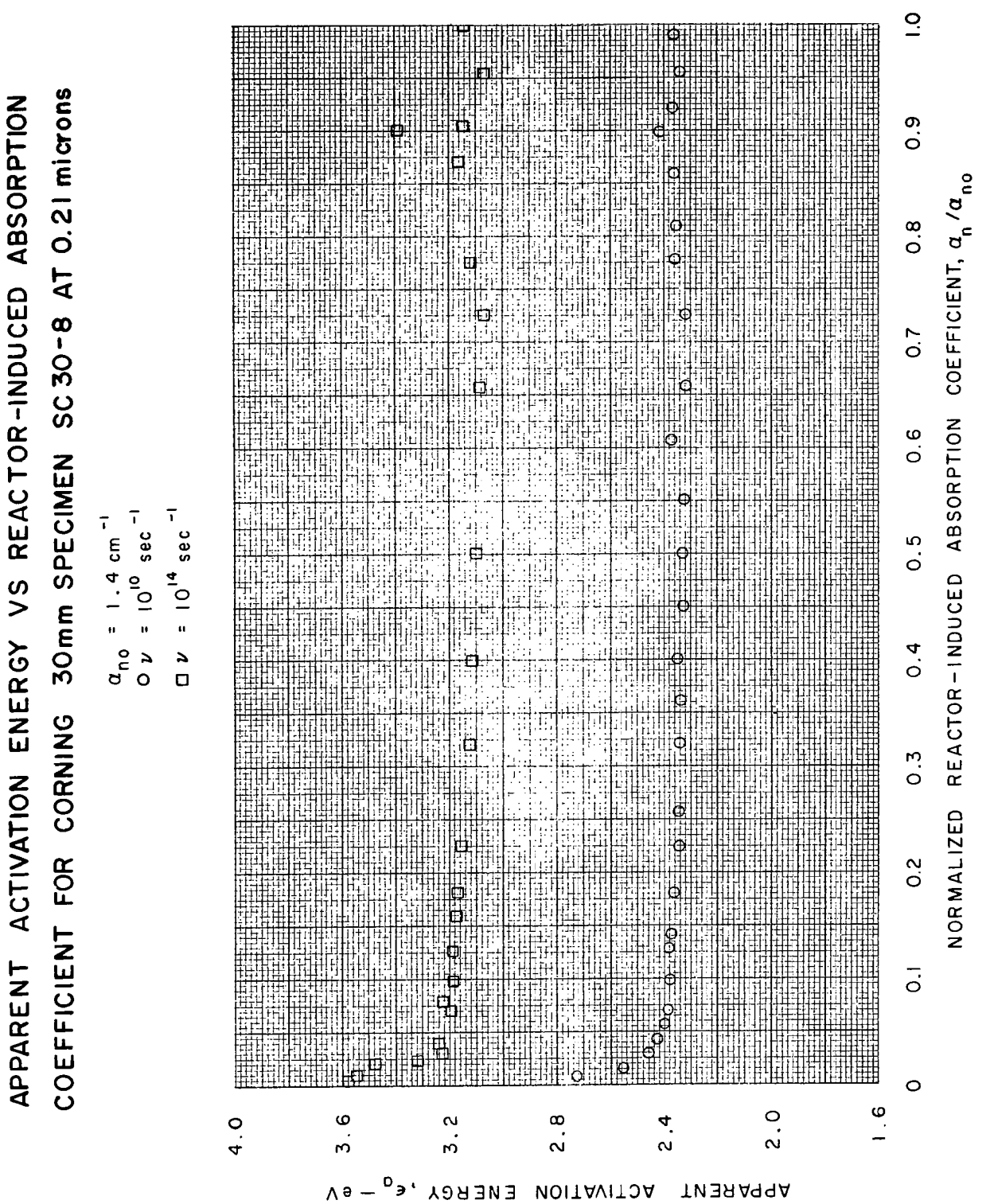
APPARENT ACTIVATION ENERGY VS REACTOR-INDUCED ABSORPTION COEFFICIENT FOR CORNING 30mm SPECIMEN SC 30-8 AT 0.21 microns
α_{no} = 1.4 cm^{-1}
O ν = 10^{10} sec^{-1}
□ ν = 10^{14} sec^{-1}
APPARENT ACTIVATION ENERGY, ϵ_o — eV
4.0
3.6
3.2
2.8
2.4
2.0
1.6
0
0.1
0.2
0.3
0.4
0.5
0.6
0.7
0.8
0.9
1.0
NORMALIZED REACTOR-INDUCED ABSORPTION COEFFICIENT, α_n / α_{no}

APPARENT ACTIVATION ENERGY VS REACTOR-INDUCED ABSORPTION COEFFICIENT FOR AMERSIL 1mm SPECIMEN SA 1-2 AT 0.210 microns

$\alpha_{no} = 22.3\,cm^{-1}$
○ $\nu = 10^{10}\ sec^{-1}$
□ $\nu = 10^{14}\ sec^{-1}$

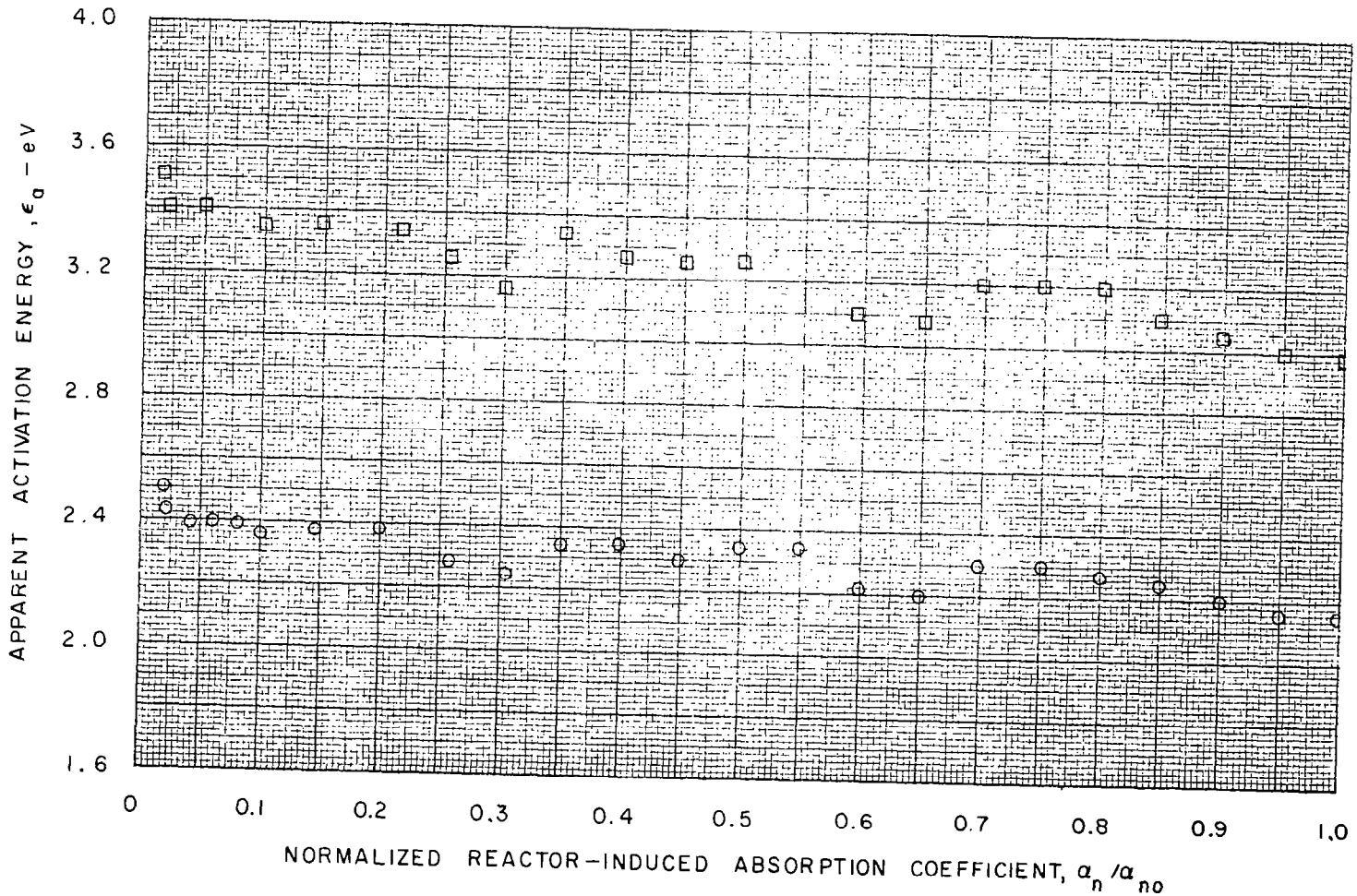

FIG. 82

APPARENT ACTIVATION ENERGY VS REACTOR-INDUCED ABSORPTION COEFFICIENT FOR AMERSIL 1mm SPECIMEN SA 1-5 AT 0.210 microns

FIG. 83

$\alpha_{no} = 35.7 cm^{-1}$
○ $\nu = 10^{10}$ sec^{-1}
□ $\nu = 10^{14}$ sec^{-1}

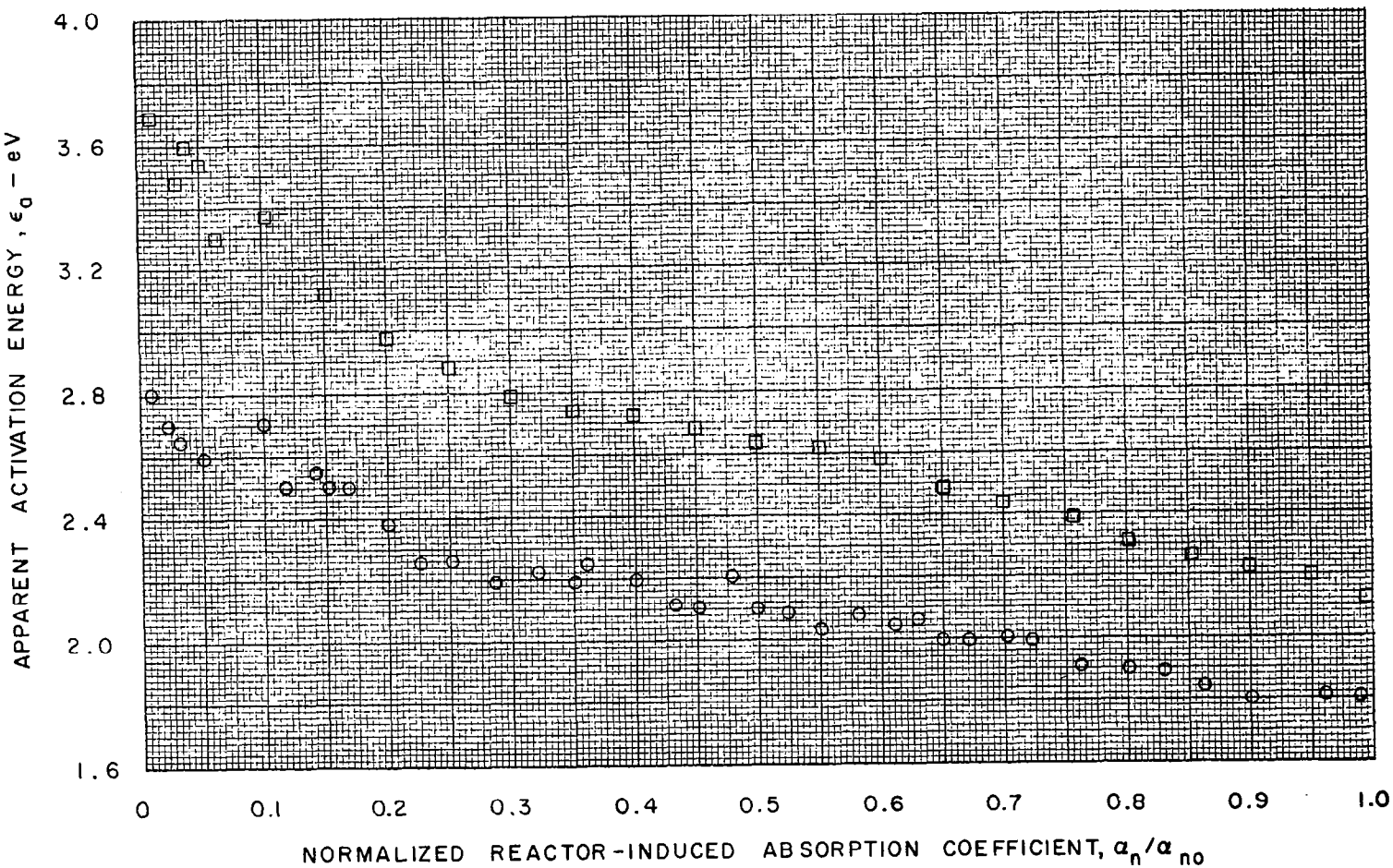

APPARENT ACTIVATION ENERGY VS REACTOR-INDUCED ABSORPTION COEFFICIENT FOR AMERSIL 30mm SPECIMEN SA 30-2 AT 0.23 microns

α_{no} = 1.2 cm^{-1}
○ ν = 10^{10} sec^{-1}.
□ ν = 10^{14} sec^{-1}

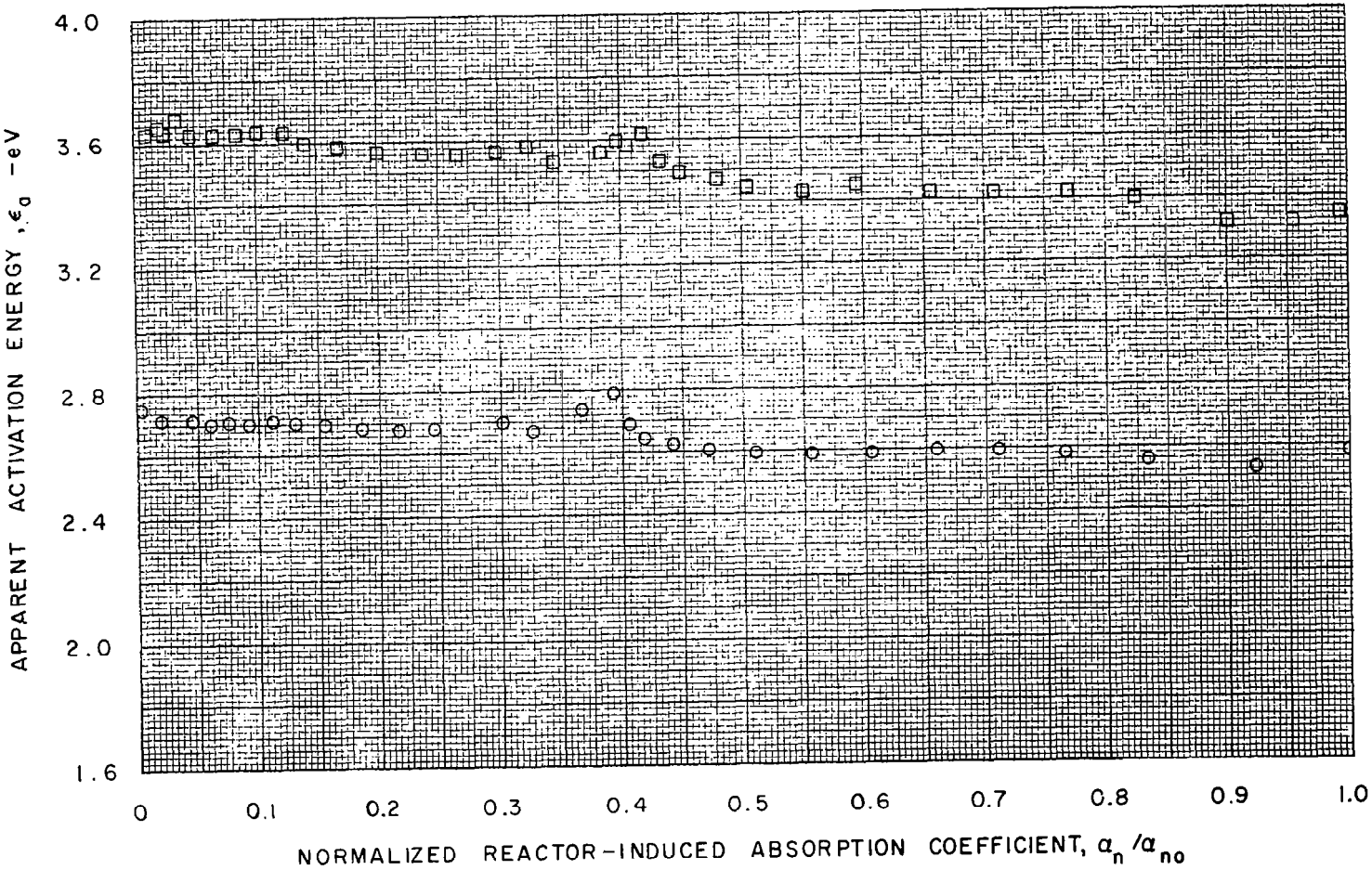

FIG. 8.4

FIG. 85

APPARENT ACTIVATION ENERGY VS REACTOR-INDUCED ABSORPTION COEFFICIENT FOR THERMAL AMERICAN 30 mm SPECIMEN ST 30-1 AT 0.210 microns

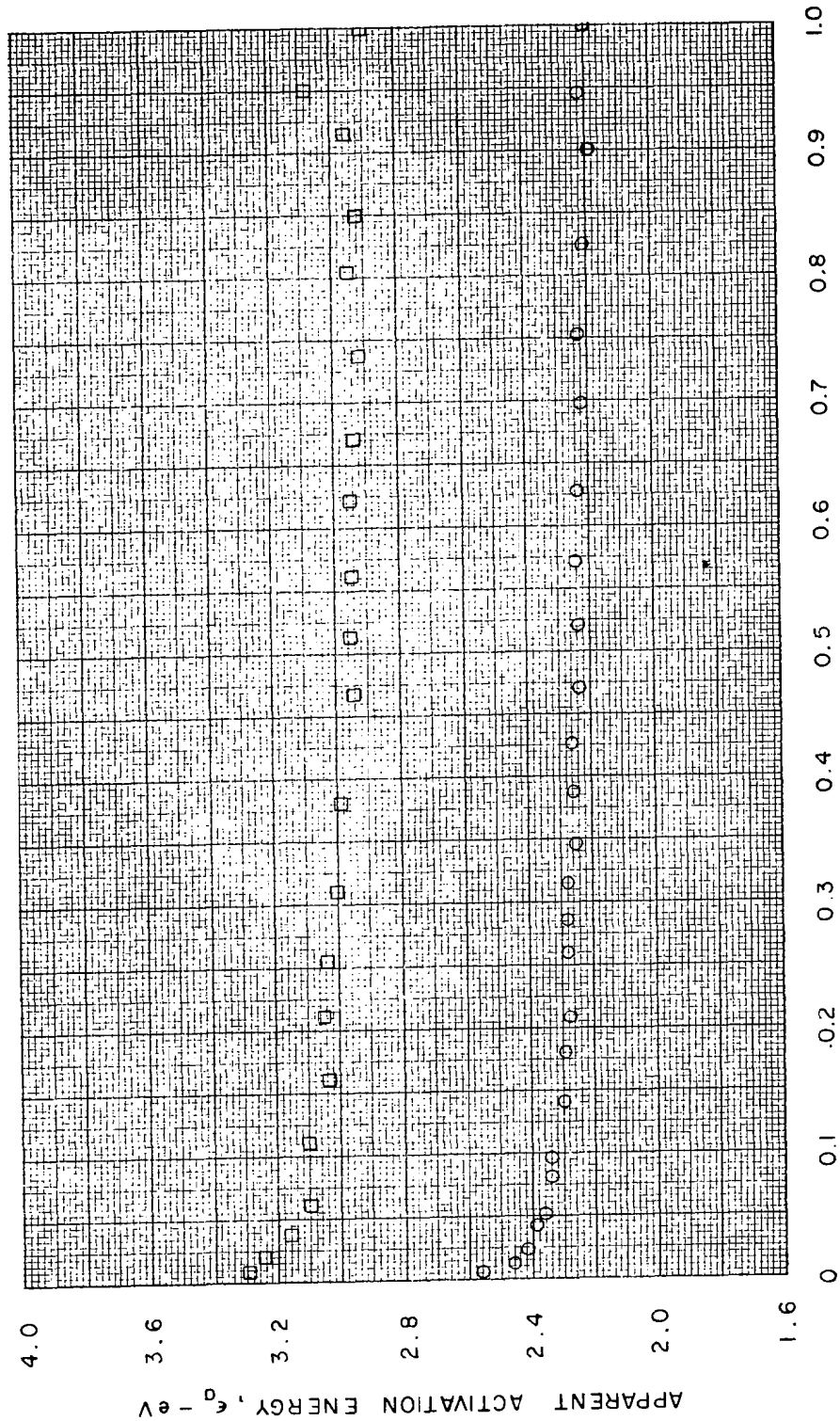

APPARENT ACTIVATION ENERGY VS REACTOR-INDUCED ABSORPTION COEFFICIENT FOR THERMAL AMERICAN 30mm SPECIMEN ST 30-4 AT 0.215 microns

$\alpha_{no} = 1.2\ cm^{-1}$

○ $\nu = 10^{10}\ sec^{-1}$

□ $\nu = 10^{14}\ sec^{-1}$

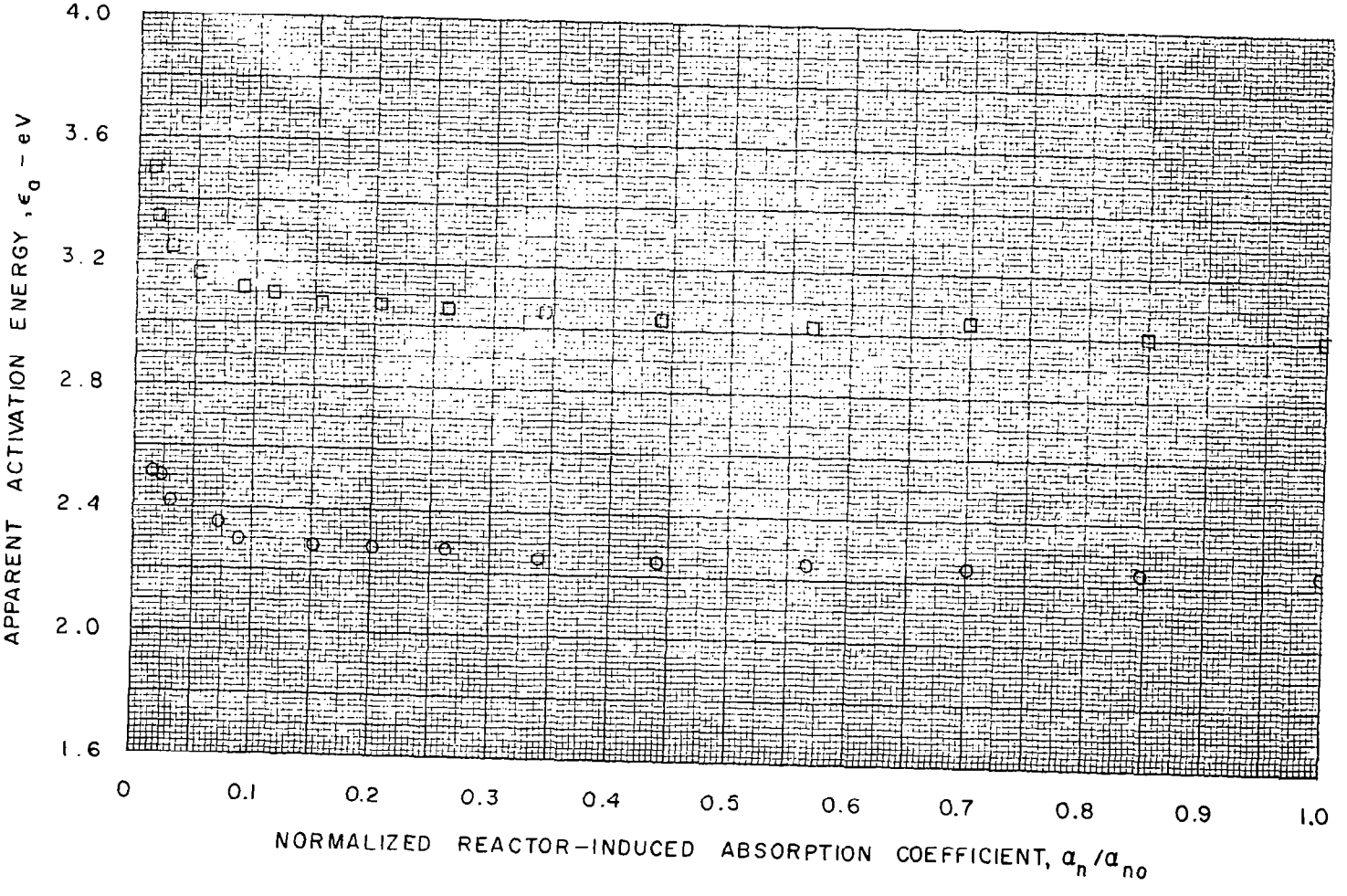

FIG. 86

APPARENT ACTIVATION ENERGY VS REACTOR-INDUCED ABSORPTION COEFFICIENT FOR THERMAL AMERICAN 30mm SPECIMEN ST 30-5 AT 0.215 microns

FIG. 87

$\alpha_{no} = 2.2\ cm^{-1}$
○ $\nu = 10^{10}\ sec^{-1}$
□ $\nu = 10^{14}\ sec^{-1}$

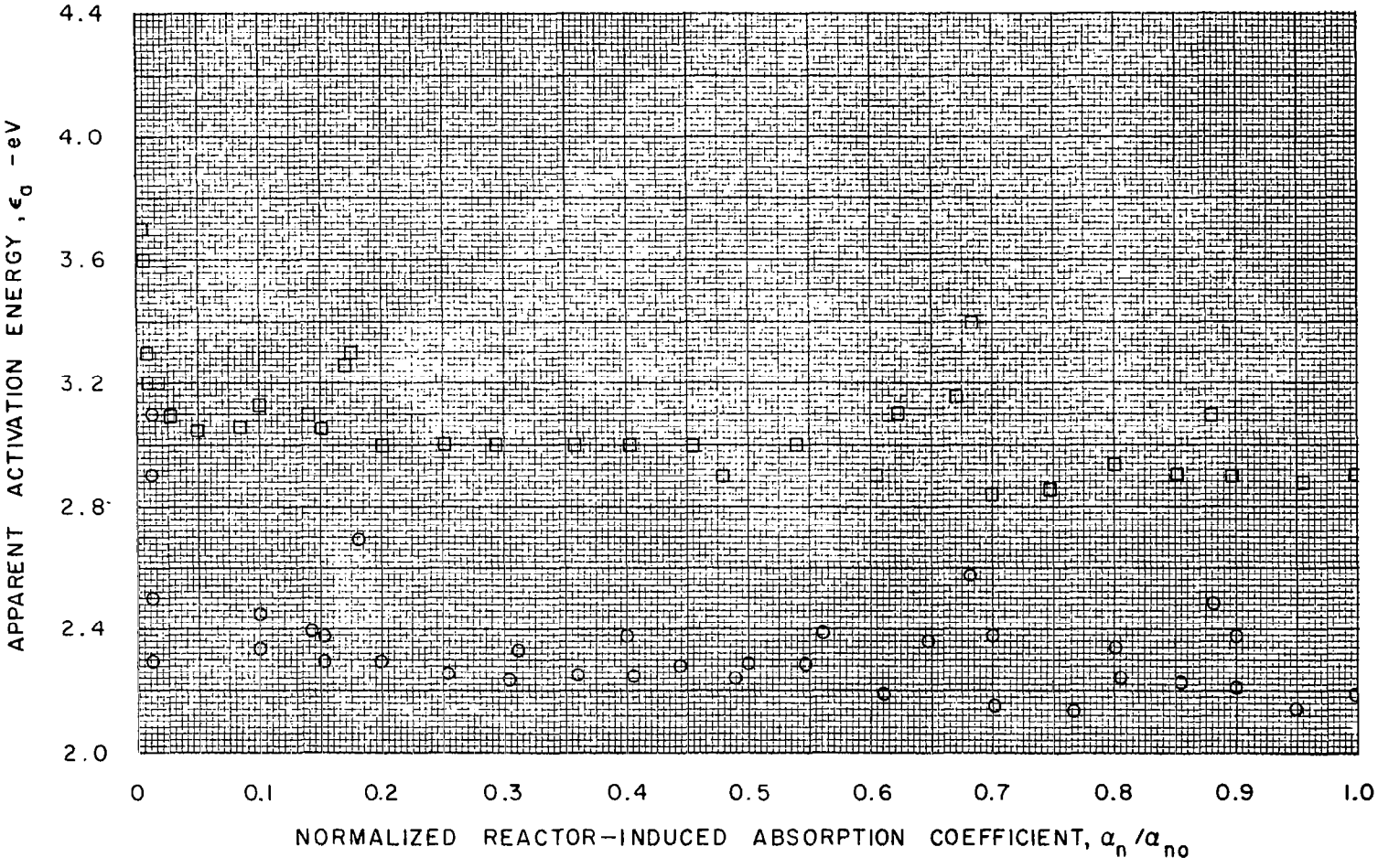

SUMMARIES OF VALUES OF APPARENT ACTIVATION ENERGY FOR CORNING, AMERSIL, AND THERMAL AMERICAN SPECIMENS

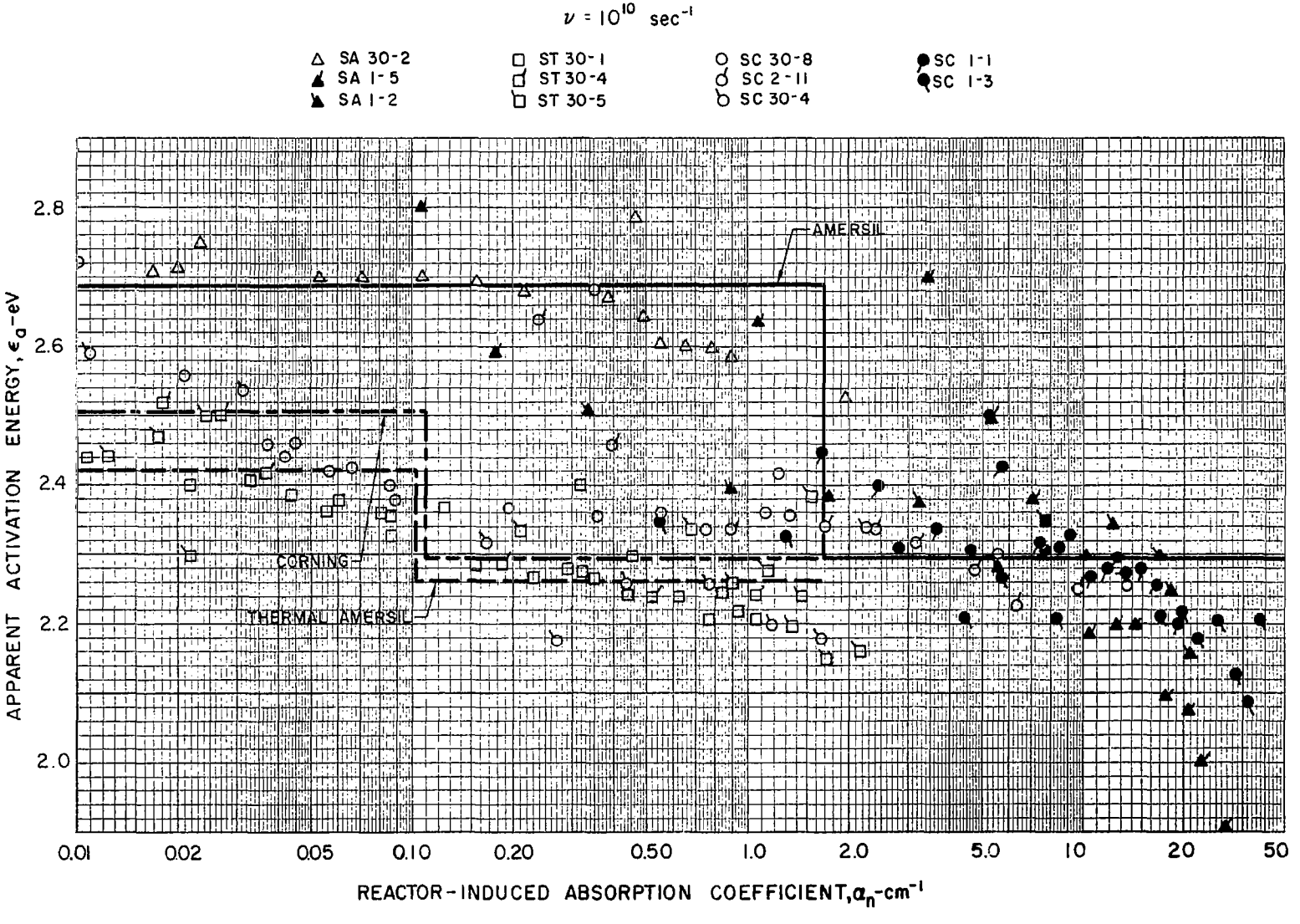

FIG. 88

FIG. 89

COMPARISON OF 22C TRANSMITTANCE OF CORNING 1 mm SPECIMEN SC 1-1 PRIOR TO REACTOR IRRADIATION AND AFTER ANNEAL OF INDUCED COLOR

SYMBOL	TEMP C	SAMPLE BEAM		REFERENCE BEAM	
		THICKNESS, mm	SPECIMEN	THICKNESS, mm	SPECIMEN
○ PRE-IRRADIATION	22	30.0	SC 1-1	1.0	NONE
□ POST-ANNEAL					

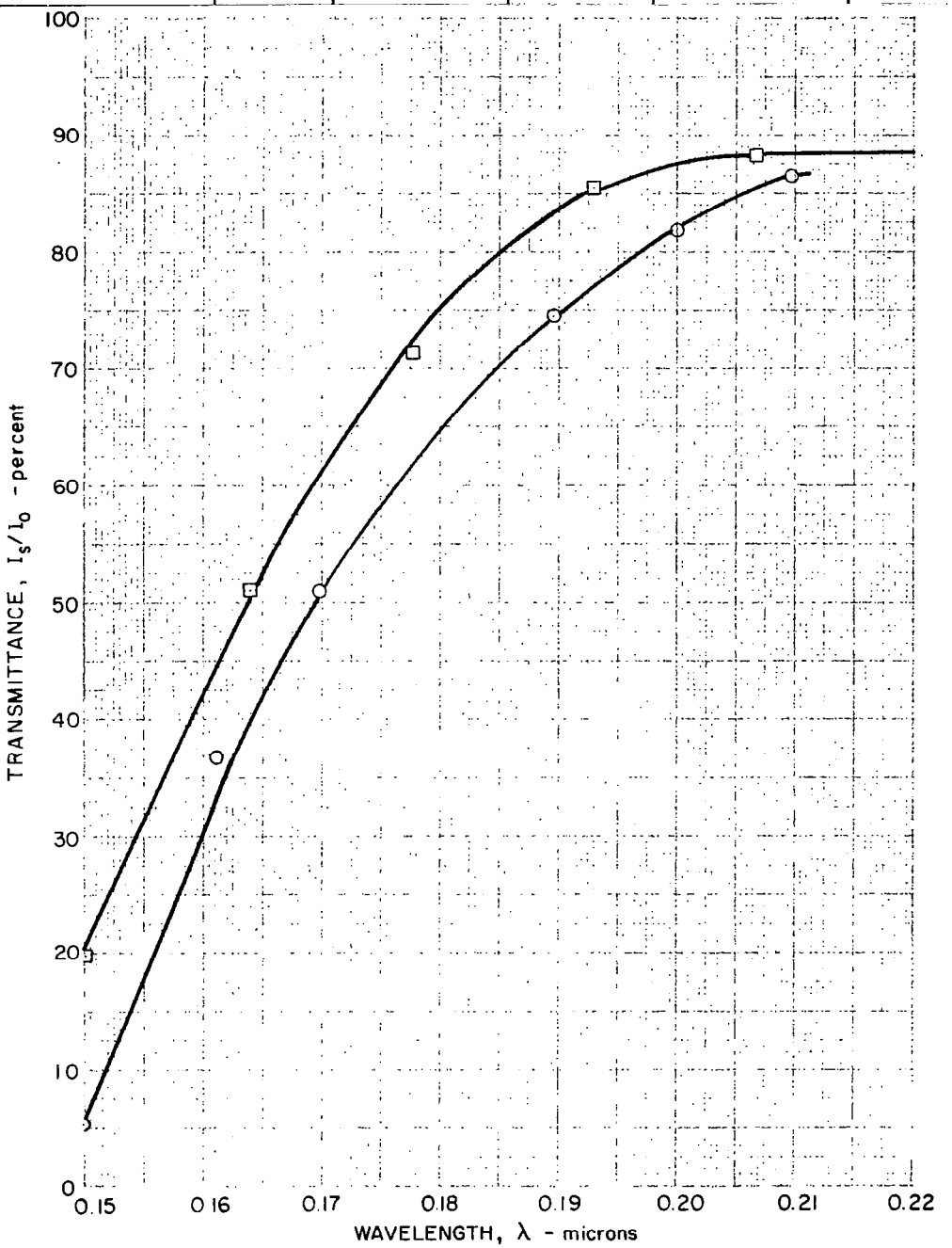

FIG. 90

COMPARISON OF 22C TRANSMITTANCE OF CORNING 2 mm SPECIMEN SC 2-11 PRIOR TO REACTOR IRRADIATION AND AFTER ANNEAL OF INDUCED COLOR

SYMBOL	TEMP C	SAMPLE BEAM		REFERENCE BEAM	
		THICKNESS, mm	SPECIMEN	THICKNESS, mm	SPECIMEN
O PRE-IRRADIATION	22	30.0	SC 2-11	1.0	NONE
□ POST-ANNEAL					

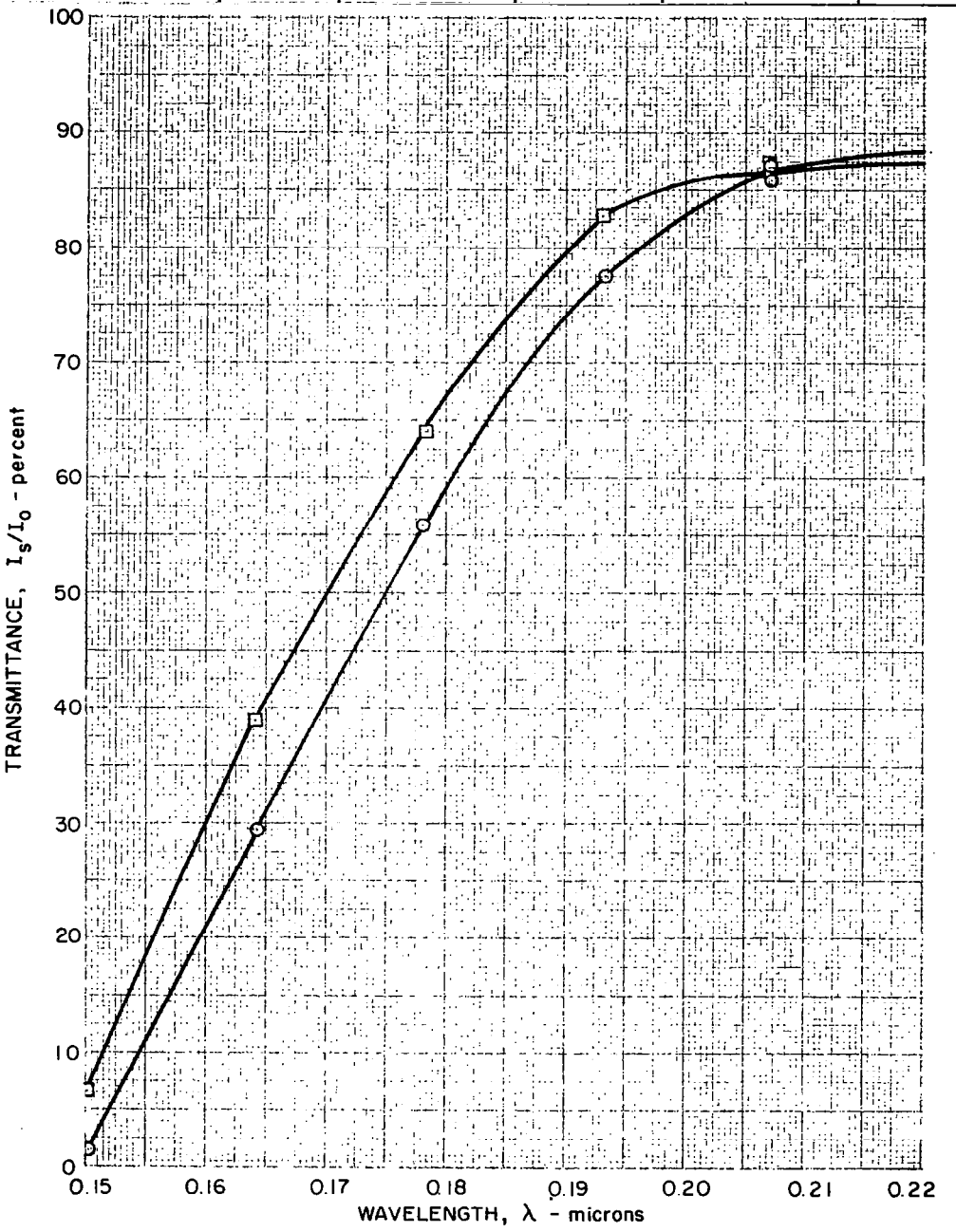

FIG. 91

COMPARISON OF 22C TRANSMISSIVITY OF CORNING 30mm SPECIMEN SC30-4 PRIOR TO REACTOR IRRADIATION AND AFTER ANNEAL OF INDUCED COLOR

SYMBOL	TEMP C	SAMPLE BEAM		REFERENCE BEAM	
		THICKNESS, mm	SPECIMEN	THICKNESS, mm	SPECIMEN
O PRE-IRRADIATION	22	30.0	SC 30-4	1.0	SC 1-3
□ POST-ANNEAL					

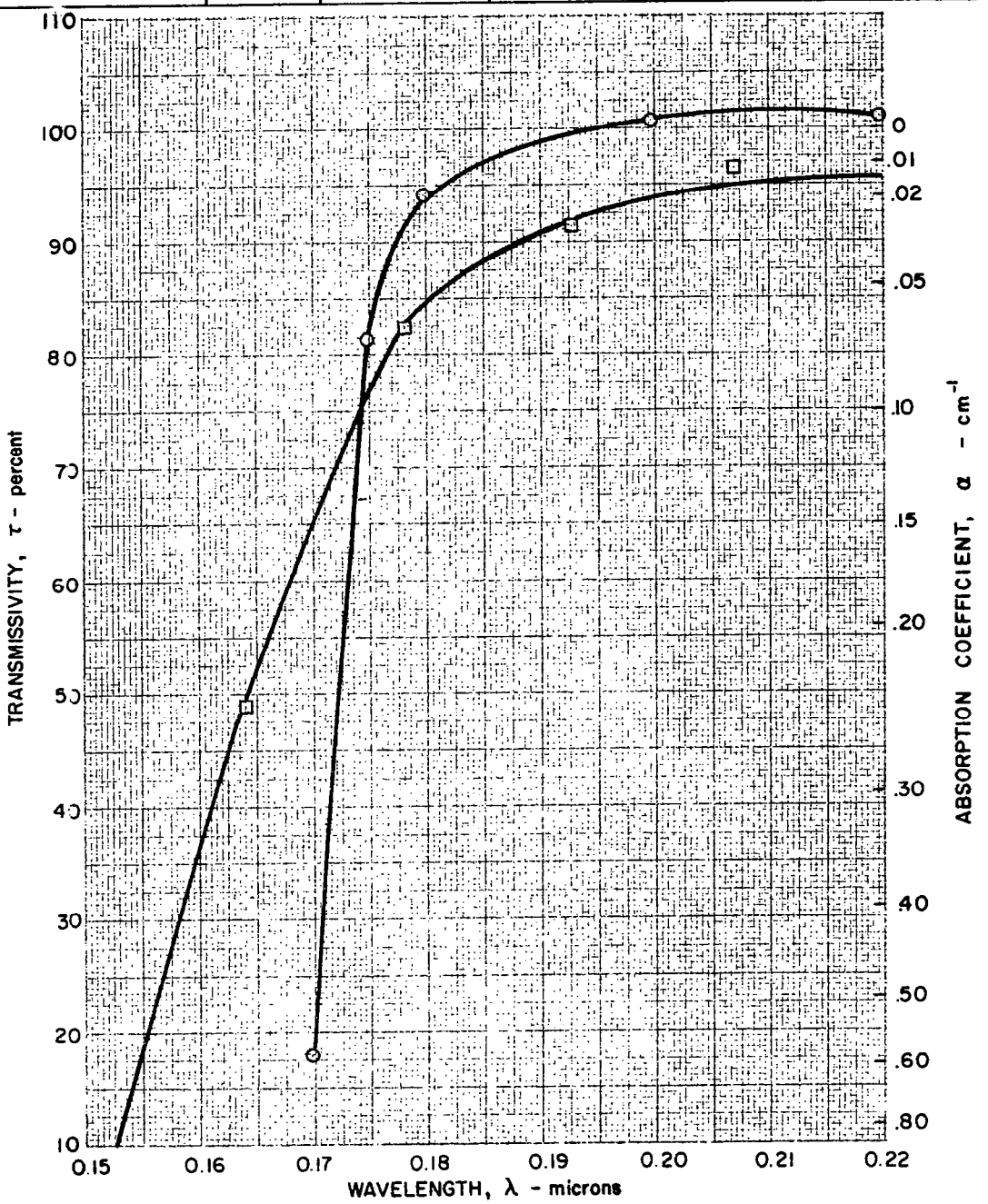

FIG. 92

COMPARISON OF 22C TRANSMISSIVITY OF CORNING 30mm SPECIMEN SC30-8 PRIOR TO REACTOR IRRADIATION AND AFTER ANNEAL OF INDUCED COLOR

SYMBOL	TEMP C	SAMPLE BEAM		REFERENCE BEAM	
		THICKNESS, mm	SPECIMEN	THICKNESS, mm	SPECIMEN
O PRE-IRRADIATION	22	30.0	SC 30-8	1.0	SC 1-2
□ POST-ANNEAL					

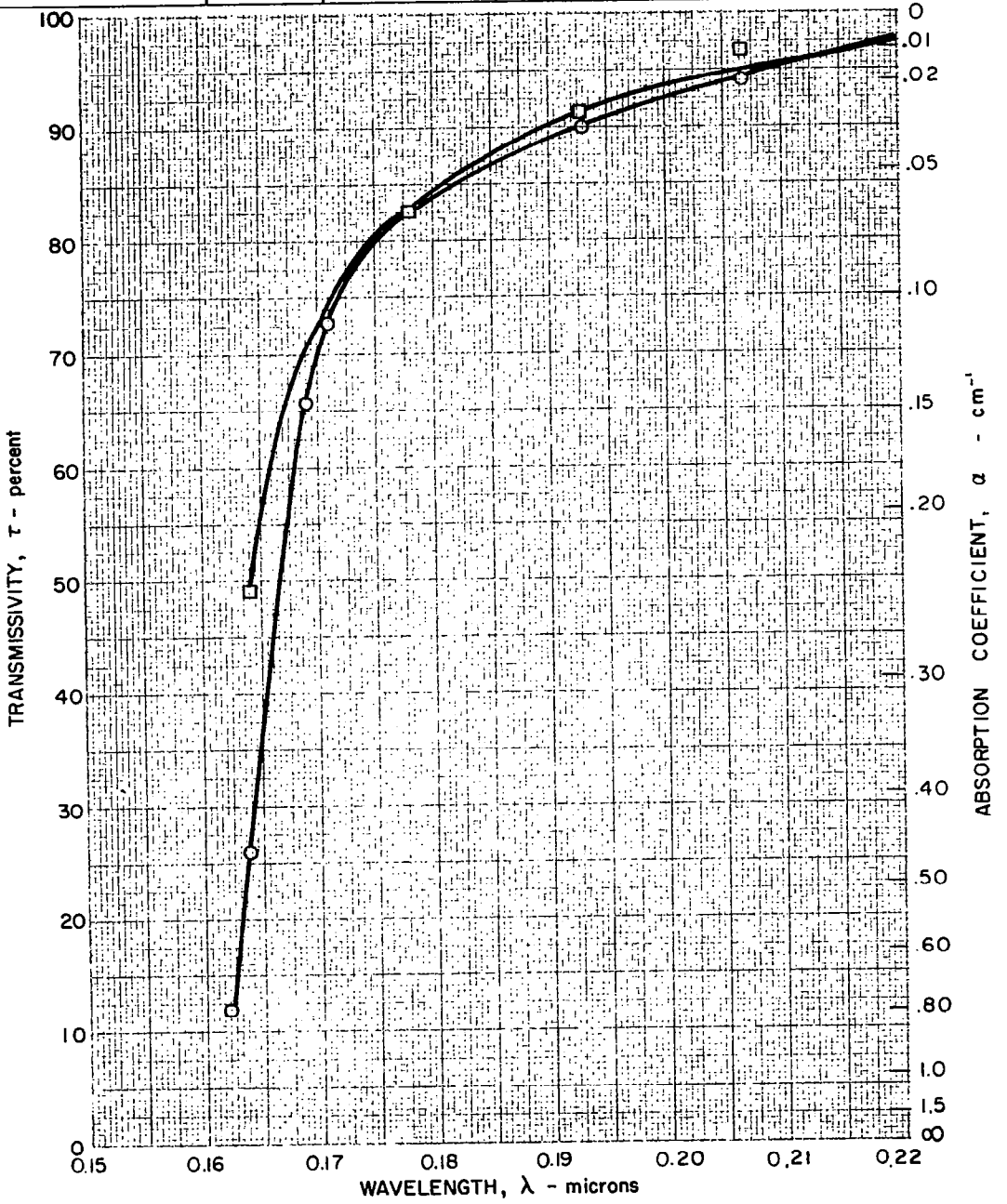

FIG. 93

COMPARISON OF 22C TRANSMISSIVITY OF AMERSIL 30 mm SPECIMEN SA 30-2 PRIOR TO REACTOR IRRADIATION AND AFTER ANNEAL OF INDUCED COLOR

SYMBOL	TEMP C	SAMPLE BEAM		REFERENCE BEAM	
		THICKNESS, mm	SPECIMEN	THICKNESS, mm	SPECIMEN
O PRE-IRRADIATION □ POST-ANNEAL	22	30.0	SA 30 - 2	1.0	SA 1 - 2

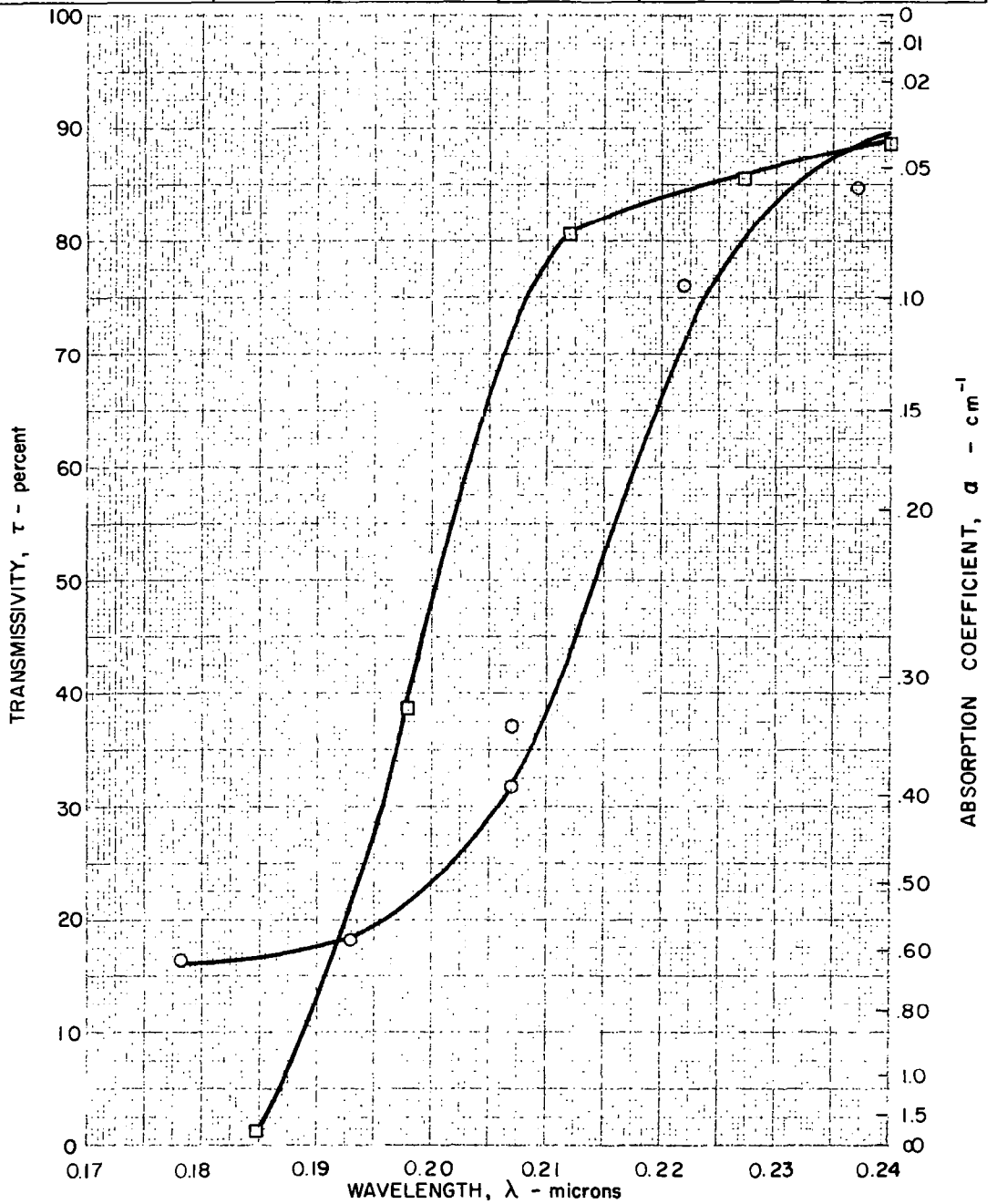

FIG. 94

COMPARISON OF 22C TRANSMISSIVITY OF AMERSIL 30mm SPECIMEN SA 30-5 PRIOR TO REACTOR IRRADIATION AND AFTER ANNEAL OF INDUCED COLOR

SYMBOL	TEMP C	SAMPLE BEAM		REFERENCE BEAM	
		THICKNESS, mm	SPECIMEN	THICKNESS, mm	SPECIMEN
O PRE-IRRADIATION	22	30.0	SA 30-5	1.0	SA 1-6
□ POST-ANNEAL					

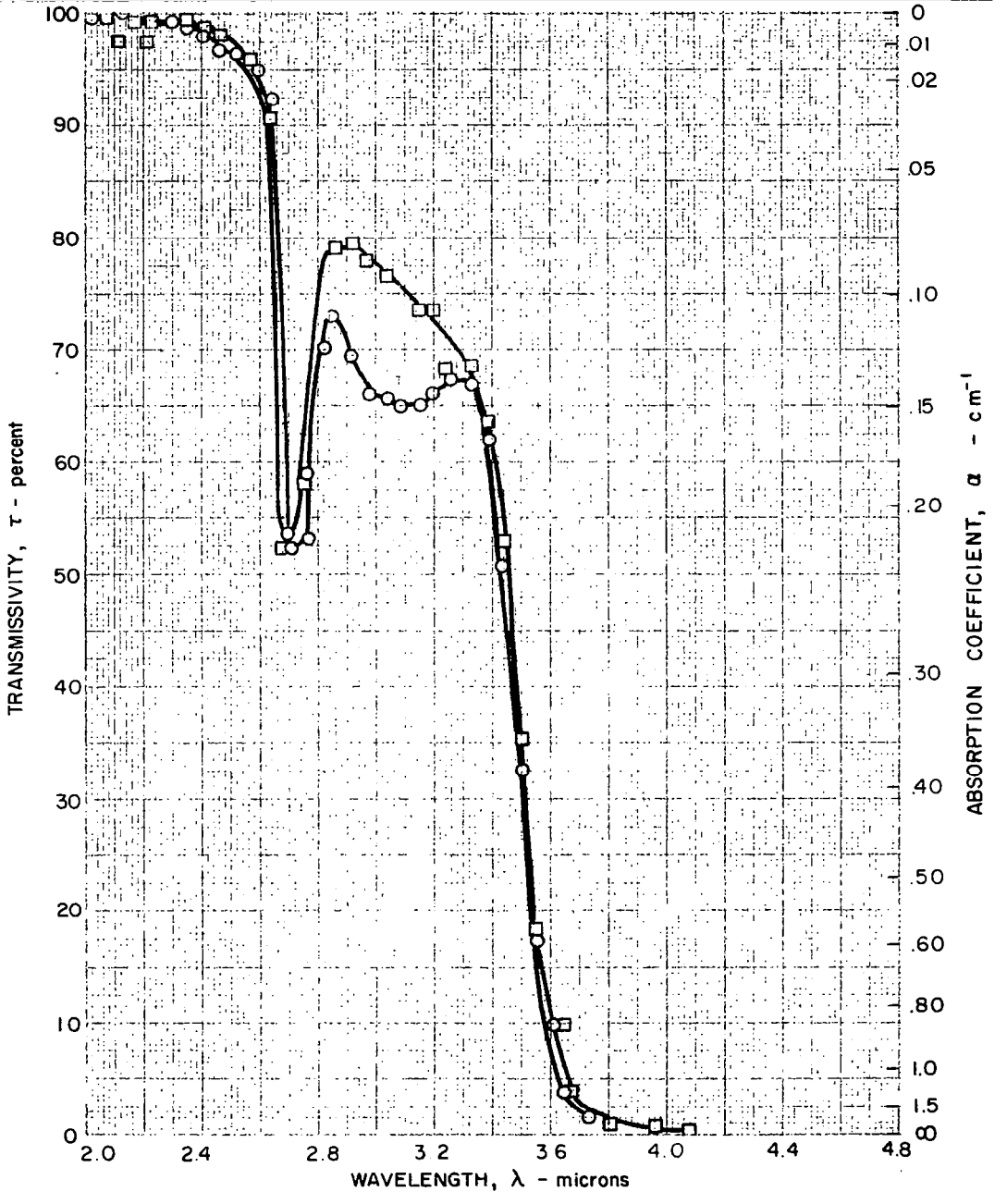

FIG. 95

COMPARISON OF 22C TRANSMISSIVITY OF THERMAL AMERICAN 30 mm SPECIMEN ST 30-I PRIOR TO REACTOR IRRADIATION AND AFTER ANNEAL OF INDUCED COLOR

SYMBOL	TEMP C	SAMPLE BEAM		REFERENCE BEAM	
		THICKNESS, mm	SPECIMEN	THICKNESS, mm	SPECIMEN
O PRE-IRRADIATION	22	30.0	ST 30-1	1.0	ST 1-3
□ POST-ANNEAL					

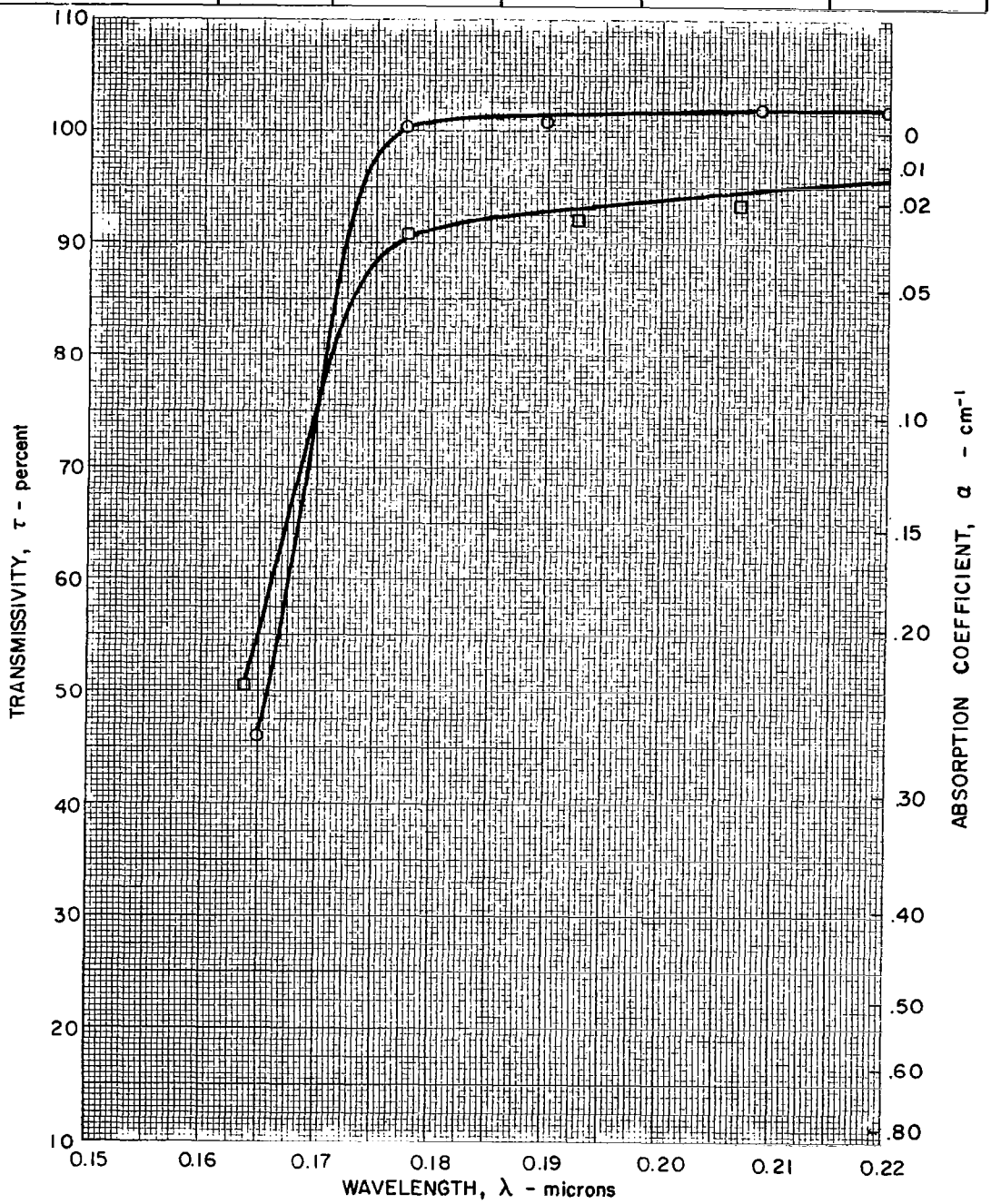

FIG. 96

COMPARISON OF 22C TRANSMISSIVITY OF THERMAL AMERICAN 30 mm SPECIMEN ST 30-4 PRIOR TO REACTOR IRRADIATION AND AFTER ANNEAL OF INDUCED COLOR

SYMBOL	TEMP C	SAMPLE BEAM		REFERENCE BEAM	
		THICKNESS, mm	SPECIMEN	THICKNESS, mm	SPECIMEN
O PRE-IRRADIATION	22	30.0	ST 30-4	1.0	ST 1-3
□ POST-ANNEAL					

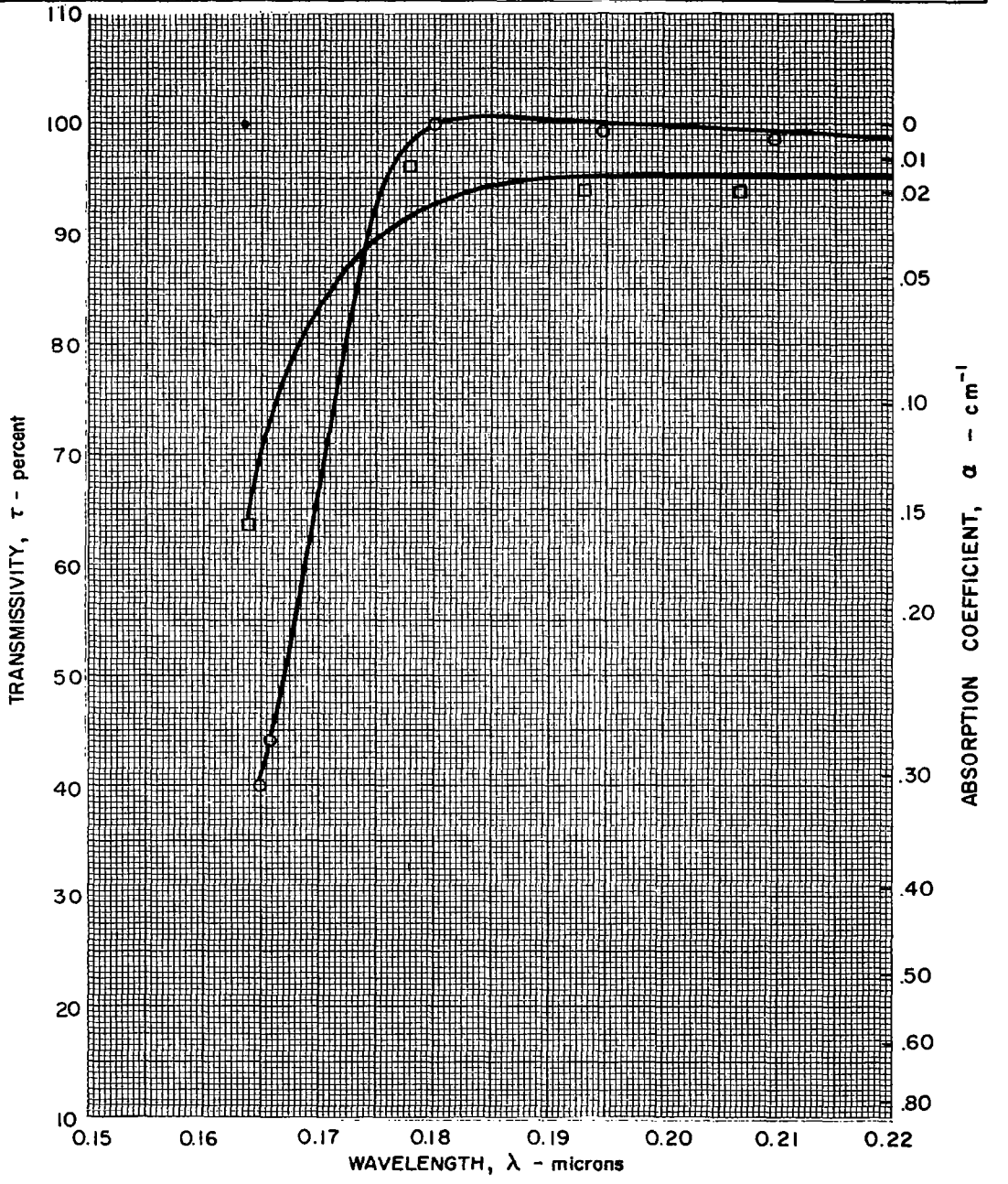

FIG. 97

COMPARISON OF 22C TRANSMISSIVITY OF THERMAL AMERICAN 30 mm SPECIMEN ST 30-5 PRIOR TO REACTOR IRRADIATION AND AFTER ANNEAL OF INDUCED COLOR

SYMBOL	TEMP. C	SAMPLE BEAM		REFERENCE BEAM	
		THICKNESS, mm.	SPECIMEN	THICKNESS, mm.	SPECIMEN
O PRE-IRRADIATION	22	30.0	ST 30-5	1.0	ST 1-3
□ POST-ANNEAL					

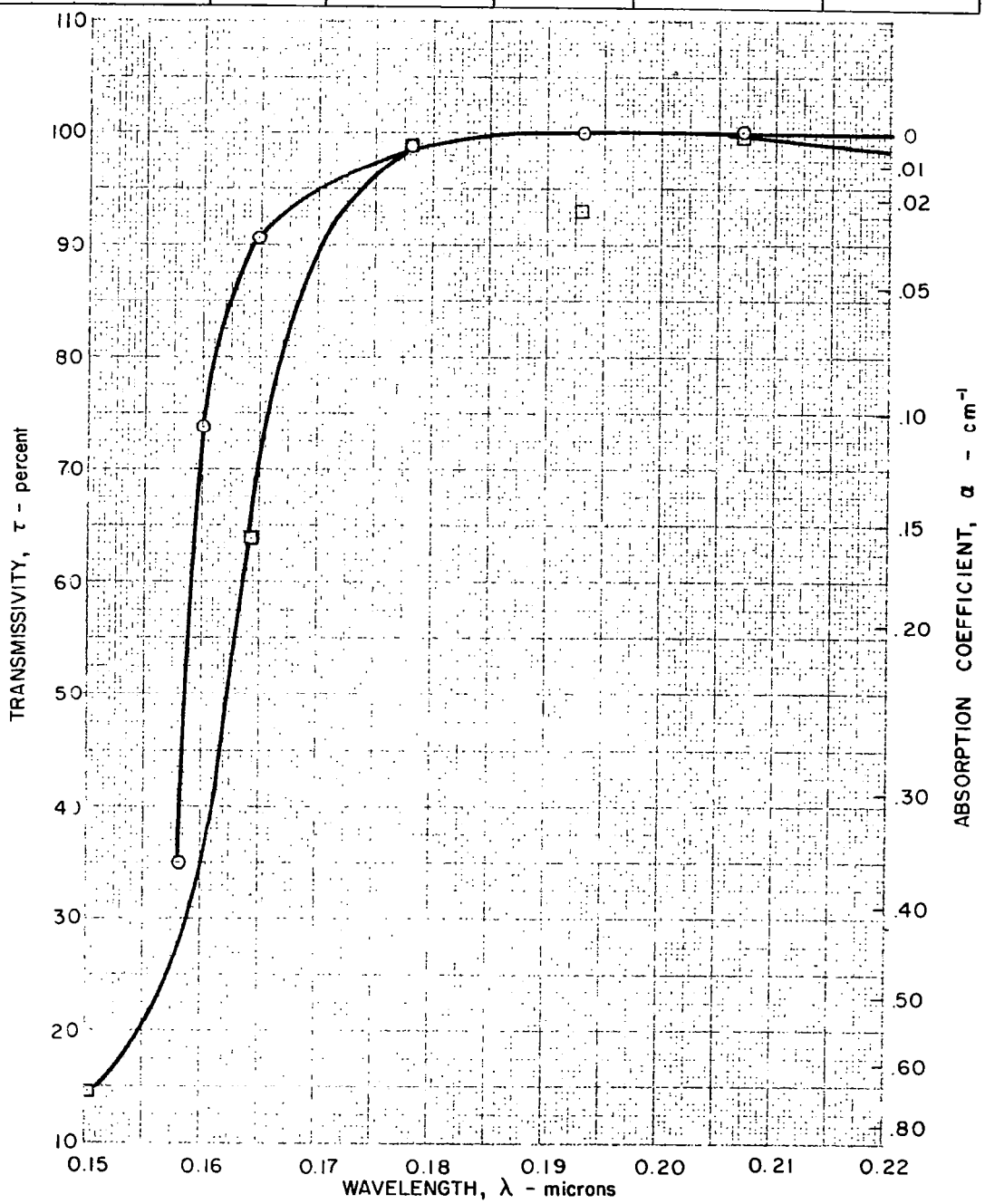

COMPARISON OF 22 C TRANSMISSIVITY OF 1 mm. SPECIMENS PRIOR TO REACTOR IRRADIATION AND AFTER ANNEAL OF INDUCED COLOR

SYMBOL	TEMP C	SAMPLE BEAM		REFERENCE BEAM	
		THICKNESS, mm	SPECIMEN	THICKNESS, mm	SPECIMEN
○ PRE - IRRADIATION □ POST - ANNEAL	22	1.0	SA 1-5	1.0	SA 1-6
◒ PRE - IRRADIATION ◨ POST - ANNEAL	22	1.0	SC 1-3	1.0	SC 1-2
● PRE - IRRADIATION ■ POST-ANNEAL	22	1.0	ST 1-6	1.0	ST 1-3

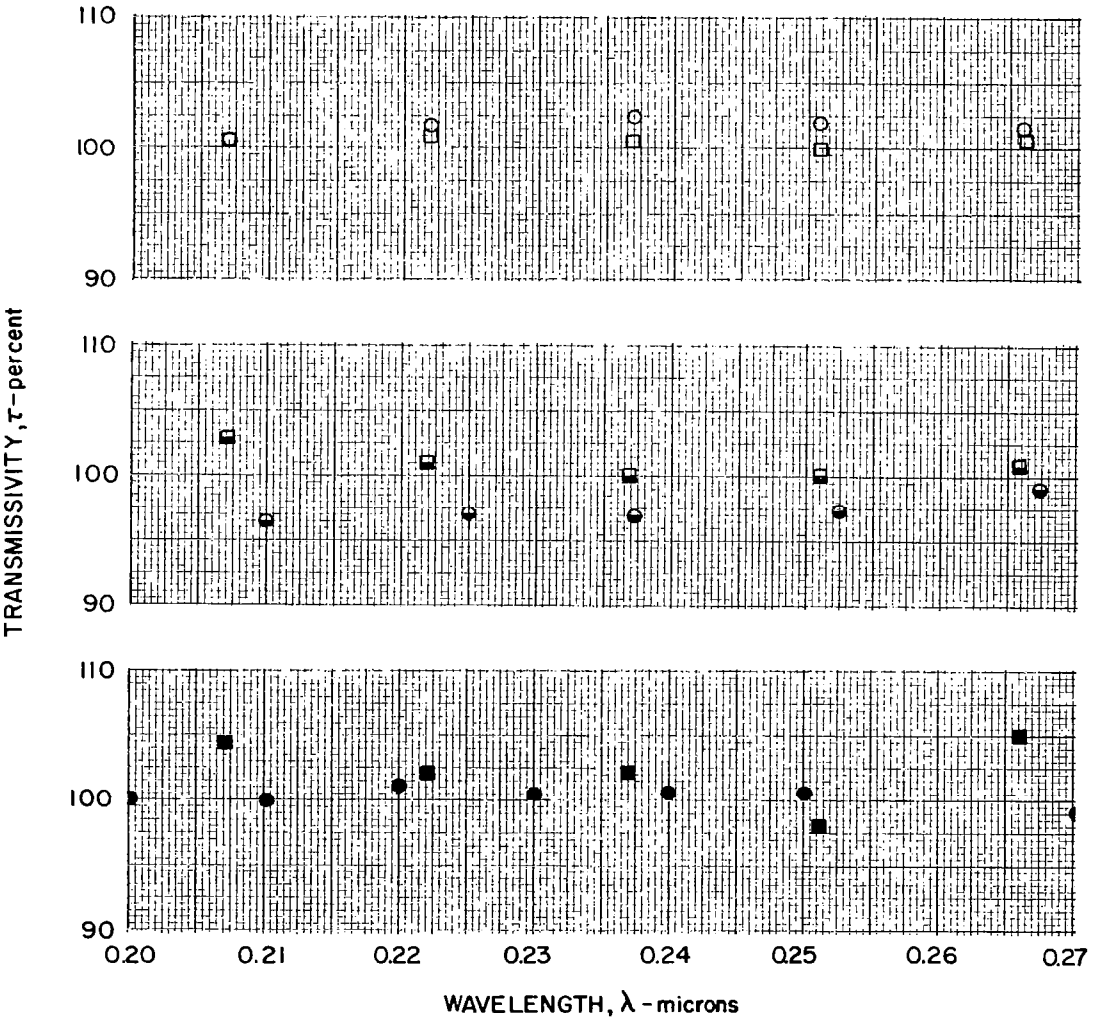

FIG. 99

COMPARISON OF 22C ABSORPTION COEFFICIENT DATA OF CORNING SPECIMENS PRIOR TO REACTOR IRRADIATION AND AFTER ANNEAL OF INDUCED COLOR

SYMBOL		SPECIMEN VS REFERENCE
PRE-IRRADIATION	-----	NOTED ON CURVES
POST-ANNEAL	○	SC 30-8 VS SC 1-2
	△	SC 2-11 VS SC 1-1
	□	SC 30-4 VS SC 1-3

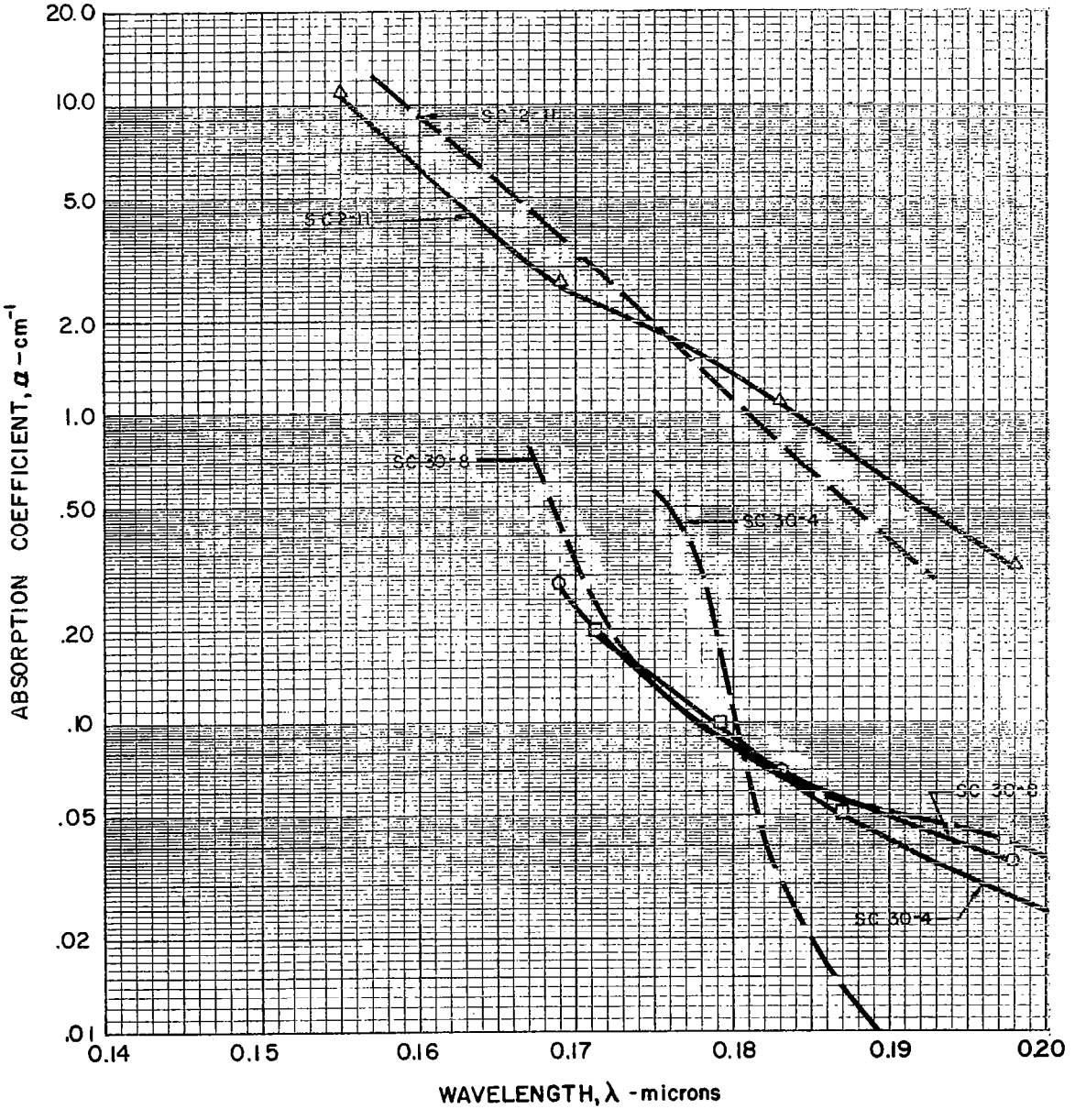

COMPARISON OF 22C ABSORPTION COEFFICIENT DATA OF AMERSIL SPECIMENS PRIOR TO REACTOR IRRADIATION AND AFTER ANNEAL OF INDUCED COLOR

SYMBOL		SPECIMEN VS REFERENCE
PRE-IRRADIATION	----	NOTED ON CURVE
POST-ANNEAL	O	SA 30-2 VS SA 1-2

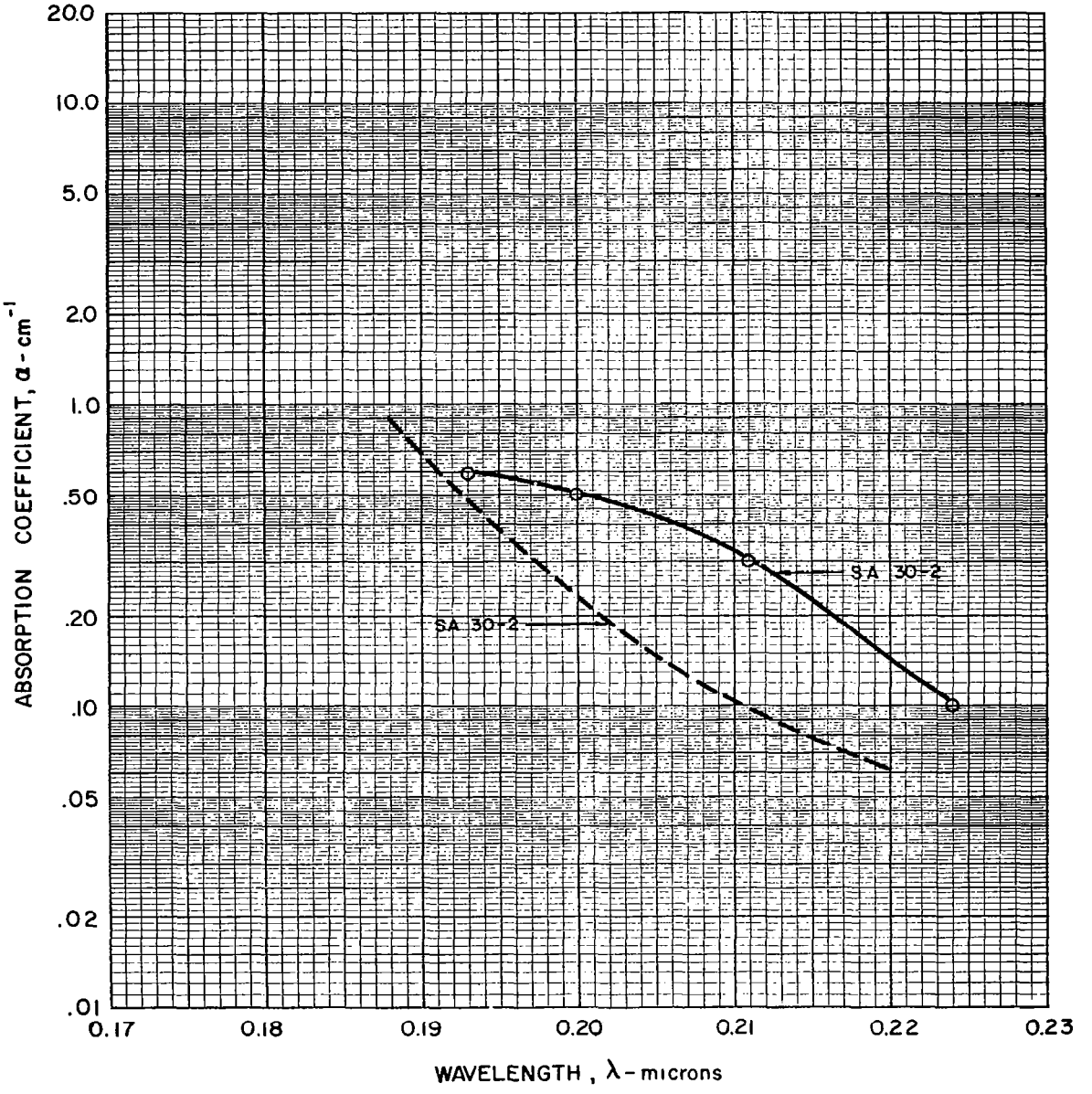

FIG. 101

COMPARISON OF 22 C ABSORPTION COEFFICIENT DATA OF THERMAL AMERICAN SPECIMENS PRIOR TO REACTOR IRRADIATION AND AFTER ANNEAL OF INDUCED COLOR

SYMBOL		SPECIMEN VS REFERENCE
PRE-IRRADIATION	----	NOTED ON CURVES
POST-ANNEAL	○	ST 30-4 VS ST 1-3
	△	ST 30-1 VS ST 1-6
	□	ST 30-5 VS STi-3